# Functional Analysis of Secondary Metabolite Biosynthesis-Related Genes in *Alternaria brassicicola*

by

**Kwang-Hyung Kim**

Dissertation submitted to the faculty of the Virginia Polytechnic Institute and State University in partial fulfillment of the requirements for the degree of

**Doctor of Philosophy**

In

**Biological Sciences**

Christopher B. Lawrence, Chair

John B. McDowell, Member

Liwu Li, Member

Dorothea Tholl, Member

September 7, 2009

Blacksburg, Virginia

Keywords: Secondary metabolite, *Alternaria brassicicola*, Nonribosomal peptide synthetase, Polyketide synthase, fungal pathogenicity

# Functional Analysis of Secondary Metabolite Biosynthesis-Related Genes in *Alternaria brassicicola*

Kwang-Hyung Kim

**ABSTRACT**

*Alternaria brassicicola* is a necrotrophic pathogen that causes black spot disease on virtually all cultivated Brassicas, *A. brassicicola* is renowned for its ability to prodigiously produce secondary metabolites. To test the hypothesis that secondary metabolites produced by *A. brassicicola* contribute to pathogenicity, we identified seven nonribosomal peptide synthetases (NPSs) and 10 polyketide synthases (PKSs) in the *A. brassicicola* genome. The phenotype resulting from knockout mutations of each *PKS* and *NPS* gene was investigated with an emphasis on discovery of fungal virulence factors. A highly efficient gene disruption method using a short linear double stranded DNA construct with minimal elements was developed, optimized, and used to functionally disrupt all *NPS* and *PKS* genes in *A. brassicicola*. Three *NPS* and two *PKS* genes, and one *NPS*-like gene appeared to be virulence factors based upon reduced lesion development of each mutant on inoculated green cabbage and Arabidopsis compared with the wild-type strain. Furthermore some of the KO mutants

exhibited developmental phenotypic changes in pigmentation and conidiogenesis. To further characterize the roles of several genes of interest in *A. brassicicola* development and pathogenesis, the genes *AbNPS2*, *AbPKS9*, and *NPS*-like *tmpL* were selected for in-depth functional analysis. We provide substantial evidence that the AbNPS2-associated metabolite is involved in conidial cell wall construction, possibly as an anchor connecting two cell wall layers. We also characterized a biosynthetic gene cluster harboring the *AbPKS9* gene and demonstrated that this cluster is responsible for the biosynthesis of depudecin, an inhibitor of histone deacetylases and a minor virulence factor. Finally, we demonstrated that a NPS-like protein named TmpL is involved in a filamentous fungi-specific mechanism for regulating levels of intracellular reactive oxygen species during conidiation and pathogenesis in both plant and animal pathogenic fungi. Collectively our results indicate that small molecule nonribosomal peptides and polyketides in *A. brassicicola* play diverse, but also fundamental, roles in fungal development and pathogenesis.

# ACKNOWLEDGEMENTS

First, before any other, I would like to give thanks to my heavenly Father, to whom I owe this accomplishment. Truly, without Him, obtaining this degree would not have been possible. Through this journey I have learned so much about God, myself, and life. I have gained much more patience.

The work in this dissertation would not have been possible without the support of my advisor, Dr. Christopher Lawrence. I have learned so much during this experience and I would like to thank you for giving me the opportunity to work under your guidance, encouraging me during challenging times of graduate studies and research work, and helping to develop a positive interpersonal relationship towards people.

I extend my thanks to the rest of my committee, Drs. John McDowell, Liwu Li, and Dorothea Tholl for their continuous assistance and valuable suggestions throughout my graduate career. You exude such warmth and kindness and have always been an inspiration to me.

I thank Dr. Yangrae Cho, who was a PostDoc when I joined the program, for providing me with guidance early on in my time in this molecular biology world. Cho Bacsanim! You were my mentor and teacher whom I could trust especially with your scientific mindset and attitude.

I extend a grateful thank to Dr. Sang-Wook Park, who fortuitously joined our lab in my fourth year of graduate school, for being a fantastic aid to my studies by taking the time to simultaneously provide ideas to help advance my research.

I would also like to give thanks for the friends in the 3rd floor hallway and coworkers I have had in the Lawrence lab for making the lab a place filled with a lot of fun, enthusiasm and adventures, which eventually made it possible for me to conduct 5 years of research here at Virginia Tech. Oh! Guys! Without you, I can't imagine where I would be today. ☺

To my family, my wife Hwan Hee and lovely daughters Sion and Joo-an, you have shown me so much support. I love you with all my heart. In my mind, you were the radiating light during this process. Thank you for your encouraging words and your never-ending support. Thank you for believing in me. Thank you for your endless trust towards me. Thank you Dad and Mom for being the best parents a boy could have. I love you and thank you for always praying for me and encouraging my dreams. I definitely dedicate all my achievements to you Dad and Mom… And my brothers Tae Hyung and Hyungsunim, and Se Hyung… Thank you so much for your words of love and support.

Last but certainly not the least, I am deeply indebted to the Northstar family for their hospitality, valuable friendship, treating me like a family member and making me feel like home in this foreign country. Yes! I would like to name them all here: Pastor Bob and Sandra Jackson, Kenny and Linda Johnson, Jim and Cynthia Rancourt, Pastor Jeff and Carolyn Noble, Chris and Tonia Anderson, and… Oh My! It's too many…

# TABLE OF CONTENTS

# LIST OF TABLES

# LIST OF FIGURES

# Chapter I

## General Introduction and Overview of Research

## *Alternaria brassicicola*

Very little information is currently available concerning the pathogenic determinants produced by *Alternaria brassicicola* (Schwein.) Wiltshire, the causal agent of black spot diseases of many economically important *Brassica* species (Braverman, 1979). The necrotrophic nature of *A. brassicicola* typically leads to extensive damage of the plant harvest product (Humpherson-Jones, 1989; Neergaard, 1945). As a necrotrophic pathogen, *A. brassicicola* secretes numerous secondary metabolites, which include host-selective and nonhost-selective phytotoxins that kill cells from a large spectrum of cultivated and wild plants found within the Brassicaceae. This introductory chapter focuses on some of the latest findings regarding *A. brassicicola* pathogenicity.

### *Alternaria*: A model genus producing secondary metabolites, especially toxins

*Alternaria* species are causal agents of black or brown spot diseases of many fruits, vegetables and field crops (King, 1994). The disease is spread during the growing season by wind-blown or rain-splashed spores (MacKinnon et al., 1999). The pathogen attacks most parts of the plant and it is thought to induce its chlorotic effect by secretion of phytotoxins. Necrotrophs like *Alternaria* represent the largest class of

plant pathogens, yet our understanding of host parasite interactions involving this class of pathogens is lacking. The majority of the research that has been performed on *Alternaria* pathogenesis mechanisms of plants has been primarily centered upon the role of phytotoxins in disease. In fact, more toxins have been characterized from this genus than from any other fungal genus. All of the plant pathogenic *Alternaria* species to date have been reported to produce host-selective toxins (HSTs) and/or produce nonhost-selective toxic substances with very diverse biochemical structures (Agrios, 1997; Rotem, 1994). For many of the plant pathogenic *Alternaria* species, toxin production has been clearly demonstrated to be essential in enabling disease development on a particular host. *A. alternata* is ubiquitous in nature and mainly leads a saprophytic lifestyle, however, the transition from a nonspecific and nonpathogenic type to a host-specific type involves the production of host-selective toxins (Rotem, 1994). For example, there are at least 7 known host-parasite interactions in which HSTs produced by *Alternaria alternata* pathotypes are responsible for disease (Akamatsu et al., 1997; Otani et al., 1998). This makes *Alternaria*-plant interactions ideal model systems for studying the role of toxins in pathogenesis.

As mentioned above, other toxins produced by *Alternaria* species are both of the host-selective and nonhost-selective nature. Toxins produced by *A. alternata* pathotypes are mainly low molecular weight secondary metabolites. However, some of these toxins, such as the AAL toxin, produced by *A. alternata* f.sp. *lycopersici*, have been shown to be a sphingolipid-like molecule structurally similar to fumonisins (Gilchrist, 1998). Other toxins of diverse structure include cyclic despipeptide-based

molecules such as the AM toxin from *A. alternata* f.sp. *mali* (Johnson et al., 2000). Like many of the pathogenic species, *A. solani* has been reported to produce non-HSTs such as alternaric acid, alternariols, solanapyrone, and zinniol, however there has also been a report of a HST being produced by this species (Rotem, 1994). *A. brassicicola*, the focus species of this study has also been reported to produce several diverse types of phytotoxic molecules. A protein HST AB toxin was reported to be produced by *A. brassicicola* on host plant (Otani et al., 1998). *A. brassicicola* has also been reported to produce toxic metabolites including despipeptides and fucicoccin-like compounds (MacKinnon et al., 1999; McKenzie et al., 1988). Both HSTs and non-HSTs could be involved in any or all stages of infection by *Alternaria* species. Unlike HSTs, non-HSTs may not be the primary determinant of disease but may serve as important virulence factors (Rotem, 1994).

### *Alternaria brassicicola* – Brassica pathosystem

Brassicaceae, the crucifer plant family, consists of approximately 3,500 species in 350 distinct genera. However, the most important crop species from an economic perspective are found within the single genus, *Brassica*. These crop species include *B. oleracea* (vegetables), *B. rapa* (vegetables, oilseeds, and forages), *B. juncea* (vegetables and seed mustard), and *B. napus* (oilseeds) (Westman et al., 1999). *A. brassicicola* causes black spot disease (also called dark leaf spot) on virtually every important *Brassica* species (Sigareva and Earle, 1999; Westman et al., 1999). Black spot disease is of worldwide economic importance (Humpherson-Jones, 1985; Humpherson-Jones, 1989; Humpherson-Jones and Phelps, 1989; Maude and

Humpherson-Jones, 1980). For example, black spot can be a devastating disease resulting in 20-50% yield reductions in crops such as canola or rape (Rotem, 1994). Like other diseases caused by *Alternaria* species, black spot appears on the leaves as necrotic lesions, which are often described as black and sooty with chlorotic yellow halos surrounding the lesion sites (Fig. 1) (Rotem, 1994). *A. brassicicola*, however, is not limited to infection of leaves, and can infect all parts of the plant including pods, seeds, and stems, and is of particular importance as a post-harvest disease (Rimmer and Buchwaldt, 1995).

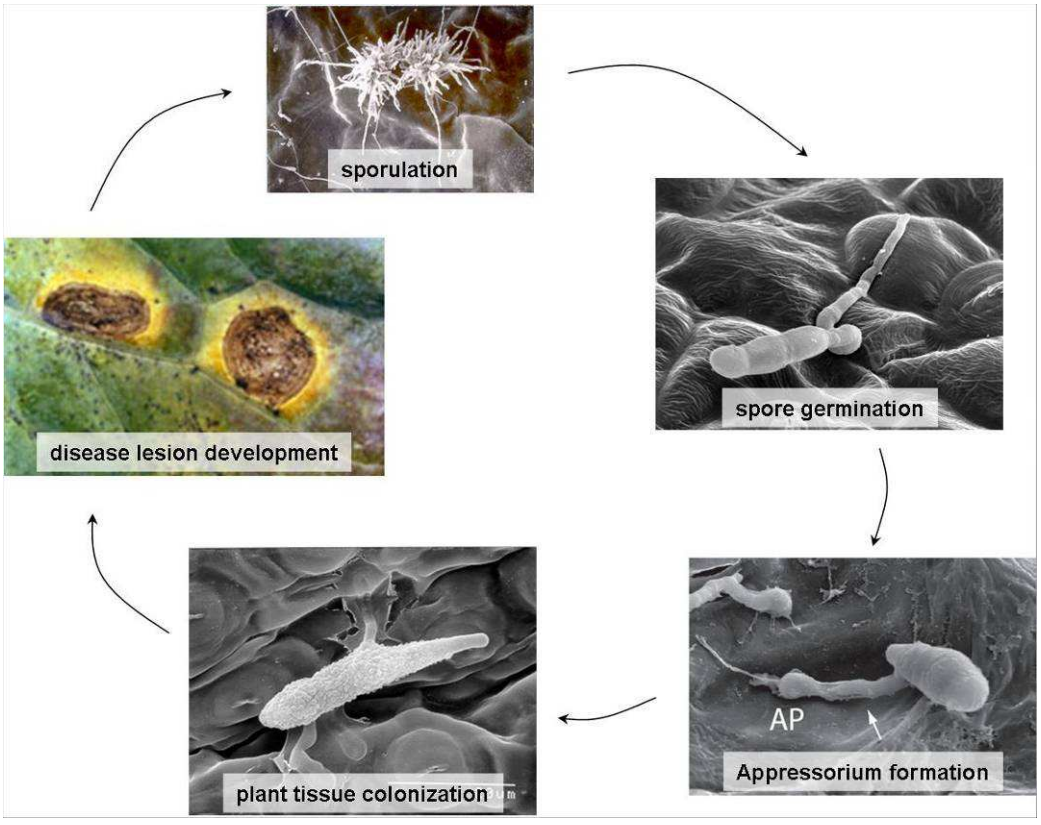


**Figure 1. *Alternaria brassicicola* disease cycle.**

*A. brassicicola* infection begins when fungal conidia, under favorable environmental conditions, produce one or more germ tubes on the plant surface (Fig. 1). Following germination, this fungus invades host tissues by developing a series of specialized infection structures including appressoria and necrotrophic penetration and infection hyphae (Fig.1). These specialized cells mediate the initial direct penetration of host epidermal cells by breaching the plant cuticle and cell wall layers, probably through a combination of localized secretion of a variety of fungal enzymes, which include fungal cutinases, lipases, galacturonidases, and endoglucanases (Berto et al., 1999; Isshiki et al., 2001; Thomma, 2003; Yao and Köller, 1995). Previous studies have shown that successful penetration of host epidermal cells by *A. brassicicola* may depend on the production of small phytotoxic metabolites that selectively or non-selectively damage host plants (MacKinnon et al., 1999; Oka et al., 2005; Pattanamahakul and Strange, 1999). In addition to toxins, it has been reported that *A. brassicicola* produces a number of other interesting metabolites, such as the histone deacetylase (HDAC) inhibitor depudecin (Kim et al., 2009; Matsumoto et al., 1992), an antibiotic complex termed brassicicolin A which shows a host-specific toxicity to *B. napus* (Gloer et al., 1988; Pedras et al., 2009), non-toxic polyketide compounds phomapyrone and infectopyrone (Pedras et al., 2009), and a nonribosomally-synthesized peptide related to conidial cell wall integrity (Kim *et al.*, 2007). Thus, some progress has been made in identifying gene functions necessary for the initial establishment of the fungus on the host. However, genetic processes and disease determinants governing specific molecular interactions between the necrotrophic fungus and the host plant, such as infection structure development, toxic metabolite

and enzyme production, and detoxification mechanism, need to be better understood. This understanding may open new strategies for broad-spectrum crop disease intervention against necrotrophic pathogens.

*A. brassicicola* is typically seed transmitted, though transmission by insects has also been reported (Dillard et al., 1998). Between 1976 and 1978 in the United Kingdom, 86% of the commercial Brassica seeds produced were contaminated with *A. brassicicola* (Maude and Humpherson-Jones, 1980). The primary disease consistently affecting the cabbage seed industry in the U.S. is also *Alternaria* leaf spot, caused by *A. brassicicola* and the related species *A. brassicae*. Infection decreases seed yield, quality, and germination rates. Seed lots may be rejected if germination drops below 85 to 90% and infected seed lots must be treated accordingly, increasing costs associated with seed production. Spread of the disease during the growing season is typically by rain and wind that dislodge spores. Optimal conditions for sporulation and infection include a minimum wet period of 13 hours and ambient temperatures of 20-30ºC (Humpherson-Jones and Phelps, 1989; Rotem, 1994). Consequently, black spot disease has been of particular importance in regions of the world with cool, wet weather during the growing season, such as in the United Kingdom, Thailand, and the northeastern United States (Pattanamahakul and Strange, 1999). High-levels of resistance/immunity to this fungus have been reported in weedy cruciferous plants such as *Arabidopsis thaliana* and *Capsella bursa-pastoris*, but no satisfactory source of resistance has been identified among cultivated *Brassica* species 6(Conn et al., 1988; Sigareva and Earle, 1999; Westman et al., 1999). Of the very few *Brassica*

species or breeding lines that have been reported to possess some level of resistance, the genetic basis appears to involve additive and dominant gene action (King, 1994). Importantly, necrotrophs are traditionally hard to control with host resistance, which is usually quantitative in nature.

**The *Alternaria brassicicola* genome sequencing project**

In 2004, the USDA Microbial genome sequencing program funded random shotgun sequencing of the *A. brassicicola* genome (isolate ATCC 96836). The 6.4 x shotgun sequencing, BAC and fosmid end sequencing, physical map construction, and MPSS experiments were completed at Washington University Genome Center (St. Louis, USA) and Solexa Inc., Hayward, USA. A genome assembly was generated and the assembly is composed of 838 supercontigs averaging 36,147 bp in length and having an N50 value of 2,400,717 bp (the length such that 50% of all nucleotides contained in supercontigs are of at least this size). The supercontigs are composed of 4,039 contigs with 84% of the contigs longer than 1000 bp and 98.8% of the bases having a phred quality above 20. The total length of the sequenced portion is ~31 Mb, consistent with the previous estimate of 29.6 Mb for genome size using pulse-field gel electrophoresis. Approximately 80% of the assembled genome (25 Mb) is distributed on 12 supercontigs suggesting a relatively robust assembly for only 6 x coverage. For the prediction of genes in the genome assembly, version 2.4 of the FGENESH software (http://www.softberry.com) was used with an *Alternaria* trained parameter matrix. A total of 10,688 genes were predicted when using the contig sequences as input, or 9,814 using the supercontigs. Similar values were obtained when using other

gene prediction programs such as SNAP. Mega BLAST was used to map a set of 6,430 ESTs (from fungus grown *in vitro* and plant infection libraries) to support the *A. brassicicola* gene prediction and included BLASTX results from similarity searches against the Uniprot protein database and against other related gene models from taxonomically-related fungi. Results of MPSS of a mRNA library derived from late stage *Alternaria* infected cabbage leaves have provided additional experimental evidence of transcription for a subset of the gene models (~4,500). HMMER analysis of predicted proteins based on gene models has been performed utilizing protein functional domain databases individually (Pfam, Tigrfam, Superfam) and part of the InterPro suite of tools (http://www.ebi.ac.uk/interpro/). Collectively, all genome sequences and annotation data are currently available to the public in our *A. brassicicola* genome website (http://alternaria.vbi.vt.edu/lannot/index.shtml).

## Fungal secondary metabolites

Filamentous fungi synthesize a wide variety of secondary metabolites, collectively referred to as natural products. These are generally low molecular weight molecules that are traditionally thought to not be required for growth or development of the producing organism under laboratory conditions, but are thought to aid the fungus in competing successfully with other organisms in its natural habitat. Accordingly, many secondary metabolites tend to be compounds that have toxic or inhibitory effects on other organisms. Because of these bioactive properties, many fungal secondary metabolites have been adopted by humans for use as

pharmaceuticals such as antibiotics, cholesterol-lowering agents, tumor inhibitors, and immunosuppressants for transplant operations. Other natural products of fungi have negative impacts on society, including phyto- and mycotoxins produced by plant pathogenic fungi and enhancers of virulence in fungal pathogens of humans and other animals. Because of the impact of these compounds, fungal secondary metabolites have received considerable attention from the scientific community.

Alexander Flemming discovered the antibiotic substance penicillin from the fungus *Penicillium notatum* in 1928, for which he shared the Nobel Prize in Physiology or Medicine in 1945 with Howard Walter Florey and Ernst Boris Chain. This discovery led to the development of a fungal secondary metabolite, a nonribosoomal peptide-based chemical, as a drug and marked the beginning of the modern antibiotic era. Since then more than 100,000 secondary metabolites of low molecular weight (less than 2,500 Da) have been isolated from various plant and microbial species (Demain, 1986). The classes of chemical compounds isolated to date include terpenes (also known as isoprenoids), alkaloids, nonribosomal peptides, polyketides, and shikimate metabolites, and their pharmaceutical activities are wide-ranging (Stadler and Keller, 2008). Biosynthetic pathways of these natural products starting from small precursor molecules derived from primary metabolism have been characterized in many fungal organisms. With the advent of recombinant DNA technology the biosynthesis of the metabolites can now be studied on a genetic level, and this led to the isolation of numerous genes associated with secondary metabolite production, some of which will be discussed here.

## Polyketides

Polyketides (derived from polyketone) form the largest family of structurally diverse secondary metabolites synthesized in both prokaryotic and eukaryotic organisms and have been most extensively examined in bacteria and fungi. In fungi, polyketides include a range of compounds such as the mycotoxins aurofusarin (Morishita et al., 1968), aflatoxin (Bhatnagar et al., 2003), and zearalenone (Gora et al., 2004) and spore pigments (Fujii et al., 2001; Mayorga and Timberlake, 1992). Many functions have been proposed for polyketides (Weinberg, 1971). However, the most plausible explanation for the diversity of secondary metabolites is that the ability to produce a wide variety of compounds is ecologically and evolutionarily advantageous as a resource for bioactive compounds (Challis and Hopwood, 2003; Firn and Jones, 2000). For example, several actinomycetes synthesize two chemically unrelated antimicrobial metabolites that act against the same target organism (Challis and Hopwood, 2003; Demain, 1986). Thus, unrelated compounds may be selected for possessing similar activities when important to organism survival.

### *Biosynthesis of polyketides*

The biosynthesis of polyketides has been studied in depth. It is clear that polyketides, independent of their structural diversity, have a common biosynthetic origin. Polyketides are derived from highly functionalized carbon chains, whose assembly mechanism bears close resemblance to the fatty acid synthetic pathway (O'Hagan, 1991). The assembly process is controlled by multifunctional enzyme complexes called polyketide synthases or PKSs.

Common to all fungal polyketides is their biosynthetic origin. They are produced by repetitive Claisen condensations of an acyl-coenzyme A (CoA) starter molecule with malonyl-CoA elongation units to form a chain of $C_2$ units with alternating ketones in a fashion reminiscent of fatty acid biosynthesis and the resulting chain can be either linear or aromatic. The functions of PKS domains are summarized in Table 1. The minimal PKSs consist of three domains: a β-ketoacyl synthase (KS)

**Table 1. Functions of PKS domains.**

| Domain | Function |
|---|---|
| β-ketoacyl synthase (KS) | forms a new carbon-carbon bond by Claison condensation via 3 steps: acyl transfer, decarboxylation, condensation |
| Acyl transferase (AT) | substrate recruitment and loading: AT primes the ACP with acetyl or propionyl moiety and extends the chain with malonyl or methylmalonyl moieties (in a chain-extending module) |
| Acyl carrier protein (ACP) | handling of the acyl chain to the KS active site |
| Dehydratase (DH) | reductive domain (β-keto processing reactions): hydroxyl to enoyl group; belongs to non-metal dehydratases |
| Methyltransferase (ME) | Methylation |
| Ketoreductase (KR) | reductive domain (β-keto processing reactions): keto to hydroxyl group; belongs to short-chain dehydrogenase family, |
| Enoylreductase (ER) | reductive domain (β-keto processing reactions): enoyl to alkyl group; belongs to medium chain dehydrogenase family |

domain, an acyl transferase (AT) domain, and an acyl carrier protein (ACP) domain. Such an enzyme is said to be nonreducing and the resulting polyketide is aromatic with unmodified ketone groups. In addition to the three requisite domains, PKSs may also have ß-ketoreductase (KR) and dehydratase (DH) and, occasionally, enoyl reductase (ER) domains to reduce the ketone groups to various extents (Fujii et al., 2001; O'Hagan, 1991). The resulting enzymes typically produce linear polyketide compounds. Reducing PKSs often also have a methyltransferase (ME) domain. Variability in the type, number, and activity of these domains after each condensation cycle contributes further to diversity of the metabolites generated by fungal PKSs. During polyketide biosynthesis a starter acyl unit, acetate, is transferred from CoA onto the active site thiol of the KS (Fig. 2). A thiolester linkage is also formed between a malonate extender unit from CoA and the pantetheine thiol of the holo form of the ACP. These loading reactions are generally catalyzed by specific AT enzymes. The KS catalyzes the decarboxylative Claisen condensation between the acyl and malonyl units to generate acetoacetyl ACP. This process is repeated several times. Each condensation is followed by a cycle of modifying reactions that involves the enzymes KR, DH, ER, and ME in the subsequent reduction steps.

At this stage, a major difference between fatty acid and polyketide biosynthesis becomes apparent. Fatty acid synthases catalyze the full reduction of each β-keto moiety prior to further chain extension in every cycle. Polyketide biosynthesis, however, shows a higher degree of complexity as the reduction steps following condensation can be fully, or partially, omitted, giving highly functionalized chains, as

already mentioned above. The assembled polyketide chain can also undergo further modifications such as cyclization, reduction or oxidation, alkylation, and arrangement after release from the polyketide synthase.

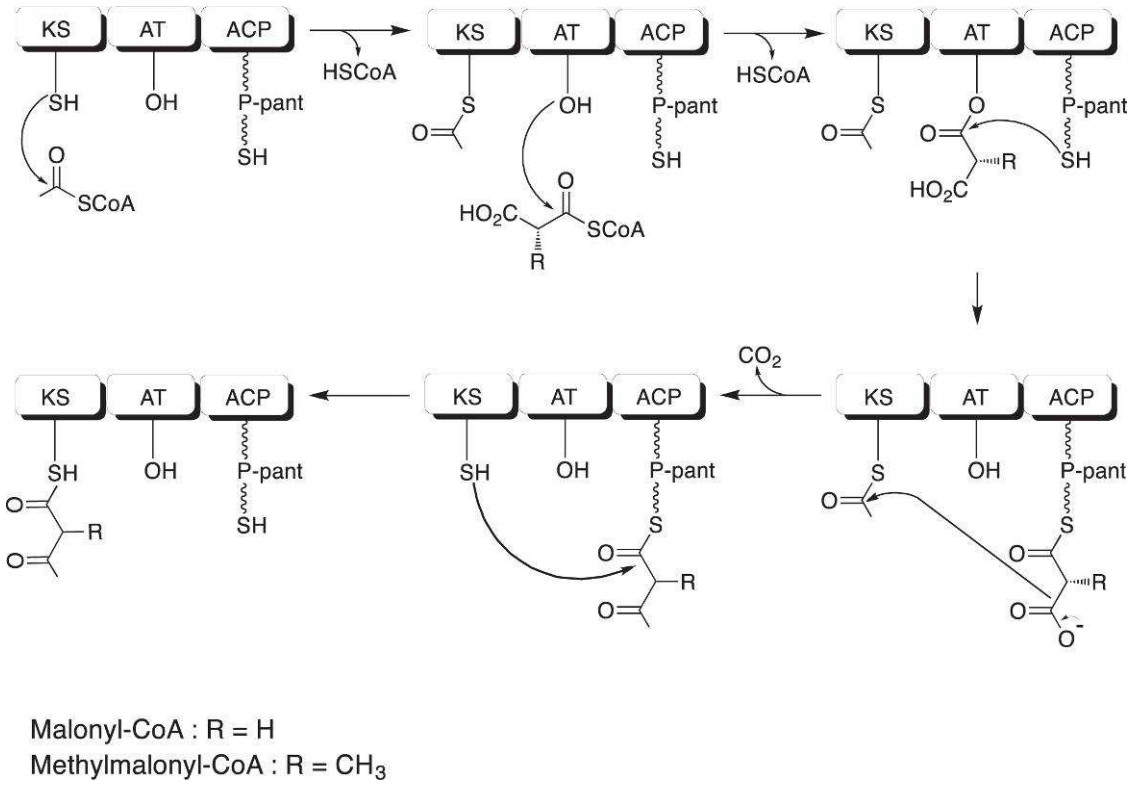


**Figure 2. Polyketide synthesis by a polyketide synthase.** Acetate (the starter unit) is first loaded from the coenzyme A (CoA) to a cysteine residue in the active site of a ketoacyl synthase (KS) domain. Malonate (the extender unit) is then transferred by an acyltransferase (AT) domain from malonyl-CoA to an acyl carrier protein (ACP)-bound 4'-phosphopantetheine residue. Carbon nucleophile formed by decarboxylation of the malonate loaded on ACP then attacks the carbonyl carbon of the starter acyl residue on the KS to form the nascent β-ketoacyl chain on the ACP, which is then loaded to a cysteine residue on the KS.

***Iterative Type I fungal PKS***

The two main categories of PKS are referred to as Type I and Type II (Hardie et al., 1986). Type I is characteristic of fungi and vertebrates and consists of only a large multifunctional enzyme which contains all the necessary enzymatic activity embedded in its catalytic domains. Type II, found in bacteria, carries out all the main chemical transformations using discrete mono-functional enzymes. If the same active sites are used more than once, then the synthase is described as iterative (Hopwood, 1997). To date, a general theme has been observed that fungal PKSs are generally iterative Type I enzymes. Some fungal PKSs and their products are well characterized. These include PKSs involved in biosynthesis of conidial pigment and melanin, fungal polyketide mycotoxins, lovastatin which is a cholesterol lowering drug naturally produced by *Aspergillus terreus* (references, see below).

Fungal spore pigmentation contributes both to the survival and pathogenicity of fungal propagules in the environment. The green pigment contained in the asexual spores of the ascomycetous fungus *Aspergillus nidulans* protects them from damage caused by ultraviolet radiation. The *wA* gene product had been shown to be responsible for the production of a yellow intermediate of this pigment (Mayorga and Timberlake, 1990), and in 1992 it was shown that the *wA* gene coded for an iterative Type I PKS (Mayorga and Timberlake, 1992). *Colletotrichum lagenarium pks1* has previously been cloned from a cosmid library by complementation of a melanin-deficient mutant. *C. lagenarium*, a plant pathogenic fungus, requires melanin to retain its infectious ability (Vidal-Cros et al., 1994). However, in *A. alternata* it was shown

that melanin was not a virulence factor (Tanabe et al., 1995). Aflatoxin and sterigmatocystin are potent, polyketide-derived, carcinogenic mycotoxins produced by fungi of the genus *Aspergillus* and constitute a major agricultural problem (Hartley et al., 1963). Race T of the fungal pathogen *Cochliobolus heterostrophus* produces T-toxin, a polyketide derived virulence factor responsible for the high virulence of *C. hetorostrophus* towards Texas male sterile (T) maize (Yang et al., 1996). Fumonisin, a mycotoxin frequently contaminating maize, is produced by a number of fungi within the *Gibberella fujikuroi* group of crop pathogens (Proctor et al., 1999). The gene encoding the PKS responsible for the production of the highly reduced polyketide backbone of fumonisin has been isolated from a genomic library. *Alternaria solani* is a causal fungus of early blight disease of potato and tomato. Two kinds of phytotoxins, alternaric acid (Brian et al., 1949) and solanapyrones (Ichihara et al., 1983), were isolated from the different strains of the fungus. Feeding experiments for these reduced complex-type compounds showed the polyketide origin of both compounds (Oikawa et al., 1998).

## Nonribosomal peptides

One of the largest and most important groups of microbial secondary metabolites comprises peptides that are synthesized by enzymes instead of ribosomes. Of the thousands of known nonribosomal peptides (NRPs), many are cyclic, but others are linear or a mixture of cyclic and linear. NRPs represent a large subclass of bioactive natural products (Sieber and Marahiel, 2005). Remarkably diverse biological

activities of NRPs have been elucidated over the past decades as a result of extensive searches for and characterizations of the NRPs. Most work, however, has been focused on metabolites with antibiotic/immunosuppressive activities, due to their medical and industrial value. Surprisingly little is known about biological function of NRPs in producing organisms. It is noteworthy that benefits of NRPs to their producers remain unclear in most cases (Finking and Marahiel, 2004). Some proposed activities include roles as signal molecules for coordination of growth and differentiation (Horinouchi and Beppu, 1990; Marahiel et al., 1997; Schaeffer, 1969), as aids in the breakdown of cellular metabolic products (Davies, 1990), as defense compounds that kill competing microorganisms (Vining, 1990), as siderophores to assist in iron uptake (Challis (Challis et al., 2000), and as virulence effectors (Haese et al., 1993; Johnson et al., 2000).

Penicillin and derivatives thereof, one of the earliest discovered and still one of the most widely used antibiotics, is an example of a NRP with antibacterial and antifungal activities. Such antibiotics as tyrocidine, fengycin and vancomycin are also NRPs. Cyclosporin, another example of a NRP, has immunosuppressive properties and remains the most widely used agent for post-transplant immunosuppression (Ducan and Craddock, 2006). Biosurfactants, such as surfactin and arthrofactin, are examples of NRPs with surface tension lowering activity (Mulligan, 2005; Roongsawang et al., 2003). In addition to its surfactant property, antiviral and antimycoplasmic activities of surfactin have been reported (Vollenbroich et al., 1997). Most bacteria and fungi produce small molecules with strong iron-chelating activity

under iron-depleted conditions. These microbial metabolites are collectively called siderophores, many of which are NRPs, and play key roles in iron metabolism of producing organisms. The following sections describe a biosynthetic mechanism of NRPs by nonribosomal peptide synthetase (NPS) enzymes.

***Biosynthesis of nonribosomal peptides***

NPSs are large, multifunctional enzymes typically comprised of numerous semiautonomous catalytic domains in a linear series. The domains are arranged in a predictable distance from each other and in a characteristic sequence that reflects the order of their activity in the assembly and tailoring of the peptide or peptide-containing product. The functions of NPS domains are summarized in Table 2.

In NPSs, the adenylation domain (A-domain) is responsible for selection and activation of the substrate (Fig. 3A). The A-domain recognizes and activates a cognate amino or carboxy acid substrate as an amino acyl adenylate, consuming ATP (May et al., 2002; Stachelhaus and Marahiel, 1995). The A-domain is the primary determinant of substrate specificity in the nonribosomal peptide synthesis system, although the condensation domain also shows specificity to some extent (see below) (Lautru and Challis, 2004). Determination of crystal structure of the phenylalanine-activating A-domain of gramicidin S synthetase A (PheA) from Bacillus brevis (Conti et al., 1997) facilitated the search for the key residues defining substrate specificity of the A-domain, leading to identification of a L- phenylalanine-binding pocket and the residues making contact with phenylalanine (Lautru and Challis, 2004). Sequence alignment of different A-domains revealed that the residues corresponding to the ten

residues in direct contact with L- phenylalanine in PheA are conserved among A-domains with the same substrate specificity (Challis et al., 2000; Stachelhaus et al., 1999). These ten residues were called the “nonribosomal code”. However, the nonribosomal code was deduced from analyses of A-domains of bacterial NPS. Compared to bacterial NPSs, available sequence and corresponding structural/functional data on fungal NPSs are limited and thus a nonribosomal code specific for fungal NPSs has not been established yet. Furthermore, it is not clear if the bacterial code is applicable to fungal NPS proteins (Walton et al., 2004). In conclusion, our current knowledge on mechanisms of substrate selection by A-domain is still under development and further determination of A-domain structures will be required to refine the nonribosomal code (Lautru and Challis, 2004).

**Table 2. Functions of NPS domains.**

| **Domain** | **Function** |
|---|---|
| Adenylation (A) | selection of substrates<br>activation of substrates |
| Thiolation (T) | carrier of activated substrates |
| Condensation (C) | formation of peptide bond<br>selection of substrates<br>peptide release* |
| Epimerization (E) | epimerization of a L-amino acid to a D-amino acid |
| *N*-methylation (M) | methylation of substrates |
| Thioesterase (TE) | peptide release |
| Reductase (R) | peptide release |

* This function of the condensation domain is restricted to those located at the C-terminal end of the NPS.

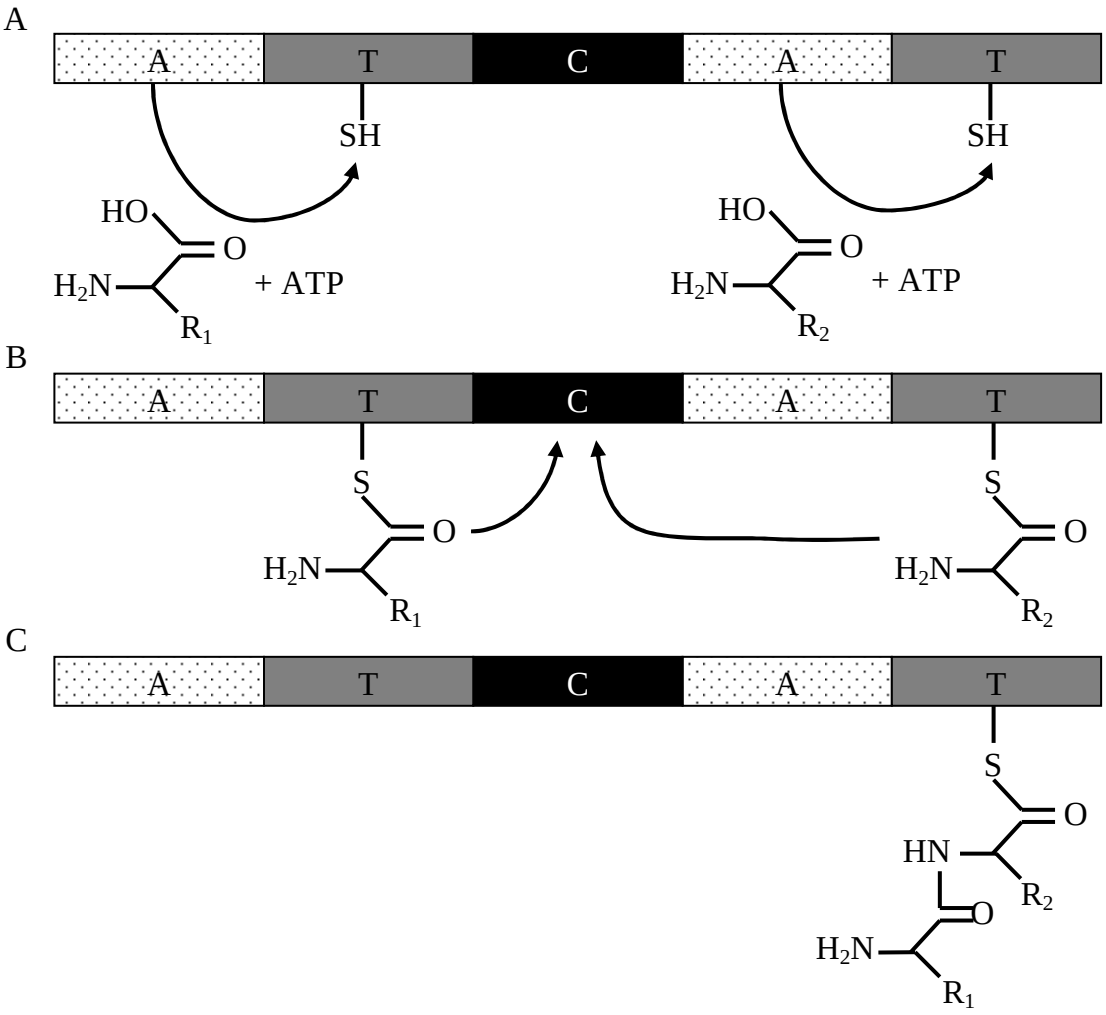


**Figure 3. Peptide synthesis by a nonribosomal peptide synthetase.** **A.** The adenylation domain (A) recognizes and activates the substrate consuming ATP. **B.** The thiolation domain (T) is the scaffold for the activated substrates. **C.** The condensation domain (C) assists in formation of a peptide bond between activated substrates on adjacent T domains.

In ribosomal machinery, tRNA is the carrier of activated substrates. A peptidyl carrier protein or thiolation domain (T-domain) of NPS is the counterpart of tRNA (Fig. 3B) (Finking and Marahiel, 2004). The T-domain requires a cofactor, 4'-

phosphopantetheine (4'PP), for its function. 4'PP is transferred from coenzyme A to the hydroxyl group of a conserved serine residue in the T-domain, posttranslationally by 4'-phosphopantetheinyl transferase (PPTase)**.**

The condensation domain (C-domain) is responsible for peptide bond formation between two amino acyl substrates bound to two adjacent T-domains (Fig.3C) (Bergendahl et al., 2002; Stachelhaus et al., 1998). The C-domain catalyzes a reaction between an amino/imino/hydroxyl group of one activated substrate and an acyl group of the other activated substrate. According to the multiple carrier model of nonribosomal peptide synthesis (Stein et al., 1996), the C-domain has an acceptor and a donor site to accommodate the two activated substrates (Finking and Marahiel, 2004). An activated substrate bound to the T-domain upstream of the C-domain comes into the donor site and an activated substrate bound to the downstream T-domain enters the acceptor site. Nucleophilic attack of an acyl group of the substrate in the donor site by an amino/imino/hydroxyl group of the substrate in the acceptor site results in peptide bond formation between the two substrates. As noted, the C-domain plays a role in determination of substrate specificity, in addition to peptide bond formation. The acceptor sites of C-domains show strong stereoselectivity (L- or D-amino acid) (Benshaw et al., 1999; Ehmann et al., 2000; Linne and Marahiel, 2000) and some selectivity to the side chains of the aminoacyl thioester (Ehmann et al., 2000). In contrast, no significant substrate specificity has been described for donor sites of C-domains (Benshaw et al., 1999; Linne et al., 2003; Marshall et al., 2001).

Such substrate selectivity of acceptor site may explain how directionality of peptide synthesis is regulated (Lautru and Challis, 2004; Linne and Marahiel, 2000).

While a combination of A-, T- and C-domains is responsible for incorporation of substrates and elongation of peptide chains, there may be additional domains that play a role in modification of substrates. For example, an epimerization domain produces a D-amino acid by epimerization of a L-amino acid (Pfeifer et al., 1995) and a *N*-methylation domain catalyzes transfer of a S-methyl group from a S-adenosylmethionine to an α-amino group of an amino acid substrate. These tailoring domains contribute to structural diversity of NPS metabolites.

In addition to those for initiation, modification and elongation, nonribosomal peptide synthesis requires specific domains for termination and release of peptide chains (Table 3). This final step of nonribosomal peptide synthesis is, at least in bacteria, most commonly carried out by thioesterase domains (TE-domain), variants of serine hydrolases (Keating et al., 2001). An active-site serine of the TE-domain accepts a mature peptide chain from an adjacent T-domain, forming a covalent acyl-O-TE-domain intermediate. Subsequent hydrolysis of the intermediate releases a peptide chain as a linear or a cyclic peptide (Pazirandeh et al., 1991; Schneider and Marahiel, 1998). In fungi, this type of peptide release has been reported in biosynthesis of δ-(L-α-aminoadipyl)-L-cysteinyl-D-valine (ACV), the precursor of β-lactam antibiotics, by the ACV synthetase of *Aspergillus nidulans* (Kallow et al., 2000).

There are several examples of nonribosomal peptide synthesis where the TE-domain is absent and replaced by a C-domain variant or a reductase domain (Keating et al., 2001). An example of the former is observed in the NPS (SimA) responsible for biosynthesis of cyclosporin in the fungus *Tolypocladium niveum* (Keating et al., 2001; Weber et al., 1994). The C-domain, which is assumed to function as an amide synthase in this reaction, catalyzes head to tail condensation of a peptide chain, coupling an amino group of the first amino acid of the chain to a carbonyl group of the last amino acid of the chain, to produce a cyclic amide product (Keating et al., 2001). Based on domain organization of the NPSs (i.e. a C-terminal extra C-domain), Konz and Marahiel (1999) predicted that peptide release by head to tail condensation is also operational in biosynthesis of enniatin (Haese et al., 1993) and HC-toxin (Scott-Craig et al., 1992), both of which are phytotoxins produced by filamentous fungi. In the second type of peptide release without the TE-domain, the reductase domain releases a mature peptide chain as an aldehyde through NAD(P)H-coupled reduction of a thioester bond (Keating et al., 2001). This type of peptide release is observed in biosynthesis of the essential amino acid lysine by Lys2p in *S. cerevisiae* (Keating et al., 2001). Although not functionally characterized, reductase-like domains were identified in some fungal NPSs [*e.g.* the NPS of *A. nidulans* (EAA59538) and the NPS of *Gibberella zeae* (EAA75314)] in the database (von Dohren, 2004). Peptaibiols are linear peptides of fungal origin, and are characterized by the presence of an unusual amino acid, α-aminobutyric acid, and a C-terminal α-aminoalcohol group (Reiber et al., 2003). Reduced C-terminals of peptaibols indicate that peptide release by the reductase domain is operational in biosynthesis of peptaibols.

**Table 3. Peptide release in nonribosomal peptide synthesis**

| Domain | Activity | Example | Reference |
|---|---|---|---|
| Thioesterase domain | hydrolysis of a peptide chain | ACV synthesis by *Aspergillus nidulans* | (Kallow et al., 2000) |
| Condensation domain | head to tail condensation of a peptide chain | cyclosporin synthesis by *Tolypocladium niveum* | (Weber et al., 1994) |
| Reductase domain | reduction of a thioester bond | lysine synthesis by *Saccharomyces cerevisiae* | (Ehmann et al., 2000) |

***Modular Organization of NPSs***

A module is defined as the unit responsible for incorporation of a single substrate into a growing peptide chain (Finking and Marahiel, 2004). C-, A- and T-domains are minimal components of a single elongation module, with the exception of the first module (initiation module) that consists of only A- and T-domains (Finking and Marahiel, 2004). Some NPSs (*i.e.* monomodular NPSs) carry only a single module, while others (*i.e.* multimodular NPSs) consist of multiple modules arrangement. At first glance, it seems straightforward to predict structure of any NPS metabolite based on module organization of the corresponding NPS. For example, surfactin synthetases Srf A, B and C have seven modules in total, and biosynthesize the cyclic lipoheptapeptide surfactin (Finking and Marahiel, 2004; Peypoux et al., 1999). Cyclosporin, which consists of eleven substrates, is biosynthesized by the NPS SimA carrying eleven modules in the filamentous fungus *Tolypocladium niveum* (Weber and Leitner, 1994). However, there are examples for which the simple assumption that the number of modules of a NPS corresponds to the number of

substrates in a NPS metabolite does not apply. Gramicidin S, which consists of ten amino acids, is biosynthesized by the gramicidin S synthetases GrsA and B carrying a total of five modules (Kratzschmar et al., 1989; Turgay et al., 1992). The apparent discrepancy between the structure of Gramicidin S and the module organization of GrsA and B is explained by iterative use of the GrsA and B templates. In the first round, GrsA and B synthesize a pentapeptide which is maintained on the C-terminal TE-domain. In the second round, GrsA and B again synthesize a pentapeptide and the two pentapeptides are combined by a TE-domain, yielding a homodimeric product (Finking and Marahiel, 2004). The iterative use of a NPS template is also observed in biosynthesis of enniatin by the enniatin synthetase (Esyn) isolated from *Fusarium scirpi* (Glinski et al., 2002). Taken together, it is not necessarily simple to predict structure of a NPS metabolite based on module arrangement of a NPS protein, which points out the importance of biochemical characterization of NPS enzymes and their products. Flexibility of modular organizations of NPSs may partly account for structural diversity of NPS metabolites.

## Overview of research

The fungus, *A. brassicicola* is an economically important pathogen of Brassicas. Moreover this fungus is a premier representative of a devastating class of fungal plant pathogens, the necrotrophs. Annotation of the complete sequence of the *A. brassicicola* genome has led to a deeper understanding of the biology of this important plant pathogen; we have identified numerous gene clusters we predicted to be

involved in the production of novel metabolites, documented the expansion of specific gene families that may contribute to virulence, and mapped the position of genes known to be involved in virulence in other fungal pathogens (Lawrence et al., unpublished). However, our understanding of virulence remains limited. As an initial step elucidating the underpinnings of *A. brassicicola* necrotrophic pathogenesis, we've chosen representative secondary metabolite-producing genes, nonribosomal peptide synthetases (*NPS*) and polyketide synthases (*PKS*) to functionally characterize their roles in fungal biology and virulence.

**In Chapter II**, functional analysis of all *NPS* genes and *PKS* genes in *A. brassicicola* was conducted using a linear minimal element (LME) construct approach that was developed as an *A. brassicicola* targeted gene disruption method. The LME constructs were used to functionally disrupt all *NPS* and *PKS* genes, resulting in more than 95 % of targeted gene disruption efficiency. Phenotypic analyses of each *NPS* and *PKS* gene disruption mutant revealed in some cases interesting developmental changes and/or reduced virulence.

**In Chapter III**, the function of *AbNPS2*, one of the *A. brassicicola NPS* genes associated with conidial cell wall construction was investigated. Gene expression and mutation analyses showed that *AbNPS2* plays an important role in conidial development and virulence although the reduction in virulence was due primarily to low viability of conidia.

**In Chapter IV**, biosynthesis and role in virulence of the histone deacetylase inhibitor depudecin from *A. brassicicola* were investigated. We demonstrated that *AbPKS9,* one of the *A. brassicicola PKS* genes, and six genes defining a biosynthetic gene cluster were responsible for the depudecin biosynthesis and created depudecin-minus mutants to test the role of depudecin in virulence.

**In Chapter V**, the function of a *NPS*-like gene, *tmpL* in fungal development and virulence was investigated. TmpL is a novel transmembrane protein necessary for regulation of intracellular ROS levels, tolerance to external ROS, and required for infection of plants by the necrotroph, *A. brassicicola* and mammals by the human pathogen, *Aspergillus fumigatus*. This chapter demonstrated that the regulation of intracellular levels of reactive oxygen species (ROS) is critical for fungal differentiation and virulence.

Finally, a summary and conclusions of the research presented in this dissertation are provided **in Chapter VI**.

# Literature Cited


Agrios, G.N. (1997) Plant Pathology. San Diego, CA: Academic Press, pp.300-333.

Akamatsu, H., Itoh, Y., Kodama, M., Otani, H., and Kohmoto, K. (1997) AAL-toxin-deficient mutants of Alternaria alternata tomato pathotype by restriction enzyme mediated integration. Phytopathology, 87, 967-972.

Benshaw, P.J., Walsh, C.T., and Stachelhaus, T. (1999) Aminoacyl-CoAs as probes of condensation domain selectivity in nonribosomal peptide synthesis. Science, 284, 486-489.

Bergendahl, V., Linne, U., and Marahiel, M.A. (2002) Mutational analysis of the C-domain in nonribosomal peptide synthesis. Eur J Biochem, 269(2), 620-629.

Berto, P., Commenil, P., Belingheri, L., and Dehorter, B. (1999) Occurrence of a lipase in spores of *Alternaria brassicicola* with a crucial role in the infection of cauliflower leaves. FEMS Microbiol Lett., 180(2), 183-189.

Bhatnagar, D., Ehrlich, K.C., and Cleveland, T.E. (2003) Molecular genetic analysis and regulation of aflatoxin biosynthesis. Appl Microbiol Biotechnol, 61(2), 83-93.

Braverman, Y. (1979) Experiments on direct and secondary poisoning by fluoroacetamide (1081) in wildlife and domestic carnivores. J Wildl Dis, 15(2), 319-325.

Brian, P.W., Curtis, P.J., Hemming, H.G., Unwin, C.H., and Wright, J.M. (1949) Alternaric acid, a biologically active metabolic product of the fungus Alternaria solani. Nature, 164, 534.

Challis, G.L., and Hopwood, D.A. (2003) Synergy and contingency as driving forces for the evolution of multiple secondary metabolite production by Streptomyces species. Proc. Natl. Acad. Sci. USA, 100, 14555-14561.

Challis, G.L., Ravel, J., and Townsend, C.A. (2000) Predictive, structure-based model of amino acid recognition by nonribosomal peptide synthetase adenylation domains. Chem Biol, 7(3), 211-224.

Conn, K.L., Tewari, J.P., and Dahiya, J.S. (1988) Resistance to alternaria brassicae and phytoalexin-elicitation in rapeseed and other crucifers. Plant Sci., 56, 21-25.

Conti, E., Stachelhaus, T., Marahiel, M.A., and Brick, P. (1997) Structural basis for the activation of phenylalanine in the non-ribosomal biosynthesis of gramicidin S. EMBO J, 16(14), 4174-4183.

Davies, J. (1990) What are antibiotics - archaic functions for modern activities. Molecular Microbiology, 4, 1227-1232.

Demain, A.L. (1986) Regulation of secondary metabolism in fungi. Pure Appl. Chem., 58, 219-226.

Dillard, H.R., Cobb, A.C., and Lamboy, J.S. (1998) Transmission of Alternaria brassicicola to cabbage by flea beetles (Phyllotreta cruciferae). Plant disease, 82, 153-157.

Ducan, N., and Craddock, C. (2006) Optimizing the use of cyclosporine in allogeneic stem cell transplantation. Bone Marrow Transplantation, 38, 169-174.

Ehmann, D.E., Trauger, J.W., Stachelhaus, T., and Walsh, C.T. (2000) Aminoacyl-SNACs as small-molecule substrates for the condensation domains of nonribosomal peptide synthetases. Chem. Biol., 7, 765-772.
Finking, R., and Marahiel, M.A. (2004) Biosynthesis of nonribosomal peptides. Annual Review of Micorobiology, 58, 453-488.
Firn, R.D., and Jones, C.G. (2000) The evolution of secondary metabolism - a unifying model. Mol Microbiol, 37(5), 989-994.
Fujii, I., Watanabe, A., Sankawa, U., and Ebizuka, Y. (2001) Identification of Claisen cyclase domain in fungal polyketide synthase WA, a naphthopyrone synthase of Aspergillus nidulans. Chem Biol, 8(2), 189-197.
Gilchrist, D.G. (1998) Programmed cell death in plant disease: the purpose and promise of cellular suicide. Annu Rev Phytopathol, 36, 393-414.
Glinski, M., Urbanke, C., Hornbogen, T., and Zocher, R. (2002) Enniatin synthetase is a monomer with extended structure: evidence for an intramolecular reaction mechanism. Archives of Microbiology, 178, 267-273.
Gloer, J.B., Poch, G.K., Short, D.M., and McCloskey, D.V. (1988) Structure of brassicicolin A: a novel isocyanide antibiotic from the phylloplane fungus Alternaria brassicicola. J. Org. Chem., 53(16), 3758-3761.
Gora, M., Luczynski, M.K., Smoczynski, L., Obremski, K., Polak, M., Swist, M., Zielonka, L., and Gajecki, M. (2004) Modification of zearalenone structure in model and natural conditions. Pol J Vet Sci, 7(3), 181-185.
Haese, A., Schubert, M., Herrmann, M., and Zocher, R. (1993) Molecular characterization of the enniatin synthetase gene encoding a multifunctional enzyme catalysing N-methyldepsipeptide formation in Fusarium scirpi. Mol Microbiol, 7(6), 905-914.
Hardie, D.G., McCarthy, A.D., and Braddock, M. (1986) Mammalian fatty acid synthase: a chimeric protein which has evolved by gene fusion. Biochem Soc Trans, 14(3), 568-570.
Hartley, R.D., Nesbitt, B.F., and O'Kelly, J. (1963) Toxic metabolites of Aspergillus flavus. Nature, 198, 1056-1058.
Hodgkin, T., and Macdonald, M.V. (1986) The effect of a phytotoxin from Alternaria brassicicola on Brassica pollen. New Phytol., 104, 631-636.
Hopwood, D.A. (1997) Genetic contributions to understanding polykitide synthases. Chem. Rev., 97, 2465-2497.
Horinouchi, S., and Beppu, T. (1990) Gene expression in Streptomyces. Tanpakushitsu Kakusan Koso, 35, 2567-2583.
Humpherson-Jones, F.M. (1985) The incidence of Alternaria spp. and Leptosphaeria maculans in commercial brassica seed in the United Kingdom. Plant Pathol., 34(3), 385-390.
Humpherson-Jones, F.M. (1989) Survival of *Alternaria brassicae* and *Alternaria brassicicola* on crop debris of oilseed rape and cabbage. Ann. appl. Biol., 115, 45-50.
Humpherson-Jones, F.M., and Phelps, K. (1989) Climatic factors influencing spore produciton in Alternaria brassicae and Alternaria brassicicola. Ann. appl. Biol., 114, 449-458.

Ichihara, A., Tazaki, H., and Sakamura, S. (1983) Solanapyrones A, B, and C, phytotoxic metabolites from the fungus Alternaria solani. Tetrahedron Lett., 24, 5373-5376.

Isshiki, A., Akimitsu, K., Yamamoto, M., and Yamamoto, H. (2001) Endopolygalacturonase is essential for citrus black rot caused by *Alternaria citri* but not brown spot caused by *Alternaria alternata*. Mol. Plant Microbe Interact., 14, 749-757.

Johnson, R.D., Johnson, L., Itoh, Y., Kodama, M., Otani, H., and Kohmoto, K. (2000) Cloning and characterization of a cyclic peptide synthetase gene from Alternaria alternata apple pathotype whose product is involved in AM-toxin synthesis and pathogenicity. Mol Plant Microbe Interact, 13(7), 742-753.

Kallow, W., Kennedy, J., Arezi, B., Turner, G., and von Dohren, H. (2000) Thioesterase domain of delta-(l-alpha-Aminoadipyl)-l-cysteinyl-d-valine synthetase: alteration of stereospecificity by site-directed mutagenesis. J Mol Biol, 297(2), 395-408.

Keating, T.A., Ehmann, D.E., Kohli, R.M., Marshall, C.G., Trauger, W., and Walsh, C.T. (2001) Chain termination step in nonribosomal peptide synthetase assembly lines: directed acyl-S-enzyme breakdown in antibiotic and siderophore biosynthesis. ChemBioChem, 2, 99-107.

Kim, K.-H., Wight, W., Lawrence, C.B., and Walton, J.D. (2009) Biosynthesis and role in virulence of the histone deacetylase inhibitor depudecin from Alternaria brassicicola. Mol. Plant Microbe Interact., In Press.

Kim, K.H., Cho, Y., La Rota, M., Cramer, R.A., Jr., and Lawrence, C.B. (2007) Functional analysis of the *Alternaria brassicicola* non-ribosomal peptide synthetase gene *AbNPS2* reveals a role in conidial cell wall construction. Mol. Plant Pathol., 8(1), 23-39.

King, S.R. (1994) Screening, selection, and genetics of resistance to *Alternaria* diseases in *Brassica oleracea*. Cornell University, Ithaca, New York.

Konz, D., and Marahiel, M.A. (1999) How do peptide synthetases generate structural diversity? Chem. Biol., 6, R39-R48.

Kratzschmar, J., Krause, M., and Marahiel, M.A. (1989) Gramicidin S biosynthesis operon containing the structural genes grsA and grsB has an open reading frame encoding a protein homologous to fatty acid thioesterases. J Bacteriol, 171(10), 5422-5429.

Lautru, S., and Challis, G.L. (2004) Substrate recognition by nonribosomal peptide synthetase multi-enzymes. Microbiology, 150(Pt 6), 1629-1636.

Linne, U., and Marahiel, M.A. (2000) Control of directionality in nonribosomal peptide synthesis: role of the condensation domain in preventing misinitiation and timing of epimerization. Biochemistry, 39(34), 10439-10447.

Linne, U., Stein, D.B., Mootz, H.D., and Marahiel, M.A. (2003) Systematic and quantitative analysis of protein-protein recognition between nonribosomal peptide synthetases investigated in the tyrocidine biosynthetic template. Biochemistry, 42(17), 5114-5124.

MacKinnon, S.L., Keifer, P., and Ayer, W.A. (1999) Components from the phytotoxic extract of *Alternaria brassicicola*, a black spot pathogen of canola. Phytochemistry, 51, 215-221.

Marahiel, M.A., Stachelhaus, T., and Mootz, H.D. (1997) Modular Peptide Synthetases Involved in Nonribosomal Peptide Synthesis. Chem Rev, 97(7), 2651-2674.

Marshall, C.G., Burkart, M.D., Keating, T.A., and Walsh, C.T. (2001) Heterocycle formation in vibriobactin biosynthesis: alternative substrate utilization and identification of a condensed intermediate. Biochemistry, 40(35), 10655-10663.

Matsumoto, M., Matsutani, S., Sugita, K., Yoshida, H., Hayashi, F., Terui, Y., Nakai, H., Uotani, N., Kawamura, Y., and Matsumoto, K. (1992) Depudecin: a novel compound inducing the flat phenotype of NIH3T3 cells doubly transformed by ras- and src-oncogene, produced by Alternaria brassicicola. J Antibiot (Tokyo), 45(6), 879-885.

Maude, R.B., and Humpherson-Jones, F.M. (1980) studies on the seed-borne phases of dark leaf spot (Alternaria brassicicola) and grey leaf spot (Alternaria brassicae) of brassicas. Ann. appl. Biol., 95(311-319).

May, J.J., Kessler, N., Marahiel, M.A., and Stubbs, M.T. (2002) Crystal structure of DhbE, an archetype for aryl acid activating domains of modular nonribosomal peptide synthetases. Proc Natl Acad Sci U S A, 99(19), 12120-12125.

Mayorga, M.E., and Timberlake, W.E. (1990) Isolation and molecular characterization of the Aspergillus nidulans wA gene. Genetics, 126(1), 73-79.

Mayorga, M.E., and Timberlake, W.E. (1992) The developmentally regulated Aspergillus nidulans wA gene encodes a polypeptide homologous to polyketide and fatty acid synthases. Mol Gen Genet, 235(2-3), 205-212.

McKenzie, K.J., Robb, J., and Lennard, J.H. (1988) Toxin production by *Alternaria* pathogens of oilseed rape (*Brassica napus*). Crop Res., 28, 67-81.

Morishita, E., Takeda, T., and Shibata, S. (1968) Metabolic products of fungi. XXIX. The structure of aurofusarin. (2). Chem Pharm Bull (Tokyo), 16(3), 411-413.

Mulligan, C.N. (2005) Environmental applications for biosurfactants. Environ Pollut, 133(2), 183-198.

Neergaard, P. (1945) Danish species of *Alternaria* and *Stemphylium*. London, UK: Oxford University Press.

O'Hagan, D. (1991) The polyketide metabolites. West Sussex, England: Ellis Horwood Limited,.

Oikawa, H., Yokota, T., Sakano, C., Suzuki, Y., Naya, A., and Ichihara, A. (1998) Solanapyrones, phytotoxins produced by Alternaria solani: biosynthesis and isolation of minor components. Biosci. Biotechnol. Biochem., 62, 2016-2022.

Oka, K., Akamatsu, H., Kodama, M., Nakajima, H., Kawada, T., and Otani, H. (2005) Host-specific AB-toxin production by germinating spores of *Alternaria brassicicola* is induced by a host-derived oligosaccharide. Physiol. Mol. Plant Pathol., 66, 12-19.

Otani, H., Kohnobe, A., Kodama, M., and Kohmoto, K. (1998) Production of a host-specific toxin by germinating spores of *Alternaria brassicicola*. Physiol. Mol. Plant Pathol., 52, 285-295.

Pattanamahakul, P., and Strange, R.N. (1999) Identification and toxicity of *Alternaria brassicicola*, the causal agent of dark leaf spot disease of *Brassica* species grown in Thailand. Plant Pathol., 48, 749-755.

Pazirandeh, M., Chirala, S.S., and Wakil, S.J. (1991) Site-directed mutagenesis studies on the recombinant thioesterase domain of chicken fatty acid synthase expressed in Escherichia coli. J Biol Chem, 266(31), 20946-20952.

Pedras, M.S., Chumala, P.B., Jin, W., Islam, M.S., and Hauck, D.W. (2009) The phytopathogenic fungus Alternaria brassicicola: phytotoxin production and phytoalexin elicitation. Phytochemistry, 70(3), 394-402.

Peypoux, F., Bonmatin, J.M., and Wallach, J. (1999) Recent trends in the biochemistry of surfactin. Appl Microbiol Biotechnol, 51(5), 553-563.

Pfeifer, E., Pavela-Vrancic, M., von Dohren, H., and Kleinkauf, H. (1995) Characterization of tyrocidine synthetase 1 (TY1): requirement of posttranslational modification for peptide biosynthesis. Biochemistry, 34(22), 7450-7459.

Proctor, R.H., Desjardins, A.E., Plattner, R.D., and Hohn, T.M. (1999) A polyketide synthase gene required for biosynthesis of fumonisin mycotoxins in Gibberella fujikuroi mating population A. Fungal Genet Biol, 27(1), 100-112.

Reiber, K., Neuhof, T., Ozegowski, J.H., von Dohrend, H., and Schwecke, T. (2003) A nonribosomal peptide synthetase involved in the biosynthesis of ampullosporins in Sepedonium ampullosporum. J Pept Sci, 9(11-12), 701-713.

Rimmer, S.R., and Buchwaldt, L. (1995) Diseases. In Brassica oilseeds (D.S. Kimber, and D.I. MacGregor, eds), Wallingford, UK: CAB International, pp 111-140.

Roongsawang, N., Hase, K., Haruki, M., Imanaka, T., Morikawa, M., and Kanaya, S. (2003) Cloning and characterization of the gene cluster encoding arthrofactin synthetase from Pseudomonas sp. MIS38. Chem Biol, 10(9), 869-880.

Rotem, J. (1994) The Genus Alternaria. Biology, Epidemiology, and Pathogenicity. St. Paul: APS Press.

Schaeffer, P. (1969) Sporulation and the production of antibiotics, exoenzymes, and exotonins. Bacteriological Reviews, 33, 48-71.

Schneider, A., and Marahiel, M.A. (1998) Genetic evidence for a role of thioesterase domains, integrated in or associated with peptide synthetases, in non-ribosomal peptide biosynthesis in Bacillus subtilis. Arch Microbiol, 169(5), 404-410.

Scott-Craig, J.S., Panaccione, D.G., Pocard, J.A., and Walton, J.D. (1992) The cyclic peptide synthetase catalyzing HC-toxin production in the filamentous fungus Cochliobolus carbonum is encoded by a 15.7-kilobase open reading frame. J Biol Chem, 267(36), 26044-26049.

Sieber, S.A., and Marahiel, M.A. (2005) Molecular mechanisms underlying nonribosomal peptide synthesis: approaches to new antibiotics. Chem Rev, 105(2), 715-738.

Sigareva, M.A., and Earle, E.D. (1999) Camalexin induction in intertribal somatic hybrids between Camelina sativa and rapid-cycling Brassica oleracea. Theor. Appl. Genet., 98, 164-170.

Stachelhaus, T., and Marahiel, M.A. (1995) Modular structure of peptide synthetases revealed by dissection of the multifunctional enzyme GrsA. J Biol Chem, 270(11), 6163-6169.
Stachelhaus, T., Mootz, H.D., Bergendahl, V., and Marahiel, M.A. (1998) Peptide bond formation in nonribosomal peptide biosynthesis. Catalytic role of the condensation domain. J Biol Chem, 273(35), 22773-22781.
Stachelhaus, T., Mootz, H.D., and Marahiel, M.A. (1999) The specificity-conferring code of adenylation domains in nonribosomal peptide synthetases. Chem Biol, 6(8), 493-505.
Stadler, M., and Keller, N.P. (2008) Paradigm shifts in fungal secondary metabolite research. Mycol Res, 112(Pt 2), 127-130.
Stein, T., Vater, J., Kruft, V., Otto, A., Wittmann-Liebold, B., Franke, P., Panico, M., McDowell, R., and Morris, H.R. (1996) The multiple carrier model of nonribosomal peptide biosynthesis at modular multienzymatic templates. J Biol Chem, 271(26), 15428-15435.
Thomma, B.P.H.J. (2003) *Alternaria* spp.: from general saprophyte to specific parasite. Mol. Plant Pathol., 4(4), 225-236.
Turgay, K., Krause, M., and Marahiel, M.A. (1992) Four homologous domains in the primary structure of GrsB are related to domains in a superfamily of adenylate-forming enzymes. Mol Microbiol, 6(4), 529-546.
Vidal-Cros, A., Viviani, F., Labesse, G., Boccara, M., and Gaudry, M. (1994) Polyhydroxynaphthalene reductase involved in melanin biosynthesis in Magnaporthe grisea. Purification, cDNA cloning and sequencing. Eur J Biochem, 219(3), 985-992.
Vining, L.C. (1990) Functions of secondary metabolites. Annu Rev Microbiol, 44, 395-427.
Vollenbroich, D., Ozel, M., Vater, J., Kamp, R.M., and Pauli, G. (1997) Mechanism of inactivation of enveloped viruses by the biosurfactant surfactin from Bacillus subtilis. Biologicals, 25(3), 289-297.
von Dohren, H. (2004) Biochemistry and general genetics of nonribosomal peptide synthetases in fungi. Adv Biochem Eng Biotechnol, 88, 217-264.
Walton, J.D., Panaccione, D.G., and Hallen, H.E. (2004) Peptide synthesis without ribosomes. In ADVANCES IN FUNGAL BIOTECHNOLOGY FOR INDUSTRY, AGRICULTURE, AND MEDICINE (J.S. Tkacz, and L. Lange, eds), New York, NY: Kluwer Academic/Plenum Publishers, pp 127-162.
Weber, G., and Leitner, E. (1994) Disruption of cyclosporine synthetase gene of Tolypocladium niveum. Current Genetics, 26, 461-467.
Weber, G., Schorgendorfer, K., Schneider-Scherzer, E., and Leitner, E. (1994) The peptide synthetase catalyzing cyclosporine production in Tolypocladium niveum is encoded by a giant 45.8-kilobase open reading frame. Curr Genet, 26(2), 120-125.
Weinberg, E.D. (1971) Secondary metabolism-raison d'être. Perspect. Biol. Med., 14, 565.
Westman, A.L., Kresovich, S., and Dickson, M.H. (1999) Regional variation in *Brassica nigra* and other weedy crucifers for disease reaction to *Alternaria*

*brassicicola* and *Xanthomonas campestris* pv. *campestris*. Euphytica, 106, 253-259.

Yang, G., Rose, M.S., Turgeon, B.G., and Yoder, O.C. (1996) A polyketide synthase is required for fungal virulence and production of the polyketide T-toxin. Plant Cell, 8, 2139-2150.

Yao, C., and Köller, W. (1995) Diversity of cutinases from plant pathogenic fungi: Different cutinases are expressed during saprophytic and pathogenic stages of *Alternaria brassicicola*. Mol. Plant Microbe Interact., 8, 122-130.

# Chapter II

## Functional Analysis of the Nonribosomal Peptide Synthetase Genes and Polyketide Synthase Genes in *Alternaria brassicicola* Using a Linear Minimal Element (LME) Construct-Mediated Targeted Gene Disruption Method

## Abstract

(Part of this work was published in ***Cho et al., 2006, MPMI, 19:7-15***)

*Alternaria brassicicola* causes black spot disease of cultivated Brassicas and based on its necrotrophic lifestyle, *A. brassicicola* belongs to a genus renowned for its ability to prodigiously produce secondary metabolites. To test the hypothesis that secondary metabolites produced by *A. brassicicola* contribute to pathogenicity, 8 *NPS* or *NPS*-like genes and 10 *PKS* genes were identified by mining the *A. brassicicola* genome sequence database in our lab. Domain annotation of each gene excluded one *NPS*-like gene from the list due to the absence of necessary enzymatic domains. In *A. brassicicola*, mutant generation has been the most rate-limiting step for the functional analysis of individual genes due to low efficiency of both transformation and targeted integration. To improve the targeted gene disruption efficiency as well as to expedite gene disruption construct production, we adopted a short linear construct with minimal elements, an antibiotic resistance selectable marker gene and a 250- to 600-bp-long partial target gene. The linear minimal element (LME) constructs were used to functionally disrupt all *NPS* and *PKS* genes, resulting in more than 95 % of targeted gene disruption efficiency when using the LME construct, suggesting that this method

is advantageous for high throughput gene disruption in *A. brassicicola*. Deletion of each *NPS* and *PKS* gene and phenotypic analyses showed that 3 *NPS* and 2 *PKS* genes and a *NPS*-like gene (*tmpL*) are required for normal virulence on green cabbage and Arabidopsis, and some of the KO mutants showed interesting phenotypic changes in pigmentation and conidiogenesis.

# Introduction

Secondary metabolites are a remarkably diverse class of cellular products that often exhibit taxonomic specificity (Frisvad et al., 2008). Secondary metabolites are generally considered "nonessential" for organismal growth under culture conditions (Bennett, 1983). In microbes, these unique biochemicals are frequently produced in culture after a period of active growth has depleted the substrate (Bennett, 1995; Bode et al., 2002) and biosynthesis often coincides with differentiation, especially sporulation (Bennett, 1983). However, the circumstances of production and their role in life cycles in the natural environment are not well understood.

The study of fungal secondary metabolites including nonribosomal peptides and polyketides has been limited by the difficulty of detecting and characterizing the secondary metabolite itself. Complete analysis of the genetic potential of fungi to produce secondary metabolites became possible only recently when the genomic sequences of several fungal species became available. Now, the selective cloning of genes encoding those secondary metabolite-producing enzymes such as nonribosomal peptide synthetases (NPS) and polyketide synthases (PKS) can precede identification

of a product and contribute to the overall analysis of secondary metabolite diversity and function in an organism.

The imperfect filamentous fungus *Alternaria brassicicola* (Schwein, Wiltshire) causes black spot disease on a broad range of cultivated and weedy members within *Brassica* species. Notably, *A. brassicicola* has been used as a true necrotrophic fungus for studies with Arabidopsis. Having genome sequences and functional methodologies developed for both plant and pathogen is advantageous for the elucidation of events occurring at the host–pathogen interface that ultimately determine the outcome of the interaction.

Targeted gene disruption or gene replacement, such as recombinational insertion of circular disruption constructs, recombinational replacement (Yang et al., 2004), or transposon arrayed gene knockout (Adachi et al., 2002; Hamer et al., 2001; Lo et al., 2003), is highly desirable for targeted mutational analysis in conjunction with a genome or large expressed sequence tag (EST) sequencing project. With the completion of the *A. brassicicola* genome sequencing, development of high-efficiency gene disruption technology for functional analysis is critical for the identification of virulence factors. This technology also will be useful for identifying the functions of other genes of interest involved in a fungal secondary metabolism.

*A. brassicicola*, in contrast to studies with other *Alternaria* spp., previously has been reported to exhibit very low efficiency for both transformation and targeted gene disruption. Yao and Köller (1995) reported a rare case of gene disruption in *A.*

*brassicicola* for a cutinase gene *cutab1*. In this study, high-velocity microprojectiles (delivered via gene gun) were used to introduce circular plasmid constructs harboring a partial *cutab1* cDNA into conidia. Two targeted gene mutants were identified out of 30 hygromycin B resistant transformants, whereas a polyethylene glycol (PEG)-mediated protoplast transformation method failed to generate any transformants. In the present study, we adopted a relatively easy and economical PEG-mediated protoplast transformation method for targeted gene disruption. Our study had two goals: first, to identify all the *NPS* and *PKS* genes in the genome of *A. brassicicola*, and second, to determine the phenotype resulting from mutation of each *NPS* and *PKS* gene identified using the targeted gene disruption method, with emphasis on discovery of any that might be involved in fungal virulence. Eight *NPS* or *NPS*-like genes and 10 *PKS* genes were found in the *A. brassicicola* genome and characterized in this study.

# Results

**Linear minimal element constructs: new logic for fungal gene disruption**.

There are several established methods to disrupt target genes using diverse constructs. A representative circular disruption construct contains an internal fragment of a target gene cloned together with a selectable marker gene in a plasmid vector (Fig. 1A). A classic linear construct, represented by the replacement construct, flanks an antibiotic resistance or other appropriate selectable marker genes with two fragments representing 5′ and 3′ regions of a target gene (Fig. 1B). Derivatives of replacement constructs have been widely used in diverse filamentous fungi to either replace short segments within a target gene with a selectable marker gene or disrupt a

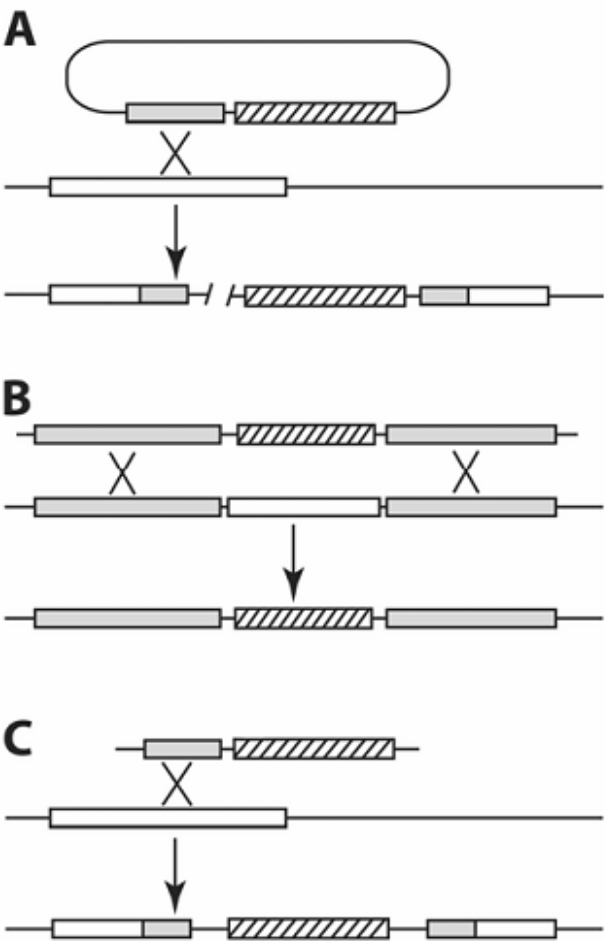


**Figure 1. Diagram depicting incorporation of transforming DNA at a target genomic locus.** Shown are targeted gene disruption or replacement mechanisms starting with A, a circular construct, B, a linear recombinational gene replacement construct, and C, a linear minimal element (LME) construct. Hatched box = a selectable marker gene, white box = a target genomic locus (A, B, and C) and gray box = partial target gene (A and C) or target flanking regions (B). Homologous recombination events are shown with a large "X" between target genomic locus and a partial target gene (A and C) or between target gene flanking regions (B).

target gene (Bussink and Osmani, 1999; Shah-Mahoney et al., 1997; Shiotani and Tsuge, 1995; Voigt et al., 2005). We generated a linear construct with a partial target gene at only one end and an antibiotic resistance selectable marker gene at the other

end (Fig. 1C), and designated this as a linear minimal element (LME) disruption construct to distinguish from other types of linear constructs (Cho et al., 2006). Insertion of classic linear constructs by a single homologous recombination was reported as an undesirable side-effect in several cases due to the circularization of the linear constructs after transformation (Bussink and Osmani, 1999; Shah-Mahoney et al., 1997; Yang et al., 2004). In contrast, if the LME construct were circularized efficiently in the cell, gene disruption might occur by a single homologous recombination (Fig. 1C).

**Transformation and targeted gene disruption efficiency using LME constructs.**

We initially created over 15 individual disruption constructs, using the pCB1636 vector harboring partial cDNA sequences corresponding to *A. brassicicola* genes identified in various cDNA libraries from our laboratory, to ultimately evaluate their role in pathogenicity (Table 1). We produced LME disruption constructs by PCR-based amplification of the gene-specific fragments and the hygromycin B (hygB) resistance gene (*hph*) cassette with M13 forward and M13 reverse primers using plasmid constructs as template DNA. To establish a new gene disruption method, we transformed the LME constructs primarily into an *A. brassicicola* isolate ATCC96836. We tested LME constructs for their ability to efficiently disrupt genes encoding putative toxic proteins, hydrolytic enzymes, a signaling pathway component, a transcription factor, and an essential protein (Table 1). Numbers of transformants generated in these experiments ranged from 3 to 40 that emerged within 2 weeks on the selection plate for each gene except an essential gene (Table 1). Additional

transformants surfaced after 16 days. Late-emerging transformants were not counted in this study because previously emerged colonies grew too large and overlapped the late-emerging colonies. On average, 15 transformants emerged within 16 days when we transformed 10 µg of LME disruption constructs in $4 \times 10^6$ protoplasts with an optimized protocol. We obtained 100 % gene disruption efficiency according to PCR and Southern hybridization experiments in most of these experiments (Table 1). In addition, no evidence of ectopic insertion was observed in the vast majority of targeted gene disruption mutants. One or two rounds of single-spore isolation on PDA media containing hygB were sufficient to purify mutants and eliminate contamination with wild-type nuclei. We qualitatively assessed stability of gene disruption mutants after one round of single-spore isolation. Three different hygB resistant mutants for genes predicted to encode a fus3 MAP kinase, chymotrypsin, and N-acetylglucosaminidase were cultured on PDA media lacking hygB for approximately 1 week, and hyphal tips were repeatedly transferred on to new PDA plates. The repeated subculturing on PDA media did not change hygB resistance of the disruption mutants during the repeated hyphal tip transfers, even after five times. After isolation of new conidia produced during late stages of plant infection, we also tested growth ability of mutant conidia on hygB-containing PDA media several times with over 10 different mutants. In every case, recovered spores remained highly resistant to hygB at the levels used in our studies. Thus, we strongly believe that this transformation method produces highly stable, hygB-resistant transformants.

**Table 1. Efficiency of transformation and gene knockout in *Alternaria brassicicola* using linear minimal element (LME) constructs**

| Gene | Number of transformants/ 1 x $10^{6-7}$ protoplasts | Knock-out percentile (no. of mutants/no. examined)[a] | Verification method |
|---|---|---|---|
| Fus3 MAP Kinase | 20 | 100 (20/20) | PCR/Southern |
| Hog MAP Kinase | 13 | ND | … |
| Chymotrypsin | 10 | 83 (4/5) | PCR |
| N-acetylglucosaminidase | 12 | 100 (6/6) | Southern, PCR |
| Glycosyl hydrolase | 15 | ND | … |
| Pectate lyase | 10 | 100 (5/5) | PCR |
| Zinc finger | 31 | 100 (8/8) | Southern, PCR |
| Altb1 Allergen | 3 | 100 (4/4) | Southern, PCR |
| ATP/ADP transporter | 4 | 98 (196/200) | Viability |
| Lipase1-1 | >200 | 100 (5/5) | PCR |
| Lipase1 | >10 | 100 (8/8) | Southern |
| Lipase2 | 8 | 100 (6/6) | Southern |
| Lipase3 | 15 | 93 (13/14) | Southern |
| Cutinase (CL394) | 14 | 100 (6/6) | PCR |
| MFS transporter | 8 | 100 (8/8) | PCR |

[a]ND = not determined.

**Table 2. Sequence similarities of the *NPS* and *PKS* genes in *A. brassicicola***

| Gene | Gene ID | Genebank homolog | E-value | Inferred or known function |
|---|---|---|---|---|
| ***NPS* genes** | | | | |
| *AbNPS1* | AB3659 | *Hypocrea virens, tex1* | 0.0 | Peptaibol biosynthesis (Wiest et al., 2002) |
| *AbNPS2* | AB8354~6 | *Cochliobolus heterostrophus, NPS4* | 0.0 | Cell wall biosynthesis (Kim et al., 2007) |
| *AbNPS3* | AB7453 | *Cochliobolus heterostrophus, NPS10* | 0.0 | Unknown |
| *AbNPS4* | AB4869 | *Penicillium nordicum, NRPS* | 0.0 | Unknown |
| *AbNPS5* | AB8172 | *Aspergillus fumigatus, NRPS* | 1e-121 | Unknown |
| *AbNPS6* | AB1758 | *Cochliobolus heterostrophus, NPS2* | 2.3e-56 | Siderophore biosynthesis (Oide *et al*., 2006) |
| *AbNPS7* | AB4798 | *Cochliobolus heterostrophus, NPS6* | 2.6e-48 | Siderophore biosynthesis (Oide *et al*., 2007) |
| *AbNPS8* (*NPS*-like) | AB4611 | *Cochliobolus heterostrophus, NPS12* | 0.0 | Intracellular ROS homeostasis (Kim et al., 2009) |
| ***PKS* genes** | | | | |
| *AbPKS1* | AB5106 | *Alternaria solani, Alt5* | 0.0 | Alternapyrone biosynthesis (Fujii et al., 2005) |
| *AbPKS2* | AB5242 | *Pyrenophora tritici-repentis, ppsA* | 0.0 | Unknown |
| *AbPKS3* | AB6179~80 | *Cochliobolus heterostrophus, PKS8* | 0.0 | Unknown |
| *AbPKS4* | AB4669 | *Cochliobolus heterostrophus, PKS12* | 0.0 | Unknown |
| *AbPKS5* | AB7780 | *Cochliobolus heterostrophus, PKS15* | 0.0 | Unknown |
| *AbPKS6* | AB4556 | *Cochliobolus heterostrophus, PKS16* | 0.0 | Unknown |
| *AbPKS7* | AB2277 | *Cochliobolus heterostrophus, PKS18* | 0.0 | Melanin biosynthesis (Kim, unpublished) |
| *AbPKS8* | AB4567~8 | *Cochliobolus heterostrophus, PKS25* | 0.0 | Unknown |
| *AbPKS9* | AB1916 | *Gibberella moniliformis, PKS14* | 2.4e-160 | Depudecin biosynthesis (Kim et al., 2009) |
| *AbPKS10* | AB3659~60 | *Pyrenophora tritici-repentis*, PTRG_04244 | 0.0 | Lovastatin biosynthesis (The Broad Institute) |

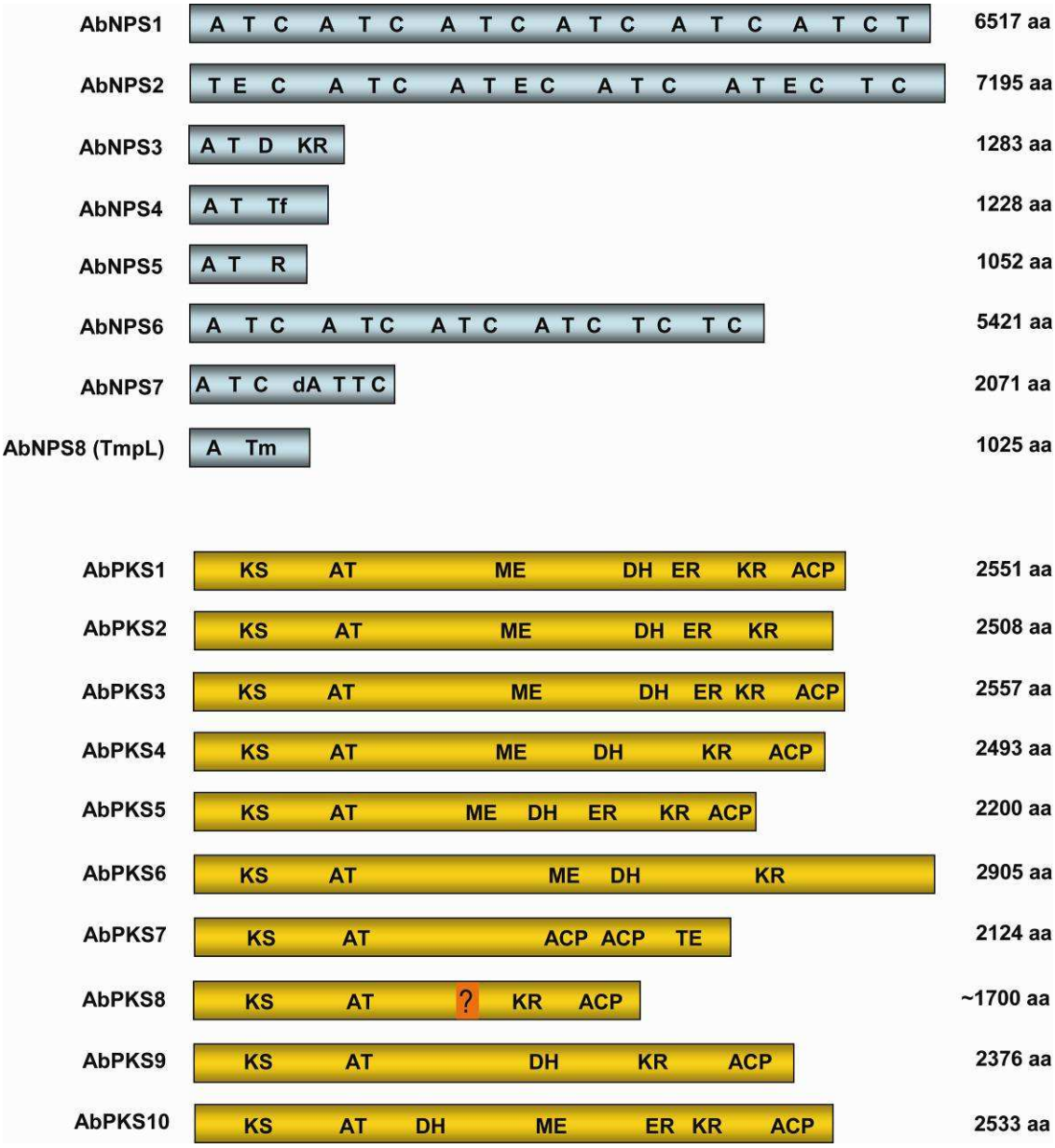


**Figure 2. Structural organization of *A. brassicicola* predicted NPS and PKS proteins.** Abbreviations: A, adenylation; dA, degenerate adenylation; T, thiolation; C, condensation; E, epimerization; Tf, transferase; R, reductase; Tm, transmembrane; D, dehydrogenase; ; KR, ketoreductase; KS, beta-ketoacyl synthase; AT, acyl transferase; ACP, acyl carrier protein; DH, dehydratase; ER enoyl reductase; ME, methyl transferase; TE, thioesterase. Each box represents an open reading frame, the size of which is indicated on the right in amino acids (aa). The question mark in AbPKS8 indicates incomplete sequence.

**Identification of *NPS* and *PKS* genes**

Utilizing the genomic sequence of *A. brassicicola* we have identified 8 *NPS* or *NPS*-like genes and 10 *PKS* genes, named *AbNPS1* to *AbNPS8* and *AbPKS1* to *AbPKS10*, respectively. To identify the *NPS* and *PKS* genes, we used the consensus sequence of the phosphopantetheine (PP)-binding and/or adenylation domain conserved in *NPS* genes and the KS domain, the most highly conserved domain in type I *PKS* genes as queries in HMM (Hidden Markov Model) search. In this regard, we searched a sequence database of *A. brassicicola* genome with a profile HMM. PSI-BLAST searches were also used to retrieve all previously published fungal PKS and NPS protein sequences from National Center for Biotechnology Information (NCBI). Sequence similarity searches were applied to the *A. brassicicola* genome database using BLASTN, BLASTP, and TBLASTN in the NCBI stand-alone BLAST tool (Table 2).

The complete set of domains comprising each *NPS* and *PKS* gene was determined by searches using a conserved domain database (NCBI; http://www.ncbi.nlm.nih.gov/Structure/cdd/cdd.shtml) and an InterProScan (EMBL-EBI; http://www.ebi.ac.uk/InterProScan/). These domains were verified by aligning the predicted protein sequences with domains identified in previously characterized NPS and PKS proteins using CLUSTALW.

The modular organization of each of the eight *NPS* genes is shown in Figure 2. Predicted protein sequences grouped the eight genes into two structural categories: *AbNPS1*, *AbNPS2*, *AbNPS6*, and *AbNPS7* genes encoding mulimodular proteins,

whereas *AbNPS3*, *AbNPS4*, *AbNPS5*, and *AbNPS8* are encoding monomodular proteins, each with a distinctive C-terminal end. *AbNPS3* has a polyketide synthase domain near its C terminus, and is thus an NPS/PKS hybrid; it terminates with a dehydrogenase (DH) domain followed by a ketoreductase (KR) domain found in the PKS proteins. AbNPS4 and AbNPS5 terminate with a tansferase domain and a reductase domain, respectively, suggesting an alternative mechanism of termination reported in a bacterial NPS system (Silakowski et al., 2000). Among the monomodular NPSs, *AbNPS8* contained only an adenylation domain without thiolation and condensation domains which are typical components in the multi-modular organization of *NPS* genes, followed by six transmembrane domains. Therefore, *AbNPS8* was considered not a true *NPS* gene, renamed as *tmpL*, and further characterized in Chapter 5.

According to the domain analysis of *PKS* genes (Fig. 2), there was one nonreducing PKS (*AbPKS7*) and nine reducing PKSs (*AbPKS1-6* and *AbPKS8-10*). All the *PKS* genes identified showed a typical iterative domain organization of *PKS* genes. The full open reading frame (ORF) of the *AbPKS8* had extended over two contigs in *A. brassicicola* genome assembly, thus there was a sequence gap between contigs. However we failed to amplify and sequence the gap region, possibly due to too long gap sequences to amplify efficiently with PCR.

**Functional analysis of *NPS* and *PKS* genes**

To investigate the function of the identified *NPS* and *PKS* genes, we generated LME KO constructs based on the retrieved sequence, and all genes were disrupted

individually using each LME construct. As a consequence of the targeted gene disruption, about 10-20 transgenic strains per each transformation were recovered from the selection media. After single spore isolation, sets of mutants corresponding to each gene were characterized at the molecular level. PCR was used to identify mutants disrupted at each gene locus as well as ectopic mutants, with genomic DNA from each mutant as the template.

Growth, conidiation, morphological alteration, pathogenicity, and sensitivity to oxidative stress were analyzed for the set of disrupted transformants of each gene to determine how the functional disruption affected normal fungal growth and development. Four KO mutants were tested for each *PKS* and *NPS* gene. All ~100 conidia from each mutant strain germinated normally; the mycelial growth, as measured by colony area relative to the wild-type, was similar to the wild-type for all mutants. Abnormal conidial shape was noticed from transformants disrupted in *AbNPS2* and *AbNPS8* (*tmpL*) genes. Interestingly conidia of *AbNPS2* deletion mutants appeared to be hydrophilic and *AbPKS7* deletion mutants were albino mutants having no melanin. All mutants were screened for altered virulence on susceptible green cabbage and in some cases Arabidopsis. Mutants disrupted in *AbNPS2, AbNPS4, AbNPS7*, *AbNPS8* (*tmpL*), *AbPKS1,* and *AbPKS8* displayed significant reductions in virulence (20 % to 80 %), indicating that the products of those genes are necessary for high virulence of *A. brassicicola* on green cabbage. Interestingly, the *AbNPS2* deletion mutants showed an age-dependent reduction in virulence; 7-day-old *abnps2* mutants showed a comparable virulence to wild-type strain, while 21-day-old mutants were

**Table 3. Virulence and phenotype test results of targeted gene disruption mutants.**

| Mutant | Virulence | Relative growth | Phenotype analysis | | |
|---|---|---|---|---|---|
| | | | Pigmentation | Conidial shape | Other traits |
| ***NPS* mutants** | | | | | |
| *abnps1* | Normal | 100% | Normal | Normal | |
| *abnps2* | Age-dependent reduction | 100% | Normal | Abnormal | Water-wettable |
| *abnps3* | Normal | 100% | Normal | Normal | |
| *abnps4* | 60% reduced | 100% | Normal | Normal | |
| *abnps5* | Normal | 100% | Normal | Normal | |
| *abnps6* | Normal | 100% | Normal | Normal | Sensitive to oxidative stress |
| *abnps7* | 80% reduced | 100% | Normal | Normal | Sensitive to oxidative stress |
| *abnps8*(*tmpL*) | 80% reduced | 100% | Lighter-pigmented | Abnormal | Sensitive to oxidative stress |
| ***PKS* mutants** | | | | | |
| *abpks1* | 20% reduced | 100% | Normal | Normal | |
| *abpks2* | Normal | 100% | Normal | Normal | |
| *abpks3* | Normal | 100% | Normal | Normal | |
| *abpks4* | Normal | 100% | Normal | Normal | |
| *abpks5* | Normal | 100% | Normal | Normal | |
| *abpks6* | Normal | 100% | Normal | Normal | |
| *abpks7* | Normal | 100% | White | Normal | Melanin-deficient |
| *abpks8* | 50% reduced | 100% | Normal | Normal | |
| *abpks9* | 10% reduced | 100% | Normal | Normal | Lack of depudecin |
| *abpks10* | Normal | 100% | Normal | Normal | |

less virulent than the wild-type strain. Some of the mutants (*abnps6, abnps7* and *abnps8*) were hypersensitive to oxidative stress. Growth rates of those mutant strains were significantly reduced ($P<0.05$) in the presence of hydrogen peroxide, compared to the wild-type. The *PKS* and *NPS* genes showing an interesting phenotype and virulence changes were selected for further functional characterization in the following chapters.

# Discussion

Various genes involved in fungal pathogenicity have been identified by conventional forward genetics and recently phase-specific protein identification (Kars et al., 2005). However, recent genome-wide approaches have enabled us to discover large numbers of candidate genes in *A. brassicicola* that require subsequent verification by reverse genetics approaches. Starting with the *A. brassicicola* genome sequence, in this study we explored new approaches for systematically knocking out targeted genes to discover the major virulence factors such as proteins involved in the secondary metabolite biosynthesis: nonribosomal peptide synthetases and polyketide synthases.

### Production and optimization of the efficient targeted gene disruption method

The combination of partial target gene sequences disrupted by vector sequences as well as the orientation of vector sequences in mutants indicates that targeted gene disruption in our system was accomplished by a single homologous recombination preceded by circularization of the linear construct, and not by

nonhomologous DNA end joining (Convery et al., 2005; Critchlow and Jackson, 1998; Pastink et al., 2001). With the LME constructs consisting of minimal components, we were able to produce transformants in every trial with approximately 35 genes. We were able to generate approximately 15 transformants per construct with 10 µg of purified PCR products in approximately $4 \times 10^6$ protoplast with an optimized protocol in *A. brassicicola* isolate tested. Targeted gene disruption efficiency was improved dramatically with the LME constructs compared with standard plasmid disruption constructs. These results may be attributed to the small size of the linear constructs or intrinsic differences between plasmids and linear DNA. The typical minimal linear construct (2 kb) is approximately three fold smaller than the plasmid (5.5 kb) used in this study. Alternatively, the linear DNA might enhance both transformation and targeted gene disruption efficiencies as shown in *A. alternata* (Shiotani and Tsuge, 1995) due to uncharacterized reasons. However, substantial differences in transformation efficiency were not observed between LME and plasmids disruption constructs. The major difference observed between the two methods was in reliable targeting efficiency.

In most cases, gene disruption efficiency was 100% in *A. brassicicola* isolate ATCC96836 with the LME disruption construct. Importantly, the majority of mutants contain a single copy of transforming DNA. Our results show greatly increased efficiency compared with examples of approximately 40% gene disruption efficiency in other systems with either Agrobacterium-mediated transformation or transposon-mediated library construction (Adachi et al., 2002; Hamer et al., 2001; Mullins et al.,

2001). Moreover, our results are comparable with the targeted gene disruption efficiency of *N. crassa* in nonhomologous DNA end-joining machinery mutant background (Ninomiya et al., 2004) and *Alternaria alternata* with linearized disruption constructs (Shiotani and Tsuge, 1995). Although both examples showed 100% gene targeting efficiency, the LME disruption method has merits over them in its simplicity to create the constructs and isolate pure mutants, and in the tendency of a single-copy insertion of the disruption constructs into the genome.

This method is applicable for the integration of EST or genome sequence information with the functional analysis of each gene by a reverse genetics approach. Combined with PCR-based construct generation (Yang et al., 2004), it appears possible to use LME constructs for an initial high-throughput screen to study the effect of individual genes on biological functions. It is conceivable to make a synthetic oligo library for every single gene identified in silico (Cho and Walbot, 2001), followed by PCR amplification of the target gene with a selectable marker gene.

In this study, we have described a relatively straightforward, extremely efficient method for disrupting genes in *A. brassicicola*. This approach appears quite suitable for development of a high-throughput functional genomics platform for analyzing gene function in an organism whose genome sequence is publicly available. Other than the role of host-selective fungal toxins in pathogenesis, our basic understanding of the subtleties underlying interactions of plants with necrotrophic fungi is still in its infancy. For example, it is becoming apparent that only specific gene family members encoding secreted plant cell wall-degrading enzymes are

required for full virulence of necrotrophs such as *A. alternata* and *Botrytis cinerea* on specific plants and plant parts (Isshiki et al., 2001; Kars et al., 2005). The high-throughput approach described here will allow for the systematic functional analysis of large sets of candidate genes such as secondary metabolite-producing enzyme-encoding genes identified through bioinformatic analysis of the *A. brassicicola* genome sequence.

**Functional analysis of *NPS* and *PKS* genes in *A. brassicicola* genome**

Production of secondary or "specialized" metabolites is involved in diverse processes in fungi including niche competition, host parasitism, and development (Keller et al., 2005). *A. brassicicola* has a necrotrophic pathogenesis strategy and thus is thought to secrete a plethora of secondary metabolites. Nonribosomal peptides and polyketides consist of the largest and most important groups of microbial secondary metabolites (Keller et al., 2005). Accordingly, the comprehensive functional analysis of all *NPS* and *PKS* genes in *A. brassicicola* will show not only their variety of roles in developmental processes but also in necrotrophic fungal virulence. In this study we identified 8 *NPS* or *NPS*-like genes and 10 *PKS* genes in *A. brassicicola* genome and presented the first comprehensive functional analysis of all *NPS* and *PKS* genes from a single filamentous fungus.

It is clear from our genome-wide analysis of *A. brassicicola* and from similar analyses with additional fungal genomes (Yoder and Turgeon, 2001) that secondary metabolite-producing genes such as *NPS* and *PKS* are abundant in filamentous ascomycetes. *C. heterostrophus*, for example, has 12 *NPS* and 25 *PKS* genes (Kroken

et al., 2003; Lee et al., 2005), and *M. grisea* has 11 *NPS* and 23 *PKS* genes (Dean et al., 2005). Although *A. brassicicola* genome contains less *NPS* and *PKS* genes compared to these ascomycetes, these numbers still rival the numbers reported for *Streptomyces* and *Mycobacterium* spp., bacterial genera renowned for their pharmaceutically important secondary metabolite output (Omura et al., 2001). Of the 17 *A. brassicicola NPS* and *PKS* genes, only a few had a detectable phenotype when mutated, suggesting that the presumed small metabolite products of the NPS and PKS proteins usually do not have obvious biological activity. This fact increases the difficulty of detecting both the secondary metabolites and the corresponding secondary metabolite-producing genes in the absence of genome sequence. This difficulty is exacerbated by the fact that most of the *A. brassicicola NPS* and *PKS* genes appear to be transcribed at low levels (≤2% that of the GAPDH gene control) under standard laboratory culture conditions (data not shown). Low expression suggests that the small molecule biosynthetic pathways represented by the *A. brassicicola NPS* and *PKS* genes may be cryptic under common laboratory culture conditions and that special measures may be necessary to detect biological activity of the small molecules predicted by the presence of these genes in the genome. Furthermore, there may be little correlation between RNA and protein levels, or with factors relating to enzyme activity and secretion of the final metabolite.

To determine the function of individual *NPS* and *PKS* genes, we created a valuable resource in the form of confirmed gene disruption mutants corresponding to each gene and the resulting mutants examined for changes in development and

pathogenicity. Some mutations led to detectable phenotypes, i.e. reduced virulence, water-wettable phenotype, abnormal conidial shape, hypersensitivity to oxidative stress, and so on. Among them *AbNPS2*, *AbPKS9*, and *AbNPS8* (*tmpL*) were further characterized in the following chapter 3, 4 and 5, respectively.

*AbNPS6* and *AbNPS7* were previously identified as NPS enzymes responsible for siderophore biosynthesis by Turgeon and colleagues (Oide et al., 2007; Turgeon et al., 2008). *AbNPS6* biosynthesizes the intracellular siderophore, ferricrocin, while *AbNPS7* biosynthesizes an extracellular siderophore, dimethyl coprogen and derivatives (Oide et al., 2007). Deletion of *AbNPS7* results in a strain that is not only reduced in virulence on its host, but also sensitive to oxidative and low iron stress and in asexual conidiation.

Based on the striking phenotype of the disrupted mutants, we identified *AbPKS7* as the PKS enzyme responsible for the biosynthesis of melanin pigment in *A. brassicicola*. The *abpks7* mutants formed albino mycelia and conidia on potato-dextrose agar plates, whereas the parent wild-type formed dark brown mycelia and conidia. Similar to *Alternaria alternata* $Alm^-$ mutants (*ALM* is an *A. alternate* ortholog of the *AbPKS7*) (Tanabe et al., 1995), the *abpks7* mutants had a comparable virulence to wild-type strain, indicating that the ability to produce melanin may not be relevant to the pathogenicity of *A. brassicicola*. However, melanization of *Colletotrichum lagenarium* (Kubo et al., 1991), *C. lindemuthianum* (Wolkow et al., 1983), and *Magnaporthe grisea* (Yamaguchi and Kubo, 1992) is essential for penetration of their

host plants, suggesting that there are great diversity among fungi in the roles of melanin.

As future research, through a genome-wide comparative study with other fungal genes, the *NPS* and *PKS* genes identified in our study will provide phylogenetic relationship among filamentous fungi. For *NPS* genes, cross-genome comparisons indicated that most filamentous ascomycetes carry many genes encoding NPS (Turgeon et al., 2008). Most *NPS* genes are not conserved from one species to the next, although some appear to be discontinuously distributed. For example, *C. heterostrophus* carries four *NPS* genes that are common to other filamentous ascomycetes, whereas the remaining eight *NPS* genes may or may not have a counterpart in one or more additional fungal species (Turgeon et al., 2008). Accordingly, comparisons among studies of *NPS* and *PKS* genes will further our understanding of the evolution and ecological significance of these diverse group of compounds. Further analysis of the mutants like *abnps4* and *abpks8* strains that showed more than 50 % reduced virulence compared with the wild-type strain, and identification of the secondary metabolite compounds produced by those genes will enable us to assign functions to each gene in *A. brassicicola* and elucidate the role they play in the life cycle of the fungus, especially in the pathogenesis. In addition, another advantage from the detailed characterization of the pathogenicity factor candidates derived from this research is ultimately efficient control of fungal disease of important crops. Considering the diversity of strategies that fungal pathogens use as well as their ability to quickly adapt, it is difficult to predict which developments will

lead to durable and broad-spectrum disease resistance. No matter what sophisticated methodologies may be discovered, it is clear that effective plant protection will require a much better understanding of the diverse roles of multiple fungal pathogenicity factors.

## Materials and methods

### *Fungi*

*A. brassicicola* isolate ATCC96836 was used in this study, which is the isolate sequenced. *A. brassicicola* was routinely cultured on PDA media (Difco, Kansas City, MO, U.S.A.) at RT.

### *Generation of disruption constructs*

Based on the cDNA sequence, two primers with an enzymatic site at each end were designed to amplify a 250- to 500-bp fragment within the coding region of each gene. PCR products were digested with the two endonucleases and ligated into the multiple cloning site of pCB1636 plasmid (Sweigard et al., 1995). The plasmid construct was transformed in *Escherichia coli* DH5α (Invitrogen, Carlsbad, CA, U.S.A.) to produce over 10 µg of plasmid. The plasmid constructs were sequenced to verify the presence of target gene sequences in the vector. These constructs were used in either transformation experiments in their circular form or PCR reactions to generate linear DNA. Constructs were used as template DNA to amplify between M13 forward and M13 reverse priming sites that contained the hygB phosphotransferase gene under control of the *trpC* fungal promoter and the cloned partial targeted gene. The PCR

products were purified with the PCR Clean Up kit (Qiagen, Palo Alto, CA, U.S.A.) and further concentrated to a concentration of 1 µg/µl in a Speedvac (Eppendorf, Barkhausenweg, Germany).

***A. brassicicola transformation***

Transformation was carried out with either plasmid disruption constructs or linear PCR products based on the transformation protocol of *A. alternata* (Akamatsu et al., 1997), with modifications. Approximately $5 \times 10^6$ fungal conidia were harvested from a PDA culture plate and inoculated into 50 ml of GYEB (1% glucose and 0.5 % yeast extract) media. They were cultured for 36 h with shaking at 100 rpm at 25 ºC. The mycelia were harvested by centrifugation at 2,000 × g for 5 min and washed with 0.7 M NaCl followed by centrifugation again under the same conditions as before. The mycelia were digested in 6 ml of Kitalase (Wako Chemicals, Richmond, VA, U.S.A.) at 10 mg/ml in 0.7 M NaCl for 3 to 4 h at 28 ºC with constant shaking at 110 rpm. The protoplasts were collected by centrifugation at 700 × g for 10 min at 4 ºC, washed twice with 10 ml of 0.7 M NaCl and then with 10 ml of STC buffer (1 M Sorbitol, 50 mM Tris-HCL, pH 8.0, and 50 mM $CaCl_2$). The protoplasts were resuspended in STC at a concentration of $4 \times 10^6$ in 70 µl, after which 10 µg of plasmid or PCR products in 10 µl of $ddH_2O$ was added to the protoplast and gently mixed. The transformation mix was incubated on ice for 30 min. Heat shock transformation was per-formed by incubating the transformation mixture at 42 ºC for 2 to 10 min. The transformation mix was incubated at room temperature after the addition of 800 µl of 40 % PEG solution. Then, 200 µl of the transformation mixture was added to 25 ml of mol-ten

regeneration medium (1 M sucrose, 0.5 % yeast extract, 0.5 % casein amino acids, and 1 % agar,) in a 50-ml tube and subsequently poured into a 100-by-15-mm petri dish. After 24 h, the plates were overlaid with 25 ml of hygB (Sigma-Aldrich, St. Louis, U.S.A.) containing PDA at 30 µg/ml. Individual hygB-resistant transformants were transferred to a fresh hygB-containing plate between 10 and 15 days after each transformation. Each transformant was purified further by transferring a single spore to a fresh hygB-containing plate.

***Identification and annotation of NPS and PKS genes***

To identify *PKS* genes, we used the consensus sequence of the KS domain, the most highly conserved domain in type I PKSs and FASs, as a query in hmmsearch - search a sequence database with a profile HMM of the sequence database of *A. brassicicola* genome. The PSI-BLAST searches were also used to retrieve all previously published fungal PKS protein sequences from National Center for Biotechnology Information (NCBI). Sequence similarity searches were applied to the local *A. brassicicola* database using BLASTN, BLASTP, and TBLASTN in the NCBI stand-alone BLAST tool. Among the hits, fatty acid synthases were manually identified and discarded. To identify *NPS* genes, we used the consensus sequence of the phosphopantetheine (PP)-binding or adenylation (A) domain using the same searching method for *PKS* genes. Sequence similarity searches were done against the local *A. brassicicola* genomic database. Among the hits were genes other than *NPS* that also encode proteins with A domains, such as aminopeptidases and ATPase; these were discarded. Manual annotation of the *NPS* and *PKS* sequences and alignment of each against the others

and against known *NPS* and *PKS*, respectively, were used to define the structures of these genes. To manually annotate each *PKS* and *NPS* gene, the conserved sequences of each domain and module are used first and then known *PKS* and *NPS* sequence information are used for each domain and module identification.

***Virulence test***

To test virulence, conidia are harvested from strains grown on PDA agar plates for 7 days at 25°C and are suspended in sterile water at a concentration of $1 \times 10^5$ spores/ml. 10 µl of conidial suspension is dropped on the surface of cabbage leaf. The leaves are incubated for 5 days in the Petri dishes at RT with 100 % relative humidity.

***Growth and germination test***

Fifty conidia from each mutant and from the wild-type were picked onto PDA plates, and mycelial growth was monitored for 96 h. The growth rate was determined by measuring diameters of six independent colonies from each mutant and from the wild-type every 24 h. Conidial germination was measured on cover glasses (Fishier Scientific, Hampton, NH, USA). Conidia were harvested from 7-day-old culture on PDA in sterile distilled water and adjusted to $1 \times 10^4$ conidia per ml. Drops (30 µl) were placed on cover glasses, then placed in a moistened box and incubated at RT for 36 h. The percentage of germinated conidia was determined by microscopic examination of at least 100 conidia per replicate in at least three independent experiments.

# Literature Cited


Adachi, K., Nelson, G.H., Peoples, K.A., Frank, S.A., Montenegro-Chamorro, M.V., DeZwaan, T.M., Ramamurthy, L., Shuster, J.R., Hamer, L., and Tanzer, M.M. (2002) Efficient gene identification and targeted gene disruption in the wheat blotch fungus Mycosphaerella graminicola using TAGKO. Curr Genet, 42(2), 123-127.

Akamatsu, H., Itoh, Y., Kodama, M., Otani, H., and Kohmoto, K. (1997) AAL-Toxin-Deficient Mutants of Alternaria alternata Tomato Pathotype by Restriction Enzyme-Mediated Integration. Phytopathology, 87(9), 967-972.

Bennett, J.W. (1983) Differentiation and secondary metabolism in mycelial fungi. In Secondary metabolism and differentiation in fungi (J.W. Bennett, and A. Ciegler, eds), New York, NY: Marcel Dekker, pp 1-32.

Bennett, J.W. (1995) From molecular genetics and secondary metabolism to molecular metabolites and secondary genetics. Can. J. Botany, 73, S917-S924.

Bode, H.B., Bethe, B., Hofs, R., and Zeeck, A. (2002) Big effects from small changes: possible ways to explore nature's chemical diversity. Chembiochem, 3(7), 619-627.

Bussink, H.J., and Osmani, S.A. (1999) A mitogen-activated protein kinase (MPKA) is involved in polarized growth in the filamentous fungus, Aspergillus nidulans. FEMS Microbiol Lett, 173(1), 117-125.

Cho, Y., Davis, J.W., Kim, K.H., Wang, J., Sun, Q.H., Cramer, R.A., Jr., and Lawrence, C.B. (2006) A high throughput targeted gene disruption method for Alternaria brassicicola functional genomics using linear minimal element (LME) constructs. Mol Plant Microbe Interact, 19(1), 7-15.

Cho, Y., and Walbot, V. (2001) Computational methods for gene annotation: the Arabidopsis genome. Curr Opin Biotechnol, 12(2), 126-130.

Convery, E., Shin, E.K., Ding, Q., Wang, W., Douglas, P., Davis, L.S., Nickoloff, J.A., Lees-Miller, S.P., and Meek, K. (2005) Inhibition of homologous recombination by variants of the catalytic subunit of the DNA-dependent protein kinase (DNA-PKcs). Proc Natl Acad Sci U S A, 102(5), 1345-1350.

Critchlow, S.E., and Jackson, S.P. (1998) DNA end-joining: from yeast to man. Trends Biochem Sci, 23(10), 394-398.

Dean, R.A., Talbot, N.J., Ebbole, D.J., Farman, M.L., Mitchell, T.K., Orbach, M.J., Thon, M., Kulkarni, R., Xu, J.R., Pan, H., Read, N.D., Lee, Y.H., Carbone, I., Brown, D., Oh, Y.Y., Donofrio, N., Jeong, J.S., Soanes, D.M., Djonovic, S., Kolomiets, E., Rehmeyer, C., Li, W., Harding, M., Kim, S., Lebrun, M.H., Bohnert, H., Coughlan, S., Butler, J., Calvo, S., Ma, L.J., Nicol, R., Purcell, S.,

Nusbaum, C., Galagan, J.E., and Birren, B.W. (2005) The genome sequence of the rice blast fungus Magnaporthe grisea. Nature, 434(7036), 980-986.

Frisvad, J.C., Andersen, B., and Thrane, U. (2008) The use of secondary metabolite profiling in chemotaxonomy of filamentous fungi. Mycol Res, 112(Pt 2), 231-240.

Hamer, L., Adachi, K., Montenegro-Chamorro, M.V., Tanzer, M.M., Mahanty, S.K., Lo, C., Tarpey, R.W., Skalchunes, A.R., Heiniger, R.W., Frank, S.A., Darveaux, B.A., Lampe, D.J., Slater, T.M., Ramamurthy, L., DeZwaan, T.M., Nelson, G.H., Shuster, J.R., Woessner, J., and Hamer, J.E. (2001) Gene discovery and gene function assignment in filamentous fungi. Proc Natl Acad Sci U S A, 98(9), 5110-5115.

Isshiki, A., Akimitsu, K., Yamamoto, M., and Yamamoto, H. (2001) Endopolygalacturonase is essential for citrus black rot caused by Alternaria citri but not brown spot caused by Alternaria alternata. Mol Plant Microbe Interact, 14(6), 749-757.

Kars, I., Krooshof, G.H., Wagemakers, L., Joosten, R., Benen, J.A., and van Kan, J.A. (2005) Necrotizing activity of five Botrytis cinerea endopolygalacturonases produced in Pichia pastoris. Plant J, 43(2), 213-225.

Keller, N.P., Turner, G., and Bennett, J.W. (2005) Fungal secondary metabolism - from biochemistry to genomics. Nat Rev Microbiol, 3(12), 937-947.

Kroken, S., Glass, N.L., Taylor, J.W., Yoder, O.C., and Turgeon, B.G. (2003) Phylogenomic analysis of type I polyketide synthase genes in pathogenic and saprobic ascomycetes. Proc Natl Acad Sci U S A, 100(26), 15670-15675.

Kubo, Y., Nakamura, H., Kobayashi, K., Okuno, T., and Furusawa, I. (1991) Cloning of a melanin biosynthetic gene essential for appressorial penetration of Colletotrichum lagenarium. Mol. Plant-Microbe Interact., 5, 440-445.

Lee, B.N., Kroken, S., Chou, D.Y., Robbertse, B., Yoder, O.C., and Turgeon, B.G. (2005) Functional analysis of all nonribosomal peptide synthetases in Cochliobolus heterostrophus reveals a factor, NPS6, involved in virulence and resistance to oxidative stress. Eukaryot Cell, 4(3), 545-555.

Lo, C., Adachi, K., Shuster, J.R., Hamer, J.E., and Hamer, L. (2003) The bacterial transposon Tn7 causes premature polyadenylation of mRNA in eukaryotic organisms: TAGKO mutagenesis in filamentous fungi. Nucleic Acids Res, 31(16), 4822-4827.

Mullins, E.D., Chen, X., Romaine, P., Raina, R., Geiser, D.M., and Kang, S. (2001) Agrobacterium-Mediated Transformation of Fusarium oxysporum: An Efficient Tool for Insertional Mutagenesis and Gene Transfer. Phytopathology, 91(2), 173-180.

Ninomiya, Y., Suzuki, K., Ishii, C., and Inoue, H. (2004) Highly efficient gene replacements in Neurospora strains deficient for nonhomologous end-joining. Proc Natl Acad Sci U S A, 101(33), 12248-12253.

Oide, S., Krasnoff, S.B., Gibson, D.M., and Turgeon, B.G. (2007) Intracellular siderophores are essential for ascomycete sexual development in heterothallic Cochliobolus heterostrophus and homothallic Gibberella zeae. Eukaryot Cell, 6(8), 1339-1353.

Omura, S., Ikeda, H., Ishikawa, J., Hanamoto, A., Takahashi, C., Shinose, M., Takahashi, Y., Horikawa, H., Nakazawa, H., Osonoe, T., Kikuchi, H., Shiba, T., Sakaki, Y., and Hattori, M. (2001) Genome sequence of an industrial microorganism Streptomyces avermitilis: deducing the ability of producing secondary metabolites. Proc Natl Acad Sci U S A, 98(21), 12215-12220.

Pastink, A., Eeken, J.C., and Lohman, P.H. (2001) Genomic integrity and the repair of double-strand DNA breaks. Mutat Res, 480-481, 37-50.

Shah-Mahoney, N., Hampton, T., Vidaver, R., and Ratner, D. (1997) Blocking the ends of transforming DNA enhances gene targeting in Dictyostelium. Gene, 203(1), 33-41.

Shiotani, H., and Tsuge, T. (1995) Efficient gene targeting in the filamentous fungus Alternaria alternata. Mol Gen Genet, 248(2), 142-150.

Silakowski, B., Kunze, B., Nordsiek, G., Blocker, H., Hofle, G., and Muller, R. (2000) The myxochelin iron transport regulon of the myxobacterium *Stigmatella aurantiaca* Sg a15. Eur J Biochem, 267(21), 6476-6485.

Sweigard, J.A., Carroll, A.M., Kang, S., Farrall, L., Chumley, F.G., and Valent, B. (1995) Identification, cloning, and characterization of PWL2, a gene for host species specificity in the rice blast fungus. Plant Cell, 7(8), 1221-1233.

Tanabe, K., Park, P., Tsuge, T., Kohmoto, K., and Nishimura, S. (1995) Characterization of the mutants of Alternaria alternata Japanese pear
pathotype deficient in melanin production and their pathogenicity. Ann. Phytopathol. Soc. Jpn., 61, 27-33.

Turgeon, B.G., Oide, S., and Bushley, K. (2008) Creating and screening Cochliobolus heterostrophus non-ribosomal peptide synthetase mutants. Mycol Res, 112(Pt 2), 200-206.

Voigt, C.A., Schafer, W., and Salomon, S. (2005) A secreted lipase of Fusarium graminearum is a virulence factor required for infection of cereals. Plant J, 42(3), 364-375.

Wolkow, P.M., Sisler, H.D., and Vigil, E.L. (1983) Effect of inhibitors of melanin biosynthesis on structure and function of appressoria of *Colletotrichum lindemuthianum*. Physiol. Plant Pathol., 22, 55-71.

Yamaguchi, I., and Kubo, Y. (1992) Target sites of melanin biosynthesis inhibitors. In Target Sites of Fungicide Action (W. Koller, ed, London: CRC Press, pp 101-118.

Yang, L., Ukil, L., Osmani, A., Nahm, F., Davies, J., De Souza, C.P., Dou, X., Perez-Balaguer, A., and Osmani, S.A. (2004) Rapid production of gene replacement constructs and generation of a green fluorescent protein-tagged centromeric marker in Aspergillus nidulans. Eukaryot Cell, 3(5), 1359-1362.

Yao, C., and Köller, W. (1995) Diversity of cutinases from plant pathogenic fungi: different cutinases are expressed during saprophytic and pathogenic stages of *Alternaria brassicicola*. Mol. Plant-Microbe Interact., 8, 122-130.

Yoder, O.C., and Turgeon, B.G. (2001) Fungal genomics and pathogenicity. Curr Opin Plant Biol, 4(4), 315-321.

# Chapter III

## Functional Analysis of the *Alternaria brassicicola* Nonribosomal Peptide Synthetase Gene *AbNPS2* Reveals a Role in Conidial Cell Wall Construction


## Abstract

(This work was published in ***Kim et al., 2007, Mol. Plant Pathol., 8:23-39***)

*Alternaria brassicicola* is a necrotrophic pathogen causing black spot disease on virtually all cultivated Brassica crops worldwide. In many plant pathosystems fungal secondary metabolites derived from nonribosomal peptide synthetases (NPS) are phytotoxic virulence factors or are antibiotics thought to be important for niche competition with other microorganisms. However, many of the functions of NPS genes and their products are largely unknown. In this study, we investigated the function of one of the *A. brassicicola* NPS genes, *AbNPS2*. The predicted amino acid sequence of AbNPS2 showed high sequence similarity with *A. brassicae*, AbrePsy1, *Cochliobolus heterostrophus*, NPS4 and a *Stagonospora nodorum* NPS. The *AbNPS2* ORF was predicted to be 22 kb in length and encodes a large protein (7195 aa) showing typical NPS modular organization. Gene expression analysis of *AbNPS2* in wild-type fungus indicated that it is expressed almost exclusively in conidia and conidiophores, broadly in the reproductive developmental phase. *AbNPS2* gene disruption mutants showed abnormal spore cell wall morphology and a decreased hydrophobicity phenotype. Conidia of *abnps2* mutants displayed an aberrantly inflated cell wall and an increase in lipid bodies compared to wild-type. Further phenotypic analyses of *abnps2* mutants showed decreased spore germination rates both *in vitro*

and *in vivo*, and a marked reduction in sporulation *in vivo* compared to wild-type fungus. Moreover, virulence tests on Brassicas with *abnps2* mutants revealed a significant reduction in lesion size compared to wild-type but only when aged spores were used in experiments. Collectively, these results indicate that *AbNPS2* plays an important role in development and virulence.

## Introduction

*A. brassicicola* is the causal agent of black spot disease of many economically important Brassica species worldwide (Braverman, 1979; Humpherson-Jones and Phelps, 1989). In a dramatic example, *A. brassicicola* has been shown to be responsible for up to 50% yield loss in infected fields of winter rape in Germany (MacKinnon *et al.*, 1999). Like other diseases caused by *Alternaria* species, black spot appears on the leaves as necrotic lesions, which are often described as black and sooty with chlorotic yellow halos surrounding the lesion sites (Agrios, 1997). *A. brassicicola*, however, is not limited to infection of leaves, and can infect all parts of the plant including pods, seeds, and stems, and is of particular importance as a post-harvest disease (Rimmer and Buchwaldt, 1995). Despite this, little is known about the pathogenic determinants produced by this fungus that enable penetration and colonization of plant tissues. The production of small phytotoxic metabolites that selectively or non-selectively damage host plants has been reported in *A. brassicicola* over the last two decades (MacDonard and Ingram, 1986; MacKinnon *et al.*, 1999; Otani *et al.*, 1998). In addition to these toxins it has been reported that *A. brassicicola* produces a number of other interesting natural products, such as the antitumoric,

HDAC inhibitor depudecin (Matsumoto *et al.*, 1992), and an antibiotic complex termed brassicicolin (Ciegler and Lindenfelser, 1969; Gloer *et al.*, 1988).

A complex and fascinating aspect of fungal biology is the production of secondary metabolites. Fungal secondary metabolites are considered part of the chemical arsenal required for niche specialization and have garnered intense interest by virtue of their biotechnological and pharmaceutical applications (Kleinkauf and von Dohren, 1996; Schwarzer and Marahiel, 2001; Smith *et al.*, 1990a; von Dohren *et al.*, 1997). Some secondary metabolites are well known virulence factors in fungal-plant interactions, causing crop damage, yield losses, and food supply contamination (Bennett, 1989; Lee *et al.*, 1986; Osbourn, 2001).

One of the largest and most important groups of fungal secondary metabolites, nonribosomal peptides (NRP), are comprised of peptide-based molecules and nonribosomally synthesized by peptide synthetases (Schwarzer *et al.*, 2003). Nonribosomal peptide systhetases (NPS) are large, multifunctional enzymes typically comprised of numerous semiautonomous catalytic domains in a linear series (Marahiel *et al.*, 1979; Marahiel *et al.*, 1997; Shen *et al.*, 2004). The domains are arranged in a predictable distance from each other and in a characteristic sequence that reflects the order of their activity in the assembly and tailoring of the peptide or peptide-containing product. A minimal NPS module is composed of domains that catalyze the single reaction steps like activation, covalent binding, optional modification of the incorporated monomer substrate, and condensation with the amino acyl or peptidyl group on the neighboring module (Schwarzer and Marahiel, 2001). Generally, the number and order of modules present in a NPS determine the length and structure of

the resulting NRP. The activation domain recognizes a substrate amino (or hydroxy) acid, usually specifically, and activates it as its acyl adenylate by reaction with ATP. This active ester is then covalently linked as its thioester to the enzyme-bound 4′-phosphopantetheine located within the module. The reaction continues by the direct transfer to another acylamino acid intermediate on the adjacent downstream module mediated by the condensation domain to form a peptide bond. In some cases, modifications (epimerization, N- or C-methylation or cyclization) are catalyzed by additional domains or by modified domains within a module. In some NPSs, a thioesterase domain is found at the C-terminal end of the protein and is thought to release the NRP from the NPS by cyclization or hydrolysis (Cosmina *et al.*, 1993).

Fungal NRPs have been found to have a wide range of biological activity from being involved in plant pathogenesis to the production of beneficial antibiotics. Although the production of nonribosomal peptide-associated metabolites by the thiotemplate mechanism is well supported in the literature, the biological significance and benefit of these molecules to the producing organisms remains elusive. However, evidence has been presented demonstrating that NRPs may function as signal molecules for coordination of growth and differentiation (Guillemette *et al.*, 2004; Horinouchi and Beppu, 1990; Marahiel *et al.*, 1979; Schaeffer, 1969). NRPs may also participate in the breakdown of cellular metabolic products (Davies, 1990). Some NRPs such as penicillin clearly have antimicrobial activity and kill competing microorganisms (Vining, 1990). Other NRPs act as siderophores and assist in iron uptake (Challis and Ravel, 2000). Finally, NRPs may serve as host virulence factors

often possessing phytotoxic activities (Haese *et al.*, 1993; Johnson *et al.*, 2000; Panaccione *et al.*, 1992; Scott-Craig *et al.*, 1992).

The genomic sequences of over fifty fungi have been determined, including the fungi *Neurospora crassa*, *Aspergillus nidulans*, *Stagonospora nodorum*, and *Magnaporthe grisea*, to name a few (Dean *et al.*, 2005; Galagan *et al.*, 2003; Hynes, 2003; Jones *et al.*, 2004). As more genomes become available and are analyzed for their *NPS* genes, it will be interesting to see how the types and numbers of *NPS* genes (as well as secondary metabolite-associated genes in general) correlate with ecological niche and the interaction with their host, either animal or plant. Here we report on a putative *NPS* gene, *AbNPS2*, from *A. brassicicola*, which is involved in conidiation and more specifically conidial cell wall stabilization. We also annotate and describe the organization of the *AbNPS2* region in the *A. brassicola* genome and compare this to the orthologous region in the closely related Dothideomycete, *S. nodorum*. This is the first report that a fungal NPS is associated with conidial cell wall construction. The role of this gene in fungal development and plant pathogenesis is discussed.

# Results

### Structure and annotation of *AbNPS2*

Seven putative *NPS* genes were identified in the *A. brassicicola* genome via HMMER and BLAST analyses. They were designated as *AbNPS1* to *AbNPS7*, for *Alternaria brassicicola* non-ribosomal peptide synthetase. Among the seven *NPS* genes, *AbNPS2* gene was functionally characterized in this study. The predicted ORF of *AbNPS2* was found to be 22066 bp long and encodes a putative protein of 7195

amino acids with typical NPS modular organization with exceptions described hereafter (Fig.1A). The predicted AbNPS2 protein contains four repeats of the conserved catalytic domain (adenylation (A) domain) responsible for the activation of each constituent amino acid incorporated into the final synthesized peptide. Using conserved sequence motifs for individual NPS domains, six peptidyl carrier protein or thiolation (T) domains, six condensation (C) domains, and three epimerization (E) domains were also identified within the NPS sequence. Based on this analysis, the synthetase consists of 19 domains, organized into four modules and is predicted to produce an L-D-L-D-tetrapeptide due to the existence of two epimerization (E) domains. It was notable that the structure of AbNPS2 had no traditional initiation module consisting of an A and a T domains, but started with a T domain, and the last elongation module of AbNPS2 was followed by a C-T-C module, not by a typical terminal thioesterase (TE) domain. Based on the identified modules and gene organization, *AbNPS2* belongs to the nonlinear (Type C) NPS group differing from the classical $(C\text{-}A\text{-}T)_n$ architecture of linear NPSs (Mootz *et al.*, 2002).

Results of BLASTP using GenbankNR and local fungal genome databases suggested that *AbNPS2* and three of the *NPS* genes from other fungi investigated might comprise an orthologous group. The most significant hits were to putative NPS's from *A. brassicae* (score = 12610, ID = 90%), *C. heterostrophus* (score = 10400, ID = 72%), and *S. nodorum* (score = 8335, ID = 64%). Interestingly, all of these organisms along with *A. brassicicola* are taxonomically classified as Dothideomycetes. The most significant hit to a non-fungal NPS was the gramicidin synthetase from *Brevibacillus brevis* (score = 1640, ID = 27%). In addition to the

identical domain and module arrangement, the adenylation domain substrate specificity sequences [as defined by Stachelhaus *et al.* (1999)] from the four Dothideomycete NPS's were identical (Table 1).

**Table 1. Specificity code of AbNPS2 orthologs' adenylation domains**

| NPS | A Domain 1 | A Domain 2 | A Domain 3 | A Domain 4 |
|---|---|---|---|---|
| *C. heterostrophus* | DNEDCGOIN- | DAIAFVGCV- | DAILVGAVV- | DALFTGVIF- |
| *A. brassicicola* | DNEDCGMIN | DAITFIGCI- | DAILVGAVV- | DVGFVGGVF- |
| *A. brassicae* | DNEDCGMIN- | DAIAFVGAV- | DAILVGAVV- | DVGFVGGVF- |
| *S. nodorum* | DNEDAGQIN- | DAIAVVGCV- | DAILVGAVV- | DVGFVGGVF- |

**Organization of the *AbNPS2* region in the *A. brassicicola* genome**

Analysis of a preliminary assembly of the *A. brassicicola* genome employing the use of the gene prediction program FGENESH (with an Alternaria-specific gene prediction matrix) (Salamov and Solovyev, 2000) and a customized EnsEMBL annotation pipeline (Potter *et al.*, 2004) revealed a total of 61 genes predicted to be present in a 200 kb region containing the *AbNPS2* gene. Comparison of these predicted genes with gene models from other available fungal genome projects showed that only the Dothideomycete, *S. nodorum* had a similar organization flanking its NPS ortholog. All except eight of 61 predicted genes in this interval have *S. nodorum* homologs. The majority of the matching genes models (37 of 61) are located on one segment of *S. nodorum*'s genome (supercontig 4) while 14 are located on

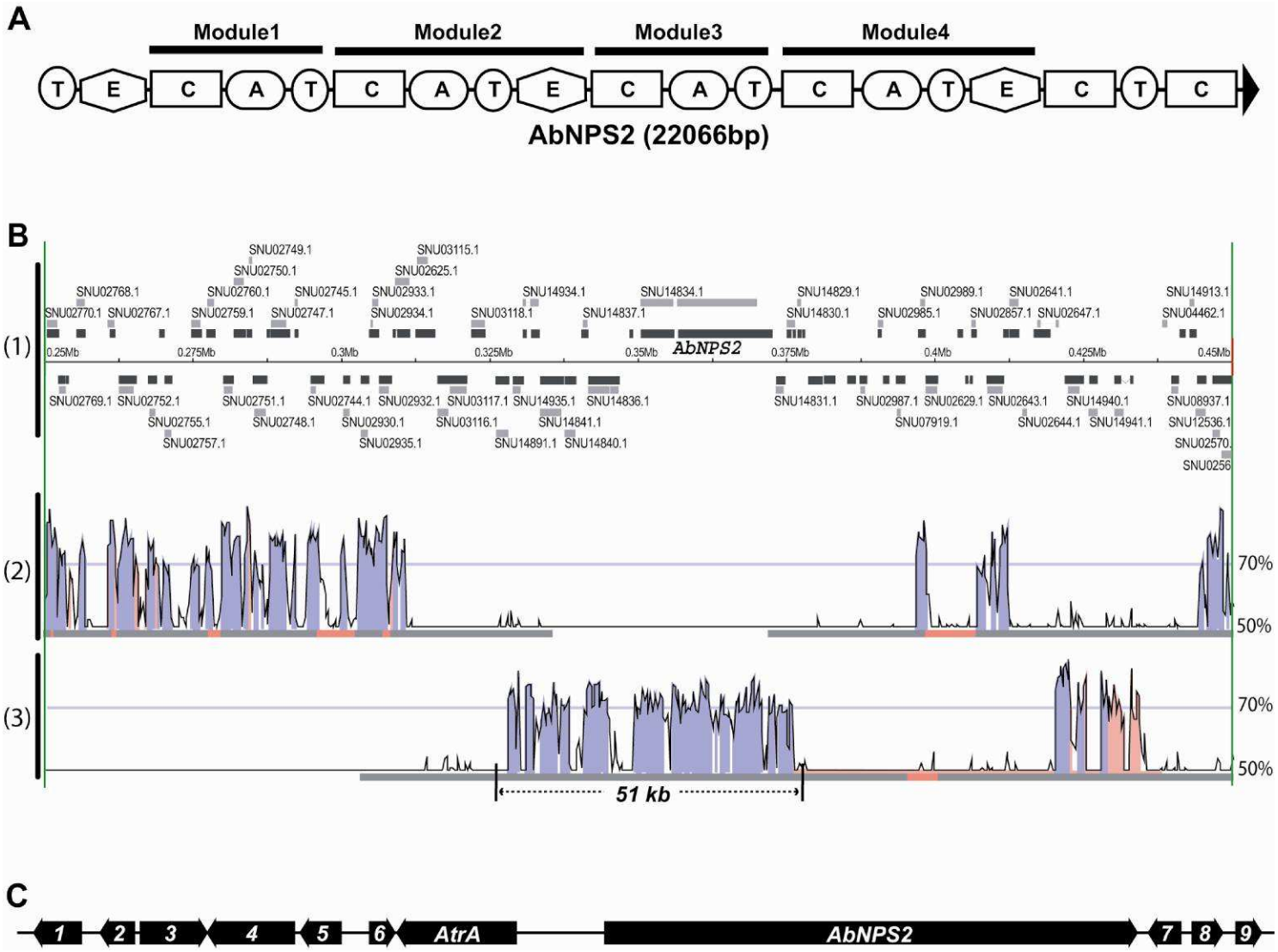
A
Module1
Module2
Module3
Module4
T E C A T C A T E C A T C A T E C T C
AbNPS2 (22066bp)
B
(1)
(2)
(3)
AbNPS2
70%
50%
51 kb
C
1 2 3 4 5 6 AtrA AbNPS2 7 8 9

**Figure 1. *AbNPS2* gene structure and micro-synteny at the *AbNPS2* locus**.
**A.** Domain and module organization of AbNPS2. The predicted protein encoded by the *AbNPS2* gene is comprised of 7195 amino acid residues. This protein contained four repeats of the conserved catalytic domain (A-domain) responsible for the activation of each constituent amino acid in the final synthesized peptide. The synthetase consists of 19 domains, organized into four modules. Abbreviations: A, adenylation; C, condensation; E, epimerization; T, thiolation.
**B.** Comparisons of gene organization between supercontig 10 in the *A. brassicicola* genome and the *Stagonospora nodorum* genome. (1) Predicted gene content in 200 kb of *A. brassicicola* genomic sequence from 250 kb to 450 kb of supercontig 10. Dark grey rectangles represent FGENESH predicted *A. brassicicola* genes (exons connected with lines). Light grey rectangles represent best genomic matches (BLASTX) to *S. nodorum* predicted proteins, which are labeled with the identifiers provided by the Broad Institute. (2) and (3) MVista/MLagan alignment to *S. nodorum* supercontig 4 (2) and supercontig 34 (3) within Broad's assembly. Only significant matches above 50% (DNA-DNA) similarity are depicted in the MVista plots.
**C.** Organization of the 51 kb genomic region near *AbNPS2* indicated at (3) of B. The arrows represent a putative gene and its transcriptional direction. For detailed information on the predicted genes within the *AbNPS2* gene cluster, see Table 2.

another segment of the genome (supercontig 34), indicating some conservation of synteny after chromosomal rearrangement (Fig. 1B).

Of particular importance is the fact that 11 of the 14 *A. brassicicola* genes syntenic to supercontig 34 of *S. nodorum* correspond to *AbNPS2* and its immediately adjacent genes (Fig. 1C). These genes are co-linear and have the same transcription orientation albeit with some gene deletions relative to the gene organization in *S. nodorum*. It is possible that the conserved gene content and order reflect a functional clustering around the *NPS* gene in both species (for instance, transporting and modifications of the NPS-derived metabolite). Surrounding the *AbNPS2* gene there

were an ABC transporter and two additional transport protein homologs including a MFS transporter and a C4-dicarboxylate transporter/malic acid transport protein. A carboxypeptidase and deoxycytidylate deaminase homologs were also found which may play roles in further modification of the peptides (Table 2).

It is important to note that at present the only two Dothideomycete draft genome sequences publicly available are that of *A. brassicicola* and *S. nodorum*. However the genomes of several other plant pathogenic Dothideomycetes, including *Leptosphaeria maculans, Mycosphaerella graminicola,* and *Pyrenophora tritici-repentis* are currently being sequenced.

**Table 2. Sequence similarities of the genes located at 51kb regions around *AbNPS2* gene**

| Gene | Putative function | Best BLASTX[a] |
|---|---|---|
| *1* | Carboxypeptidase | SNU14891.1 |
| *2* | Deoxycytidylate deaminase | SNU14935.1 |
| *3* | Ubiquitin activating enzyme E1 like (transport-related) | SNU14934.1 |
| *4* | Cell surface glycoprotein | SNU14841.1 |
| *5* | MFS (major facilitator superfamily) transporter | SNU14840.1 |
| *6* | Unknown | SNU14837.1 |
| *AtrA* | ABC (ATP binding cassette) transporter | SNU14836.1 |
| *AbNPS2* | Nonribosomal peptide synthetase | SNU14834.1 |
| *7* | C4-dicarboxylate transporter/malic acid transport protein | SNU14831.1 |
| *8* | Unknown | SNU14830.1 |
| *9* | Unknown | SNU14829.1 |

[a] Best BLASTX against *S. nodorum* sequence database

**Genealogy of *A. brassicicola* AbNPS2**

To help confirm the putative orthology of the *A. brassicicola* AbNPS2 with other Dothideomycete NPS proteins, a genealogy of adenylation domains from NPSs identified in the BLAST analyses was constructed. As seen in Fig. 2**,** adenylation domains from the putative Dothideomycete specific NPS cluster together with 100% bootstrap support in all sub-clades provided further evidence for the predicted orthology of these NPSs. In addition, the individual A domains from the orthologous NPSs are most closely related to each other, rather than other A domains from the same NPS (i.e. A1 from *A. brassicicola* is most closely related to A1 from *A. brassicae*) indicating that this NPS was likely present in the Dothideomycete ancestor. In addition, each A domain from AbNPS2 and its orthologs is most closely related to A domains from Soradariomycota and Eurotiomycota. Thus, the genealogy also suggests that the individual A domains that comprise the final AbNPS2 possibly had unique evolutionary histories including domain duplication and subsequent mutations, but most likely occurred in the Dothideomycete ancestor. The resulting structure of AbNPS2 found only to date in Dothideomycetes is likely then the result of these domain duplications and subsequent module rearrangements. However, the possibility of horizontal gene transfer or the role of gene loss from other Ascomycete lineages cannot be ruled out.

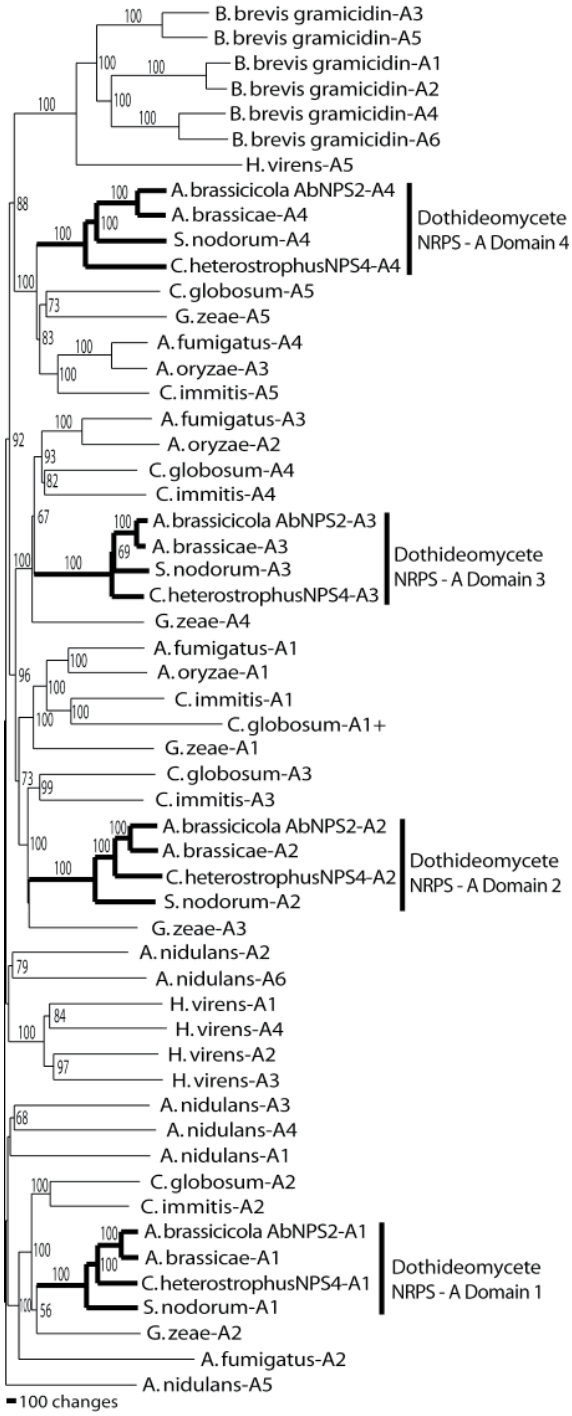


**Figure 2. Adenylation module phylogeny based on predicted amino acid sequence.** Shown are the phylogeny constructed with 50 Adenylation modules from 11 fungal and one bacterial NPS genes that have top sequence similarity among NPS in public databases. Numbers on the branches are Neighbor joining bootstrap supports over 50% based on 100 replicates.

### *AbNPS2* is expressed during the reproductive developmental phase

To examine *AbNPS2* expression in diverse fungal developmental stages, over 20 transformants were generated harboring an *AbNPS2* promoter-GFP fusion construct without disrupting the nascent *AbNPS2* gene. None of the transformants showed visible phenotypic changes discernable from the wild-type except the expression of green fluorescence. The spatial and temporal expression patterns of the *AbNPS2* were investigated by the expression of GFP in the transformants using fluorescent confocal microscopy (Fig. 3A-C). GFP expression was not detectable in the vegetative mycelia grown in GYEB media for 72 hours with gentle shaking in the dark. In contrast, GFP expression became detectable soon after the mycelia was transferred to the solid GYEA media and exposed to ambient air in the dark (Fig. 3B). During this time the mycelia started to accumulate melanin in the hyphal tips, formed conidiophores and subsequently mature conidia. The intensity of green fluorescence increased during the conidiation process reaching a maximum in young, albeit mature conidia (Fig. 3A-C).

To further the understanding of developmental phase-specific expression of *AbNPS2*, the expression of GFP was monitored during the growth of the transformants on the solid GYEA media in the dark. As the GFP expressing conidia germinated, the fluorescence signal migrated to the young germ tube (Fig. 3D and E). We speculate that the signal was due to the highly stable GFP proteins transported from the conidia, although we do not completely rule out the possibility that the gene is expressed during the early germination processes. Transmission electron microscopy supported the possibility of the cytoplasm migration from the spore to the germ tube (Inset of

Fig. 3E). The signal, however, was completely undetectable 4 hours after germination (8 hours after inoculation) and was not expressed in the hyphal networks invasively growing in and on the GYEA media. Aerial hyphae started to develop at the center of colony approximately 24 hours after inoculation (Fig. 3H). However, GFP expression was undetectable. About 36 hours after the inoculation (Fig. 3I), aerial hyphae started to differentiate into conidiophores leading to the production of mature conidia. The fluorescent signal became detectable at this time, increased during the conidiation process, and supported our earlier observations that *AbNPS2* is expressed primarily during the conidiation process. However, we cannot rule out the possibility that environmental stresses such as nitrogen or carbon starvation or other unknown factors may induce *AbNPS2* gene expression in vegetatively growing hyphae. To support data collected from the *AbNPS2* promoter-GFP fusion experiments, the *AbNPS2* transcript level was examined by northern hybridization (Fig. 3 bottom panels). Consistent with the GFP fluorescence image data, transcripts were detected in conidiophores and conidia produced in the dark but not in mycelia vegetatively-grown in both GYEB and GYEA.

*AbNPS2* gene expression was further examined *in vivo* during host plant infection (data not shown). Consistent to the *in vitro* expression patterns, GFP-fluorescence was detectable only in the conidophores and conidia but not in appressoria or in invasively growing hyphal networks. This further supported the data that *AbNPS2* is expressed during the reproductive developmental phase and not during invasive vegetative growth *in vitro* or *in vivo*.

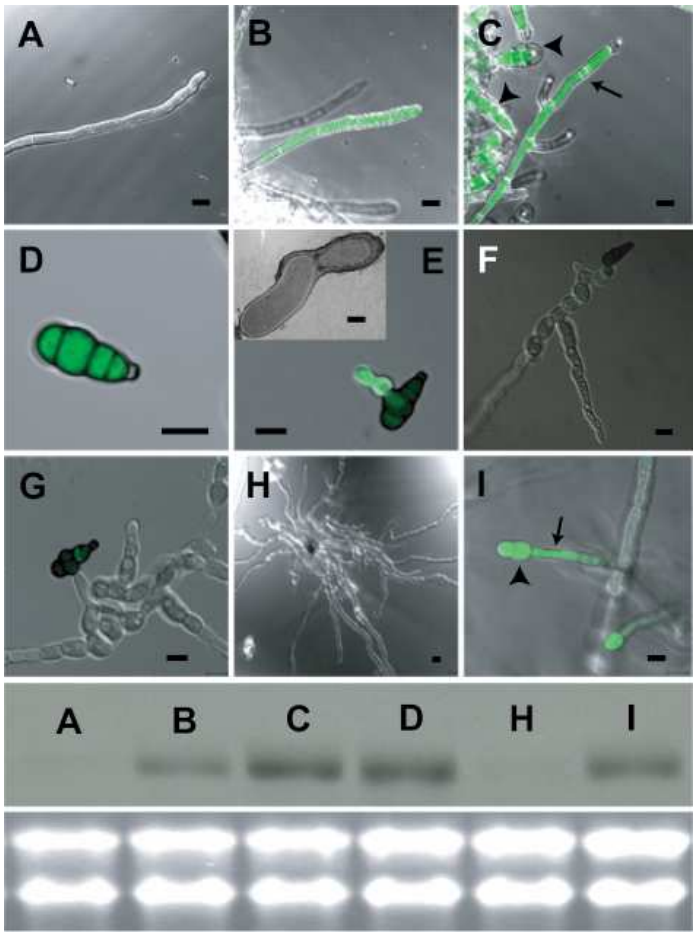


**Figure 3. Developmental phase specific expression of *AbNPS2*.** Top three panels are confocal microscopic images of GFP expression in *A. brassicicola* transformed by an *AbNPS2* promoter and a GFP coding sequence fusion construct. (A) Mycelia grown for 72 hours in GYEB liquid-culture media. (B) 8 hours after transfer from liquid culture to a solid GYEA plate. (C) 16 hours after transfer from liquid culture to a GYEA plate. The arrow and arrow heads indicate a conidiophore and conidia, respectively. (D) A typical conidium formed on a GYEA plate. (E) Early germination stage 4 hours after inoculation. Inset depicts an electron micrograph showing the cytoplasmic migration from the spore to the germ tube. (F) Vegetative growth phase 8 hours after inoculation. (G) Vegetative growth phase 12 hours after inoculation. (H) Vegetative growth phase 24 hours after inoculation. (I) Early stage of conidial development 36 hours after inoculation on GYEA plates. An arrow and arrow heads indicate a conidiophore and conidia, respectively. The bottom panels depict northern hybridization results using a 550 bp probe corresponding to the *AbNPS2* coding region used for making disruption construct. Ribosomal RNA bands stained with ethidium bromide (bottom panel) are shown for the quantitative assessment of RNA loading. Bars indicate 10 μm (A - I) and 2 μm (Inset of E).

**Targeted disruption of *AbNPS2***

To investigate the function of *AbNPS2*, we generated Six *abnps2* null mutants by disrupting the target gene using linear minimal element (LME) constructs (Cho *et al.*, 2006) (Fig. 4A). Two of the six mutants were randomly selected for phenotypic characterization in this study. PCR was initially used to identify transformants disrupted at the *AbNPS2* locus as well as ectopic mutants (data not shown). Based on these results two targeted gene disruption mutants and an ectopic insertion mutant

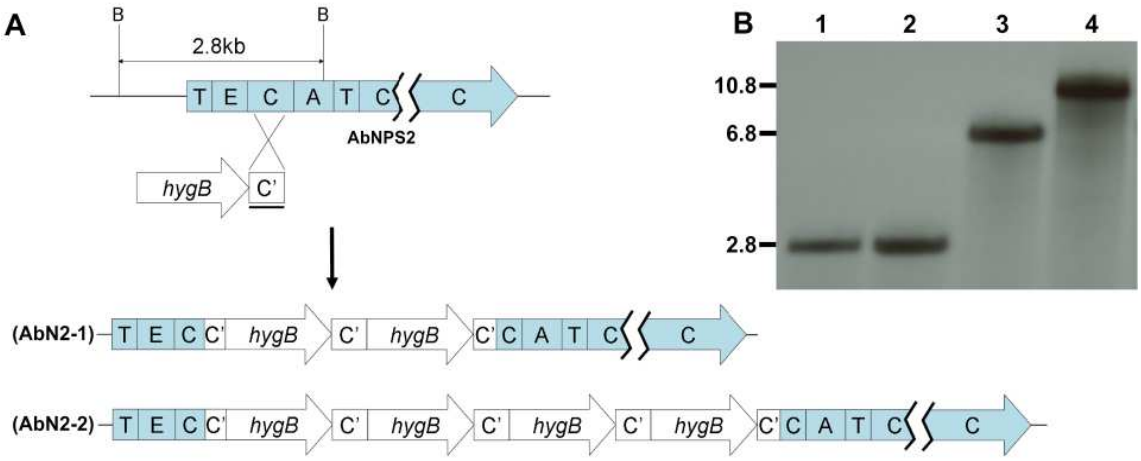


**Figure 4. Targeted disruption of the *AbNPS2* gene.** **A.** Shown are wild-type *AbNPS2* gene locus, a disruption cassette, and two loci disrupted by the cassette. The disruption cassette is a linear minimal element (LME) construct (Cho *et al.*, 2006) comprised of a hygromycin phosphotransferase (Hyg B) cassette and a partial target gene sequence. Two mutated genomic loci AbN2-1 and AbN2-4 are depicted to show two and four tandem insertions of LME constructs, respectively. **B.** Southern blot analyses sequentially showing wild-type, ectopic insertion, and two targeted gene disruption mutants. The letter B on the genomic locus indicates enzymatic sites for *Bsr*GI that were used for genomic DNA digestion. Region used for labeling the hybridization probe is marked with a bar under the LME disruption construct. Abbreviations: A, adenylation; C, condensation; E, epimerization; T, thiolation.

were verified by Southern hybridization (Fig. 4). Consistent with the PCR results, the wild-type hybridization pattern consisted of a single band (2.8 kb) shifted to 6.8 kb and 10.8 kb in AbN2-1 and AbN2-2 transformants, indicating targeted gene disruption by two and four copies of the LME constructs in each mutant, respectively (Fig. 4B). We confirmed no additional integration of the constructs in any other location in the genome by Southern hybridization with *Hyg B* probes (data not shown). In addition, we qualitatively assessed stability of *abnps2* disruption mutants by 5 sequential hyphal tip transfers to fresh PDA plates lacking Hyg B in approximately one week intervals. The repeated subculturing on PDA media did not change Hyg B resistance of the *abnps2* mutants during the repeated hyphal tip transfers after five generations.

### *abnps2* mutants show decreased hydrophobicity phenotype and an aberrant conidial cell wall

Typical wild-type conidia of *A. brassicicola* are very hydrophobic. When water drops were placed on the lawn of aerial hyphae bearing conidia, they remained beaded and easily rolled around on the surface for up to 10 hours. In contrast, water drops on the *abnps2* mutants at a similar developmental phase were immediately absorbed through the lawn of aerial hyphae and conidia. In addition to the rapid absorption of the water, the mutants showed a slightly vagarious conidial surface discernable from the wild-type under a phase contrast light microscope (data not shown). Therefore we decided to investigate the aberrant morphology of the mutant conidia using transmission electron microscopy (TEM). For the wild-type conidia the outermost layer appeared smooth and the cell wall structure appeared compact (Fig. 5 D and F). In contrast, the outermost layer of *abnps2* mutant conidia appeared fluffy

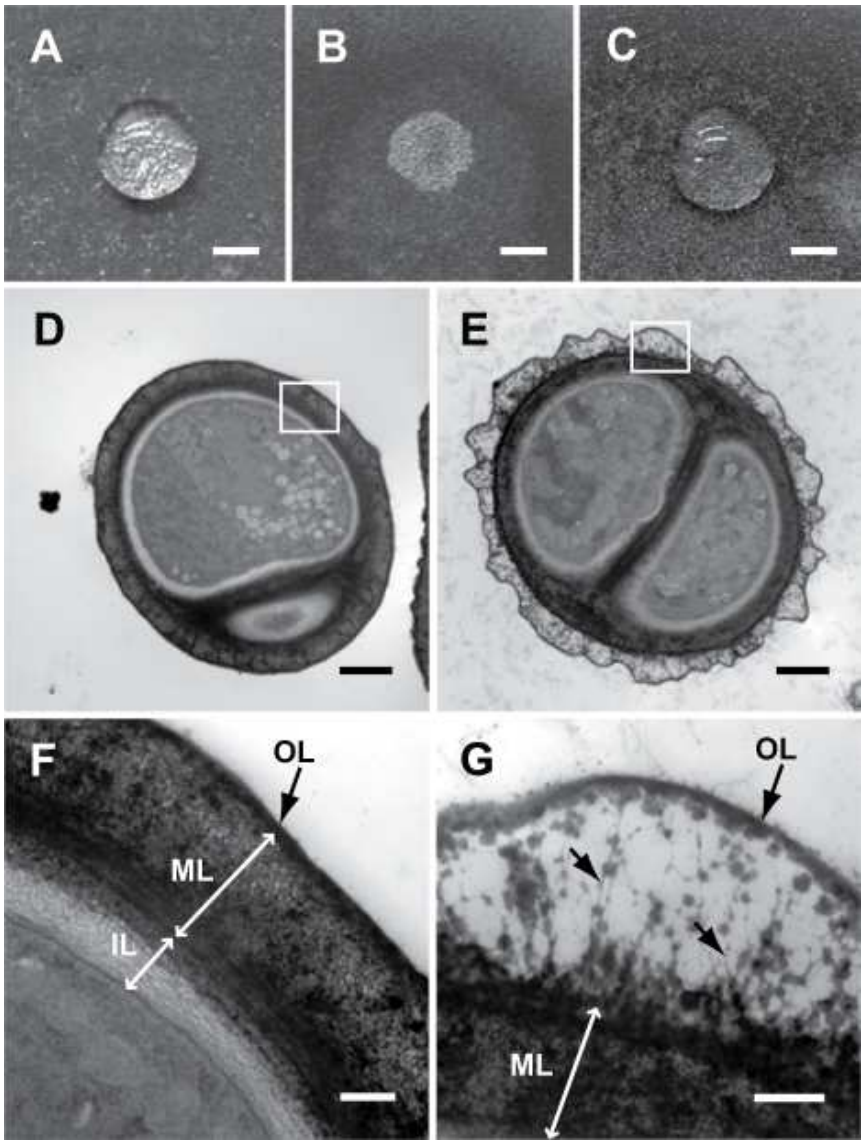


**Figure 5. Decreased hydrophobicity phenotype and electron micrographs of *abnps2* mutant.** Top panel pictures depict the fate of 30 µl water drops deposited on PDA plates covered with conidia. A. Wild-type conidia showing hydrophobic surface. B. AbN2-1 mutant conidia showing water wettable surface. C. Ectopic insertion mutant conidia showing a similar hydrophobic phenotype as the wild-type. Four pictures at the second and third panels are transmission electron micrographs depicting the aberrant ultrastructure of *abnps2* mutants (E and G), compared to the wild-type (D and F). F and G, Magnification of the rectangles in D and E, respectively. Arrow heads point to microfibrils in the middle cell wall layer. Bars indicate 20 mm (A, B, C), 2 µm (D, E) and 200 nm (F, G). Abbreviations: OL= outermost cell wall layer, ML = middle cell wall layer, IL = inner cell wall layer.

and the outermost layer of the cell wall structure was separated from the middle electron dense layer (Fig. 5E and G). There were filamentous structures, loosely connecting the detached outermost layer with the middle layer (Fig. 5G). We suspected that the AbNPS2-derived metabolite product is involved in cell wall formation and/or cell wall architecture. Specifically, it appears as though the AbNPS2-derived metabolite product may be a component or facilitates the linkage of the outermost layer and the middle layer of the fungal spore cell wall.

### *AbNPS2* is important for conidial viability and virulence

Virulence and conidia production were compared among two *abnps2* mutants, an ectopic insertion mutant and the wild-type *in vivo* on the host plant (green cabbage) leaves. When approximately 1000 (7 days old) conidia of each strain collected from PDA plates were inoculated onto detached plant leaves, the difference was negligible in the size of necrotic lesions formed. However, the disruption mutants produced approximately 40% less conidia than the wild-type and the ectopic insertion mutant (Fig. 6A). We further examined the mycelial growth rate and conidia production *in vitro* on PDA plates, however, there were no significant difference in conidial production and mycelial growth rates among all three strains (Fig. 6A). This result suggested that *abnps2* mutant is more sensitive to biological stresses imposed during plant infection than the wild-type because of its cell wall abnormalities.

To understand the biological significance of the mutant phenotype with the abnormal cell wall structures, we examined the germination rate of the mutant conidia that were collected from PDA plates after 7, 14, and 21 days of culture incubation

(DCI). On cover glasses, 7- and 14-day-old wild-type conidia germinated over 90% and the 21-day-old wild-type conidia had a 60% germination rate. There was no significant difference in the germination rates for the ectopic insertion mutant and the wild-type conidia. Germination rates of the *abnps2* mutants were lower than both the wild-type and the ectopic mutant in all three aged groups (Fig. 6). It is especially noteworthy that the germination rate precipitously decreased to 50-58% for the 14-day-old *abnps2* mutants and further decreased to 40–45% level for 21-day-old mutants. The trend of the observed decreased germination rates *in vitro* was similar *in vivo* although the average germination rate of all tests was somewhat lower than the *in vitro* assay in general. Germination rates became progressively lower as the conidia aged on the PDA plates for both wild-type and mutants. The difference between the wild-type and the mutant was in the efficiency of the germination rates. To investigate the effects of decreased germination rate in regards to pathogenicity, virulence assays were carried out with conidia collected from PDA plates after 7, 14 and 21 DCI. After the *in planta* inoculation of 500 conidia in 10 µl water, the disease severity was estimated by measuring the lesion size. Plants inoculated with conidia from 7-day-old culture of the wild-type strain and *abnps2* mutants developed almost the same size of typical black spot lesions on the leaves, but inoculations performed with 14-day-old *abnps2* mutants resulted in formation of a statistically significant smaller lesion size compared to the wild-type of same aged group. A significant reduction in lesion size on the individual leaves was even more evident in 21-day-old *abnps2* mutants 5 days after inoculation compared to the wild-type (Fig. 6D and E). In consideration of the possibility that the reduced pathogenicity of the aged mutants could result from other

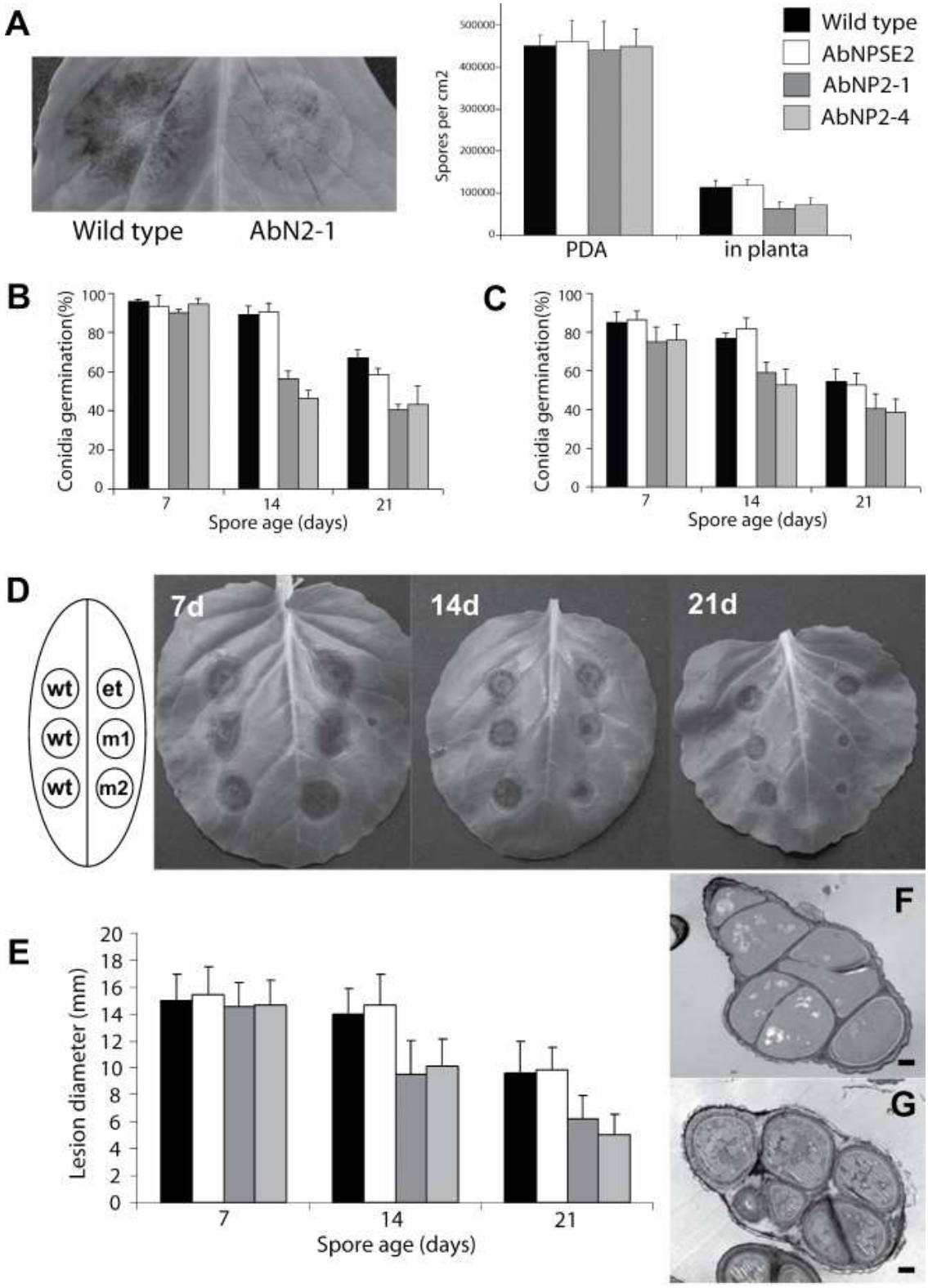
A
Wild type
AbN2-1
Spores per cm2
500000
400000
300000
200000
100000
0
PDA
in planta
Wild type
AbNPSE2
AbNP2-1
AbNP2-4
B
Conidia germination(%)
100
80
60
40
20
0
7
14
21
Spore age (days)
C
Conidia germination(%)
100
80
60
40
20
0
7
14
21
Spore age (days)
D
wt
et
wt
m1
wt
m2
7d
14d
21d
E
Lesion diameter (mm)
20
18
16
14
12
10
8
6
4
2
0
7
14
21
Spore age (days)
F
G

**Figure 6. Reduced virulence associated with reduced germination rate in *abnps2* mutant.** **A.** Conidiation test on PDA and *in vivo*. Picture (left) shows the conidiation *in vivo* of wild-type and AbN2-1 mutant strain 7 days post inoculation. **B and C.** Germination test *in vitro* (B) and *in vivo* on green cabbage (C) of wild-type, ectopic, *abnps2* mutant strains. **D and E.** Pathogenicity assay on green cabbage leaves using conidia from 7-day-(7d), 14-day-(14d), and 21-day-old (21d) culture of wild-type, ectopic, *abnps2* mutants strains. The diagram (left side of D) indicates inoculation sites of each strain. **F and G.** Electron micrographs of 21-day-old wild-type (F) and *abnps2* mutant (G) conidia. Note that the wild-type conidia were normally filled with cellular organelles, glycogen and lipid droplets, and intact intercellular walls visible (F). The lipid granules were expanded and intercellular walls aberrant in *abnps2* mutants compared to the wild-type (G). Bars indicate 2 μm. Columns and error bars on graphs represent averages and SD, respectively, of four independent experiments (A, B, C and E). Statistical analyses were performed to test the differences in germination rates and lesion diameters among the four strains by least significant difference pairwise comparisons ($p \leq 0.05$).

defectiveness of the *abnps2* mutant during infection, we closely investigated the infection process using electron microscopy. Following initial germination there were no observed differences between the wild-type and *abnps2* mutants in appressoria formation and penetration into plant epidermal cells (data not shown).

Conidia collected from PDA plates after 21 DCI were examined using transmission electron microscopy to understand the possible reason for the reduction in conidial germination rate over time in *abnps2* mutants compared to the wild-type. The wild-type conidia were filled with typical cellular organelles, glycogen and lipid droplets. The lipid granules were few in number and small in size, and an intact plasma membrane was visible (Fig. 6F). In *abnps2* mutant conidia, however, the lipid granules were largely expanded and occupied almost the entire cell (Fig. 6G). The

intercellular walls between each conidial cell component appeared relatively weakened compared to the wild-type resulting in a rounder shape of each cell similar to protoplasts that lack a cell wall.

## Discussion

The function of secondary metabolism has been a topic of lively debate. The various theories have been compared and contrasted many times (Bennett, 1995; Dietera *et al.*, 2003; Haavik, 1979; Hungria *et al.*, 2004; Keller *et al.*, 2005; Lee *et al.*, 2005; Omura *et al.*, 2001; Pfeifer and Khosla, 2001; Vanek and Janecek, 1997; Weinberg, 1971). One of the more interesting hypotheses is that secondary metabolites might function to control the ordered sequence of events that occurs during fungal differentiation (Keller *et al.*, 2005; Weinberg, 1971). Anatomic differentiation and the initiation of secondary metabolism are phase dependent and often occur simultaneously after active growth has ceased. For example, the peptide antibiotics of bacteria are usually elaborated during sporulation (Calvo *et al.*, 2002; Katz and Demain, 1977; Yu and Keller, 2005). The phase-specific development of selected polyketides, gibberellins, ergot alkaloids, penicillin, and cephalosporin has been reviewed by Martin and Demain (1978). Our studies of the *AbNPS2* gene from *A. brassicicola* strongly demonstrated the close relationship between fungal differentiation and secondary metabolism. *AbNPS2* is predicted to encode a large multifunctional enzyme putatively having a role in stabilizing the conidial cell wall and consequently affecting its viability. The putative secondary metabolite produced via AbNPS2 could serve as a physical bridge in the conidial cell wall or function as a

regulator of conidial cell wall biosynthesis. The exact nature of the role of AbNPS2 and the secondary metabolite associated with this NPS remains to be elucidated. The secondary metabolite produced by AbNPS2 may serve as a marker for the switch from the vegetative phase to the reproductive phase during fungal differentiation. This gene has a number of unique characteristics, including its expression patterns and its role in conidial development and viability.

**Structure and Genomic Organization of the AbNPS2 Region**

The predicted protein encoded by the *AbNPS2* gene was the largest protein among the identified seven NPSs in *A. brassicicola*. The identified domain structure indicated that there are four typical C-A-T or C-A-T-E elongation modules (Mootz *et al.*, 2002), allowing the insertion of two L-amino acids and two D-amino acids in the synthesized polypeptide. Work from the laboratories of Brick and Marahiel has led to the crystal structure of the N-terminal 556-amino-acid residue segment of the gramicidin S synthetase A (GrsA) (Conti *et al.*, 1997). By comparing this structure with sequences of adenylation domains to those with known amino acid specificity, a set of rules was established to predict the specificity of the adenylation domain (Stachelhaus *et al.*, 1999). By comparison with the activation domain of GrsA, it is possible to speculate that the sequences found in the four adenylation domains of AbNPS2 results in four substrate specificity pockets: one for an amino acid with positively charged side chain and three for amino acids with hydrophobic side chains. This speculation was also suggested by Guillemette (2004) with AbrePsy1 in *A. brassicae*, which is an ortholog of AbNPS2.

AbNPS2 had the unique N-terminal domain arrangement starting with a T domain instead of an A domain suggesting there are likely some other genes in the cluster that are involved in the synthesis or a possibility that these preliminary domains (T and E) may not be functional. In addition the last elongation module of AbNPS2 was followed by a C-T-C module, not by a typical terminal thioesterase (TE) domain. A deviation from the traditional module arrangement is often associated with nonlinear peptide products, which constitute a considerable fraction of the NPSs in nature (Mootz *et al.*, 2002). Another characteristic of the nonlinear NPSs can be the use of small soluble molecules such as amines to be incorporated into the nonribosomally assembled peptide. Such an incorporation needs specialized C domains since the amines lack a carboxyl group for a covalent attachment to the enzyme as thioester (Keating *et al.*, 2000a, 2000b), indicating the special use of the unusual C domains in C-T-C module. Another possibility regarding the role of C-T-C module is that AbNPS2 may use the four modules iteratively and consequently form a repeated peptide in multiples of four (Mootz *et al.*, 2002; Yuan *et al.*, 2001). For example, an iterative NPS of *Fusarium scirpi* uses its modules three times in the assembly of an enniatin (Glinski *et al.*, 2002), which has a T-C didomain at the C-terminal end like AbNPS2. It is believed that the oligomerization intermediates are stalled on this additional T domain with the C domain catalyzing both the transfer and final cyclization (Konz and Mahariel, 1999).

In many microbial systems genes responsible for secondary metabolite production, modification, and secretion are often found to be clustered (Brakhage, 1997; Keller *et al.*, 2005; Kleinkauf and von Dohren, 1996; Smith *et al.*, 1990a; Smith

*et al.*, 1990b; Yu and Keller, 2005). Here we present data suggesting that this is also the case for *AbNPS2* in *A. brassicicola*. Idenification of some transporter- and enzyme-encoding genes around *AbNPS2* and the fact that the gene organization around the *NPS* gene is conserved in both Dothideomycete species suggest the possibility of the presence of a gene cluster for the *AbNPS2* gene product and related genes in same secondary metabolite biosynthetic pathway. Keller *et al.* (2005) have hypothesized that the conservation of clustering for genes involved in the same secondary metabolite biosynthetic pathway might provide an evolutionary advantage. One possible example would be that by maintaining related genes in close proximity to each other, a hypothetical global regulator of secondary metabolism can access the gene cluster and switch on/off the whole pathway at once by mechanisms such as chromatin remodeling.

**AbNPS2 expression is related to conidiation, a reproductive developmental phase**

Filamentous fungi undergo distinct life-cycle phases of growth (accumulation of undifferentiated hyphae) and reproduction (elaboration of fruiting structures). Switching between these two phases is highly regulated (Adams and Yu, 1998; Fischer, 2002) and initiation is governed by perception of a combination of physiological and environmental conditions and cues (Calvo *et al.*, 2002). *AbNPS2* promoter-GFP fusion analysis and RNA blot analysis clearly showed that the pattern of *AbNPS2* expression is related to the conidiation process. The morphological changes associated with the reproductive phase were coupled with *AbNPS2* gene expression and the putative production of a yet to be identified secondary metabolite

produced via AbNPS2 and the products of clustered modifying genes. It has been reported that fungal secondary metabolism and sporulation (conidiation) are associated both temporally and functionally (Adams and Yu, 1998; Calvo *et al.*, 2002). Illustrating the latter, secondary metabolites in *Aspergillus* and *Fusarium* (including the mycotoxin zearalenone) are associated with the onset of sporulation (Calvo *et al.*, 2001; Mazur *et al.*, 1991). Some secondary metabolites act as pigments protecting spores (Kawamura *et al.*, 1999). Sterigmatocystin is a fungal secondary metabolites that appears to be important for sporulation in *A. nidulans* (Wilkinson *et al.*, 2004). There are many proposed and/or verified roles of fungal secondary metabolites, especially those made by NPSs (Haese *et al.*, 1993; Johnson *et al.*, 2000; Lee *et al.*, 2005; Panaccione *et al.*, 1992). For example functional analysis of *NPS6* in *C. heterostrophus* revealed that the product of this NPS may protect the fungus from oxidative stress and is critical for full virulence (Lee *et al.*, 2005).

**AbNPS2 may synthesize a conidial cell wall component**

AbNPS2 is related to surface hydrophobicity of conidia as shown in Fig. 5. Disruption of *AbNPS2* resulted in a water-soaked, easily wettable phenotype *in vitro*. Similar phenotypes were reported in several hydrophobin deletion mutants in fungi (Bell-Pedersen *et al.*, 1992; Spanu, 1998; Stringer *et al.*, 1991; van Wetter *et al.*, 1996), which suggested that the synthesized metabolic product of AbNPS2 might be related to a process of hydrophobic coating of fungal aerial structures (Wessels, 1997). In addition to the rapid absorption of the water, however, the mutants showed a slightly vagarious conidial surface discernable from the wild-type under a phase

contrast light microscope, which has never been reported for any hydrophobin-disrupted mutant. Therefore we turned our interest to the conidial cell wall itself instead of the surface hydrophobic proteins of conidia.

The cell walls of most filamentous fungi have a fibrillar structure consisting of chitin, ß-glucans, and a variety of heteropolysaccharides (De Groot *et al.*, 2005; Latge *et al.*, 1988; Perez and Ribas, 2004). Targeted mutation of *AbNPS2* resulted in aberrant conidial cell walls in *A. brassicicola*. It is very rare to obtain discernable morphological phenotypes associated with expression of the *NPS* in filamentous fungi. Furthermore most NPS products described thus far have been secreted molecules such as antibiotics, siderophores, and toxins but not structural components. The pigment melanin was the only cell wall component encoded by secondary metabolite-producing genes in fungi reported thus far (Bennett, 1983). Transmission electron microscopy showed that the outermost layer of conidial cell wall of *abnps2* mutant was separated from the original cell wall body. Our microscopic studies revealed that three layers were recognized in sections of conidia of the *A. brassicicola* wild-type strain: the innermost one electron transparent, the middle layer appearing electron dense, and the outermost layer which was very thin (15 to 20 nm thick) and also quite electron dense. This cell wall organization usually results from the intimate association of the different constituents through hydrogen bonding, hydrophobic and electrostatic interactions and even by the establishment of covalent bonds, all of them occurring in a rather precise and specific manner (Ruiz-Herrera, 1991). The electron micrographs demonstrate that the middle layer contains substantially larger amounts of amorphous compounds and intertwining microfibrils which stain more or less

strongly, whereas the outermost layer had a granular or amorphous structure of high electron density. In general, reports suggest that fibrillar polysaccharides are accumulated mostly in the inner layers of the cell walls, whereas glycoproteins are more abundant in the external layers (Wessels *et al.*, 1990). Hunsley and Burnett (1970) concluded that the external coat was made of amorphous β-glucans placed over a reticulum of glycoproteins. More internally, it was suggested, a protein layer followed where chitin microfibrils were embedded. Based on our data and these reports it is possible that the *abnps2* deletion mutants were lacking a compound connecting or attaching the glycoprotein and/or amorphous compounds in the outermost protein layer to the microfibrillar polysaccharides in the outer part of the middle layer. The presence of residues of the fibrillar net between the middle layer and the outermost layer in Fig. 5G supports the notion that the role of the secondary metabolite produced by AbNPS2 is to stabilize and make the conidial cell wall more rigid, resulting in conidia with an improved ability to survive in adverse environmental conditions.

**Implications of AbNPS2**

The mechanical and osmotic stability of most plant and microorganism cells is achieved by their cell walls, constructed of different polysaccharide moieties to which various proteins are attached. The fungal cell wall is critical for cell viability and pathogenicity (Farkas, 1985). Beyond serving as a protective shell and providing cell morphology, the fungal cell wall is a critical site for exchange and filtration of ions and proteins, as well as metabolism and catabolism of complex nutrients. Disruptions

of this protein/carbohydrate cell wall matrix have resulted in high sensitivity to osmotic lysis (Peberdy, 1990) and decreased UV tolerance (Kawamura *et al.*, 1999) of fungal cells. Disruption of *AbNPS2* resulting in cell wall abnormalities did not affect the osmotic resistance but did affect UV tolerance. Treatment with UV resulted in a 25% decrease in germination rate of the *abnps2* mutants compared to the wild-type (data not shown). In addition to environmental stresses, biological stress also affected the *abnps2* mutants. The reduced conidial reproduction *in vivo* suggests that *abnps2* mutant is more sensitive to biological stress than the wild-type. In Fig. 5A, we observed the lesion size of the wild-type and *abnps2* mutants were highly similar, demonstrating the vegetative invasive growth of the wild-type and *abnps2* mutants *in vivo* was the same but only when inoculations were performed with young conidia. However, the factors in green cabbage causing reduced conidial reproduction rate of *abnps2* mutants remains to be revealed. The *abnps2* mutants were tested for increased sensitivity *in vitro* to the Arabidopsis antimicrobial phytoalexin camalexin, but no differences were observed between mutants and wild-type (data not shown).

As conidia aged *in vitro*, the frequency of conidial germination decreased in *abnps2* mutants, but the wild-type maintained a germination rate at a relatively high level in each test group compared to *abnps2* mutants. These germination assay results were consistent in *in vitro* and *in vivo* assays, suggesting that pathogenicity of older conidia of *abnps2* mutants might be less virulent mainly due to a decrease in germination rate. In some previous experiments, it was reported that decreased germination rate resulted in reduced pathogenicity (Kim *et al.*, 2005; Solomon *et al.*,

2004). In fact, virulence tests with *abnps2* mutants revealed a significant reduction in lesion size compared to the wild-type when aged spores were used in experiments. This result is supported by ultrastructural analysis demonstrating that 21-day-old *abnps2* mutant conidia were abnormal. Autolysis-like phenomena had occurred in the conidia of *abnps2* mutants, in which formation of numbers of lipid bodies and degradation of intercellular wall occurred. Although the precise biochemical mechanism underlying these phenomena is not known, similar phenomena have been reported in other fungi. These include mature basidiospores with fully grown hilar appendix (Yoon and McLaughlin, 1979) and old aged fungal hyphae grown on the media lacking nitrogen (Kamisaka *et al.*, 2004). In addition, five different genera of filamentous fungi were incubated for 60 days, which resulted in 23.5-87.3% degree of cell autolysis. The secretion of the lytic enzymes was consistent with the degree of autolysis in each fungus (Lahoz *et al.*, 1976). Our data suggests that the presence of many lipid bodies and the degradation of conidial cell wall in *abnps2* mutants resulted from premature aging of conidia accompanied with autolysis-like phenomena. The relatively weak cell wall of *abnps2* mutants might not be sufficient to prevent premature aging of conidia. Fungal cells have significant internal turgor pressure and thus undergo lysis when their cell walls are even slightly perturbed (Selitrennikoff, 2001). However, whether the outermost cell wall layer affects conidial viability remains unanswered. In addition, our evidence showing that high numbers of abnormally large lipid bodies filling the cytoplasm of mutant conidia are related to cell autolysis has not been reported yet in any microorganisms. Although further experiments should be performed to answer these questions, we speculate that the

relatively rapid decrease in germination rate and pathogenicity of the *abnps2* mutant is due to loss of a cell wall component or cell wall integrity in general. In conclusion, *AbNPS2*, a gene encoding a NPS synthesizing a secondary metabolite, plays significant roles in conidial cell wall construction and conidial development. This may be one physiological mechanism associated with the Dothideomycetes, a taxonomic group which harbors many important plant pathogenic genera, that allows for enhanced fitness and to preserve its asexual structures in space and time.

# Materials and Methods

### *Fungal strains, media, and fungal culture*

*A. brassicicola* isolate ATCC96836, the isolate used for whole genome shotgun sequencing was used in this study. *A. brassicicola* was cultured on 3.9% (w/v) potato dextrose agar (PDA) (Difco, Kansas City, Mo, USA) and 1% (w/v) glucose 0.5% (w/v) yeast extract (GYEB) broth. Fungi were grown at 25°C in the dark for both solid and liquid culture.

### *Annotation of region surrounding AbNPS2*

The final genomic sequence corresponding to *AbNPS2* was deduced following closure of two small gaps in the genome using straightforward PCR approaches and DNA sequencing in our laboratory. The predicted *AbNPS2* coding and protein sequences are available (see supplementary materials). The 200 kb region surrounding the *AbNPS2* locus was annotated in-house using an EnsEMBL annotation pipeline (Potter *et al.*, 2004) that included *ab initio* gene prediction with FGENESH (Salamov and

Solovyev, 2000) trained for *A. brassicicola*, BLASTX searches of the genomic sequence against the Uniref90 database (www.uniprot.org), HMM searches of FGENESH predicted peptides against the PFAM and TIGRFAM databases and BLASTP searches of the predicted peptides against the proteomes of other available fungal genomes (as of June 2006). The predicted function of the annotated genes in the region was determined from the combined information obtained from the BLASTX, BLASTP, and HMM results.

***Survey of micro-synteny around AbNPS2***

Candidates of homologs for the predicted genes in the *A. brassicicola* 200 kb genomic sequence flanking *AbNPS2* gene were identified from the fungal species whose proteomes were available as of June 2006 (http://fungal.genome.duke.edu/). Once the list of putative homologs was assembled for all predicted genes, it was sorted according to originating species and manually checked for evidence of co-linearity in the given species (protein identifier numbers follow a linear order in the supercontigs of sequenced fungal genomes). Among the species surveyed only predicted proteins from *S. nodorum* supercontigs 4 and 34 showed evidence of synteny. Finally, the 200 kb continuous genomic sequence was aligned to supercontigs 4 and 34 of the *S. nodorum* genome sequence using MLAGAN and shuffle-LAGAN (Brudno *et al.*, 2003a; Brudno *et al.*, 2003b) and visualized with the online version of MVISTA (Mayor *et al.*, 2000).

***Mining AbNPS2 orthologs from fungal proteome databases***

Seven NPS genes in *A. brassicicola* (*AbNPS1* - *AbNPS7*) were identified in the partially assembled genome sequence. The predicted amino acid sequence of *A. brassicicola* AbNPS2 was used as a query against a database of fungal proteomes (kindly provided by Dr. Jason E. Stajich, Duke University Medical Center and available at http://fungal.genome.duke.edu/) with the BLASTP algorithm (Altschul *et al.*, 1990; Altschul *et al.*, 1997). This database contains the predicted proteomes of 53 sequenced fungi (list available at above website). To this database, the predicted proteome of *A. brassicicola* and the model plant *Arabidopsis thaliana* were added. In addition, BLASTP against the NCBI Genbank non-redundant (NR) database was also performed. BLAST hits were manually examined by visually comparing alignments. It was determined that bit scores ≥ 2000 correlated with ~40% amino acid identity and these hits would be further examined for potential orthology. Domain and module organization of predicted NPS amino acid sequences were annotated using HMMER results from a search using NPS amino acid sequences as queries against the Pfam database (E value cutoff $1e^{-03}$) (Finn *et al.*, 2006). In addition, NPS amino acid sequences were used as queries against the online database of non-ribosomal peptide synthetases (http://203.90.127.50/~zeeshan/webpages/nrpsall.html) (Ansari *et al.*, 2004). Discrepancies between the two prediction algorithms were resolved by manual inspection of the amino acid sequences of the disputed domain. The predicted NPS code for adenylation domains was determined using the server available at http://www-ab.informatik.uni-tuebingen.de/toolbox/index.php?view=domainpred (Rausch *et al.*, 2005; Stachelhaus *et al.*, 1999).

### *Genealogy of A. brassicicola AbNPS2*

In order to examine the genealogy of AbNPS2, the most conserved domain of fungal NPS enzymes, the adenylation domain (~500 bp) was utilized. Fungal NPSs were chosen based on the BLAST analyses, and a multiple amino acid sequence alignment of 50 fungal NPS A domains from 11 species of fungi plus six additional bacterial A domains was created using CLUSTALX and the BLOSUM62 scoring matrix (Thompson *et al.*, 1997). A domains were defined with HMMER and their amino acid sequences extracted with a Perl script utilizing BioPerl (Stajich *et al.*, 2002). The multiple alignment was edited manually to include five known A domain motifs found in fungal NPS A domains, this alignment was used to create unrooted neighbor joining (NJ) and parsimonious trees using PFAAT and PHYLIP (http://evolution.genetics.washington.edu/phylip.html) packages respectively (Johnson *et al.*, 2003). The NJ tree was virtually identical to the tree created with parsimony analysis and is presented here. Columns in the multiple alignment with >50% gaps were excluded from the NJ tree. Bootstrapping with 100 replications was performed with the unrooted NJ tree.

### *DNA isolation and Southern hybridization*

*A. brassicicola* was clutured for 2-3 days in 50 ml GYEB media. Approximately 0.2 g mycelia was harvested and filtered with Miracloth (Calbiochem, Darmstadt, Germany), semi dried with paper towels, and ground into fine powder with a mortar and pestle in the presence of liquid nitrogen. Total genomic DNA from was extracted using Plant DNeasy kit (Qiagen, Palo Alto, CA).

A total 2-3 μg of genomic DNA was digested with an endonuclease *Bsr*GI (New England BioLab, Beverly, MA). The digested DNA was size-fractionated on a 0.7% agarose gel, followed by overnight transfer to a Hybond $N^+$ nylon membrane (Amersham Pharmacia Biotech, Buckinghamshire, UK). The transferred DNA was U.V. cross-linked at 120 mJ (Spectronics corporation, Westbury, NY) to the membrane and subsequently hybridized with 0.5 kb long probes that were amplified from *A. brassicicola* genomic DNA using PCR DIG Probe Synthesis Kit (Roche Diagnostics, Mannheim, Germany). The entire procedure from the hybridization to the signal detection was carried out with Block and Wash Buffer Set and CDP-Star in the DIG Detection Kit (Roche Diagnostics, Mannheim, Germany) according to the manufacturer's protocols with following specifics. Hybridization was performed at 50°C. After the hybridization, the membrane was briefly rinsed three times at room temperature in wash solution 1 (1XSSC, 0.1% SDS) and stringently washed at 68°C in wash solution 2 (0.1X SSC, 0.1% SDS) for 30 min.

***RNA isolation and Northern hybridization***

Total RNA for expression analysis was prepared from fungal mycelia grown under the following condition: shake liquid glucose-yeast extract broth (GYEB) medium, 25°C, 72 h for germination and vegetative growth. Conidiating aerial structures containing aerial mycelia, conidiophores and conidia were collected at 8 h and 16 h post-incubation as follows: about 20 mycelial balls collected from the above 72 h liquid culture were spread onto sterilized filter paper and incubated for conidiation. Conidia were harvested from strains grown on glucose-yeast extract agar (GYEA) plates for 5

days at 25°C and were washed with sterile water 3 times and collected by centrifugation for RNA extraction. For expression analysis for different fungal developmental stages 100 µl of conidial suspension ($5 \times 10^5$ conidia/ml) was spread onto GYEA plates and incubated for germination and conidiation. After 4, 8, 12, 24 and 36 hours after incubation conidia which did not germinate or show relatively late growth rate were removed under the microscope and the conidia and colonies growing well on GYEA were collected and ground in the presence of liquid nitrogen.

Total RNA was extracted using Plant RNeasy Kit (Qiagen, Palo Alto, CA), followed by DNase digestion for 15 minutes at 37°C using DNase Mini Kit (Promega, Madison, WI). Total RNA (20 µg) was fractionated on a 1.5% formaldehyde agarose gel and the gel was stained with ethidium bromide to assess quality and quantity of the RNA. The fractionated total RNA was transferred overnight from the agarose gel onto a Hybond $N^+$ nylon membrane (Amersham Pharmacia Biotech, Buckinghamshire, UK). Hybridization and detection procedures after the RNA transfer were carried out as described in the Southern hybridization section except that hybridization and washing was carried out at 42°C.

***AbNPS2 promoter and GFP fusion-protein construct***

Two primers were designed at 1 bp position with an exogenous *Apa*I site (tagggcccATGGTGAGCAAGGGCGAGGA) and at 2370 bp position with an exogenous *Hind*III site (acaagcttTGGTTCCCGGTCGGCATCTA) in relation to the GFP start codon. These primers were used to amplify GFP coding region and Hyg B cassette from template plasmids pCG16G6-Nac (Cho *et al.*, 2006). The PCR products

were cloned at the corresponding multiple cloning sites in pBluscript (SK+) to create pCB16G6-PF. Another set of primers were designed at -1 bp position (upstream of start codon) with an exogenous *Apa*I site (gagggcccCGTGGGCCGTGTGTGGTTTC) and at approximately the -1000 bp position with an exogenous *Kpn*I (gtggtaccCAGCCTCGCAGACACTCGAC) in relation to the *AbNPS2* start codon. These primers were used to amplify the *AbNPS2* promoter region and the subsequent PCR products were cloned in the corresponding multiple cloning sites of pCB16G6-PF to make pCB16g6-N2. The pCB16G6-N2 sequentially contains 1 kb *AbNPS2* promoter, a GFP open reading frame, and Hyg B cassette between M13 forward and the M13 reverse priming sites. All cloning and plasmid production were carried out as described in the following section. A fragment containing 1 kb *AbNPS2*-promoter region, GFP cassettes and Hyg B cassettes were amplified from pCB16G6-N2 with M13 forward and M13 reverse primers. The PCR products were transformed in the wild-type *A. brassicicola* to make *AbNPS2* promoter-GFP fusion mutants.

***Generation of targeted gene disruption construct and fungal transformation***

Based on *AbNPS2* sequence identified in the partially assembled *A. brassicicola* genome sequence, two primers were designed at the 911 bp position with an exogenous enzyme site *Hin*dIII (cttgaagcttTCCTTCCTGCTGTCGATGTT) and at the 1441 bp position with an exogenous *Xba*I site (ccattctagaATGCGTCTGGGAATTGGCAC) in relation to the putative start codon. These primers were used to amplify a 550 bp partial target gene from the genomic DNA. PCR products were digested with *Hin*dIII and *Xba*I, and ligated at the

corresponding multiple cloning sites in pCB1636 (Sweigard *et al.*, 1997). The ligation was transformed in *E. coli* strain DH5α (Invitrogen, Carlsbad, CA). The plasmid was isolated via miniprep (Qiagen, Palo Alto, CA) and sequence verified for the presence of insert and Hyg B cassette and used as templates for PCR amplification using M13 forward and M13 reverse primers. The PCR product was purified with PCR Cleanup kit (Qiagen, Palo Alto, CA) and further concentrated to 1 μg/μl under vacumn before fungal transformation.

Fungal transformation was carried out with linear PCR products based on the transformation protocol described previously (Cho *et al.*, 2006).

***Surface hydrophobicity assay***

The strains to be assayed were plated onto PDA and incubated at 25°C until sporulation. Sterile distilled water (30 μl) was placed on the surface of cultures and the plates were incubated for 30 min at room temperature (RT).

***Electron microscopy***

Conidia of wild-type strain ATCC96836 and *Abnps2* mutant AbN2-1 were released in sterile water from 7-day-old and 21-day-old PDA plates and collected by centrifugation at 5000 x g for 10 min. The conidial pellet was coated with 0.8% agarose and fixed in modified Karnovsky's fixative containing 2% paraformaldehyde and 2% (v/v) glutaraldehyde in 0.05 M sodium cacodylate buffer (pH 7.2) overnight at 4°C. After washing three times with 0.05 M sodium cacodylate buffer (pH 7.2) for 10 min each, samples were post-fixed with 1% (w/v) osmium tetraoxide in the same buffer for 2 hours at 4°C. The post-fixative was removed by washing briefly twice

with distilled water at room temperature and the samples were *en bloc* stained with 0.5% uranyl acetate overnight at 4°C. Then the samples were dehydrated in a graded ethanol series and embedded in Eppon resin. Ultrathin sections cut from the Eppon-embedded material with ultramicrotome (MT-X, RMC, USA) were collected on carbon-coated grids, stained with 2% uranyl acetate for 3 min, and with Reynold's lead solution (Reynolds, 1963) for 3 min. Examination was conducted with a JEM-1010 (JEOL, Tokyo, Japan) electron microscope operating at 60 kV.

***Confocal microscopy***

*AbNPS2* promoter-GFP fusion transformants were grown on GYEA plate and in GYEB broth, and prepared exactly the same as the RNA blotting samples for the confocal microscopy. Inverted laser scanning microscope (LSM-510, Carl Zeiss, Göttingen, Germany) and an argon ion laser for excitation at 488 nm wavelength and GFP filters for emission at 515–530 nm were used for this experiment. The imaging parameters used produced no detectable background signal from any source other than from GFP. Confocal images were captured using LSM-510 software (version 3.5; Carl Zeiss) and were recorded simultaneously by phase contrast microscopy and fluorescent confocal microscopy. Phase contrast images were captured with a photomultiplier for transmitted light using the same laser illumination for fluorescence.

***Conidiation assays***

The conidiation rates were compared between the wild-type, *abnps2* mutants, and ectopic insertion mutants. We examined the rates during the development *in vitro* on

PDA plates and *in vivo* on plants. For the *in vitro* assay, fungi were cultured on PDA plates with a photoperiod of 16 h using fluorescent lights for 7 days and conidia were harvested in sterile water. For the *in vivo* assay 7 day-grown 1000 conidia in 10 µl water were inoculated on detached green cabbage leaves, followed by 7 days of incubation at room temperature with 100% relative humidity under long-day conditions (16-h light/8-h dark cycle). Conidia from a size of $1cm^2$ infected leaf fragment were released in 5 ml water. Conidia produced on lesions were harvested by vortexing the test tube vigorously. Leaves were removed, and the conidia-containing suspensions were centrifuged at 5000 x g for 15 min. The conidia were resuspended in 200 µl of water, serially diluted, and counted using a hemacytometer.

***Germination rate comparisons***

Conidial germination was measured on cover glasses (Fishier Scientific, Hampton, NH, USA) and plant leaf surfaces. Conidia were harvested from 7-day-old, 14-day-old and 21-day-old cultures on PDA in sterile distilled water and adjusted to $1 \times 10^4$ conidia per ml. Drops (30 µl) were placed on cover glasses and detached leaf segments, then placed in a moistened box and incubated at RT for 36 h on cover glasses and 8 h on detached leaf segments. *In vivo* conidial germination was measured as follows: the leaf fragments with conidial drops were transferred into a test tube containing 2 ml of water, the test tube was vortexed vigorously to release conidia, and conidia were harvested from the test tube by pipetting. The percentage of germinated conidia was determined by microscopic examination of at least 100 conidia per replicate in at least three independent experiments, with three replicates per treatment.

Statistical analyses were performed to test the differences in germination rates among the four strains by least significant difference pairwise comparisons ($p \leq 0.05$).

***Virulence tests***

To test virulence, conidia of fungi were harvested from PDA agar plates incubated for either 7 days, 14 days or 21 days at 25°C, and suspended in sterile water at a concentration of $5 \times 10^4$ conidia per ml. Conidial suspensions (10 µl) were applied as drops on the surface of middle-aged leaves (fifth through sixth leaf stages). Inoculated plants were placed in a plastic box at RT and incubated at 100% humidity for 24 h in the dark, and then followed with a photoperiod of 16 h using fluorescent lights for 4 days. Lesion diameters were then measured. Statistical analyses were performed to test the differences in lesion diameters among the four strains by least significant difference pairwise comparisons ($p \leq 0.05$).

# Literature Cited


Adams, T.H. and Yu, J.H. (1998) Coordinate control of secondary metabolite production and asexual sporulation in *Aspergillus nidulans*. *Curr. Opin. Microbiol.* 1, 674-677.

Agrios, G.N. (1997) *Plant Pathology.* San Diego, CA: Academic Press.

Altschul, S.F., Gish, W., Miller, W., Myers, E.W. and Lipman, D.J. (1990) Basic local alignment search tool. *J. Mol. Biol.* 215, 403-410.

Altschul, S.F., Madden, T.L., Schaffer, A.A., Zhang, J., Zhang, Z., Miller, W. and Lipman, D.J. (1997) Gapped BLAST and PSI-BLAST: a new generation of protein database search programs. *Nucleic Acids Res.* 25, 3389-3402.

Ansari, M.Z., Yadav, G., Gokhale, R.S. and Mohanty, D. (2004) NRPS-PKS: a knowledge-based resource for analysis of NRPS/PKS megasynthases. *Nucleic Acids Res.* 32, W405-413.

Bell-Pedersen, D., Dunlap, J.C. and Loros, J.J. (1992) The Neurospora circadian clock-controlled gene, *ccg-2*, is allelic to eas and encodes a fungal hydrophobin required for formation of the conidial rodlet layer. *Genes Dev.* 6, 2382-2394.

Bennett, J.W. (1983) Differentiation and secondary metabolism in mycelial fungi. In *Secondary Metabolism and Differentiation in Fungi*. Vol. 5. Bennett, J.W. and Ciegler, A. (eds). New York: Marcel Dekker, pp. 1-32.

Bennett, J.W. (1989) Mycotoxin research: 1989. *Mycopathologia,* 107, 65-66.

Bennett, J.W. (1995) From molecular genetics and secondary metabolism to molecular metabolites and secondary genetics. *Can. J. Bot.-Revue Canadienne De Botanique,* 73, S917-S924.

Brakhage, A.A. (1997) Molecular regulation of penicillin biosynthesis in *Aspergillus (Emericella) nidulans*. *FEMS Microbiol. Lett.* 148, 1-10.

Braverman, Y. (1979) Experiments on direct and secondary poisoning by fluoroacetamide (1081) in wildlife and domestic carnivores. *J. Wildl. Dis.* 15, 319-325.

Brudno, M., Do, C.B., Cooper, G.M., Kim, M.F., Davydov, E., Green, E.D., Sidow, A. and Batzoglou, S. (2003a) LAGAN and Multi-LAGAN: efficient tools for large-scale multiple alignment of genomic DNA. *Genome Res.* 13, 721-731.

Brudno, M., Malde, S., Poliakov, A., Do, C.B., Couronne, O., Dubchak, I. and Batzoglou, S. (2003b) Glocal alignment: finding rearrangements during alignment. *Bioinformatics*, 19 Suppl 1, i54-62.

Calvo, A.M., Gardner, H.W. and Keller, N.P. (2001) Genetic connection between fatty acid metabolism and sporulation in *Aspergillus nidulans*. *J. Biol. Chem.* 276, 25766-25774.

Calvo, A.M., Wilson, R.A., Bok, J.W. and Keller, N.P. (2002) Relationship between secondary metabolism and fungal development. *Microbiol. Mol. Biol. Rev.* 66, 447-459.

Challis, G.L. and Ravel, J. (2000) Coelichelin, a new peptide siderophore encoded by the *Streptomyces coelicolor* genome: structure prediction from the sequence of its non-ribosomal peptide synthetase. *FEMS Microbiol. Lett.* 187, 111-114.

Cho, Y., Davis, J.W., Kim, K.H., Wang, J., Sun, Q.H., Cramer, R.A., Jr. and Lawrence, C.B. (2006) A high throughput targeted gene disruption method for *Alternaria brassicicola* functional genomics using linear minimal element (LME) constructs. *Mol. Plant-Microbe Interact.* 19, 7-15.

Ciegler, A. and Lindenfelser, L.A. (1969) An antibiotic complex from Alternaria brassicicola. *Experientia,* 25, 719-720.

Conti, E., Stachelhaus, T., Marahiel, M.A. and Brick, P. (1997) Structural basis for the activation of phenylalanine in the non-ribosomal biosynthesis of gramicidin S. *Embo J.* 16, 4174-4183.

Cosmina, P., Rodriguez, F., de Ferra, F., Grandi, G., Perego, M., Venema, G. and von Sinderen, D. (1993) Sequence and analysis of the genetic locus responsible for surfactin synthesis in *Bacillus subtilis*. *Mol. Microbiol.* 8, 821-831.

Davies, J. (1990) What are antibiotics-archaic functions for modern activities. *Mol. Microbiol.* 4, 1227-1232.

De Groot, P.W., Ram, A.F. and Klis, F.M. (2005) Features and functions of covalently linked proteins in fungal cell walls. *Fungal Genet. Biol.* 42, 657-675.

Dean, R.A., Talbot, N.J., Ebbole, D.J., Farman, M.L., Mitchell, T.K., Orbach, M.J., Thon, M., Kulkarni, R., Xu, J.R., Pan, H., Read, N.D., Lee, Y.H., Carbone, I., Brown, D., Oh, Y.Y., Donofrio, N., Jeong, J.S., Soanes, D.M., Djonovic, S., Kolomiets, E., Rehmeyer, C., Li, W., Harding, M., Kim, S., Lebrun, M.H., Bohnert, H., Coughlan, S., Butler, J., Calvo, S., Ma, L.J., Nicol, R., Purcell, S., Nusbaum, C., Galagan, J.E. and Birren, B.W. (2005) The genome sequence of the rice blast fungus *Magnaporthe grisea*. *Nature,* 434, 980-986.

Dietera, A., Hamm, A., Fiedler, H.P., Goodfellow, M., Muller, W.E., Brun, R., Beil, W. and Bringmann, G. (2003) Pyrocoll, an antibiotic, antiparasitic and antitumor compound produced by a novel alkaliphilic *Streptomyces* strain. *J. Antibiot. (Tokyo)* 56, 639-646.

Farkas, V. (1985) The fungal cell wall. In *Fungal protoplasts: applications in genetics and biochemistry*. Peberdy, J.F. and Ferenczy, L. (eds). New York: Dekker, pp. 3.

Finn, R.D., Mistry, J., Schuster-Bockler, B., Griffiths-Jones, S., Hollich, V., Lassmann, T., Moxon, S., Marshall, M., Khanna, A., Durbin, R., Eddy, S.R.,

Sonnhammer, E.L. and Bateman, A. (2006) Pfam: clans, web tools and services. *Nucleic Acids Res.* 34, D247-251.

Fischer, R. (2002) Conidiation in *Aspergillus nidulans*. In *Molecular Biology of Fungal Development*. Osiewacz, H.D. (ed). New York: Marcel Dekker, pp. 59-86.

Galagan, J.E., Calvo, S.E., Borkovich, K.A., Selker, E.U., Read, N.D., Jaffe, D., FitzHugh, W., Ma, L.J., Smirnov, S., Purcell, S., Rehman, B., Elkins, T., Engels, R., Wang, S., Nielsen, C.B., Butler, J., Endrizzi, M., Qui, D., Ianakiev, P., Bell-Pedersen, D., Nelson, M.A., Werner-Washburne, M., Selitrennikoff, C.P., Kinsey, J.A., Braun, E.L., Zelter, A., Schulte, U., Kothe, G.O., Jedd, G., Mewes, W., Staben, C., Marcotte, E., Greenberg, D., Roy, A., Foley, K., Naylor, J., Stange-Thomann, N., Barrett, R., Gnerre, S., Kamal, M., Kamvysselis, M., Mauceli, E., Bielke, C., Rudd, S., Frishman, D., Krystofova, S., Rasmussen, C., Metzenberg, R.L., Perkins, D.D., Kroken, S., Cogoni, C., Macino, G., Catcheside, D., Li, W., Pratt, R.J., Osmani, S.A., DeSouza, C.P., Glass, L., Orbach, M.J., Berglund, J.A., Voelker, R., Yarden, O., Plamann, M., Seiler, S., Dunlap, J., Radford, A., Aramayo, R., Natvig, D.O., Alex, L.A., Mannhaupt, G., Ebbole, D.J., Freitag, M., Paulsen, I., Sachs, M.S., Lander, E.S., Nusbaum, C. and Birren, B. (2003) The genome sequence of the filamentous fungus *Neurospora crassa*. *Nature,* 422, 859-868.

Glinski, M., Urbanke, C., Hornbogen, T. and Zocher, R. (2002) Enniatin synthetase is a monomer with extended structure: evidence for an intramolecular reaction mechanism. *Arch. Microbiol.* 178, 267-273.

Gloer, J.B., Poch, G.K., Short, D.M. and McCloskey, D.V. (1988) Structure of brassicicolin A: a novel isocyanide antibiotic from the phylloplane fungus *Alternaria brassicicola*. *J. Org. Chem.* 53, 3758-3761.

Guillemette, T., Sellam, A. and Simoneau, P. (2004) Analysis of a nonribosomal peptide synthetase gene from *Alternaria brassicae* and flanking genomic sequences. *Curr. Genet.* 45, 214-224.

Haavik, H.I. (1979) On the physiological meaning of secondary metabolism. *Folia Microbiol. (Praha)* 24, 365-367.

Haese, A., Schubert, M., Herrmann, M. and Zocher, R. (1993) Molecular characterization of the enniatin synthetase gene encoding a multifunctional enzyme catalysing N methyldepsipeptide formation in *Fusarium scirpi*. *Mol. Microbiol.* 7, 905-914.

Horinouchi, S. and Beppu, T. (1990) Gene expression in Streptomyces. *Tanpakushitsu Kakusan Koso,* 35, 2567-2583.

Humpherson-Jones, F.M. and Phelps, K. (1989) Climatic factors influencing spore produciton in *Alternaria brassicae* and *Alternaria brassicicola*. *Ann. appl. Biol.* 114, 449-458.

Hungria, M., Nicolas, M.F., Guimaraes, C.T., Jardim, S.N., Gomes, E.A. and Vasconcelos, A.T. (2004) Tolerance to stress and environmental adaptability of *Chromobacterium violaceum*. *Genet. Mol. Res.* 3, 102-116.

Hunsley, D. and Burnett, J.H. (1970) The ultrastructure architecture of the walls of some hyphal fungi. *J. Gen. Microbiol.* 62, 203.

Hynes, M.J. (2003) The *Neurospora crassa* genome opens up the world of filamentous fungi. *Genome Biol.* 4, 217.

Johnson, J.M., Mason, K., Moallemi, C., Xi, H., Somaroo, S. and Huang, E.S. (2003) Protein family annotation in a multiple alignment viewer. *Bioinformatics*, 19, 544-545.

Johnson, R.D., Johnson, L., Itoh, Y., Kodama, M., Otani, H. and Kohmoto, K. (2000) Cloning and characterization of a cyclic peptide synthetase gene from *Alternaria alternata* apple pathotype whose product is involved in AM-toxin synthesis and pathogenicity. *Mol. Plant-Microbe Interact.* 13, 742-753.

Jones, T., Federspiel, N.A., Chibana, H., Dungan, J., Kalman, S., Magee, B.B., Newport, G., Thorstenson, Y.R., Agabian, N., Magee, P.T., Davis, R.W. and Scherer, S. (2004) The diploid genome sequence of *Candida albicans*. *Proc. Natl Acad. Sci. USA*, 101, 7329-7334.

Kamisaka, Y., Noda, N. and Yamaoka, M. (2004) Appearance of smaller lipid bodies and protein kinase activation in the lipid body fraction are induced by an increase in the nitrogen source in the Mortierella fungus. *J. Biochem. (Tokyo)* 135, 269-276.

Katz, E. and Demain, A.L. (1977) The peptide antibiotics of Bacillus: chemistry, biogenesis, and possible functions. *Bacteriol. Rev.* 41, 449-474.

Kawamura, C., Tsujimoto, T. and Tsuge, T. (1999) Targeted disruption of a melanin biosynthesis gene affects conidial development and UV tolerance in the Japanese pear pathotype of *Alternaria alternata*. *Mol. Plant-Microbe Interact.* 12, 59-63.

Keating, T.A., Marshall, C.G. and Walsh, C.T. (2000a) Vibriobactin biosynthesis in Vibrio cholerae: VibH is an amide synthase homologous to nonribosomal peptide synthetase condensation domains. *Biochemistry*, 39, 15513-15521.

Keating, T.A., Marshall, C.G. and Walsh, C.T. (2000b) Reconstitution and characterization of the Vibrio cholerae vibriobactin synthetase from VibB, VibE, VibF, and VibH. *Biochemistry*, 39, 15522-15530.

Keller, N.P., Turner, G. and Bennett, J.W. (2005) Fungal secondary metabolism - from biochemistry to genomics. *Nat. Rev. Microbiol.* 3, 937-947.

Kim, S., Ahn, I.P., Rho, H.S. and Lee, Y.H. (2005) MHP1, a *Magnaporthe grisea* hydrophobin gene, is required for fungal development and plant colonization. *Mol. Microbiol.* 57, 1224-1237.

Kleinkauf, H. and von Dohren, H. (1996) A nonribosomal system of peptide biosynthesis. *Eur. J. Biochem.* 236, 335-351.

Konz, D. and Mahariel, M.A. (1999) How do peptide synthetases generate structural diversity? *Chem. Biol.* 6, R39-R48.

Lahoz, R., Reyes, F. and Perez Leblic, M.I. (1976) Lytic enzymes in the autolysis of filamentous fungi. *Mycopathologia,* 60, 45-49.

Latge, J.P., Bouziane, H. and Diaquin, M. (1988) Ultrastructure and composition of the conidial wall of *Cladosporium cladosporioides*. *Can. J. Microbiol.* 34, 1325-1329.

Lee, B.N., Kroken, S., Chou, D.Y., Robbertse, B., Yoder, O.C. and Turgeon, B.G. (2005) Functional analysis of all nonribosomal peptide synthetases in *Cochliobolus heterostrophus* reveals a factor, *NPS6*, involved in virulence and resistance to oxidative stress. *Eukaryot. Cell,* 4, 545-555.

Lee, U.S., Jang, H.S., Tanaka, T., Toyasaki, N., Sugiura, Y., Oh, Y.J., Cho, C.M. and Ueno, Y. (1986) Mycological survey of Korean cereals and production of mycotoxins by Fusarium isolates. *Appl. Environ. Microbiol.* 52, 1258-1260.

MacDonard, M.V. and Ingram, D.S. (1986) Towards the selection in vitro for resistance to *Alternaria brassicicola* (Schw.) Wilts., in *Brassica napus* SSP. Oleifera (Metzg.) Sinsk., winter oilseed rape. *New Phytologist,* 104, 621-629.

MacKinnon, S.L., Keifer, P. and Ayer, W.A. (1999) Components from the phytotoxic extract of *Alternaria brassicicola*, a black spot pathogen of canola. *Phytochemistry,* 51, 215-221.

Marahiel, M.A., Danders, W., Krause, M. and Kleinkauf, H. (1979) Biological role of gramicidin S in spore functions. Studies on gramicidin-S-negative mutants of Bacillus brevis ATCC9999. *Eur. J. Biochem.* 99, 49-55.

Marahiel, M.A., Stachelhaus, T. and Mootz, H.D. (1997) Modular Peptide Synthetases Involved in Nonribosomal Peptide Synthesis. *Chem. Rev.* 97, 2651-2674.

Martin, J.F. and Demain, A.L. (1978) Fungal development and metabolite formation. In *The Filamentous Fungi*. Vol. 3. Smith, J.E. and Berry, D.R. (eds). New York: Wiley, pp. 426-450.

Matsumoto, M., Matsutani, S., Sugita, K., Yoshida, H., Hayashi, F., Terui, Y., Nakai, H., Uotani, N., Kawamura, Y. and Matsumoto, K. (1992) Depudecin: a novel compound inducing the flat phenotype of NIH3T3 cells doubly transformed by ras- and src-oncogene, produced by *Alternaria brassicicola*. *J. Antibiot. (Tokyo)* 45, 879-885.

Mayor, C., Brudno, M., Schwartz, J.R., Poliakov, A., Rubin, E.M., Frazer, K.A., Pachter, L.S. and Dubchak, I. (2000) VISTA : visualizing global DNA sequence alignments of arbitrary length. *Bioinformatics*, 16, 1046-1047.

Mazur, P., Nakanishi, K., El-Zayat, A.A.E. and Champe, S.P. (1991) Structure and synthesis of sporogenic psi factors from *Aspergillus nidulans*. *L. Chem. Soc. Chem. Commun.* 20, 1486-1487.

Mootz, H.D., Schwarzer, D. and Marahiel, M.A. (2002) Ways of assembling complex natural products on modular nonribosomal peptide synthetases. *Chembiochem.* 3, 490-504.

Omura, S., Ikeda, H., Ishikawa, J., Hanamoto, A., Takahashi, C., Shinose, M., Takahashi, Y., Horikawa, H., Nakazawa, H., Osonoe, T., Kikuchi, H., Shiba, T., Sakaki, Y. and Hattori, M. (2001) Genome sequence of an industrial microorganism *Streptomyces avermitilis*: deducing the ability of producing secondary metabolites. *Proc. Natl Acad. Sci. USA*, 98, 12215-12220.

Osbourn, A.E. (2001) Tox-boxes, fungal secondary metabolites, and plant disease. *Proc. Natl Acad. Sci. USA*, 98, 14187-14188.

Otani, H., Kohnobe, A., Kodama, M. and Kohmoto, K. (1998) Production of a host-specific toxin by germinating spores of *Alternaria brassicicola*. *Physiol. Mol. Plant Pathol.* 52, 285-295.

Panaccione, D.G., Scott-Craig, J.S., Pocard, J.A. and Walton, J.D. (1992) A cyclic peptide synthetase gene required for pathogenicity of the fungus Cochliobolus carbonum on maize. *Proc. Natl Acad. Sci. USA*, 89, 6590-6594.

Peberdy, J.F. (1990) Fungal cell walls-A Review. In *Biochemistry of cell walls and membranes in fungi*. Kuhn, P.J., Trinci, A.P.J., Jung, M.J., Goosey, M.W. and Copping, L.G. (eds). Berlin, Germany: Springer-Verlag, pp. 5-30.

Perez, P. and Ribas, J.C. (2004) Cell wall analysis. *Methods*, 33, 245-251.

Pfeifer, B.A. and Khosla, C. (2001) Biosynthesis of polyketides in heterologous hosts. *Microbiol. Mol. Biol. Rev.* 65, 106-118.

Potter, S.C., Clarke, L., Curwen, V., Keenan, S., Mongin, E., Searle, S.M., Stabenau, A., Storey, R. and Clamp, M. (2004) The Ensembl analysis pipeline. *Genome Res.* 14, 934-941.

Rausch, C., Weber, T., Kohlbacher, O., Wohlleben, W. and Huson, D.H. (2005) Specificity prediction of adenylation domains in nonribosomal peptide synthetases (NRPS) using transductive support vector machines (TSVMs). *Nucleic Acids Res.* 33, 5799-5808.

Reynolds, E.S. (1963) The use of lead citrate at high pH as an electron opaque stain in electron microscopy. *J. Cell Biol.* 17, 208-212.

Rimmer, S.R. and Buchwaldt, L. (1995) Diseases. In *Brassica oilseeds*. Kimber, D.S. and MacGregor, D.I. (eds). Wallingford, UK: CAB International, pp. 111-140.

Ruiz-Herrera, J. (1991) *Fungal cell wall; structure, synthesis, and assembly.* Boca Raton: CRC Press.

Salamov, A.A. and Solovyev, V.V. (2000) Ab initio gene finding in Drosophila genomic DNA. *Genome Res.* 10, 516-522.

Schaeffer, P. (1969) Sporulation and the production of antibiotics, exoenzymes, and exotoxins. *Bacteriol. Rev.* 33, 48-71.

Schwarzer, D. and Marahiel, M.A. (2001) Multimodular biocatalysts for natural product assembly. *Naturwissenschaften,* 88, 93-101.

Schwarzer, D., Finking, R. and Marahiel, M.A. (2003) Nonribosomal peptides: from genes to products. *Nat. Prod. Rep.* 20, 275-287.

Scott-Craig, J.S., Panaccione, D.G., Pocard, J.A. and Walton, J.D. (1992) The cyclic peptide synthetase catalyzing HC-toxin production in the filamentous fungus *Cochliobolus carbonum* is encoded by a 15.7-kilobase open reading frame. *J. Biol. Chem.* 267, 26044-26049.

Selitrennikoff, C.P. (2001) Antifungal proteins. *Appl. Environ. Microbiol.* 67, 2883-2894.

Shen, Q.T., Chen, X.L., Sun, C.Y. and Zhang, Y.Z. (2004) Dissecting and exploiting nonribosomal peptide synthetases. *Acta. Biochim. Biophys. Sin. (Shanghai)* 36, 243-249.

Smith, D.J., Burnham, M.K., Bull, J.H., Hodgson, J.E., Ward, J.M., Browne, P., Brown, J., Barton, B., Earl, A.J. and Turner, G. (1990a) Beta-lactam antibiotic biosynthetic genes have been conserved in clusters in prokaryotes and eukaryotes. *EMBO J.* 9, 741-747.

Smith, D.J., Burnham, M.K., Edwards, J., Earl, A.J. and Turner, G. (1990b) Cloning and heterologous expression of the penicillin biosynthetic gene cluster from *Penicillum chrysogenum*. *Biotechnology, (N Y)* 8, 39-41.

Solomon, P.S., Lee, R.C., Wilson, T.J. and Oliver, R.P. (2004) Pathogenicity of *Stagonospora nodorum* requires malate synthase. *Mol. Microbiol.* 53, 1065-1073.

Spanu, P.D. (1998) Deletion of *HCf-1*, a hydrophobin gene of *Cladosporium fulvum*, does not affect pathogenicity on tomato. *Physiol. Mol. Plant-Pathol.* 52, 323-334.

Stachelhaus, T., Mootz, H.D. and Marahiel, M.A. (1999) The specificity-conferring code of adenylation domains in nonribosomal peptide synthetases. *Chem. Biol.* 6, 493-505.

Stajich, J.E., Block, D., Boulez, K., Brenner, S.E., Chervitz, S.A., Dagdigian, C., Fuellen, G., Gilbert, J.G., Korf, I., Lapp, H., Lehvaslaiho, H., Matsalla, C., Mungall, C.J., Osborne, B.I., Pocock, M.R., Schattner, P., Senger, M., Stein,

L.D., Stupka, E., Wilkinson, M.D. and Birney, E. (2002) The Bioperl toolkit: Perl modules for the life sciences. *Genome Res.* 12, 1611-1618.

Stringer, M.A., Dean, R.A., Sewell, T.C. and Timberlake, W.E. (1991) *Rodletless*, a new *Aspergillus* developmental mutant induced by direct gene inactivation. *Gene Dev.* 5, 1161-1171.

Sweigard, J., Chumly, F., Carroll, A., Farrall, L. and Valent, B. (1997) A series of vectors for fungal transformation. *Fungal Gen. Newsl.* 44, 52-53.

Thompson, J.D., Gibson, T.J., Plewniak, F., Jeanmougin, F. and Higgins, D.G. (1997) The CLUSTAL_X windows interface: flexible strategies for multiple sequence alignment aided by quality analysis tools. *Nucleic Acids Res.* 25, 4876-4882.

van Wetter, M.-A., Schuren, F.H.J., Schuurs, T.A. and Wessels, J.G.H. (1996) Targeted mutation of the *SC3* hydrophobin gene of *Schizophyllum commune* affects formation of aerial hyphae. *FEMS Microbiol. Lett.* 140, 265-269.

Vanek, Z. and Janecek, J. (1997) The physiology and biosynthesis of secondary metabolites. *Acta. Biol. Hung.* 48, 339-358.

Vining, L.C. (1990) Functions of secondary metabolites. *Annu. Rev. Microbiol.* 44, 395-427.

von Dohren, H., Keller, U., Vater, J. and Zocher, R. (1997) Multifunctional Peptide Synthetases. *Chem. Rev.* 97, 2675-2706.

Weinberg, E.D. (1971) Secondary metabolism: raison d'etre. *Perspect. Biol. Med.* 14, 565-577.

Wessels, J.G. (1997) Hydrophobins: proteins that change the nature of the fungal surface. *Adv. Microb. Physiol.* 38, 1-45.

Wessels, J.G.H., Mol, P.C., Sietsma, J.H. and Vermeulen, C.A. (1990) Wall structure, wall growth, and fungal cell morphogenesis. In *Biochemistry of cell walls and membranes in fungi*. Kuhn, P.J., Trinci, A.P.J., Jung, M.J., Goosey, M.W. and Copping, L.G. (eds). Berlin, Germany: Springer-Verlag, pp. 81-93.

Wilkinson, H.H., Ramaswamy, A., Sim, S.-C. and Keller, N.P. (2004) Increased conidiation associated with progression along the sterigmatocystin biosynthetic pathway. *Mycologia*, 96, 1190-1198.

Yoon, K.S. and McLaughlin, D.J. (1979) Formation of the hilar appendix in basidiospores of *Boletus rubinellus*. *Amer. J. Bot.* 66, 870-873.

Yu, J.H. and Keller, N. (2005) Regulation of secondary metabolism in filamentous fungi. *Annu. Rev. Phytopathol.* 43, 437-458.

Yuan, W.M., Gentil, G.D., Budde, A.D. and Leong, S.A. (2001) Characterization of the *Ustilago maydis sid2* gene, encoding a multidomain peptide synthetase in the ferrichrome biosynthetic gene cluster. *J. Bacteriol.* 183, 4040-4051.

# Chapter IV

## Biosynthesis and role in virulence of the histone deacetylase inhibitor depudecin from *Alternaria brassicicola*


## Abstract

(This work was published in ***Kim et al., 2009, MPMI, 22:1258-1267***)

Depudecin, an eleven-carbon linear polyketide made by the pathogenic fungus *Alternaria brassicicola*, is an inhibitor of histone deacetylase (HDAC). A chemically unrelated HDAC inhibitor, HC-toxin, was earlier shown to be a major virulence factor in the interaction between *Cochliobolus carbonum* and its host, maize. In order to test whether depudecin is also a virulence factor for *A. brassicicola*, we identified the genes for depudecin biosynthesis and created depudecin-minus mutants. The depudecin gene cluster contains six genes (*DEP1-DEP6*), which are predicted to encode a polyketide synthase (*AbPKS9* or *DEP5*), a transcription factor (*DEP6*), two monooxygenases (*DEP2* and *DEP4*), a transporter of the major facilitator superfamily (*DEP3*), and one protein of unknown function (*DEP1*). The involvement in depudecin production of *DEP2*, *DEP4*, *DEP5*, and *DEP6* was demonstrated by targeted gene disruption. DEP5 is required for expression of all the *DEP* genes, but not the immediate flanking genes, thus defining a co-regulated depudecin biosynthetic cluster. The genes flanking the depudecin gene cluster, but not the cluster itself, are conserved in the same order in the related fungi *Stagonospora nodorum* and *Pyrenophora tritici-repentis*. Depudecin-minus mutants have a small (10%) but statistically significant

reduction in virulence on cabbage (*Brassica oleracea*), but not on Arabidopsis. The role of depudecin role in virulence is therefore less dramatic than that of HC-toxin.

## Introduction

Host-selective toxins are positive agents of specificity and virulence in a number of plant disease interactions (Walton 1996; Walton and Panaccione 1993; Friesen et al. 2008). All known HSTs are made by fungi, and most of them are small secondary metabolites. HC-toxin, a cyclic tetrapeptide made by *Cochliobolus carbonum*, is a critical determinant of virulence in the interaction between the pathogen and its host, maize. Isolates of *C. carbonum* that synthesize HC-toxin are extremely virulent on maize homozygous recessive at the nuclear *HM1* and *HM2* loci, killing plants in a few days (Sindhu et al. 2008; Walton 2006). *HM1* encodes HC-toxin reductase, which detoxifies HC-toxin by reducing an essential carbonyl group in HC-toxin (Johal and Briggs 1992; Meeley et al. 1992; Multani et al. 1998). HC-toxin is an inhibitor of histone deacetylases (HDACs) of the Type I (*RPD3/HDA1*-like), and Type II (*HD2*, plant-specific) classes, but not of the Type III (*SIR2*-like, sirtuins) class (Brosch et al. 1995; Hollender and Liu 2009). HC-toxin has been shown to inhibit Type I HDACs in maize, protozoans, yeast, and mammals both in vivo and in vitro, and has been used as a specific HDAC inhibitor in numerous studies (Brosch et al. 1995; Darkin-Rattray et al. 1996; Deubzer et al. 2008; Joung et al. 2004). There is no evidence that HC-toxin and chemically related compounds have any other sites of action.

Earlier studies on the role of HC-toxin in plant pathogenesis raise the question of the role of HDACs in plant disease – why does inhibition of HDACs facilitate the development of disease; what is the role of HDACs in disease resistance? Attempting to further our understanding of HDACs and disease is complicated by several factors. First, there are multiple sensitive HDACs in maize and other plants. Maize has 14 and Arabidopsis has 16 HDAC genes of the HC-toxin-sensitive classes (*RPD3*, *HDA1*, and *HD2*) (Gendler et al. 2008). Second, all of the core histones are subject to reversible acetylation, and each has multiple acetylatable lysine residues. HC-toxin affects acetylation of multiple core histones in maize, especially H3 and H4 (Ransom and Walton 1997). There are thus many possible permutations of histone acetylation/ deacetylation, especially when combined with multiple possible permutations of acetylation-dependent methylation, which can lead to different physiological outcomes (Jenuwein et al. 2001). Third, many other non-histone proteins have now been shown to be regulated by reversible acetylation, including tubulin, cell cycle regulators, transcription factors, DNA helicases, heat shock factors, and HDACs themselves (Brandl et al. 2009; Westerheide et al. 2009). Therefore, in regard to elucidating the role of HC-toxin and HDACs in disease resistance, there are multiple possible targets, each with multiple possible substrates.

Reversible histone acetylation is involved in many cellular processes (Brandl et al. 2009; Haberland et al. 2009), and therefore it is not surprising that HDAC mutations in plants are pleiotropic. Mutational and inhibition studies indicate that HDACs control the expression of numerous plant genes and are involved in the

regulation of processes such as embryo and flower development, the jasmonic acid (JA) and ethylene pathways, light responses, senescence, nucleolar dominance, silencing of transgenes and transposons, Agrobacterium transformability, leaf polarity, abscisic acid and abiotic stress responses, and root hair density (Hollender and Liu 2008). In cereals, *hda101* mutants of maize have pleiotropic effects on development and gene expression (Rossi et al. 2007). Overexpression of a rice HDAC gene causes changes in plant growth and architecture (Jang et al. 2003).

In regard to the role of reversible histone acetylation in plant pathogenesis, there are some suggestions of a relationship. *HDA19* expression in Arabidopsis is induced by infection with the pathogen *Alternaria brassicicola*, and overexpression of *HDA19* causes enhanced resistance and upregulation of ethylene and JA-induced pathogenesis-related (PR)-proteins (Zhou et al. 2005). However, in light of the multiple developmental abnormalities of *HDA19* mutants, it is not clear if *HDA19* has a primary or secondary role in disease resistance (Tian and Chen 2001; Wu et al. 2000, 2003). Mutants in a gene, *HUB1*, encoding a histone H2B monoubiquitinating enzyme, have earlier flowering, thinner cell walls, and increased susceptibility to *A. brassicicola* and *Botrytis cinerea* (Dhawan et al. 2009).

Another connection between histone acetylation and disease response comes from the finding that HDA6 of Arabidopsis interacts with COI1, an F-box protein required for JA signaling (De Voto et al. 2002; Thines et al. 2007). This is consistent with the known importance of JA in response to *A. brassicicola* (see below) and with transcription profiling experiments suggesting a link between COI1-regulated genes

and resistance to *A. brassicicola* (van Wees et al. 2003). JA induces expression of *HDA6* as well as *HDA19*, but not *HDA5*, *HDA8*, *HDA9*, *HDA14*, and *HD2A* (Zhou et al. 2005).

HDA19 interacts with WRKY38 and WRKY62, which are negative regulators of defense, and they are induced by salicylic acid or *Pseudomonas syringae* infection in an *NPR1*-dependent manner (Kim et al. 2008). Overexpression of *HDA19* enhances resistance, and mutation enhances susceptibility; that is, *HDA19* appears to act as a positive regulator of defense. *HDA19* might work through *ERF1*, a gene that integrates JA and ethylene pathways, because *HDA19* overexpression upregulates *ERF1* (Zhou et al. 2005).

HDACs and their target proteins can be both positive and negative regulators of gene expression (Brandl et al. 2009). If HDACs were necessary for induction of defense genes, then by inhibiting HDACs HC-toxin might suppress expression of those genes (Brosch et al. 1995). This model is consistent with the studies on *HDA19* in the *P. syringae*/Arabidopsis pathosystem (Kim et al. 2008), but does not exclude other models, e.g., that HDACs repress a negative regulator of defense. There are several additional major uncertainties, such as whether HDACs could have a different role in dicotyledons versus cereals such as maize, and to what extent the role of HDACs might be affected by the known differences in defense signaling pathways in response to bacterial biotrophic pathogens such as *P. syringae* as opposed to necrotrophs such as *C. carbonum* and species of *Alternaria*.

In order to expand our understanding of the role of HDACs in defense, we have considered the *A. brassicicola*/Arabidopsis pathosystem. *A. brassicicola* causes black spot of most cultivated *Brassica* species including broccoli, cabbage, canola, and mustard. Many species of *Alternaria* make host-selective toxins (Walton 1996). Although *A. brassicicola* is a weak pathogen on wild-type *Arabidopsis* (Kagan and Hammerschmidt 2002), it causes significant disease on *pad3* (phytoalexin-deficient) and DELLA mutants (Navarro et al. 2008; Thomma et al. 1999). Its genome has been sequenced and it is genetically tractable (Cho et al. 2006). Transcriptional changes during infection have been profiled in the fungus (Cramer and Lawrence 2004) and the host (Narasuka et al. 2003; Schenk et al. 2003; van Wees et al. 2003). Plant factors that modulate reaction to *A. brassicicola* include JA, gibberellins acting through the JA pathway, *BOS1* (encoding an R2R3MYB transcription factor), *BOS2*, *BOS3*, *BOS4*, *RLM3* (encoding a TIR-domain protein), and a lipase (Mengiste et al. 2003; Navarro et al. 2008; Oh et al. 2005; Staal et al. 2008; Veronese et al. 2004).

A critical attribute of *A. brassicicola* from the point of view of elucidating the role of reversible histone acetylation in defense is that it makes an HDAC inhibitor called depudecin (Kwon et al. 1998; Matsumoto et al. 1992). Depudecin is a small linear polyketide (Fig. 1) (Tanaka et al. 2000). Depudecin is anti-parasitic and anti-angiogenic and, like HC-toxin, causes detransformation of oncogene-transformed mammalian cells and inhibits HDAC activity in vitro and in vivo (Kwon et al. 1998, 2003; Matsumoto et al. 1992; Oikawa et al. 1995). If depudecin is a virulence factor for *A. brassicicola* on Arabidopsis one could exploit the genetic resources of both

partners to address the role of HDACs in disease resistance. Here we report the identification and characterization of the gene cluster responsible for depudecin biosynthesis in *A. brassicicola* and the disease phenotype of depudecin-minus strains. Although depudecin does contribute to virulence of this fungus, the effect is much less dramatic than the role of HC-toxin in the *C. carbonum*/maize interaction.

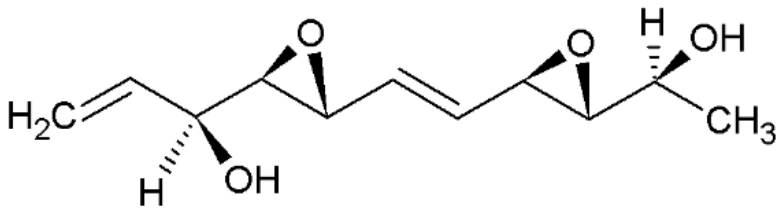


**Figure 1. Structure of the polyketide depudecin (Tanaka et al. 2000).**

# Results

### *AbPKS9* encodes the depudecin polyketide synthase

We identified nine genes encoding putative polyketide synthases (PKSs), designated *AbPKS1* through *AbPKS9*, in the genome of *A. brassicicola*. Disruption mutants for each PKS gene were generated in strain ATCC 96836 using the linear minimal element (LME) method (Cho et al. 2006). The strategies and expected results for homologous integration at *AbPKS9* are shown in Fig. 2A, B. Of the nine PKS genes, mutants of *AbPKS1* through *AbPKS8* still produce depudecin (Fig. 3A, and data

not shown). Of three transformants obtained using LME targeted to *AbPKS9*, DNA blotting indicated that two are knockout mutants and one is an ectopic transformant (Fig. 3B, panel 1). Both the wild-type and the *pks9-1* strains contain a 1.6-kb *Eco*RI fragment hybridizing to *AbPKS9* and strain *pks9-1* has a 3.6-kb band hybridizing to *hph1*, which together indicate that *pks9-1* is an ectopic transformant. In both *pks9-2* and *pks9-3* transformants, the 1.6-kb band is replaced by a ~12-kb band hybridizing to *AbPKS9* (Fig. 3B, panel 1), consistent with homologous tandem integration of five copies of the construct (see Fig. 2). The 1.6-kb wild-type band is restored in the complemented mutant PKS9-2C (Fig. 3B, panel 1). Based on TLC and HPLC analysis, neither of the knockout mutants (*pks9-2* and *pks9-3*) produces depudecin, whereas the ectopic transformant (*pks9-1*) and the complemented strain do (Fig. 3C, D).

Additional mutants of *AbPKS9* were made by double-crossover gene replacement in a different strain of *A. brassicicola*, MUCL 20297. Two independent mutants of *AbPKS9*, called *pks9-4* and *pks9-5*, were verified by DNA blotting (Fig. 4A, B). Neither produces depudecin (Fig. 4C, D). Together, these results indicate that *AbPKS9* encodes the PKS responsible for depudecin biosynthesis. In light of subsequent characterization of the depudecin biosynthetic cluster, *AbPKS9* was renamed *DEP5* (see below).

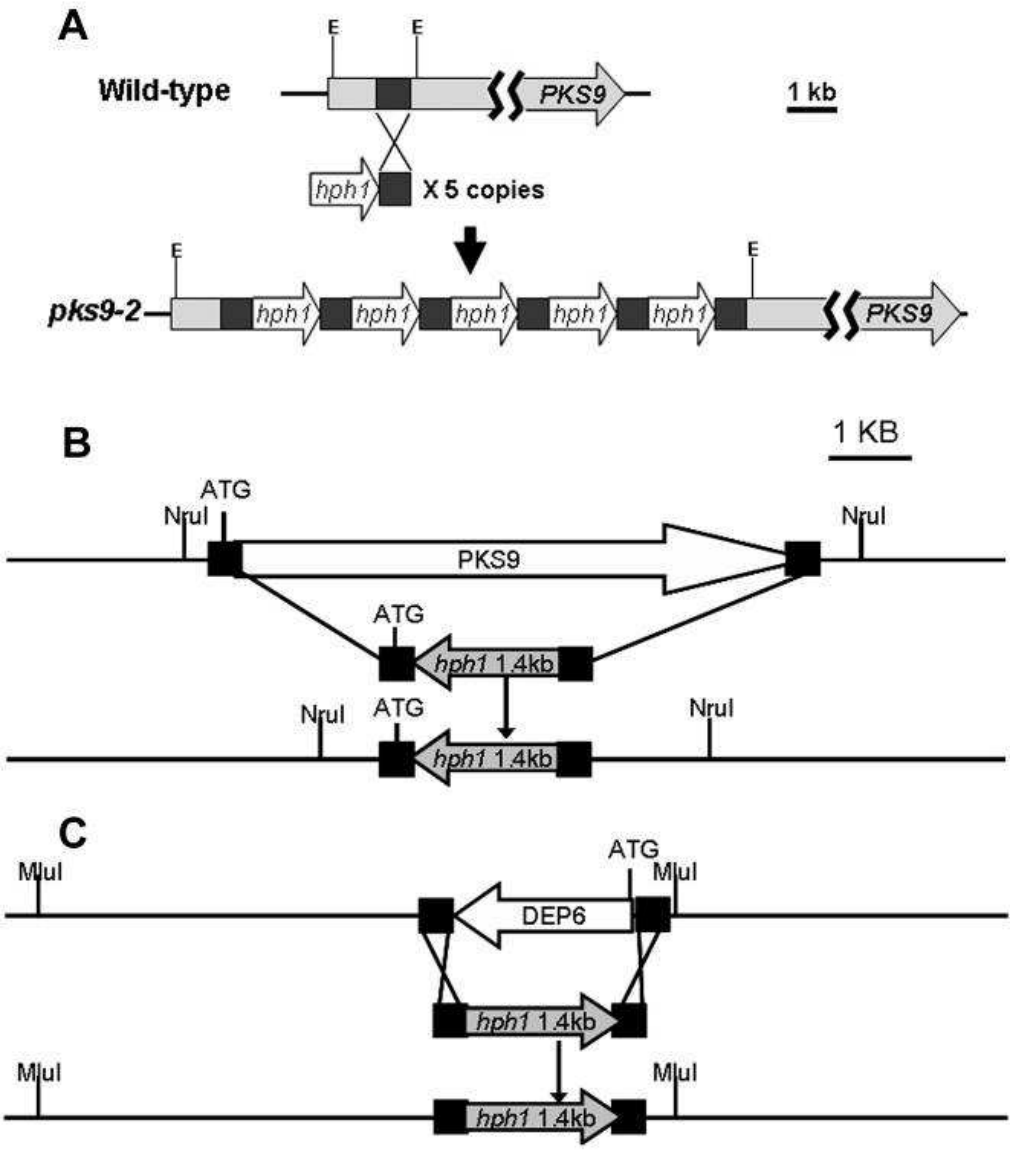


**Figure 2. Strategies for disrupting depudecin biosynthetic genes. A,** Linear minimal element (LME) strategy and predicted outcome (shown for *pks9-2* in ATCC 96836). **B,** Gene replacement strategy and predicted outcome for *DEP5* (*AbPKS9*) in MUCL 20297. **C,** Gene replacement strategy and predicted outcome for *DEP6*. *hph1* designates the gene encoding hygromycin phosphotransferase, and E designates *Eco*RI sites.

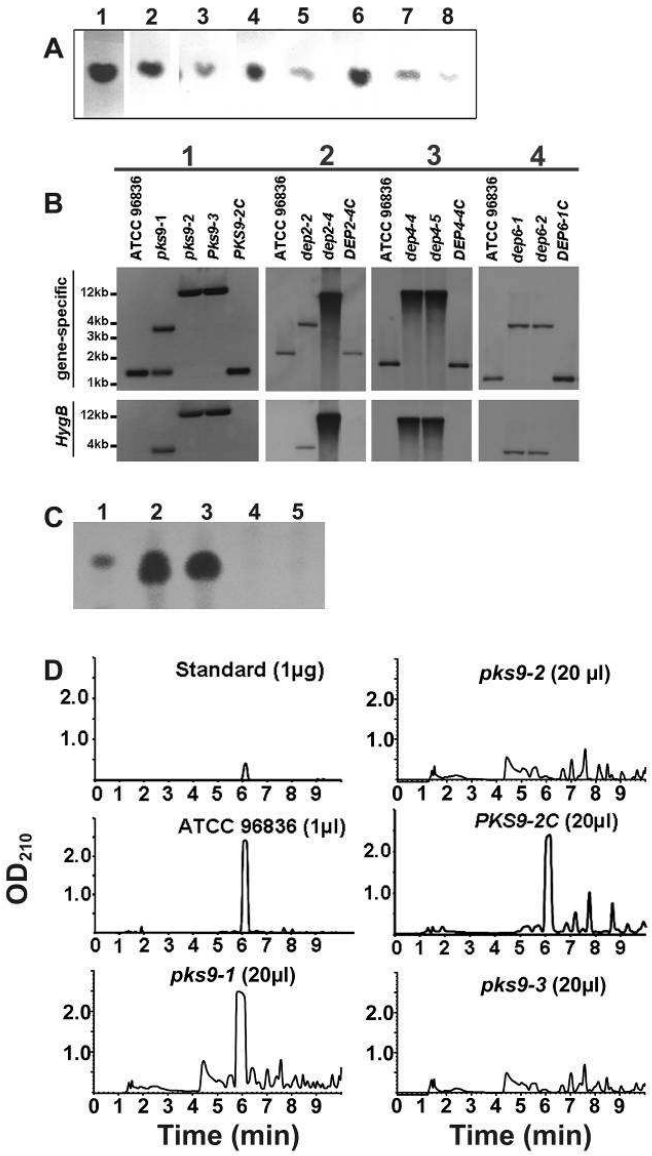


**Figure 3. Characterization of depudecin mutants and complemented strains in A. *brassicicola* ATCC 96836. A,** Lanes 1-8: TLC analysis of culture filtrates of *abpks1-abpks8* mutants. Depudecin was detected with an epoxide-specific reagent. **B,** DNA blot analysis of transformants. In each pair of panels labeled 1-4, the upper panel was hybridized with a gene-specific probe and the lower panel with a fragment of the *hph1* gene. Panel 1 shows three independent *abpks9* transformants (*pks9-1*, *pks9-2*, and *pks9-3*) and a complemented strain (PKS9-2C) of mutant *pks9-2*. DNA was cut with *Eco*RI. Panel 2 shows two independent mutants (*dep2-2* and *dep2-4*) and a complemented strain (DEP2-4C) of *dep2-4*. DNA was cut with *Pst*I. Panel 3 shows two independent mutants (*dep4-4* and *dep4-5*) and a complemented strain (DEP4-4C)

of *dep4-4*. DNA was cut with *Bam*HI. Panel 4 shows two independent mutants (*dep6-1* and *dep6-2*) and a complemented strain (DEP6-1C) of *dep6-1*. DNA was cut with *Xho*I and *Bam*HI. **C,** TLC analysis of ATCC 96836 wild-type, *pks9-1* ectopic mutant, and *pks9-2* and *pks9-3* disruption mutants. Lane 1, 5µg depudecin standard; lane 2, 10µl extract of ATCC 96836; lane 3, 10µl *pks9-1* ectopic extract; lane 4, 10 µl *pks9-2* mutant; and lane 5, 10 µl *pks9-3* mutant. **D,** HPLC analysis of transformants. Note that 20-fold more culture filtrate was injected of the four transformants than the wild-type. Depudecin was eluted from the column at ~6 min and was detected at 210 nm. The identities of the compound eluted at 6 min and the compound with the same $R_f$ on TLC as authentic depudecin were confirmed by mass spectrometry (data not shown).

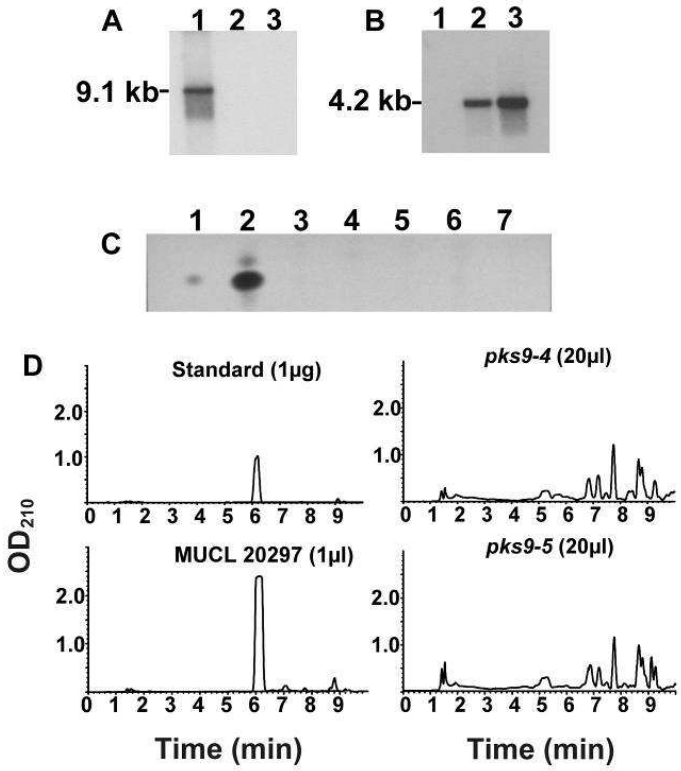


**Figure 4. Characterization of depudecin mutants in MUCL 20297.** **A,** DNA blot analysis of wild-type (lane 1) and two disruption transformants (lane 2, *pks9-4*; lane 3, *pks9-5*) probed with the deleted fragment of *AbPKS9* (*DEP5*) (see Fig. 2). **B,** DNA blot analysis of the same three strains probed with a fragment of the *hph1* gene. **C,** TLC analysis of crude extracts of wild-type and *pks9-4* and *pks9-5* replacement mutants. Lane 1, 5µg depudecin standard; lane 2, 10µl wild-type; lane 3, 10µl *pks9-4*; lane 4, 10 µl *pks9-5*. **D,** HPLC analysis of wild-type and replacement mutants. Note that 20-fold more of the two mutants than the wild-type was injected.

**The depudecin biosynthetic cluster**

The protein coding regions in 72 kb of genomic DNA surrounding *AbPKS9* were predicted with FGENESH (www.softberry.com) using the *Alternaria* model. The genes adjacent to *AbPKS9* are predicted to encode two monooxygenases, a membrane transporter of the major facilitator superfamily (MFS), and a transcription factor, all of which could have a plausible role in depudecin biosynthesis and regulation. The two monooxygenases and the transcription factor were chosen for mutational analysis. Disruption of the putative MFS transporter was not attempted because genes of this class are often necessary for self-protection, in which case a mutant would probably be lethal (Pitkin et al. 1996).

The LME strategy was used to construct mutants of the two monoxygenases (*DEP2* and *DEP4*). Two independent mutants of each gene were obtained (*dep2-2*, *dep2-4*, *dep4-4*, and *dep4-5*) (Fig. 3B, panels 2 and 3). Both *dep2* mutants fail to produce depudecin as judged by TLC and HPLC, but do produce smaller amounts of an epoxide-containing metabolite of slightly higher $R_f$ than native depudecin (Fig. 5A, lanes 3 and 4). This compound is not depudecin as judged by HPLC (Fig. 5B). Both *dep4* mutants also produce a trace of an epoxide-containing compound of the same $R_f$ as native depudecin (Fig. 5A, lanes 5 and 6). Again, however, this is not native depudecin as judged by HPLC, in which no compound of the same retention time as depudecin is seen (Fig. 5B). Complementation of the *dep2-4* and *dep4-4* mutants (DEP2-4C and DEP4-4C) restores depudecin synthesis (Fig. 5B). The mutants have no other distinguishable phenotypes (growth, color, morphology, and sporulation).

These results indicate that the two putative monooxygenase genes are also required for, and dedicated to, depudecin biosynthesis.

Two engineered mutants of the putative transcription factor gene, called *DEP6*, made with the LME method (*dep6-1* and *dep6-2*), do not produce depudecin (Fig. 3B, panel 4, and Fig. 5A, lanes 7 and 8, and Fig. 5B). Complementation of *dep6-1* restores depudecin production (DEP6-1C) (Fig. 5B). Three independent *dep6* mutants (*dep6-3*, *dep6-4*, and *dep6-5*) constructed using double-crossover gene replacement in MUC 20297 also fail to synthesize depudecin (Fig. 6). *dep6* mutants have no discernible phenotype other than loss of depudecin production. These results indicate that *DEP6*, like *AbPKS9*, *DEP2*, and *DEP4*, is required for, and dedicated to, the biosynthesis of depudecin.

**DEP6 regulates the depudecin cluster**

*DEP6* is required for biosynthesis of depudecin (Figs. 5, 6). Its sequence shows some similarity to known fungal transcription factors (see below). Therefore, it might be a pathway-specific regulator of the expression of the genes involved in depudecin biosynthesis and could be used to define the depudecin cluster. In order to test this, expression of the putative depudecin cluster genes was analyzed by RNA blotting. As shown in Fig. 7, RNA expression of *DEP2* and *DEP4* (the monooxygenases), *DEP3* (the MFS transporter), *DEP5* (*AbPKS9*), and *DEP6* itself are dependent on *DEP6.*

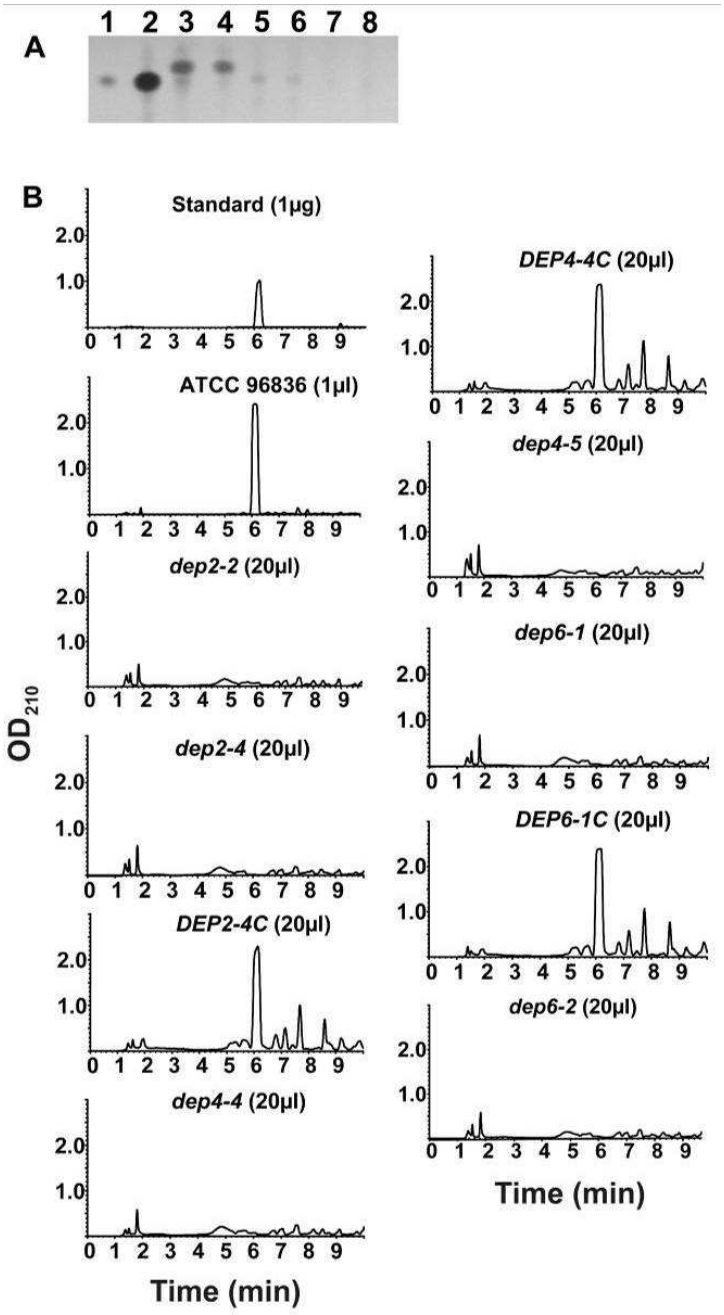


**Figure 5. Mutational characterization of genes in the depudecin cluster.** **A,** TLC analysis of depudecin production. Ten ul crude extract were applied to each lane. Lane 1, depudecin standard; lane 2, wild-type ATCC 96836; lane 3, *dep2-2*; lane 4, *dep2-4*; lane 5, *dep4-4*; lane 6, *dep4-5*; lane 7, *dep6-1*; lane 8, *dep 6-2*. **B,** HPLC analysis of wild-type, depudecin mutants (*dep2-2*, *dep2-4*, *dep4-4*, *dep4-5*, *dep6-1*, and *dep6-2*), and complemented mutants (DEP2-4C, DEP4-4C, and DEP6-1C). Depudecin is the peak eluted at ~6 min.

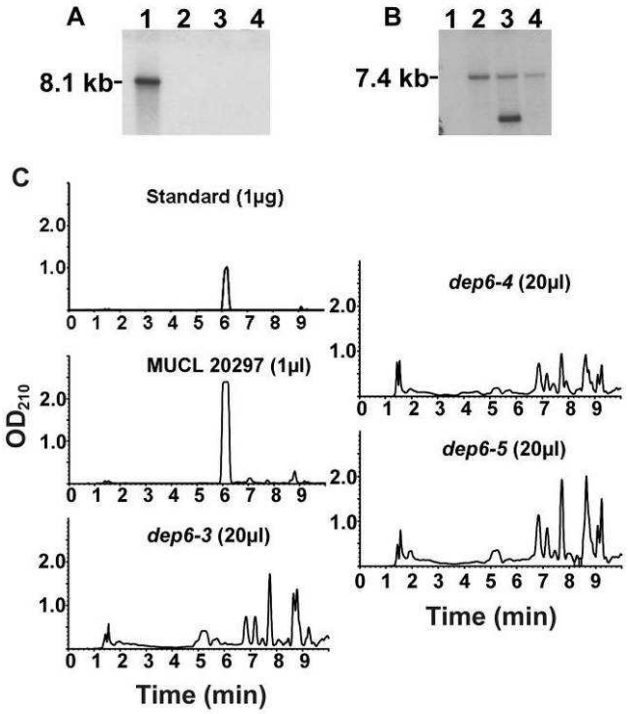


**Figure 6. Analysis of dep6 mutants in MUCL 20297.** **A**, DNA blot analysis of wild-type (lane 1) and three mutants (lane 2, *dep6-3*; lane 3, *dep6-4*; lane 4, *dep6-5*). Blot was probed with a fragment of *DEP6*. **B**, DNA blot analysis of the same strains except probed with *hph1*. *dep6-4* shows multiple bands hybridizing to *hph1*, apparently due to a multiple integration event or to an additional ectopic integration. **C**, HPLC analysis of depudecin production by the wild-type and the mutant strains.

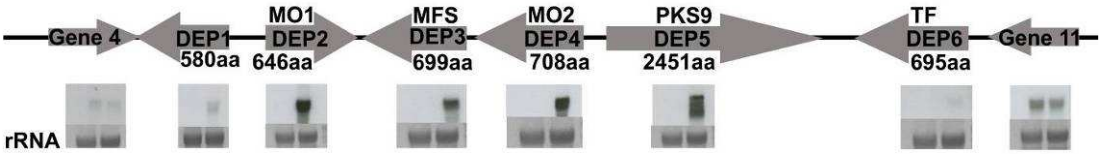


**Figure 7. The depudecin gene cluster of *A. brassicicola* ATCC 96836.** Arrows indicate the directions of transcription. RNA analysis of each gene in the *dep6* mutant are shown under the map. In each panel, the upper two panels show RNA hybridization to the indicated gene. The lower panels show the major ribosomal band stained on the blot with methylene blue. Wild-type is on the right and the *dep6* mutant on the left. MO1, monooxygenase 1; MFS, major facilitator superfamily transporter; MO2, monooxygenase 2; PKS9, polyketide synthase 9; TF, transcription factor. "Gene 4" and "Gene 11" refer to two flanking genes that are not regulated by *dep6*.

Furthermore, expression of another gene upstream of *DEP2*, called *DEP1*, is also dependent on *DEP6* (Fig. 7). On this basis, *DEP1* is part of the depudecin gene cluster. Expression of the genes immediately upstream of *DEP1* and downstream of *DEP6* (genes 4 and 11) are not affected in the *dep6* strain, and therefore are not part of the co-regulated gene cluster (Fig. 7).

**Genes of the depudecin cluster.**

Reverse transcriptase PCR and RACE were used to determine the structures and protein products of *DEP1* through *DEP6*. *DEP1* has no introns. Dep1, the protein encoded by *DEP1*, has 580 amino acids and a molecular mass of 40.3 kDa. Regulation by *DEP6* (Fig. 7) and synteny analysis (see below) suggest a role in depudecin biosynthesis. It has no detectable conserved domains. The best match by BlastP in GenBank is to a predicted protein (CIMG_02399) from *Coccidioides immitis* (score 303, expect 2e-80, 48% amino acid identity). The second best hit, a predicted protein from *Talaromyces stipitatus* is considerably poorer (score 132, expect 5e-29, 28% identity). Several additional hypothetical proteins from ascomycetes give weaker scores (>1e-22). There are no strong orthologs in other Pleosporaceae (Fig. 8). None of the putative orthologs has a known function.

*DEP2* has three introns. Its predicted product has 528 amino acids (59.1 kDa). Blastp results indicate that it has conserved domains corresponding to the pyridine nucleotide-disulfide oxidoreductase superfamily. It has an FAD-binding domain (pfam family 01494). Dep2 is also a member of COG0654 (*UbiH*) containing 2-polyprenyl-

6-methoxyphenol 4-monooxygenase and related FAD-dependent oxidoreductases. The best BlastP hit against the NR database is to a hypothetical protein (CIMG_01450) from *C. immitis* (expect score 1e-135, 53% identity ). Dep2 is also similar (expect scores <1e-50) to a number of hypothetical FAD-dependent monooxygenases from other ascomycetes. By BLASTP against SwissProt, Dep2 shows weak amino acid similarity to salicylate monooxygenase (EC 1.14.13.2) and zeaxanthin epoxidase (EC 1.14.12.4). These monooxygenases are all in class A (van Berkel et al. 2006). A number of monooxygenases of this class have been shown to be involved in secondary metabolite biosynthesis. For example, *atmM* of *Aspergillus flavus* and *paxM* of *Penicillium paxilli* are predicted to be monooxygenases involved in the biosynthesis of the indole-diterpenes aflatrem and paxilline, respectively. These compounds contain hydroxyl groups and aflatrem contains an epoxide (Young et al. 2001; Zhang et al. 2004). In the biosynthesis of depudecin, Dep2 might be responsible for the epoxidations or hydroxylations of depudecin (Fig. 1). The novel product made in the *dep2* mutants might be depudecin with one less hydroxyl and/or epoxide (Fig. 5A).

*DEP3* has eight introns. Its product is 564 aa (60.1 kDa). *DEP3* encodes a membrane transporter of the major facilitator superfamily (MFS). MFS genes are found in many fungal secondary metabolite clusters and presumed to be responsible for exporting secondary metabolites and/or to provide self-protection (Pitkin et al. 1996).

*DEP4* has four exons and its product is 581 aa in length (66.0 kDa). Its best hit is CIMG_02397 of *C. immitis* (expect score 0.0, 66% identity), followed by a large

number of hypothetical proteins in other ascomycetes. Conserved domains include COG2072 (TrkA, predicted flavoprotein involved in $K^+$ transport), and pfam00743 (flavin-binding monooxygenase). Although *DEP2* and *DEP4* are both predicted to encode monooxygenases, they are of different classes. Whereas Dep2 is in class A, Dep4 is in class B (van Berkel et al. 2006). Dep4 is related to cyclohexanone 1,2-monooxygenase (EC 1.14.13.22), 4-hydroxyacetophenone monooxygenase, and dimethylaniline monooxygenase. Like monooxygenases of class A, enzymes related to Dep4 can catalyze epoxidations (Colonna et al. 2002; van Berkel et al. 2006).

*DEP5* (also known as *AbPKS9* and as AB01916 in the recently released annotation of *A. brassicicola* at the Department of Energy Joint Genome Institute [DOE-JGI]), has five exons, and its product has 2376 amino acids (259 kDa). Dep5 is a polyketide synthase (PKS), the central enzyme in depudecin biosynthesis. Of characterized PKSs in the SwissProt database, Dep5 shows high overall amino acid similarity to the lovastatin nonaketide synthase of *Aspergillu terreus* (Hendrickson et al. 1999). Dep5 is a Type I reducing PKS with modules for ketoacyl synthase (KS), acyltransferase (AT),dehydratase (DH), and terminal acyl carrier protein (ACP).There is also probably an enoyl reductase (ER) module.

*DEP6* has four exons and encodes a 646-amino acid protein (72.6 kDa). At its amino terminus Dep6 contains a GAL4-like $Zn_2Cys_6$ binuclear cluster DNA-binding motif typical of fungal transcription factors. The best hit against GenBank NR is to SNOG_06678, a putative trancription factor in *Stagonospora nodorum*. The

dependence of expression of *DEP1* through *DEP5* on *DEP6* is consistent with it encoding a pathway-specific transcription factor (Pedley and Walton 2001).

**A related gene cluster in *Coccidioides immitis***

The best BLASTP hits against GenBank NR for three of the depudecin cluster genes are proteins from *C. immitis*, even though GenBank contains many complete genomes of fungi more closely related to *A. brassicicola* (Dothidiomycetes) than *C. immitis* (Eurotiomycetes). Furthermore, the two best hits to the products of *DEP1* and *DEP4* are *C. immitis* proteins closely linked to each other (CIMG_02399 and CIMG_02397, respectively). This raises the possibility that *C. immitis* has a gene cluster related to the depudecin cluster of *A. brassicicola*.

To test this possibility further, additional BLASTP queries were performed, especially specifically against the genome of *C. immitis* RS. The best match of Dep1 to any protein in GenBank NR is CIMG_02399 (see above). Dep3, encoding the MFS transporter, has numerous very strong hits in GenBank NR. However, the third best hit in NR, and the best hit within *C. immitis*, is CIMG_02396, which is now re-annotated as CIMG_10938 (score 676, expect 0.0, identity 63%). The best hit of Dep4 (monooxygenase) to any protein in NR is CIMG_02397 (score 769, expect 0.0, 66% identity), which is also clustered with CIMG_02399.

*PKS* genes are common in fungi, and Dep5 (AbPKS9) aligns with more than 50 proteins in GenBank NR with expect scores of 0.0. However, the fourth best hit of Dep5 against any protein is CIMG_02398 (score 2390, expect 0.0, identity 52%).

*DEP2* and *DEP6* do not continue the same pattern of clustering in *C. immitis*. The best match to Dep2 of any protein in GenBank NR is clearly also a *C. immitis* protein (CIMG_01450), but this is not clustered with CIMG_02399. Finally, the best hit of Dep6 in *C. immitis* is CIMG_10246, which has relatively poor similarity (score 103, expect 8e-22, 24% identity).

In conclusion, four of the six genes of the depudecin cluster (*DEP1*, *DEP3*, *DEP4*, and *DEP5*) have as their best, or among their best, BLASTP hits four clustered genes in *C. immitis* (CIMG_2399, CIMG_2396, CIMG_2397, and CIMG_2398, respectively). This suggests that *C. immitis* has a gene cluster that is evolutionarily related to the depudecin cluster of *A. brassicicola*, and raises the possibility that *C. immitis* makes a secondary metabolite chemically related to depudecin.

**Synteny between the depudecin cluster region of *A. brassicicola* and other Pleosporaceae.**

The predicted protein sequences flanking the depudecin cluster and the experimentally deduced proteins for *DEP1* through *DEP6* were used to search the genomes of *S. nodorum* (*Phaeosphaeria nodorum*) (Sn) and *Pyrenophora tritici-repentis* (Ptr), which are also in the family Pleosporaceae. The four contiguous genes on the left flank of the depudecin cluster of *A. brassicicola* (numbered 1-4 in Fig. 8) are contiguous in Ptr and Sn. The seven genes on the right side (genes 12-18) are also contiguous in all three fungi, although there is one local rearrangement in Sn (inversion of SNOG_8336 and SNOG_8334) (Fig. 8). In both Ptr and Sn, the syntenic

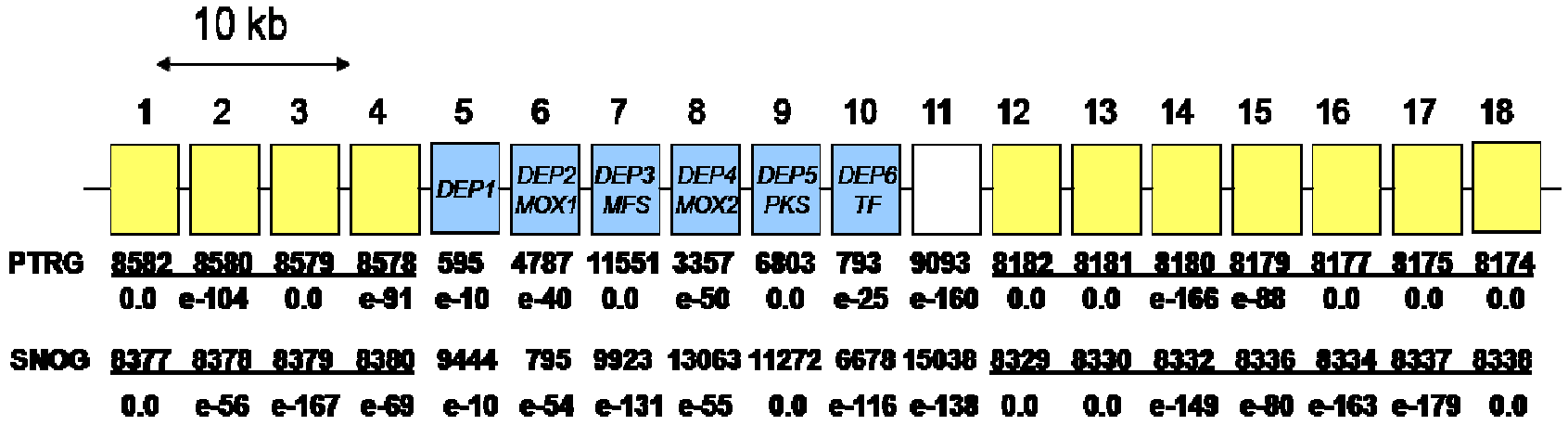


**Figure 8. Synteny between *A. brassicicola*, *P. tritici-repentis*, and *S. nodorum* in the depudecin cluster region.** The gene numbers indicate the best BLASTP hit of the corresponding *A. brassicicola* protein in the genomes of Ptr (PTRG) or Sn (SNOG). The numbers underneath the gene numbers are the expect scores of the BLASTP hit.

regions on the right and on the left are linked on the same supercontig but are not contiguous, i.e., there is a 396-gene gap in Ptr and a 51-gene gap in Sn between the left and right flanks. The closest hits to the depudecin genes themselves are scattered throughout the genomes of Ptr and Sn, representing other members of the same gene families (i.e., other PKS's, MFS transporters, monooxygenases, etc.).

These results indicate that the genomes of these three fungi are syntenous in the region surrounding the depudecin cluster, but not the cluster itself. The depudecin cluster thus appears as an indel of ~25 kb in the genomes of *A. brassicicola*, Sn, and Ptr (Fig. 8). These results also support the conclusion drawn from analysis of the *dep6* mutant that *DEP1* through *DEP6* constitute the depudecin gene cluster (Fig. 7). In this regard, gene 11 is an anomaly; it is not regulated by *DEP6* (Fig 7), nor is it syntenic with Ptr and Sn (Fig. 8). It is unlikely to be involved in depudecin biosynthesis because it is predicted to encode an α-1,3-mannosyltransferase. This gene is a single copy in Ptr and Sn. One possible explanation for how this situation arose is that the presence of gene 11 is related to the indel event, i.e., it moved by chance with the cluster to its present location in the genome of *A. brassicicola*, either from elsewhere in the genome or from another organism.

**Depudecin contributes to virulence on cabbage.**

Virulence of the wild-type, two *dep5* (*abpks9*) mutants, an ectopic insertion mutant (which had wild-type production of depudecin), and a complemented mutant of *DEP5* were compared on *Brassica oleracea* (green cabbage) leaves (Fig. 9). We observed a small but statistically significant ($p < 0.01$) reduction of ~10% in lesion size

between wild-type and mutant strains (Fig. 9B). Depudecin is thus a minor virulence factor of *A. brassicicola* on cabbage. No statistically significant difference in virulence among the strains could be seen on *Arabidopsis* (Fig. 9C; quantitation not shown).

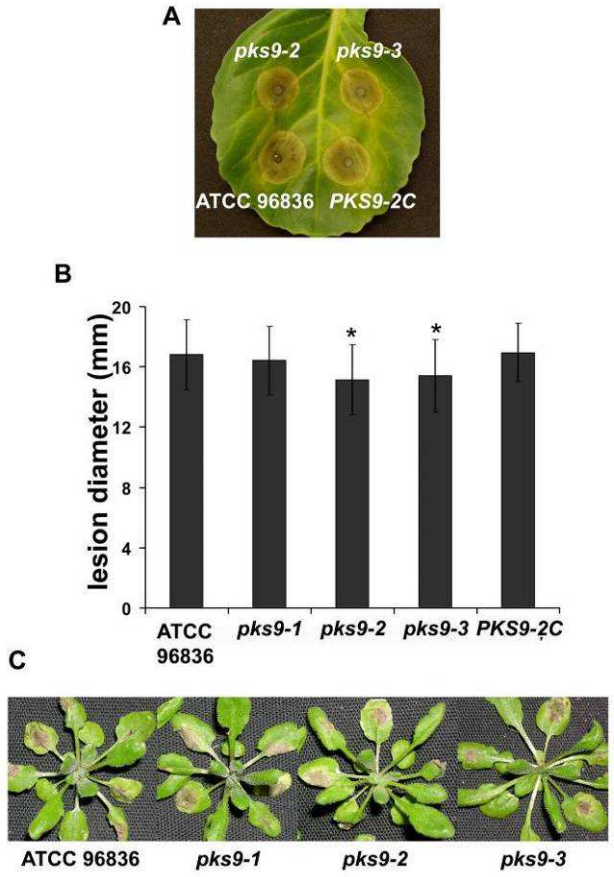


**Figure 9. Virulence analysis of A. *brassicicola dep5* (*abpks9*) mutants.** **A,** Conidial suspension (10 µl of 2 x $10^4$ conidia/ml) of ATCC 96836 wild-type, two mutants (*pks9-2* and *pks9-3*), or a complemented strain (PKS9-2C) were inoculated on green cabbage leaves. Five days after inoculation, disease severity was calculated based on the lesion diameter. **B,** Quantitation of virulence. Column heights and error bars represent average and standard deviation, respectively, of four independent experiments, each experiment measuring at least 15 lesions. Stars indicate lesion diameters statistically significant ($p<0.01$) from the others. *pks9-1* is an ectopic transformant (see Fig. 3). **C,** Virulence of the ectopic transformant and two mutants on Arabidopsis *pad3*.

## Discussion

In this study we have identified a gene cluster involved in depudecin biosynthesis and have constructed multiple depudecin-minus strains of *A. brassicicola*. The depudecin cluster appears to comprise six genes, four of which we have shown by gene disruption to be required for depudecin biosynthesis. We cannot exclude that additional, unclustered genes are also required for depudecin biosynthesis. With the exception of *DEP1*, the genes of the depudecin cluster have plausible roles in depudecin biosynthesis based on our knowledge of similar genes in other secondary metabolite pathways. *DEP6*, a putative transcription factor, is a positive regulator of the other genes of the cluster.

Based on the pathogenicity assays it appears that while depudecin does play a minor role in virulence of *A. brassicicola* on cabbage, it is not a major virulence factor like HC-toxin is for *C. carbonum* on maize. It was not possible to detect a statistically significant effect of depudecin on virulence of Arabidopsis *pad3* mutants.

There are several possible reasons why HC-toxin but not depudecin is a strong virulence factor in their respective pathosystems. One possibility is that depudecin is not made in sufficiently high concentrations, or penetrates insufficiently well, to effectively inhibit HDACs during infection of cabbage or Arabidopsis. Compared to HC-toxin, depudecin is a relatively weak HDAC inhibitor; whereas Aeo-containing cyclic peptides such as HC-toxin cause half-maximal inhibition of in vitro HDAC

activity at <10 nM, depudecin is active only at ~50 µM (Deubzer et al. 2008; Kwon et al. 1998; Monneret 2005).

Another possible explanation is that HDAC inhibition is an effective virulence strategy against grasses but not against other plants, such as Arabidopsis (Sindhu et al. 2008). That is, HDACs might be required for defense against pathogens in some plants but not others. Despite many lines of data suggesting that HDACs have at least an indirect role in defense signaling in Arabidopsis, none of the evidence is as strong as that from the *C. carbonum*/maize pathosystem (De Voto et al. 2002; Dhawan et al. 2009; Kim et al. 2008; Thines et al. 2007; Walton 2006; Zhou et al. 2005). A possibly relevant consideration in this regard is the apparent specialization of the genera *Alternaria* and *Cochliobolus*. Although both make a number of host-selective toxins, *Alternaria* tends to pathogenize dicotyledenous plants, whereas *Cochliobolus* is specialized on cereals (Walton 1996). It is possible that defense in cereals as opposed to other plants differs in the involvement of histone acetylation.

A third possible explanation for our results is that *A. brassicicola* makes additional HDAC inhibitors, which mask the loss of depudecin production. In addition to at least five known cyclic tetrapeptide inhibitors related to HC-toxin, there are a number of other natural products that are HDAC inhibitors (Monneret 2005; Walton 2006). Depudecin itself is known to be made by two fungi other than *A. brassicicola* (Amnuaykanjanasin et al. 2005; Tanaka et al. 2000). If *A. brassicicola* makes additional HDAC inhibitors, the mutant strains generated in this study will be useful for finding them.

## Materials and Methods

### *Fungal growth and depudecin analysis*

*A. brassicicola* American Type Culture Collection (ATCC) 96836 and Mycothèque Université Catholique de Louvain, Belgium (MUCL) 20297 were maintained on potato dextrose agar (PDA) (Difco) or V8-juice agar. For depudecin production, the fungus was grown in still culture in one-liter flasks containing 125 ml potato dextrose broth (PDB) (Difco) for 7 to 10 d. The cultures were filtered through Whatman #1 paper and extracted twice with equal volumes of dichloromethane. The dichloromethane fractions were evaporated under vacuum at 40ºC and redissolved in 3 ml methanol. After reconcentration under vacuum, the residue was redissolved in 100 µl methanol. This crude extract was used for both TLC and HPLC. Depudecin standard was obtained from Sigma-Aldrich and dissolved in methanol at 1 mg/ml.

For TLC, crude extract (10 µl) was spotted onto 250-µm silica plates with adsorbent strip (Whatman). Plates were developed in 1:1 acetone:dichloromethane. Depudecin was detected using an epoxide-specific reagent (Hammock et al. 1974).

For HPLC, 20 µl of extract was combined with 60 µlof acetonitrile and 20 µl of sterile distilled water. The sample was injected onto a C18 reverse phase column (Agilent Eclipse XDB-C18 silica, 5 µm, 4.6 x 150 mm) and eluted with a linear gradient of 10% (v/v) acetonitrile in water to 100% acetonitrile in 30 min at a flow rate of 1 ml/min. The eluant was monitored at 210 nm.

### *Gene disruption*

To disrupt *DEP5* (*AbPKS9*) by the LME method (Cho et al. 2006), two primers were designed, one at the 954-bp position (in relation to the start codon) with an added *Hin*dIII enzyme site and the other at the 1442-bp position with an added *Xba*I site (see Fig. 2 and Supplementary Table S1 for primer sequences). These primers were used to amplify a 509-bp fragment from genomic DNA. PCR products were digested with *Hin*dIII and *Xba*I and ligated to the corresponding sites in pCB1636 (Sweigard et al. 1997). The ligation was transformed into *E. coli* strain DH5α (Invitrogen). The plasmid was isolated and used as template for PCR amplification using M13 forward and M13 reverse primers. The PCR product was purified and concentrated to 1 µg/µl.

To disrupt *DEP6*, *DEP2*, and *DEP4* by the LME method, two primers for each gene, (DEP6KOFor and DEP6KORev for *DEP6*, DEP2KOFor and DEP2KORev for *DEP2*, and DEP4KOFor and DEP4KORev for *DEP4*), were used to amplify 751-bp partial *DEP6*, 812-bp partial *DEP2*, and 807-bp partial *DEP2* sequences from genomic DNA. Another set of two primers for each was used to amplify cassettes of *hph1* (encoding hygromycin phosphotransferase) from the plasmid pCB1636: DEP6HygFor and DEP6HygRev, DEP2HygFor and DEP2HygRev, or DEP4HygFor and DEP4HygRev. The resulting fragments for each gene were mixed and subjected to a second PCR reaction with primers DEP6KOFor and DEP6HygRev, DEP2KOFor and DEP2HygRev, or DEP4KOFor and DEP4HygRev. The resulting final products were used to transform *A. brassicicola* to make *dep6*, *dep2*, or *dep4* mutants, respectively.

In order to complement the *dep5* mutant, the wild-type *DEP5* allele from *A. brassicicola* genomic DNA was amplified using primer set P9comF and P9comR. To

complement the *dep6*, *dep2*, and *dep4* mutants, a 2.7-kb *DEP6* allele with primers TfcomF and TfcomR, a 2.6-kb *DEP2* allele with primers Mo1comF and Mo1comR, and a 3.4-kb *DEP4* allele with primers Mo2comF and Mo2comR were amplified from genomic DNA. Separately, a 1449-bp nourseothricin resistance (NAT) cassette carrying the nourseothricin acetyltransferase-encoding gene *nat1* was amplified using primer set PNRcomF and PNRcomR from plasmid pNR1 (Malonek et al. 2004). The final two PCR products, each target gene fragment, and a NAT cassette were used to transform simultaneously the *dep2*, *dep4*, or *dep6* mutant strains, and transformants were selected on PDA plates containing nourseothricin. All transformants were subjected to two rounds of single-spore isolation.

For disruption by gene replacement, primer pairs 1 and 2 were used to amplify 575-bp and 476-bp fragments from the 5' and 3' ends of *DEP5*, respectively, overlapping the transcriptional start and stop sites (see Fig. 2 and Table S1). Primer pairs 4 and 5 were used to amplify 476-bp and 507-bp fragments of *DEP6*. The internal primers had an additional 25-30 bp complementary to *hph1* of pCB1003 (Carroll et al. 1994). Primers 7 and 8 were used to amplify *hph1* and had an additional 25 bp complementary to the target gene. The upstream and downstream flanking regions of *DEP5* and *DEP6* were combined with *hph1* in a second round of PCR using the outside gene primers.

PCR products were ligated into pGem T-easy (Promega) and transformed into *E. coli* DH5α (Invitrogen). PCR products were purified with the QIAquick PCR

purification Kit (Qiagen) and used directly in transformation of protoplasts (Cho et al. 2006). Transformants were purified by two rounds of single-spore isolation.

***DNA extraction and analysis***

DNA isolations and DNA blottings were performed as described previously (Kim et al. 2007). The DNA blots shown in Fig. 3B was performed and hybridized according to the manufacturer's instruction (Roche Diagnostics, Mannheim, Germany) using digoxigenin (DIG)-labeled DNA probes. A total of 2-3 µg of genomic DNA was digested with *Eco*RI for analysis of *DEP5* (*AbPKS9*), with *Xho*I and *Bam*HI for analysis of *DEP6*, with *Pst*I for analysis of *DEP2*, and with *Bam*HI for analysis of *DEP4*. The PCR DIG Probe Synthesis Kit (Roche) was used to label a 509-bp fragment of *DEP5*, a 751-bp fragment of *DEP6*, an 812-bp fragment of *DEP2*, and 807-bp fragment of *DEP4*. A 500-bp fragment from pCB1636 and a 1-kb fragment from pNR1 were used as probes for the selection genes.

For the DNA blots shown in Fig. 4, DNA was extracted from lyophilized mats of 5-7 day-old *A. brassicicola* MUCL 20297 grown in potato dextrose broth in still culture (Pitkin et al. 1996). DNA (15 µg) was digested with *Nru*I (*dep5* mutants) or *Mlu*I (*dep6* mutants) (Fig. 2B, C). DNA was transferred to Nytran SPC (Whatman) and hybridized with $^{32}$P probes (Pitkin et al. 1996).

RNA was extracted as described (Hallen et al. 2007). Reverse transcriptase (RT)-PCR followed by 5' and 3' Rapid Amplification of cDNA Ends (RACE) was done with the SMART RACE cDNA amplification kit (Clontech). Overlapping gene

specific primers were designed from available genomic sequence. In most cases several gene-specific primers were utilized. PCR products were cloned into pGem T-easy (Promega) and transformed into *E. coli* DH5α (Invitrogen).

For RNA blotting, 15-20 µg of total RNA was used per lane. Internal gene-specific probes using primers given in Table S1 were generated directly from cDNA templates. rRNA bands on the blots were stained with 0.02% methylene blue in 0.5 M sodium acetate, pH 5.5.

***Virulence assays***

Pathogenicity assays used wild-type and mutant strains of ATCC 96836. Conidia were harvested from potato dextrose agar (PDA) plates incubated for 7 d at 25°C and suspended in sterile water at 2 x $10^4$ conidia/ml. Conidial suspensions (10 µl) were applied as drops on the surface of leaves at the fifth through sixth leaf stages. Inoculated plants were placed in a plastic box at room temperature (21°C) and kept at 100% relative humidity for 24 h in the dark, followed by 4 d under fluorescent lights with a photoperiod of 16 hr light/8 hr dark. Lesion diameters were measured. The experiments were repeated four times with >15 plants per treatment. Results were analyzed using a pair-wise t-test using JMP (SAS, Cary, NC).

Arabidopsis plants (Col-0 and *pad3*) were grown in a growth chamber at 20°C, 70% relative humidity, and a 12-hr light/dark cycle. *A. brassicicola* spores were collected from PDA culture plates in 2 ml 0.1% Tween-20. The third through the seventh true leaves from 4-week-old plants were spot-inoculated with 10 µl of $10^5$

spores/ml. Plants were covered to maintain high humidity. Lesions were measured and photographed 4 d after inoculation.

# Literature Cited


Amnuaykanjanasin, A., Punya, J., Paungmoung, P., Rungrod, A., Tachaleat, A., Pongpattanakitshote, S., Cheevadhanarak, S., and Tanticharoen, M. 2005. Diversity of type I polyketide synthase genes in the wood-decay fungus Xylaria sp. BCC 1067. FEMS Microbiol. Lett. 251:125-136.

Brandl, A., Heinzel, T., and Krämer, O. H. 2009. Histone deacetylases: salesmen and customers in the post-translational modification market. Biol. Cell 101:193-205.

Brosch, G., Ransom, R.. Lechner, T., Walton, J. D., and Loidl, P. 1995. Inhibition of maize histone deacetylase by HC-toxin, the host-selective toxin of *Cochliobolus carbonum*. Plant Cell 7:1941-1950.

Carroll, A. M., Sweigard, J. A., and Valent, B. 1994. Improved vectors for selecting resistance to hygromycin. Fungal Genet. Newslett. 41:22.

Cho, Y., Davis, J. W., Kim, K. H., Wang, J., Sun, Q. H., Cramer, R. A., Jr., and Lawrence, C. B. (2006). A high throughput targeted gene disruption method for *Alternaria brassicicola* functional genomics using linear minimal element (LME) constructs. Mol. Plant-Microbe Interact. 19:7-15.

Colonna, S., Gaggero, N., Carrea, G., Ottolina, G., Pasta, P., and Zambianchi, F. 2002. First asymmetric epoxidation catalysed by cyclohexanone monooxygenase. Tetrahedron Lett. 43:1797-1799.

Cramer, R. A., and Lawrence, C. B. 2004. Identification of *Alternaria brassicicola* genes expressed in planta during pathogenesis of Arabidopsis thaliana. Fung. Genet. Biol. 41:115-128.

Darkin-Rattray, S. J., Gurnett, A. M., Myers, R. W., Dulski, P. M., Crumley, T. M., Allocco, J. J., Cannova, C., Meinke, P. T., Colletti, S. L., Bednarek, M. A., Singh, S. B., Goetz, M. A., Dombrowski, A. W., Polishook, J. D., and Schmatz, D. M. 1996. Apicidin: a novel antiprotozoal agent that inhibits parasite histone deacetylase. Proc. Natl. Acad. Sci. U.S.A. 93:13143-13147.

Deubzer, H. E., Ehemann, V., Kulozik, A. E., Westermann, F., Savelyeva, L., Kopp-Schneider, A., Riester, D., Schwab, M., and Witt, O. 2008. Anti-neuroblastoma activity of *Helminthosporium carbonum* (HC)-toxin is superior to that of other differentiating compounds in vitro. Cancer Lett. 8:21-8.

Devoto, A., Nieto-Rostro, M., Xie, D., Ellis, C., Harmston, R., Patrick, E., Davis, J., Sherratt, L., Coleman, M., and Turner, J. G. 2002. COI1 links jasmonate signalling and fertility to the SCF ubiquitin-ligase complex in Arabidopsis. Plant J. 32:457–466.

Dhawan, R., Luo, H., Foerster, A. M., AbuQamar, S., Du, H.-N., Briggs, S. D., Scheid, O. M., and Mengiste, T. 2009. HISTONE MONOUBIQUITINATION1 interacts with a subunit of the mediator complex and regulates the defense against nectrotrophic fungal pathogens in *Arabidopsis*. Plant Cell, in press.

Friesen, T. L., Faris, J. D., Solomon, P. S., and Oliver, R. P. 2008. Host-specific toxins: effectors of necrotrophic pathogenicity. Cell Microbiol. 10:1421-1428.

Gendler, K., Paulsen, T., and Napoli, C. 2008. ChromDB: the chromatin database. Nucl. Acids Res. 36:D298-302.

Haberland, M., Montgomery, R. L., and Olson, E. N. 2009. The many roles of histone deacetylases in development and physiology: implications for disease and therapy. Nat. Rev. Genet. 10:32-42.

Hallen, H. E., Huebner, M., Shiu, S. H., Güldener, U., and Trail, F. 2007. Gene expression shifts during perithecium development in *Gibberella zeae* (anamorph *Fusarium graminearum*), with particular emphasis on ion transport proteins. Fung. Genet Biol. 44:1146-1156.

Hammock, L. G., Hammock, B. D., and Casida, J. E. 1974. Detection and analysis of epoxides with 4-(p-nitrobenzyl)-pyridine. Bull. Environ. Contam. Toxicol. 12:759-764.

Hendrickson, L., Davis, C. R., Roach, C., Nguyen, D. K., Aldrich, T., McAda, P. C., and Reeves, C. D. 1999. Lovastatin biosynthesis in *Aspergillus terreus*: characterization of blocked mutants, enzyme activities and a multifunctional polyketide synthase gene. Chem. Biol. 6:429-439.

Hollender, C., and Liu, Z. 2009. Histone deacetylase genes in Arabidopsis development. J. Integ. Plant Biol. 50:875-885.

Jang, I. C., Pahk, Y. M., Song, S. I., Kwon, H. J., Nahm, B.H., and Kim, J. K. 2003. Structure and expression of the rice class-I type histone deacetylase genes OsHDAC1-3: OsHDAC1 overexpression in transgenic plants leads to increased growth rate and altered architecture. Plant J. 33:531-541.

Jenuwein, T., and Allis, C. D. 2001. Translating the histone code. Science 293:1074-1080.

Johal, G. S., Briggs, S. P. 1992. Reductase activity encoded by the *HM1* disease resistance gene in maize. Science 258:985-987.

Joung, K. E., Kim, D. K., and Sheen, Y.Y. 2004. Antiproliferative effect of trichostatin A and HC-toxin in T47D human breast cancer cells. Arch. Pharm. Res. 27:640-645.

Kagan, I. A., and Hammerschmidt, R. 2002. Arabidopsis ecotype variability in camalexin production and reaction to infection by *Alternaria brassicicola*. J. Chem. Ecol. 28:2121-2140.

Kim, K.-C., Lai, Z., Fan, B., and Chen, Z. 2008. Arabidopsis WRKY38 and WRKY62 transcription factors interact with histone deacetylase 19 in basal defense. Plant Cell 20:2357-2371.

Kim, K. H., Cho, Y., La Rota, M., Cramer, R. A., Jr., and Lawrence, C. B. (2007). Functional analysis of the *Alternaria brassicicola* non-ribosomal peptide

synthetase gene *AbNPS2* reveals a role in conidial cell wall construction. Mol. Plant Pathol. 8:23-39.

Kwon, H. J., Owa, T., Hassig, C. A., Shimada, J., and Schreiber, S. L. 1998. Depudecin induces morphological reversion of transformed fibroblasts via the inhibition of histone deacetylase. Proc. Natl. Acad. Sci. U.S.A. 95:3356-3361.

Kwon, H. J., Kim, J. H., Kim, M., Lee, J. K., Hwang, W. S., and Kim, D.Y. 2003. Anti-parasitic activity of depudecin on *Neospora caninum* via the inhibition of histone deacetylase. Vet. Parasitol. 112:269-276.

Malonek, S., Rojas, M. C., Hedden, P., Gaskin, P., Hopkins, P., and Tudzynski, B. 2004. The NADPH-cytochrome P450 reductase gene from *Gibberella fujikuroi* is essential for gibberellin biosynthesis. J. Biol. Chem. 279:25075-25084.

Matsumoto, M., Matsutani, S., Sugita, K., Yoshida, H., Hayashi, F., Terui, Y., Nakai, H., Uotani, N., Kawamura, Y., Matsumoto, K., et al. 1992. Depudecin: a novel compound inducing the flat phenotype of NIH3T3 cells doubly transformed by ras- and src-oncogene, produced by *Alternaria brassicicola*. J. Antibiot. (Tokyo) 45:879-885.

Meeley, R. B., Johal, G. S., Briggs S. P., and Walton, J. D. 1992. A biochemical phenotype for a disease resistance gene of maize. Plant Cell 4:71 77.

Mengiste, T., Chen, X., Salmeron, J., and Dietrich, R. 2003. The *BOTRYTIS SUSCEPTIBLE1* gene encodes an R2R3MYB transcription factor protein that is required for biotic and abiotic stress responses in Arabidopsis. Plant Cell 15:2551-2565.

Monneret, C. 2005. Histone deacetylase inhibitors. Eur. J. Med. Chem. 40:1-13.

Multani, D. S., Meeley, R. B., Paterson, A. H., Gray, J., Briggs, S. P., and Johal, G. S. 1998. Plant-pathogen microevolution: molecular basis for the origin of a fungal disease in maize. Proc. Natl. Acad. Sci. U. S. A. 95:1686-1691.

Narusaka, Y., Narusaka, M., Seki, M., Ishida, J., Nakashima, M., Kamiya, A., Enju, A., Sakurai, T., Satoh, M., Kobayashi, M., Tosa, Y., Park, P., and Shinozaki, K. 2003. The cDNA microarray analysis using an Arabidopsis *pad3* mutant reveals the expression profiles and classification of genes induced by *Alternaria brassicicola* attack. Plant Cell Physiol. 44:377-387.

Navarro, L., Bari, R., Achard, P., Lisón, P., Nemri, A., Harberd, N. P., and Jones, J. D. 2008. DELLAs control plant immune responses by modulating the balance of jasmonic acid and salicylic acid signaling. Curr. Biol. 18:650-655.

Oh, I. S., Park, A. R., Bae, M. S., Kwon, S. J., Kim, Y. S., Lee, J. E., Kang, N. Y., Lee, S., Cheong, H., and Park, O. K. 2005. Secretome analysis reveals an Arabidopsis lipase involved in defense against *Alternaria brassicicola*. Plant Cell 17:2832-2847.

Oikawa, T., Onozawa, C., Inose, M., and Sasaki, M. 1995. Depudecin, a microbial metabolite containing two epoxide groups, exhibits anti-angiogenic activity in vivo. Biol. Pharm. Bull. 18:1305-1307.

Pedley, K. F., and Walton, J. D. 2001. Regulation of cyclic peptide biosynthesis in a plant pathogenic fungus by a novel transcription factor. Proc. Natl. Acad. Sci. U.S.A. 98: 14174-14179.

Pitkin, J. W., Panaccione, D. G., and Walton, J. D. 1996. A putative cyclic peptide efflux pump encoded by the *TOXA* gene of the plant-pathogenic fungus *Cochliobolus carbonum*. Microbiology 142:1557-1565.

Ransom, R. F., and Walton, J. D. 1997. Histone hyperacetylation in maize in response to treatment with HC-Toxin or infection by the filamentous fungus *Cochliobolus carbonum*. Plant Physiol. 115:1021-1027.

Rossi, V., Locatelli, S., Varotto, S., Donn, G., Pirona, R., Henderson, D.A., Hartings, H., and Motto, M. 2007. Maize histone deacetylase *hda101* is involved in plant development, gene transcription, and sequence-specific modulation of histone modification of genes and repeats. Plant Cell 19:1145-1162.

Schenk, P. M., Kazan, K., Manners, J. M., Anderson, J.P., Simpson, R. S., Wilson, I. W., Somerville, S. C., and Maclean, D. J. 2003. Systemic gene expression in Arabidopsis during an incompatible interaction with *Alternaria brassicicola*. Plant Physiol. 132:999-1010.

Sindhu, A., Chintamanani, S., Brandt, A. S., Zanis, M., Scofield, S. R., Johal, G. S. 2008. A guardian of grasses: specific origin and conservation of a unique disease-resistance gene in the grass lineage. Proc. Natl. Acad. Sci. U.S.A. 105:1762-1767.

Staal, J., Kaliff, M., Dewaele, E., Persson, M., and Dixelius, C. 2008. *RLM3*, a TIR domain encoding gene involved in broad-range immunity of Arabidopsis to necrotrophic fungal pathogens. Plant J. 55:188-200.

Sweigard, J., Chumley, F., Carroll, A., Farrall, L., and Valent, B. (1997). A series of vectors for fungal transformation. Fung. Gen. Newsl. 44:52-53.

Tanaka, M., Fujimori, T., and Nabeta, K. 2000. Biosynthesis of depudecin, a metabolite of *Nimbya scirpicola*. Biosci. Biotechnol. Biochem. 64:244-247.

Thines, B., Katsir, L., Melotto, M., Niu, Y., Mandaokar, A., Liu, G., Nomura, K., He, S. Y., Howe, G. A., and Browse, J. 2007. JAZ repressor proteins are targets of the SCF(COI1) complex during jasmonate signalling. Nature 448:661-665.

Tian, L., and Chen, Z. J. 2001. Blocking histone deacetylation in Arabidopsis induces pleiotropic effects on plant gene regulation and development. Proc. Natl. Acad. Sci. U.S.A. 98:200-205.

Thomma, B. P. H. J., Nelissen, I., Eggermont, K., and Broekaert, W. F. 1999. Deficiency in phytoalexin production causes enhanced susceptibility of *Arabidopsis thaliana* to the fungus *Alternaria brassicicola*. Plant J. 19:163-171.

van Berkel, W. J. H., Kamerbeek, N. M., and Fraaiji, M. W. 2006. Flavoprotein monooxygenases, a diverse class of oxidative biocatalysts. J. Biotechol. 124:670-689.

van Wees, S. C. M., Chang, H.-S., Zhu, T., and Glazebrook, J. 2003. Characterization of the early response of Arabidopsis to *Alternaria brassicicola* infection using expression profiling. Plant Physiol. 132:606-617.

Veronese, P., Chen, X., Bluhm, B., Salmeron, J., Dietrich, R., and Mengiste, T. 2004. The *BOS* loci of Arabidopsis are required for resistance to *Botrytis cinerea* infection. Plant J. 40:558-574.

Walton, J. D. 1996. Host-selective toxins: agents of compatibility. Plant Cell 8:1723-1733.

Walton, J. D. 2006. HC-toxin. Phytochemistry 67:1406-1413.

Walton, J. D., and Panaccione, D. G. 1993. Host-selective toxins and disease specificity: perspectives and progress. Annu. Rev. Phytopathol. 31:275-303.

Westerheide, S. D., Anckar, J., Stevens, S. M., Jr., Sistonen, L., and Morimoto, R. I. 2009. Stress-inducible regulation of heast shock factor 1 by the deacetylase SIRT1. Science 323:1063-1066.

Wu, K., Malik, K., Tian, L., Brown, D., and Miki, B. 2000. Functional analysis of a *RPD3* histone deacetylase homolog in *Arabidopsis thaliana*. Plant Mol. Biol. 44:167–176.

Wu, K., Tian, L., Zhou, C., Brown, D., and Miki, B. 2003. Repression of gene expression by *Arabidopsis* HD2 histone deacetylases. Plant J. 34:241-247.

Young, C., McMillan, L., Telfer, E., and Scott, B. 2001. Molecular cloning and genetic analysis of an indole-diterpene gene cluster from *Penicillium paxilli*. Mol. Microbiol. 39:754-764.

Zhang, S., Monahan, B. J., Tkacz, J. S., and Scott, B. 2004. Indole-diterpene gene cluster from *Aspergillus flavus*. Appl. Environ. Microbiol. 70:6875-6883.

Zhou, C., Zhang, L., Duan, J., Miki, B., and Wu, K. 2005. HISTONE DEACETYLASE19 is involved in jasmonic acid and ethylene signaling of pathogen response in Arabidopsis. Plant Cell 17:1196-1204.

# Chapter V

## TmpL, a Novel Transmembrane Protein Is Required for Intracellular Redox Homeostasis and Virulence in a Plant and an Animal Fungal Pathogen

## Abstract

(This work was published as ***Kim et al., 2009, PLoS Pathogens, In Press***)

The regulation of intracellular levels of reactive oxygen species (ROS) is critical for developmental differentiation and virulence of many pathogenic fungi. In this report we demonstrate that a novel transmembrane protein, TmpL, is necessary for regulation of intracellular ROS levels, tolerance to external ROS, and required for infection of plants by the necrotroph, *Alternaria brassicicola* and mammals by the human pathogen, *Aspergillus fumigatus*. In both fungi, *tmpL* encodes a predicted hybrid membrane protein containing an AMP-binding domain, six putative transmembrane domains, and an experimentally-validated FAD/NAD(P)-binding domain. Localization and gene expression analyses in *A. brassicicola* indicated that TmpL is associated with the Woronin body, a specialized peroxisome, and strongly expressed during conidiation and initial invasive growth *in planta*. *A. brassicicola* and *A. fumigatus ΔtmpL* strains exhibited abnormal conidiogenesis, accelerated aging, an enhanced oxidative burst during conidiation, and hypersensitivity to oxidative stress when compared to wild-type or reconstituted strains. Moreover, *A. brassicicola ΔtmpL* strains although capable of initial penetration, exhibited dramatically reduced invasive growth on Brassicas and Arabidopsis. Similarly, an *A. fumigatus ΔtmpL* mutant was dramatically less virulent than the wild-type and reconstituted strains in a murine

model of invasive aspergillosis. Constitutive expression of the *A. brassicicola yap1* ortholog in an *A. brassicicola ΔtmpL* strain resulted in high expression levels of genes associated with oxidative stress tolerance. Overexpression of *yap1* in the *ΔtmpL* background complemented the majority of observed developmental phenotypic changes and partially restored virulence on plants. Yap1-GFP fusion strains utilizing the native *yap1* promoter, exhibited constitutive nuclear localization in the *A. brassicicola ΔtmpL* background. Collectively, we have discovered a novel protein involved in the virulence of both plant and animal fungal pathogens. Our results strongly suggest that dysregulation of oxidative stress homeostasis in the absence of TmpL is the underpinning cause of the developmental and virulence defects observed in these studies.

# Introduction

Oxidative stress arises from a significant increase in the concentration of reactive oxygen species (ROS) inside the cell, and is primarily caused by either an imbalance of the cellular antioxidant capacity or a deficiency in the antioxidant system controlling ROS levels (Halliwell and Gutteridge, 2002). The damaging effects of ROS on DNA, proteins, lipids and other cell components and their role in pathological and aging processes is well established (Apel and Hirt, 2004; Halliwell and Gutteridge, 1986; Stohs, 1995). Numerous studies of pathogenic fungi have documented the crucial role of ROS produced by either fungal pathogens or their hosts in pathogenesis and defense-related activities (Egan et al., 2007; Missall et al., 2004; Nathues et al., 2004). There is also increasing evidence supporting an alternative view that ROS play

important physiological roles as signaling molecules. ROS have been shown to be critical in immunity, cell proliferation, cell differentiation, and cell signaling pathways. However, the mechanisms by which ROS and their associated enzymes regulate development in microbial eukaryotes remain to be defined (Finkel, 2003; Lambeth, 2004). Taken together, all the deleterious, pathological, and regulatory roles of ROS have generated great interest in defining the mechanisms by which ROS are produced, sensed, and managed in eukaryotes.

Because ROS readily lead to oxidative injuries, it is extremely important that the cellular ROS level be tightly controlled by complex and sophisticated redox homeostasis mechanisms. In the yeast *Saccharomyces cerevisiae*, the transcription factors Yap1 and Skn7 and a pair of related factors, Msn2 and Msn4 (Msn2/4), are implicated in controlling intracellular ROS levels (Moye-Rowley, 2003; Temple et al., 2005; Thorpe et al., 2004). Yap1 and Skn7 activate the expression of proteins that intercept and scavenge ROS. Yap1 is primarily controlled by a redox-sensitive nuclear export mechanism that regulates its nuclear accumulation when activated (Kuge et al., 1997). The Msn2/4 regulon contains only a small number of antioxidants but also includes heat shock proteins (HSPs), metabolic enzymes, and components of the ubiquitin-proteasome degradation pathway (Hasan et al., 2002). Recently, a heat shock transcription factor, Hsf1, has been added to the list of oxidative stress-responsive activators (Yamamoto et al., 2007). In addition to those found in *S. cerevisiae*, hybrid histidine kinase Mak1 and response regulator Prr1 (a Skn7 homolog), and bZIP transcription factors Atf1 and Pap1 (a Yap1 homolog) in *Schizosaccharomyces pombe*

are also involved in transducing hydrogen peroxide ($H_2O_2$) signals. These proteins are required to induce catalase gene *ctt1*$^+$ and other genes in response to $H_2O_2$ (Buck et al., 2001; Santos and Shiozaki, 2001). Although several similar proteins have been found and characterized in filamentous fungi, little is known about other transcriptional regulators or the defined regulatory mechanisms implicated in oxidative stress responses in filamentous fungi (Hagiwara et al., 2008; Molina and Kahmann, 2007; Nathues et al., 2004). However, orthologs of most components of the oxidative stress-sensing pathway described in yeasts are also known to be conserved in filamentous fungi such as *Aspergillus nidulans* and *Neurospora crassa* (Aguirre et al., 2005; Borkovich et al., 2004).

Pathogenic fungi need specialized, multi-faceted mechanisms to deal with the oxidative stress encountered *in vivo* during infection. Therefore, adaptive mechanisms that confer resistance to the oxidative stress from intra- or extracellular sources may contribute to the efficient colonization and persistence of fungal pathogens in their hosts. One of the most rapid plant defense reactions encountered by plant pathogens is the so-called oxidative burst, which constitutes the production of ROS, primarily superoxide and its dismutation product, $H_2O_2$, at the site of attempted invasion (Mehdy, 1994; Wojtaszek, 1997). The ROS produced by the oxidative burst either activate plant defense responses, including programmed cell death, or function as secondary messengers in the induction of various pathogenesis-related (*PR*) genes encoding different kinds of cell wall-degrading enzymes (Bindschedler et al., 2006; Hammond-Kosack and Jones, 1996; Torres et al., 2006). Furthermore, the presence of

$H_2O_2$ is essential for the formation of lignin polymer precursors via peroxidase activity, which provide additional plant barriers against pathogen attack (Passardi et al., 2005).

Similarly, animal phagocytic cells produce ROS to combat invading fungal pathogens. For example, following inhalation of airborne *Aspergillus fumigatus* conidia, the normal host is protected by pulmonary innate immunity, including phagocytosis by macrophages, where the killing of the engulfed conidia is known to be directly associated with ROS production (Brummer et al., 2005; Philippe et al., 2003). *In vitro* studies of neutrophil function have shown that $H_2O_2$ effectively kills fungal hyphae (Diamond and Clark, 1982) and that neutrophil-mediated damage is blocked by the addition of a commercial catalase (Diamond et al., 1978). Consequently, to counteract the potentially dangerous accumulation of ROS surrounding infection sites, fungal pathogens have developed diverse strategies. These include physically fortified or specialized fungal infection structures and various antioxidant defense systems through transporter-mediated effluxing, non-enzymatic antioxidants, and enzymatic scavenging systems, generally using NAD(P)H as reducing equivalents (Agrios, 1997; Belozerskaia and Gessler, 2007; Shibuya et al., 2006; Sun et al., 2006).

Through a combination of computational and functional genomics approaches a novel gene *tmpL*, encoding a transmembrane protein with a N-terminal AMP-binding domain and C-terminal NAD(P)/FAD-binding domain, was characterized in this study. Previously, a protein with approximately 50% identity but lacking the AMP-binding domain present in TmpL was discovered in *A. nidulans* to be important

for regulation of conidiation (Soid-Raggi et al., 2006). TmpL was initially identified during this study and referred to as the large TmpA homolog but was not functionally characterized (Soid-Raggi et al., 2006). In the present study, we characterize TmpL in both a plant and an animal fungal pathogen and provide cytochemical and genetic evidence that demonstrate a filamentous fungi-specific mechanism for control of intracellular ROS levels during conidiation and pathogenesis.

# Results

### Structure and annotation of *tmpL*

Previously, seven putative nonribosomal peptide synthetase (*NPS*) genes designated as *AbNPS1* to *AbNPS7*, for *Alternaria brassicicola* nonribosomal peptide synthetase, were identified in the *A. brassicicola* genome via HMMER and BLAST analyses in our lab (Kim et al., 2007). During this study, a *NPS*-like gene was identified with only a putative AMP-binding domain similar to an adenylation domain, followed by six transmembrane domains. There were no sequences in the adjacent region similar to thiolation and condensation domains which are typical components in the multi-modular organization of *NPS* genes. We designated this AMP-binding domain containing gene as *tmpL*, referring to the previous nomenclature but designating it as *tmpL* in lieu of large *tmpA* homolog (Soid-Raggi et al., 2006). The entire sequence of the *tmpL* gene was determined and confirmed by several sequencing events using genomic DNA and cDNA as templates for PCR based amplification and sequencing with primers based on information derived from the *A. brassicicola* genome sequence (http://www.alternaria.org). The open reading frame

(ORF) of the *tmpL* is 3450 bp long and predicted to encode a protein of 1025 amino acids. The predicted TmpL hybrid protein contains an AMP-binding domain, six putative transmembrane domains, and a FAD/NAD(P)-binding domain (Fig. 1A).

The *A. brassiciola* TmpL protein sequence was used to search for an *A. fumigatus* ortholog via BLASTP analysis in the genome sequence of strain CEA10. The highest sequence similarity was found for a protein encoded by a gene with the locus ID AFUB_085390. The protein sequences are 41% identical and use of protein domain prediction tools suggested that the *A. fumigatus* protein, like the *A. brassicicola* protein, has a putative N-terminal AMP-binding domain, followed by six transmembrane domains and a FAD/NAD(P)-binding domain at the C-terminus. Based on the high sequence and structural similarities to the *A. brassicicola tmpL* gene, we named this gene *A. fumigatus tmpL* as well. The ORF of the *A. fumigatus tmpL* is 3357 bp long, contains 8 predicted introns and encodes for a protein of 994 predicted amino acids.

The AMP-binding domain of the TmpL protein showed high similarity to adenylation domains of the NPS proteins (Schwarzer et al., 2003), which are generally involved in the activation of an amino acid substrate in the nonribosomal synthesis of polypeptides. One of the most similar sequences in the GenBank NR database was *Cochliobolus heterostrophus NPS12* (score = 2901, ID = 54%), which was reported as a putative *NPS* gene (Lee et al., 2005). However protein functional domain searches conducted against NCBI conserved domains and the InterPro database did not detect any thiolation and condensation domains in the predicted TmpL protein. This indicates

that the TmpL is indeed lacking both thiolation and condensation domains that are conserved among NPSs, and thus is not a true NPS protein.

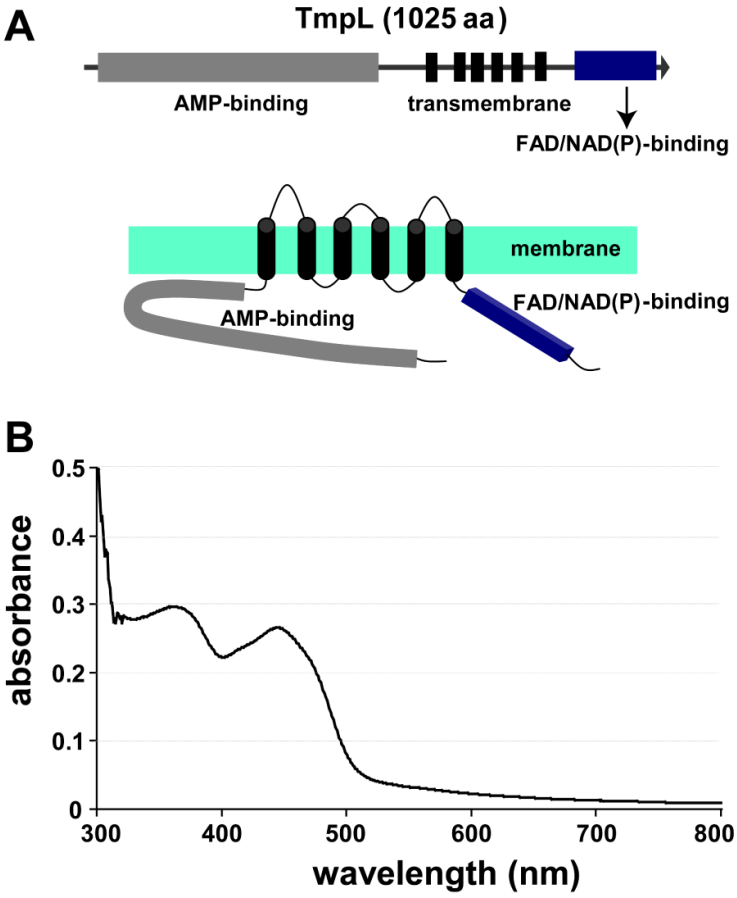


**Figure 1. TmpL is a putative membrane flavoprotein. (A)** Domain organization of TmpL. The predicted protein encoded by the *tmpL* gene is comprised of 1025 amino acid residues. This protein contained an AMP-binding, six putative transmembrane, and FAD/NAD(P)-binding domains. Bottom picture shows predicted topological map of the TmpL protein. Regions of TmpL proposed to be hydrophobic membrane-spanning domains or hydrophilic domains facing the cytosol or subcompartmental matrix were identified using the TMHMM (http://www.cbs.dtu.dk/services/TMHMM-2.0/) and PRED-TMR (http://o2.biol.uoa.gr/PRED-TMR2/). **(B)** UV-visible spectra of TmpL partial recombinant protein containing FAD/NAD(P)-binding region. The absorbance spectrum shown indicates that the protein contains bound flavin, demonstrating that TmpL is a FAD/NAD(P)-binding flavoprotein. A solution of the FAD-incubated protein (1 mg $ml^{-1}$) in 50 mM sodium phosphate buffer, pH 7.5, was analyzed.

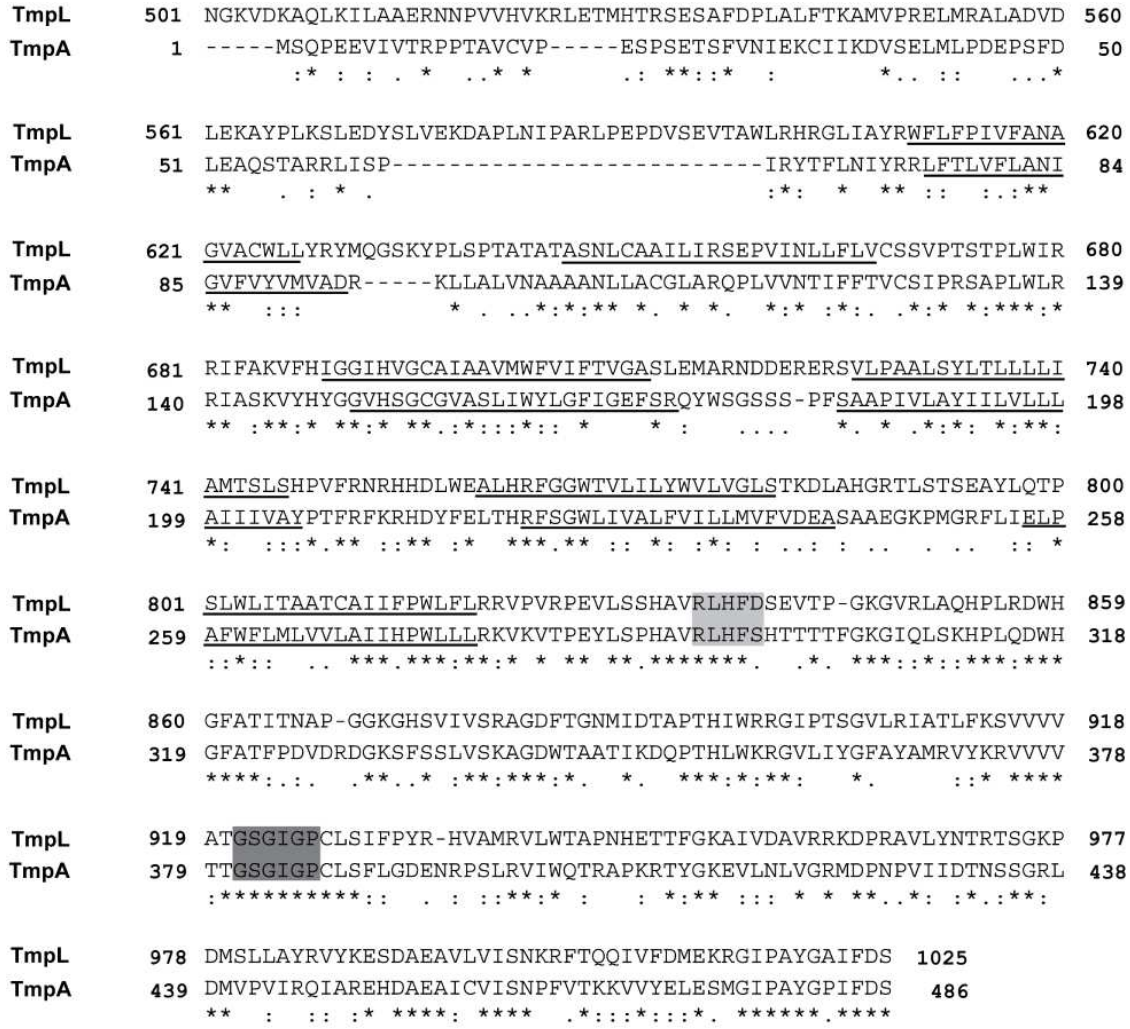


**Figure 2. Sequence comparison of *A. brassicicola* TmpL protein with *Aspergillus nidulans* TmpA protein.** The partial amino acid sequence (501-1025) of TmpL is aligned with TmpA protein (GenBank accession no. AAP13095) from *A. nidulans* using ClustalW2. Identical amino acid residues are indicated by asterisks and similar residues by dots. Predicted transmembrane domains in TmpL and TmpA are underlined. Hypothetical FAD (RLHFD) and NAD(P) (GSGIGP) phosphate-binding domains are indicated with light and dark gray boxes respectively.

**TmpL is a FAD/NAD(P)-binding flavoprotein**

Given that TmpL does not appear to be a true NPS, we next sought to determine the function of this protein in *A. brassicicola.* The transmembrane and FAD/NAD(P)-binding domains demonstrated a high sequence similarity and predicted structure to the previously identified plasma membrane flavoprotein, TmpA, in *Aspergillus nidulans* (Fig..2) (Soid-Raggi et al., 2006). As with TmpA, the sequence analysis of the FAD/NAD(P)-binding domain showed that TmpL contains two important consensus sequences which are highly conserved in flavoproteins that bind both FAD and NAD(P). They are hypothetical FAD (RLHFD) and NAD(P) (GSGIGP) phosphate-binding domains (Fig. 2), and correspond to the RXYS(T) motif for the FAD-binding domain and the GXGXXG or GT(S)G(A)IXP consensus sequences for the NAD(P)-binding domain, respectively (Dym and Eisenberg, 2001; Rossmann et al., 1974; Sridhar Prasad et al., 1998). In addition, protein structure homology modeling with TmpL C-terminal 247 amino acids using *Azotobacter vinelandii* NADPH:ferredoxin reductase as a template (Sridhar Prasad et al., 1998) via SWISS-MODEL at ExPASy (http://swissmodel.expasy.org/) showed a possible cleft formed by the two domains where the FAD and NAD(P)-binding sites were juxtaposed (data not shown). This finding was also reported in the TmpA study (Soid-Raggi et al., 2006).

To support this *in silico* data, we generated a partial TmpL recombinant protein containing the FAD/NAD(P)-binding domain via *E. coli* expression. The UV-visible spectra of the partial protein observed were characteristic of a flavoprotein (Fig. 1B).

The absorbance peaks at 367 and 444 nm indicated that the enzyme contained bound flavin. All of these analyses suggest that TmpL possesses an enzymatic function using its FAD/NAD(P)-binding domain like other NAD(P)H-dependent flavoenzymes containing FAD or FMN cofactors such as the ferric reductase (FRE) protein group. Fungal proteins belonging to the FRE group include metalloreductase (Singh et al., 2007), NADPH-cytochrome P450 reductase (Kargel et al., 1996), ferric-chelate reductase (Shatwell et al., 1996), and NADPH oxidases (NOX) (Lambeth, 2004).

**TmpL is associated with specific fungal Woronin bodies and shows conidial age-dependent association with peroxisomes**

Next, we examined the putative subcellular localization of TmpL to gain possible insights into its cellular functions. First, *in silico* analyses were performed using WoLF PSORT, SHERLOC, TARGETP, TMHMM, PRED-TMR and SIGNALP (Bendtsen et al., 2004; Horton et al., 2007; Nakai and Horton, 1999; Pasquier et al., 1999; Shatkay et al., 2007; Sonnhammer et al., 1998). SHERLOC predicted a possible subcellular localization of the TmpL protein to the peroxisomal membrane with a high probability score (0.94), while WoLF PSORT and TARGETP assigned no definitive subcellular location. TMHMM and PRED-TMR analyses predicted six possible transmembrane helices in TmpL similar to the results of initial protein conserved domain searches. There was no predictable N-terminal signal peptide sequence for co-translational insertion into a specific subcellular component by SIGNALP. Taken together, these predictions indicated that TmpL might be a peroxisomal integral membrane protein with six transmembrane helices.

To experimentally determine the localization of TmpL within the various cell types and intracellular compartments and organelles in *A. brassicicola*, a strain expressing a TmpL-GFP fusion protein was generated. Two transformants carrying a single copy of the *tmpL*:*gfp* allele tagged at the genomic locus were identified by PCR analysis and further confirmed by Southern blot analysis (data not shown). Compared with the wild-type strain, neither of the two transformants exhibited differences in growth or pathogenesis except for expression of green fluorescence in conidia, suggesting that TmpL-GFP is fully functional. One of the transformants, A1G4, was used to analyze the localization of TmpL-GFP using confocal laser scanning fluorescence microscopy. The GFP signal was detected in conidia, but no GFP signal was detected in the vegetative mycelia of the A1G4 strain grown in complete media (CM) (Fig. 3A). The GFP signals were localized in a punctate pattern in the cytoplasm as one or two tiny spots in each conidial cell, either near septae or associated with the cortical membrane. Given the previous *in silico* analyses, we hypothesized that the GFP signal might come from a specialized peroxisomal structure, the Woronin body (WB). In order to perform a co-localization test, we selected the known WB core protein HEX1 in *N. crassa*, and searched for the orthologous *abhex1* gene in *A. brassicicola*. Using the same strategy with the TmpL-GFP fusion constructs, we produced a DsRed-AbHex1 fusion protein-expressing transformant in the TmpL-GFP strain A1G4 background. DsRed-AbHex1 showed a similar punctate distribution in the cytoplasm, mostly near septal pores, but a few distant from septal pores. Figure 3A shows only DsRed-AbHex1 that are distant from septal pores co-localized with the TmpL-GFP. A separate analysis by confocal microscopy of strains that expressed

either TmpL-GFP or DsRed-AbHex1 ruled out any possible cross talk between the two fluorescence signals. Although there is no literature indicating two distinct types of WBs in fungal conidia, this might suggest that TmpL is associated with a specific WB that is not associated with septal pores. Using transmission electron microscopy (TEM) of *A. brassicicola* conidia, we confirmed several WBs located distantly from septal pores (Fig. 4). As mentioned, there was no TmpL-GFP detected in vegetative hyphae, while the DsRed-AbHex1 was distributed near septal pores (Fig. 3A) as reported in other studies (Engh et al., 2007; Managadze et al., 2007).

The WB has been described as evolving or being formed from peroxisome. The HEX1 assemblies emerge from the peroxisome by fission (budding off) and the nascent WB is subsequently associated with the cell cortex (Liu et al., 2008; Tey et al., 2005). To observe the peroxisomes and their relationship to TmpL, we co-expressed TmpL-GFP and peroxisome matrix-targeted DsRed which has a C-terminal SKL tripeptide, a peroxisome targeting singal 1 (PTS1). The TmpL-GFP was mostly associated with relatively large peroxisomes (Fig. 3B). Interestingly, depending on whether conidia were harvested from the center or edge of the colony (old to young) prior to microscopic examination, three different types of association between TmpL-GFP and DsRed-PTS1 were observed. The TmpL-GFP signals in young conidia most often showed complete association with peroxisomes. Some TmpL-GFP signals mainly in older conidia were detected in a partial association with or complete dissociation from DsRed-PTS1 (Fig. 3B). Together with TmpL-GFP localization with DsRed-AbHex1, these sequential associations might indicate a sequential process of

WB biogenesis in *A. brassicicola*: AbHex1 assemblies in large peroxisomes (Fig. 3B, a green circle), a budding event of nascent WB out of the peroxisome (Fig. 3B, white circles), and a mature WB that is completely separated from the peroxisome (Fig. 3B, red circles). This result was also supported by the observation of aged conidia from 21-day-old colonies, which rarely showed co-localization between TmpL-GFP and DsRed-PTS1 fusion proteins (data not shown).

It has been recently shown that PEX14, an essential component of the peroxisomal import machinery, is essential for the biogenesis of both peroxisome and WB. The deletion of *pex14* leads to complete mis-localization of peroxisomal matrix proteins containing PTS1 signal and HEX1 to the cytosol (Managadze et al., 2007). To determine whether deletion of the *A. brassicicola* homolog of *pex14* affects TmpL localization, we generated *Δpex14* mutant strains in a TmpL-GFP strain background using a linear minimal element (LME) gene disruption construct (Cho et al., 2006) and examined the mutants with confocal microscopy. In most of the TmpL-GFP:*Δpex14* mutant conidia, disruption of *pex14* resulted in an uneven distribution of the TmpL-GFP in the cytoplasm (Fig. 3C). The DsRed-AbHex1:*Δpex14* mutants used as control also showed cytoplasmic distribution of the DsRed-AbHex1 as reported in the study mentioned earlier (Managadze et al., 2007). Therefore, *pex14* is related to the proper localization of TmpL protein in association with WB and peroxisome proteins governed by *pex14*-related peroxisomal import machinery, further suggesting that TmpL is associated with a specific type of WB that is not associated with septal pores.

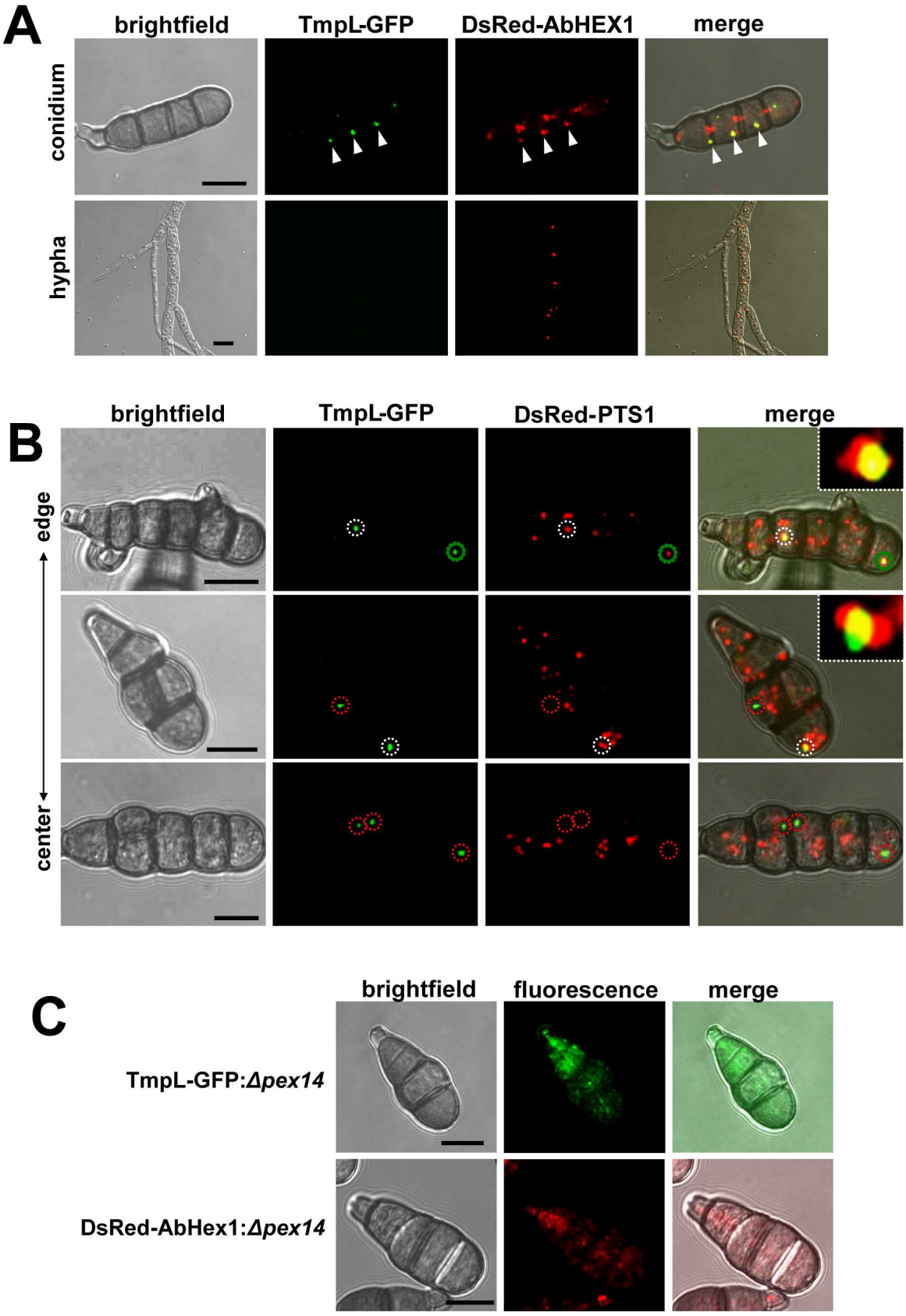
A
brightfield
TmpL-GFP
DsRed-AbHEX1
merge
conidium
hypha
B
brightfield
TmpL-GFP
DsRed-PTS1
merge
edge
center
C
brightfield
fluorescence
merge
TmpL-GFP:Δpex14
DsRed-AbHex1:Δpex14

**Figure 3. Subcellular distribution of TmpL-GFP fusion protein.**
**(A)** Colocalization analyses with a TmpL-GFP and DsRed-AbHex1 double-labeled strain in *A. brassicicola* conidium (upper panel) and vegetative hypha (lower panel) were examined using confocal microscopy. TmpL-GFP localizes over cell cortex-associated or cytoplasmic DsRed-AbHex1 signals (arrowheads), not the septal pore-associated signals. Note that no TmpL-GFP signal is observed in the growing vegetative hypha. Bars = 10 µm. **(B)** Colocalization analyses with a TmpL-GFP and DsRed-PTS1 double-labeled strain in *A. brassicicola* conidia. DsRed-PTS1 fluorescence reveals peroxisomes. A large peroxisome is completely associated with TmpL-GFP signal (a green dotted circle, top panel). The other circles denote a partial association between TmpL-GFP and DsRed-PTS1 signals (white dotted circles, top and middle panels) and a complete dissociation of TmpL-GFP with DsRed-PTS1 signals (red dotted circles, middle and bottom panels). Note that different conidial age determined by collected sites, from the center to the edge of fungal colony, shows different types of association between two fluorescence signals. Insets indicate a magnified view of each white dotted circle representing a partial association between TmpL-GFP and DsRed-PTS1 signals. Bars = 10 µm.
**(C)** Localization analyses with *Δpex14* mutants on a background of either a TmpL-GFP or DsRed-AbHex1 mutant strain. Note that the deletion of *pex14* resulted in cytoplasmic redistribution of TmpL-GFP and DsRed-AbHex1 fluorescence signals. Bars = 10 µm.

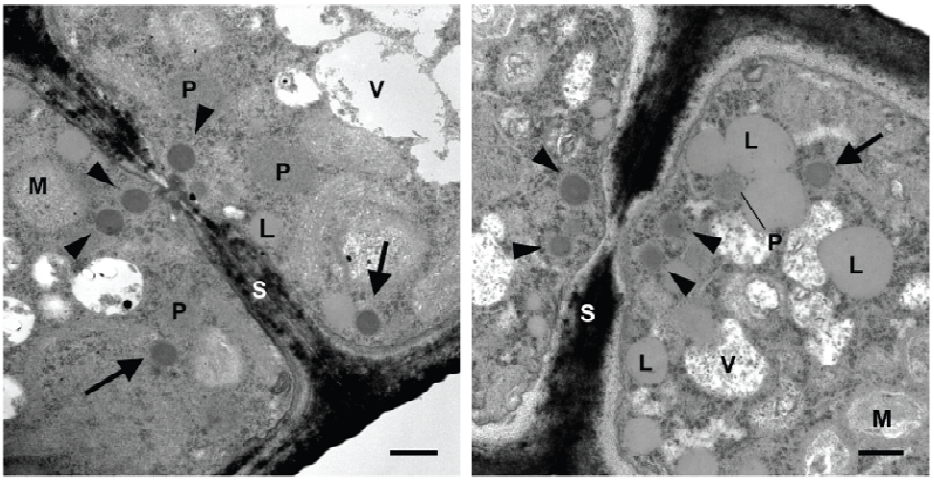


**Figure 4.** Transmission electron micrographs of *A. brassicicola* wild-type conidia showing Woronin body localization. Note that there are two locations of Woronin bodies: near septal pores (arrowheads) and apart from the septal pores, in cytoplasm (arrows). Bars = 500 nm. Abbreviations: L, lipid body; M, mitochondria; P, peroxisome; S, septa; V, vacuole.

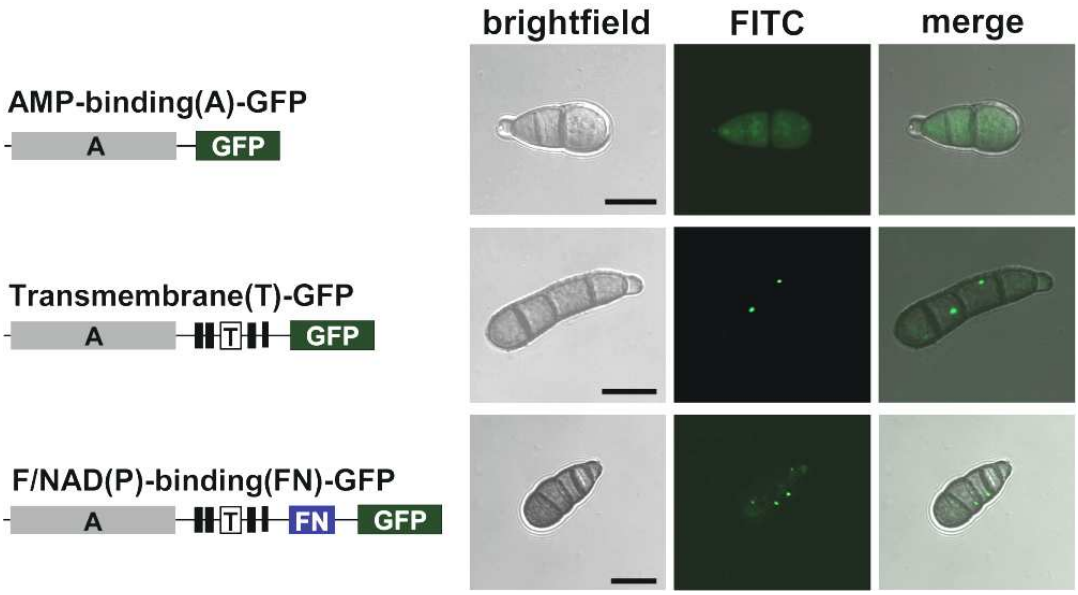


**Figure 5. The transmembrane domain of TmpL protein carries organelle targeting signal.** Organelle targeting of partial or complete TmpL-GFP fusion proteins. At left schematic representations: gray boxes represent the AMP-binding (A) domain of TmpL protein; six tandem black boxes represent the transmembrane (T) domain; and a blue box represents the FAD/NAD(P)-binding (FN) domain. Right micrographs show GFP signal localization patterns of each fusion protein in *A. brassicicola* conidia. Bars = 10 µm.

**The organelle targeting information is located in the transmembrane region of TmpL**

HEX1 and its orthologs in filamentous fungi possess a PTS1 at their C-terminal end that target it to the peroxisomal matrix (Galagan et al., 2003). However, as other known peroxisomal membrane proteins, the predicted TmpL sequences do not carry any defined localization signal peptides or PTS peptides. To identify the organelle targeting information in TmpL, we produced three transformants by appending GFP marker protein at three locations of TmpL: the AMP-binding domain, transmembrane domain, and FAD and NAD(P)-binding domain. This produced

truncated TmpL-GFP fusion proteins under the control of the wild-type tmpL promoter (Fig. 5). Using each construct, we generated three different GFP-tagged strains and examined their localization pattern. The AMP-binding-GFP fusion protein resulted in cytoplasmic distribution of the GFP signal, while the transmembrane- and FAD and NAD(P)-binding-GFP fusion proteins were concentrated in a punctate pattern in the cytoplasm (Fig. 5). This suggests that the transmembrane domain carries the targeting signal to the organelle membrane.

### ***tmpL*** **is strongly expressed during conidiation and initial invasive growth** ***in planta***

To gain further insights into the possible function of TmpL, we next examined *tmpL* mRNA abundance in diverse fungal developmental stages. Relative abundance of *tmpL* mRNA transcripts during vegetative growth, conidiation, and plant colonization were estimated by quantitative real-time polymerase chain reaction (QRT-PCR) (Fig. 6A). The abundance of *tmpL* mRNA during vegetative growth in liquid CM was extremely low compared with the internal reference gene, *A. brassicicola* glyceraldehyde 3-phosphate dehydrogenase (*GAPDH*). Interestingly, the mRNA abundance of *tmpL* increased almost six fold at 12 hr post-inoculation (hpi) on plant leaves (i.e., approximately at the time when penetration and infection hyphae develop from appressoria), compared with that of conidia (0 hpi). This result was also supported by *in planta* observation of the TmpL-GFP strain using epifluorescence microscopy (Fig. 6B). At 24 and 48 hpi, however, the mRNA abundance was significantly decreased from the 12 hpi level. From 48 hpi, the mRNA abundance gradually increased until 120 hpi. To examine *tmpL* mRNA abundance during

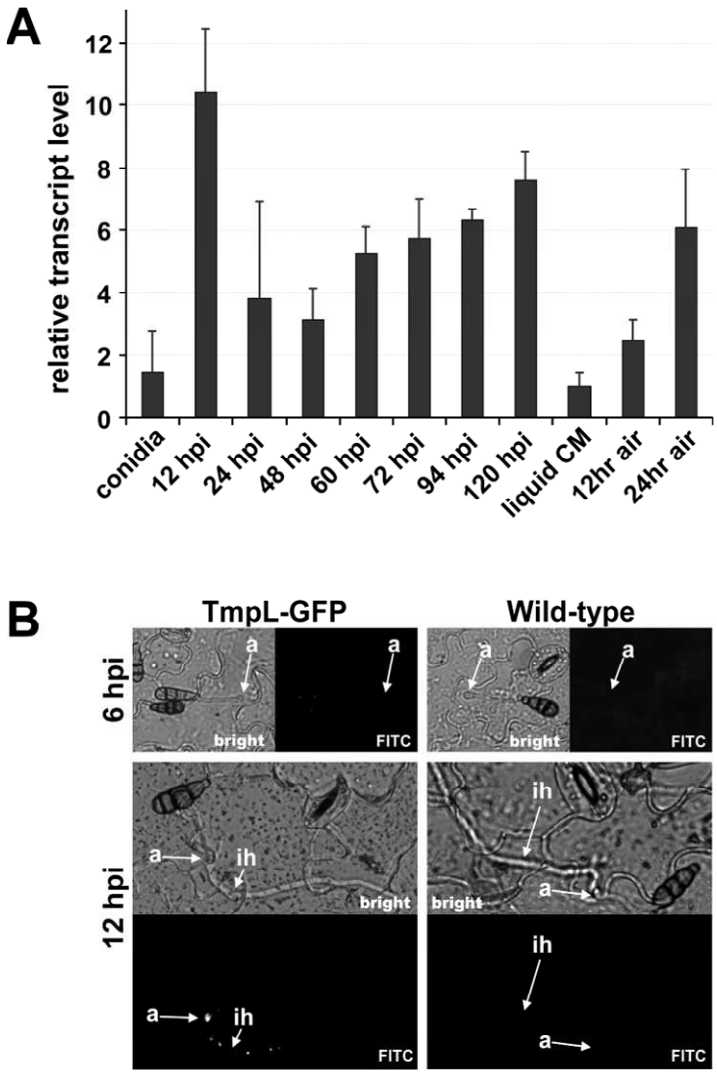


**Figure 6. Phase specific expression of *A. brassicicola tmpL*.** **(A)** The phase specific expression of *tmpL* was quantified by quantitative real-time (QRT)-PCR after synthesis of cDNA of each developmental RNA including infectious growth, vegetative growth, and condiation. Relative abundance of *tmpL* transcript during infectious growth (from ungerminated conidia to *in planta* fungal cells 120 hpi) and conidial development (from 12 hr air-exposed mycelia to 24 hr air-exposed mycelia) was normalized by comparing with vegetative growth in liquid CM (set to transcript level 1). **(B)** Epifluorescence microscopy of *in planta* GFP expression for the TmpL-GFP mutant strain. The germ tubes and appressoria did not show any GFP signal on the plant surface at 6 hpi. However, GFP signal was detectable at 12 hpi in a punctate pattern in the appressoria and infection hyphae growing within the plant tissue, consistent with the QRT-PCR results. The wild-type strain was used as a control. Abbreviations: a, appressorium; ih, infection hypha.

conidiation, vegetative mycelia grown in liquid CM were exposed to ambient air to stimulate conidiophore formation and subsequent conidia production. *tmpL* mRNA abundance was gradually elevated up to six-fold during conidiation compared with vegetative growth in liquid CM. Overall, these data indicate that *tmpL* transcript is strongly accumulated during conidiation and during infection *in planta*.

**Targeted mutagenesis of *tmpL* results in abnormal conidiogenesis and accelerated loss of conidial integrity with aging**

To further characterize the role of TmpL in fungal development and pathogenesis, a targeted gene replacement strategy was adopted to produce *tmpL* deletion mutants in *A. brassicicola* (Fig. 7) and *A. fumigatus* (Fig. 8). For the complementation of the *A. brassicicola ΔtmpL* (Ab*ΔtmpL*) strain we introduced both the full-length *tmpL* gene and nourseothricin resistance gene (*NAT)* fragments into the Ab*ΔtmpL* strain. Re-introduction of full-length *tmpL* gene in *A. fumigatus ΔtmpL* (Af*ΔtmpL*) strain was conducted as well by introducing full length *tmpL* with *hph* gene for hygromycin resistance ectopically into the Af*ΔtmpL* strain. The resulting complemented strains were named AbtmpL rec and AftmpL rec for *A. brassicicola* and *A. fumigatus* mutant strains, respectively. All strains were rigorously confirmed with Southern blot and PCR analyses (Fig. 7 and 8).

Analysis of developmental characteristics, including germination, growth, and conidiation on CM and *in planta*, of *A. brassicicola tmpL* deletion mutants indicated that they were indistinguishable from wild-type and an ectopic mutant A1E1. The

mutant strains also showed no defects related to osmotic stress, cell wall perturbation, or responses to antifungal drugs (data not shown). However, it was noted that the Ab*ΔtmpL* strains displayed less pigmentation in culture (Fig. 9A). Light microscopy showed that the conidia of the mutants were less pigmented and were narrower than the wild-type. Few multicellular conidia with longitudinal septa were detected among the mutants, which may explain the larger minor axis in wild-type conidia. In addition, increased conidial chain branching was observed in Ab*ΔtmpL* strains compared with the wild-type (Fig. 9A). Further investigation of the abnormal mutant conidia using TEM revealed that the conidial cell wall was significantly more electron-dense and thicker in the wild-type than the Ab*ΔtmpL* strain (wild-type, 746 ± 116 nm, n = 53; Ab*ΔtmpL*, 504 ± 83 nm, n = 64; $p<0.01$). The reconstituted strain AbtmpL rec showed the rescue of the less pigmented conidia and abnormal conidiogenesis seen in the Ab*ΔtmpL* strains (data not shown)

Another interesting difference between *A. brassicicola* wild-type and *ΔtmpL* strains was noticed in older fungal colonies. The conidial suspension of a 21-day-old Ab*ΔtmpL* strain appeared more yellow in color than a comparable wild-type suspension (Fig. 9B). We analyzed the conidial suspensions to obtain a secondary metabolite profile using high performance liquid chromatography but the profiles were comparable (data not shown). A protein quantification assay, however, detected large differences in the amount of protein. The 21-day-old Ab*ΔtmpL* strain released more cytoplasm than the wild-type as judged by the amount of total protein quantified in the conidial suspensions (Fig. 9B). This result was further supported by our finding that

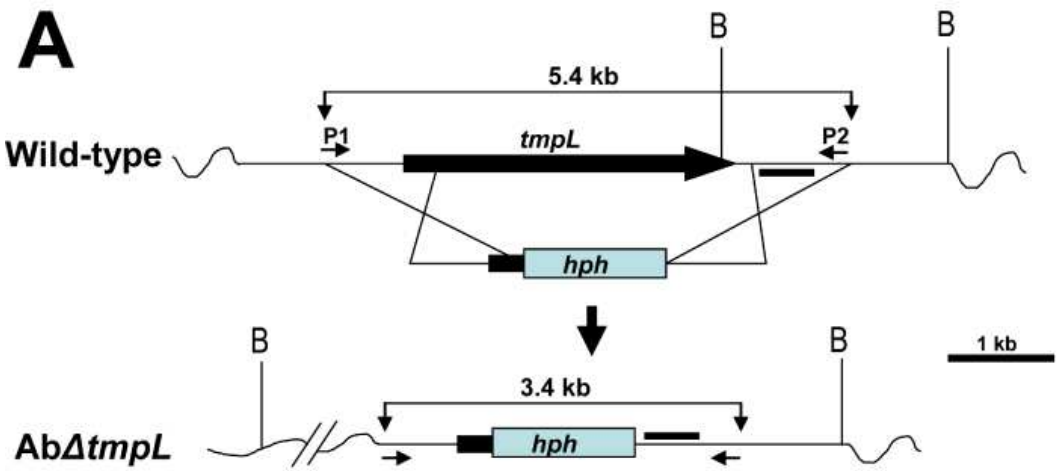
A
B
B
5.4 kb
P1
tmpL
P2
Wild-type
hph
B
B
1 kb
3.4 kb
hph
AbΔtmpL

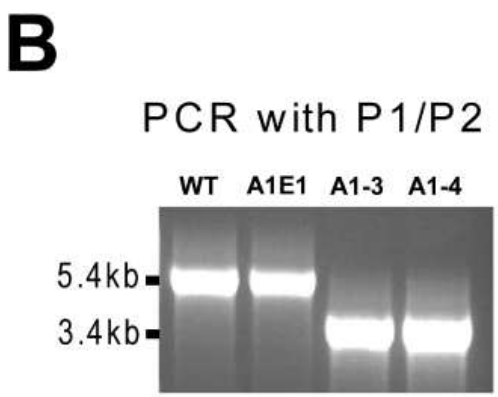
B
PCR with P1/P2
WT
A1E1
A1-3
A1-4
5.4kb
3.4kb

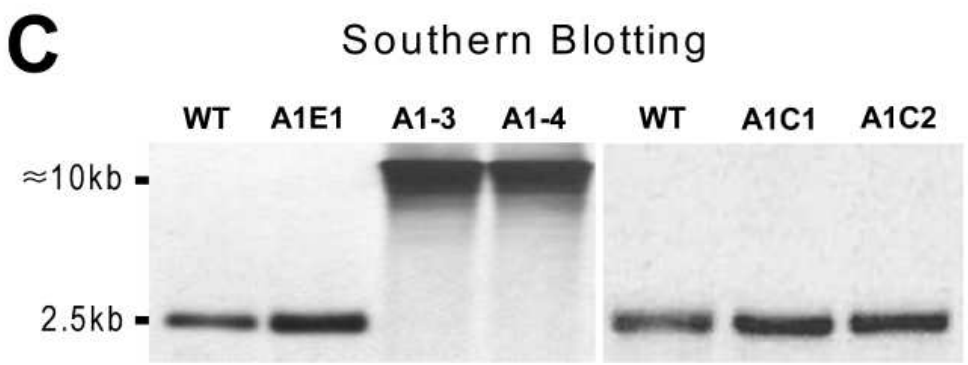
C
Southern Blotting
WT
A1E1
A1-3
A1-4
WT
A1C1
A1C2
≈10kb
2.5kb

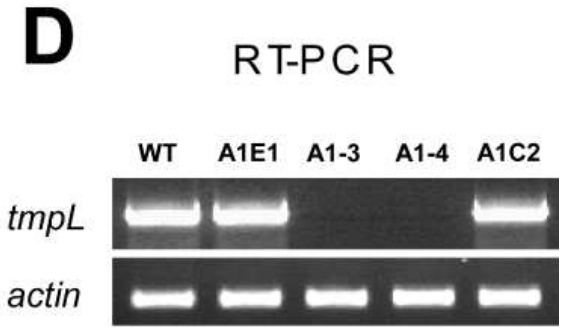
D
RT-PCR
WT
A1E1
A1-3
A1-4
A1C2
tmpL
actin

**Figure 7. Targeted gene replacement of the *A. brassicicola tmpL* locus.** **(A)** A gene replacement construct was generated by fusion PCR method and used for transformation of fungal protoplasts of *A. brassicicola* isolate ATCC93866. Shown are wild-type *tmpL* gene locus, a replacement cassette, and Ab*ΔtmpL* mutant locus replaced by the cassette. The mutated genomic locus of Ab*ΔtmpL* mutant is depicted to show homologous recombination of the replacement cassette. **(B)** *A. brassicicola* wild-type (WT), ectopic mutant (A1E1), and replacement of wild-type *tmpL* with a single copy of *hph* cassette by homologous recombination in two Ab*ΔtmpL* mutants (A1-3 and A1-4) were first screened by PCR with primers (P1/P2). **(C)** Southern blot analysis of *A. brassicicola* wild-type strain (WT), ectopic mutant (A1E1), two *ΔtmpL* mutants (A1-3 and A1-4), and two reconstituted mutants (A1C1 and A1C2). The wild-type and a hygromycin-resistant mutant A1E1 both contained a 2.5 kb *Bsr*GI fragment, but Southern blotting with *hph* fragment showed a 5 kb band in A1E1 (data not shown), indicating ectopic integration of a possible truncated replacement construct. A band shift to about 10 kb was detected in both Ab*ΔtmpL* mutants, indicating that homologous recombination occurred at a single site. The complemented mutants, A1C1 and A1C2, generated from a mutant strain A1-3 showed the same 2.5 kb band to the wild-type, indicating Ab*ΔtmpL* mutant A1-3 have been complemented by a full-length *tmpL* gene fragment. The letter B on the genomic locus (A) indicates enzymatic sites for *Bsr*GI that were used of genomic DNA digestion. The region used for labeling the hybridization probe is marked with a bar under the replacement cassette. **(D)** Reverse transcription (RT)-PCR showing *tmpL* transcripts from mycelia actively producing conidia of *A. brassicicola* wild-type (WT), ectopic mutant (A1E1), two *ΔtmpL* mutants (A1-3 and A1-4), and reconstituted mutant (A1C2). RT-PCR showed that *tmpL* transcripts are not detected among Ab*ΔtmpL* mutants during active conidiogenesis when mycelia were exposed to ambient air. *actin* was used as an internal control.

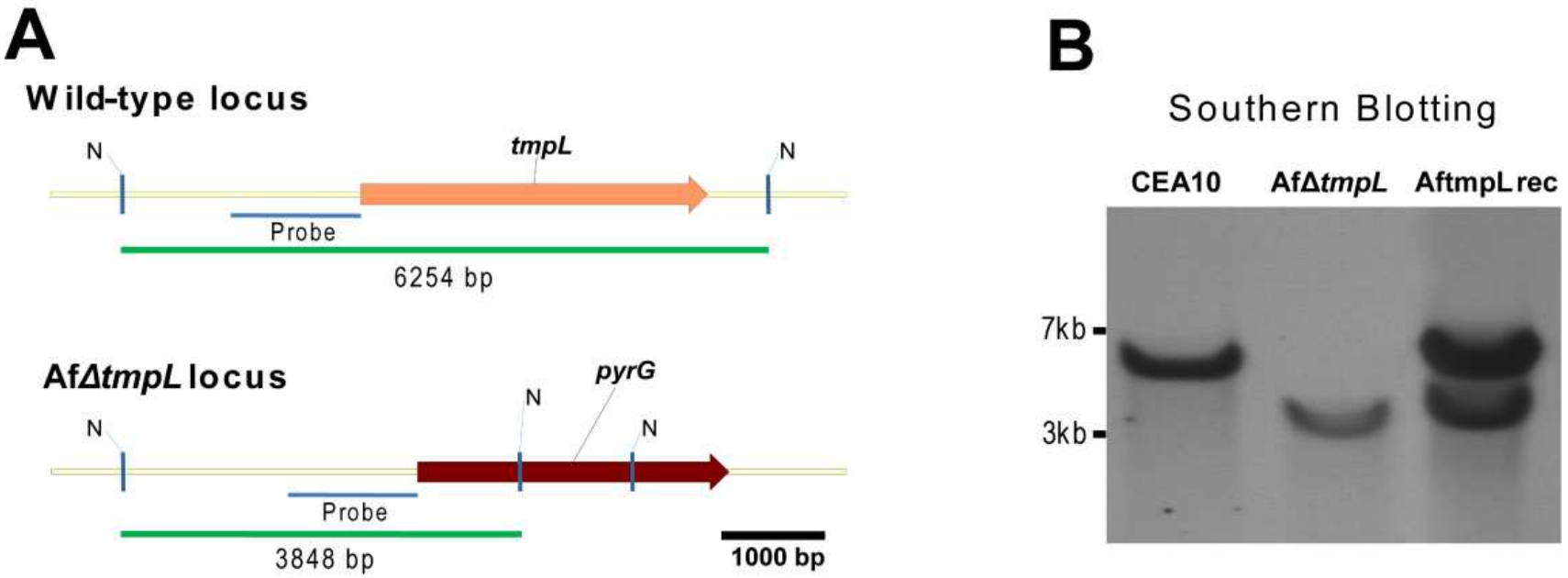


**Figure 8. Targeted gene replacement of the *A. fumigatus tmpL* locus.** **(A)** *A. fumigatus* wild-type *tmpL* gene locus was replaced by the *A. parasiticus pyrG* cassette, resulting in Af*ΔtmpL* mutant locus. The mutated genomic locus of Af*ΔtmpL* mutant is depicted to show homologous recombination of the replacement cassette. **(B)** Southern blot analysis of *A. fumigatus* wild-type strain (CEA10), *ΔtmpL* mutant (Af*ΔtmpL*), and reconstituted strain (AftmpL rec). The wild-type strain CEA10 contained a 6.3 kb *Nco*I fragment. A band shift to about 3.8 kb was detected in Af*ΔtmpL* strain, indicating that homologous recombination occurred at a single site. The reconstituted strain AftmpL rec showed the same 6.3 kb band to the wild-type and 3.8 kb band to the Af*ΔtmpL* strain, indicating the Af*ΔtmpL* mutant has been ectopically complemented by a full-length *tmpL* gene fragment. The letter N on the genomic locus (A) indicates enzymatic sites for *Nco*I that were used of genomic DNA digestion. The region used for labeling the hybridization probe is marked with a bar (Probe).

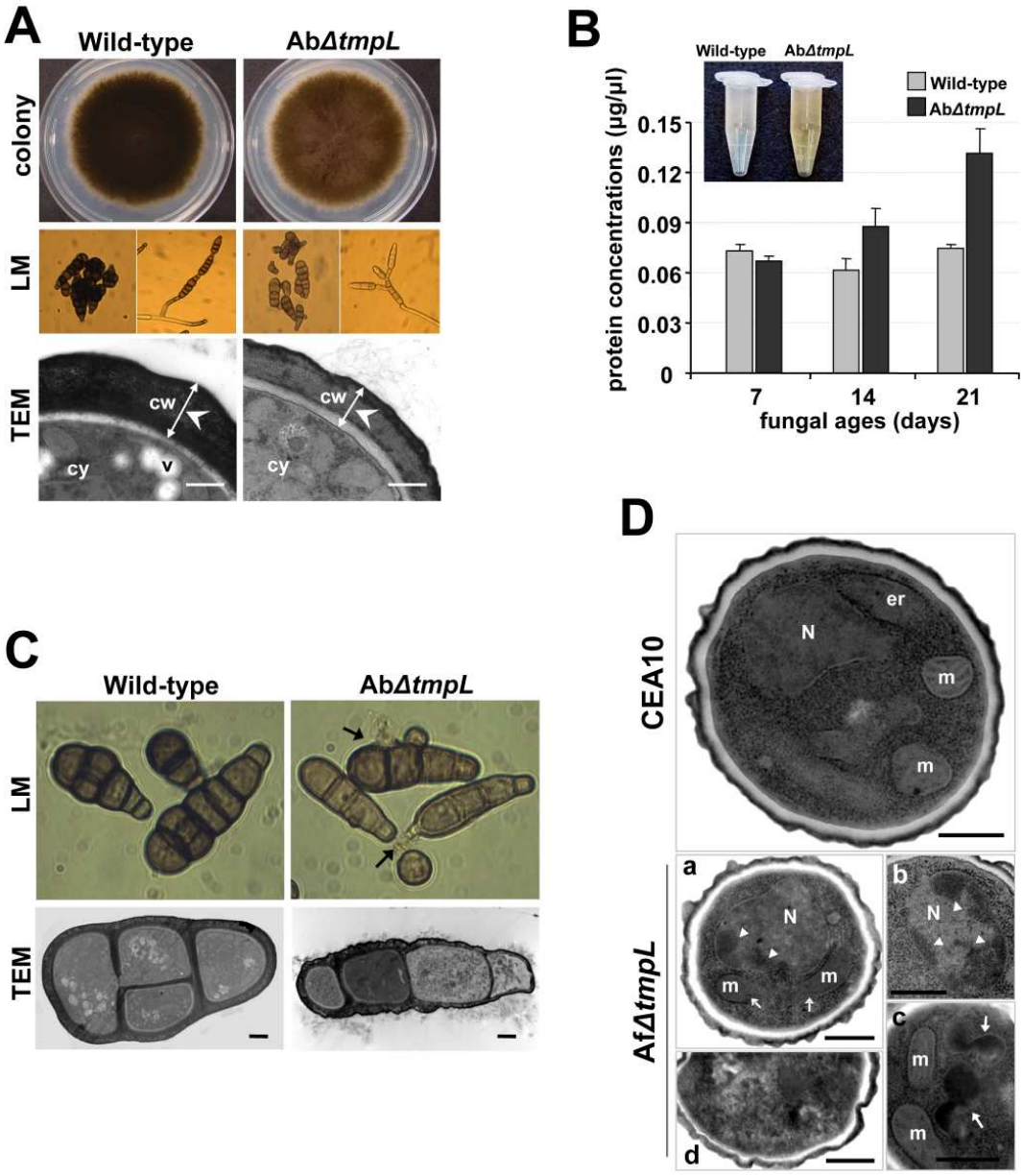


**Figure 9. Abnormal conidiogenesis and rapid loss of cell integrity in aged conidia of the *ΔtmpL* mutants.** **(A)** Fungal colony grown on solid CM plates (colony). Light micrographs (LM) of less-pigmented conidia and abnormal branching of the conidial chain of the Ab*ΔtmpL* mutants compared to the normal conidiogenesis of the wild-type. Transmission electron micrographs (TEM) depicting the less electron-dense and thinner cell wall of an Ab*ΔtmpL* mutant conidium compared to a wild-type conidium. Bars = 500 nm. Abbreviations: cw, conidial cell wall; cy, conidial cytoplasm; v, vacuole. **(B)** Quantification of protein concentration from conidial suspensions of *A. brassicicola* wild-type and *ΔtmpL* mutant. Note color difference of conidial suspensions between the wild-type and mutants (inset). Values indicate the total

quantity of protein released by different-aged fungal cultures from each strain. Average values and SD of three independent quantitations are shown. **(C)** Light and transmission electron micrographs of 21-day-old conidia of *A. brassicicola* wild-type and *ΔtmpL* mutant. Arrows indicate cytoplasmic bleeding through cell burst of the Ab*ΔtmpL* mutant conidia. Bars = 2 µm. **(D)** Transmission electron micrographs showing sections of 10-day-old conidia of *A. fumigatus* wild-type CEA10 and *ΔtmpL* mutant strains. Compared to the normal nucleus and subcellular structures of the wild-type conidia, more than half of the Af*ΔtmpL* mutant conidia showed at least one of the apoptotic histological markers: (a) discontinuous or missing mitochondrial outer membrane, (b) chromatin condensation and margination (arrowheads; a and b), (c) accumulation of huge electron dense materials (arrows) in cytoplasm, and (d) conidia with features of necrotic cell death. Bars = 500 nm. Abbreviations: er, endoplasmic reticulum; m, mitochondria; N, nuclei.

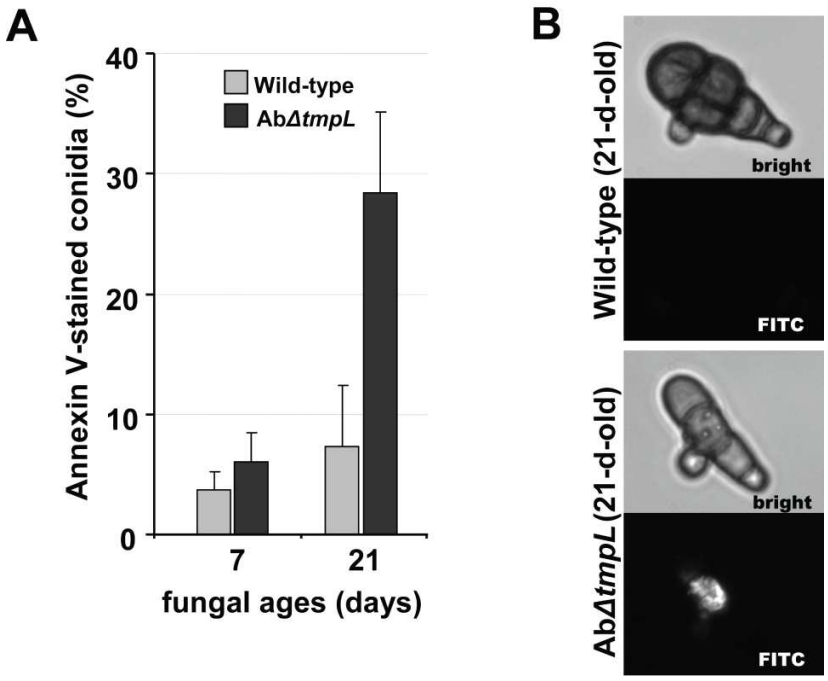


**Figure 10. Detection of cell death in *A. brassicicola* wild-type and *ΔtmpL* conidia stained with annexin V-FITC.** **(A)** Conidia collected from 7- and 21-d-old fungal colonies grown on solid CM were subjected to annexin V-FITC staining. Percentage of conidia showing fluorescence that are classified as dead cells was measured. Columns and error bars represent average and SD, respectively, of two independent experiments. **(B)** Representative micrographs showing an annexin V-FITC positive conidial cell of the 21-d-old Ab*ΔtmpL* mutant, while no staining in the 21-d-old wild-type conidia.

the 21-day-old Ab*ΔtmpL* conidia showed frequent cell bursts in water under light microscopy, which resulted in exuding large amounts of cytoplasm (Fig. 9C, LM). Ultrastructural analysis revealed more frequent cell necrosis-like phenotypes in cells of the Ab*ΔtmpL* conidia compared with seemingly intact wild-type conidia (Fig. 9C, TEM). In order to clarify the TEM observation, we determined the percentage of old conidia that stained positive with annexin V-FITC, a compound that specifically stains apoptotic or dead cells by binding to phosphatidylserine present on the outer leaflet (Champagne et al., 1999; De Smet et al., 2004). The annexin V-stained conidia from 21-day-old Ab*ΔtmpL* strain were increased significantly to 30 %, whereas the annexin V-positive wild-type conidia had increased less than 10 % after 21 days of growth on CM (Fig. 10). These phenotypic abnormalities suggest that the membrane protein TmpL is required for proper fungal conidiation and maintenance of fungal cell integrity with aging in *A. brassicicola*.

*A. fumigatus ΔtmpL* strains displayed no noticeable phenotypic change when grown on glucose minimal media (GMM) plates compared with the wild-type strain CEA10. Unlike *A. brassicicola ΔtmpL* strains, *A. fumigatus ΔtmpL* strains displayed normal pigmentation and cell wall thickness in conidia compared with CEA10 (data not shown). However, when we examined aged conidia using TEM, obvious differences were observed in the Af*ΔtmpL* strain conidia (Fig. 9D). The 10-day-old *A. fumigatus* wild-type conidia featured cells with normal structure and clearly identifiable organelles, nuclei surrounded by a nuclear membrane, and mitochondria with well-preserved outer and inner membranes (Fig. 9D, CEA10). TEM of the

reconstituted strain AftmpL rec conidia were comparable to the wild-type conidia (data not shown). However, Af*ΔtmpL* conidia had an abnormal subcellular morphology (Fig. 9D, Af*ΔtmpL*). The mitochondria were less well defined and often displayed discontinuous or missing outer membranes (Fig. 9D, a). Chromatin condensation and margination was observed in many nuclei (Fig. 9D, a and b) and amorphous electron-dense fragments were frequently aggregated in the cytoplasm (Fig. 9D, c). Signs of cell death, such as distorted organelles and numerous small vacuoles, were also observed in some conidia (Fig. 9D, d). These features appeared frequently, but not all were observed in every cell.

**Deletion of *tmpL* leads to hypersensitivity to oxidative stresses and excess oxidative burst in fungal cells during conidiation and plant penetration**

Given the peroxisomal association of TmpL and the dramatic phenotype during conidiation observed in *ΔtmpL* strains, we suspected a possible involvement of TmpL in oxidative stress responses. To investigate this hypothesis, wild-type and *ΔtmpL* mutants of *A. brassicicola* were examined for sensitivity to two different sources of oxidative stress, the superoxide generator $KO_2$ and $H_2O_2$. The Ab*ΔtmpL* strain showed increased sensitivity to oxidative stress compared with the wild-type (Fig. 11A). The minimal inhibitory concentration (MIC) of $KO_2$ for *A. brassicicola* wild-type was 12.5 mM and for the Ab*ΔtmpL* strain, 7.5 mM; the MIC of $H_2O_2$ for wild-type, 7.5 mM and for Ab*ΔtmpL*, 5 mM. The reconstituted strain AbtmpL rec showed comparable sensitivity to oxidative stress with the wild-type, indicating deletion of *tmpL* caused the hypersensitivity to oxidative stress. In order to investigate the functional conservation of the *A. fumigatus tmpL*, we also examined *A. fumigatus*

*ΔtmpL* strains for sensitivity to oxidative stress. We tested germling sensitivity to $H_2O_2$ for the *A. fumigatus* strains (Fig. 11B). The germlings of the Af*ΔtmpL* strain were more sensitive to $H_2O_2$ than the wild-type (p=0.0018). The reconstituted strain AftmpL rec showed comparable sensitivity to $H_2O_2$ as the wild-type, and a slight, but statistically not significant, increase in tolerance to oxidative stress created by $H_2O_2$ in the germling test (Fig. 11B).

Visualization of the accumulation of reactive oxygen species (ROS) was examined to investigate oxygen metabolism during conidiation and plant infection in *A. brassicicola* wild-type and *ΔtmpL* strains. We first investigated the production of ROS by using nitroblue tetrazolium (NBT), which forms a dark-blue water-insoluble formazan precipitate upon reduction by superoxide radicals. Using this technique, it appeared that the Ab*ΔtmpL* strain colonies and conidia accumulated higher amounts of superoxide than the wild-type (Fig. 12A). Such increased accumulation of superoxide was also detected in the Ab*ΔtmpL* strain inoculated on onion epidermis. Formazan precipitates were typically more intense in the mature appressoria and emerging infection hyphae of the Ab*ΔtmpL* strain, normally after 12 hpi (Fig. 12B). However, wild-type appressoria and infection hyphae had less formazan precipitate than the Ab*ΔtmpL* strain.

To investigate production of other ROS in conidia of *A. brassicicola* strains, we used 2′,7′-dichlorodihydrofluorescein diacetate ($H_2$DCFDA). This cell-permeable ROS indicator remains nonfluorescent until it is deacetylated by intracellular esterases and oxidized to yield DCF. The $H_2$DCF can be oxidized by several ROS generated by

intracellular peroxidases, but not directly by $H_2O_2$ (Myhre et al., 2003; Royall and Ischiropoulos, 1993). Conidia released from 7-day-old colonies were subject to the $H_2$DCFDA staining. More than half of the Ab*ΔtmpL* strain conidia examined were stained by $H_2$DCFDA while only few wild-type conidia showed green fluorescence (Fig. 12C). Staining with 3,3′-diaminobenzidine tetrahydrochloride (DAB) visualized that mature appressoria of the Ab*ΔtmpL* strain on green cabbage cotyledons also accumulated more $H_2O_2$ than wild-type appressoria at 12 hpi (Fig.12D). Together these data indicate that deletion of *tmpL* in *A. brassicicola* caused an intracellular burst of ROS in conidia and infection structures.

This accumulation of ROS was also visualized in *A. fumigatus* wild-type and the *ΔtmpL* strain conidia using $H_2$DCFDA (Fig. 12E). $H_2$DCFDA staining of conidia from 3-day-old colonies showed a greater intensity of fluorescence in the Af*ΔtmpL* conidia than in the wild-type CEA10 conidia. This brighter fluorescence was detected mainly in the smaller, younger Af*ΔtmpL* conidia (Fig. 12E, inset). ROS production appeared to be greater in the conidiophores of Af*ΔtmpL* than wild-type conidiophores, especially in the phialides and not the inflated vesicle of the conidiophore. This indicates that the oxidative burst first takes place mostly within phialides and then young conidia that are formed on the phialides in the absence of the *tmpL* gene in *A. fumigatus*. Taken together, these data indicate that deletion of *tmpL* in *A. fumigatus* resulted in the same phenotype as the *A. brassicicola ΔtmpL* strains: a burst of ROS in conidia and conidiophores.

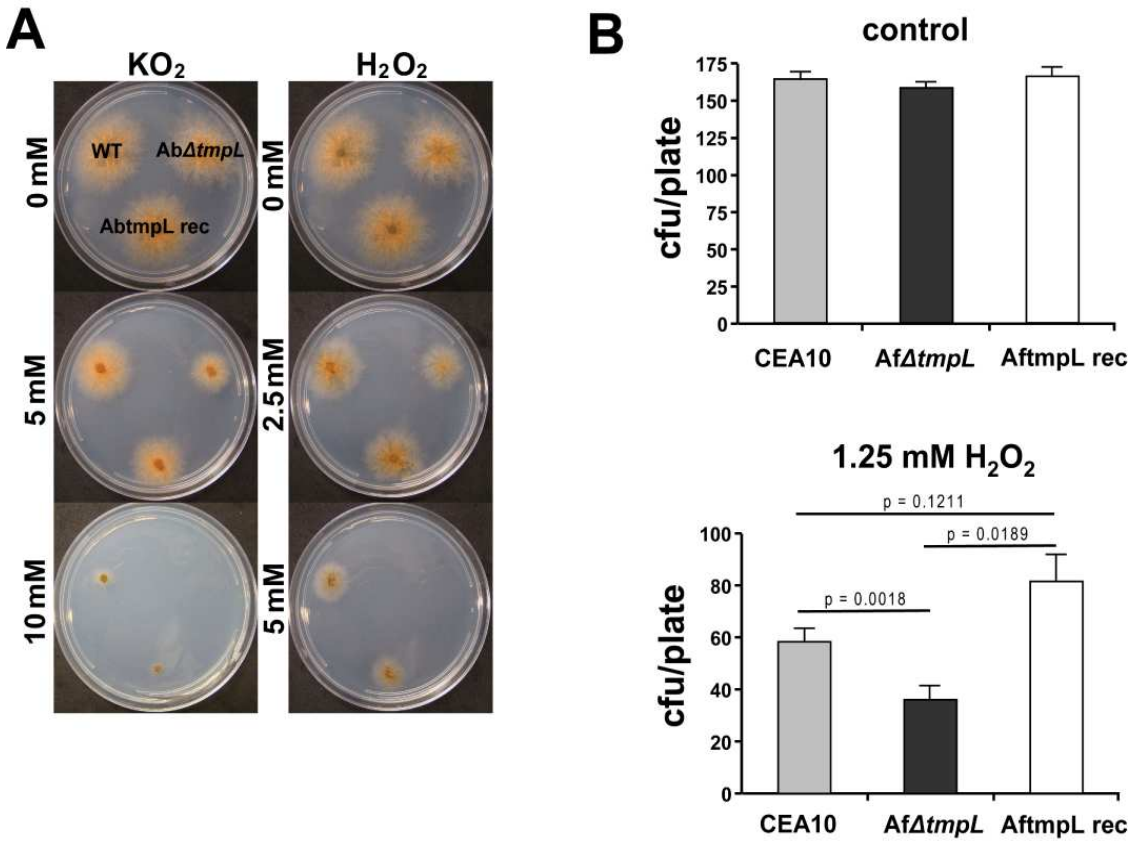


**Figure 11. The *ΔtmpL* mutants are hypersensitive to the oxidative stressors.** **(A)** Increased sensitivity of *A. brassicicola ΔtmpL* mutants to oxidative stress generated by $KO_2$ or $H_2O_2$ compared with wild-type. Conidial suspensions of *A. brassicicola* wild-type (WT), *ΔtmpL* mutant (Ab*ΔtmpL*), and reconstituted strain (AbtmpL rec) were cultured on minimal agar medium containing different concentrations of $KO_2$ or $H_2O_2$ and evaluated 5 days after inoculation. **(B)** Increased sensitivity of *A. fumigatus ΔtmpL* mutant germlings to oxidative stress generated by $H_2O_2$ compared with wild-type. Plates with the germlings of A. fumigatus wild-type strain (CEA10), *ΔtmpL* mutant (Af*ΔtmpL*), and reconstituted strain (AftmpL rec) were overlaid with 1.25mM $H_2O_2$ solution, incubated at 37˚C for 10 minutes. After washing the plate with sterile distilled water the plates were incubated until colonies were big enough to count. Samples were prepared in triplicate, and error bars on graph represent SD of two independent experiments.

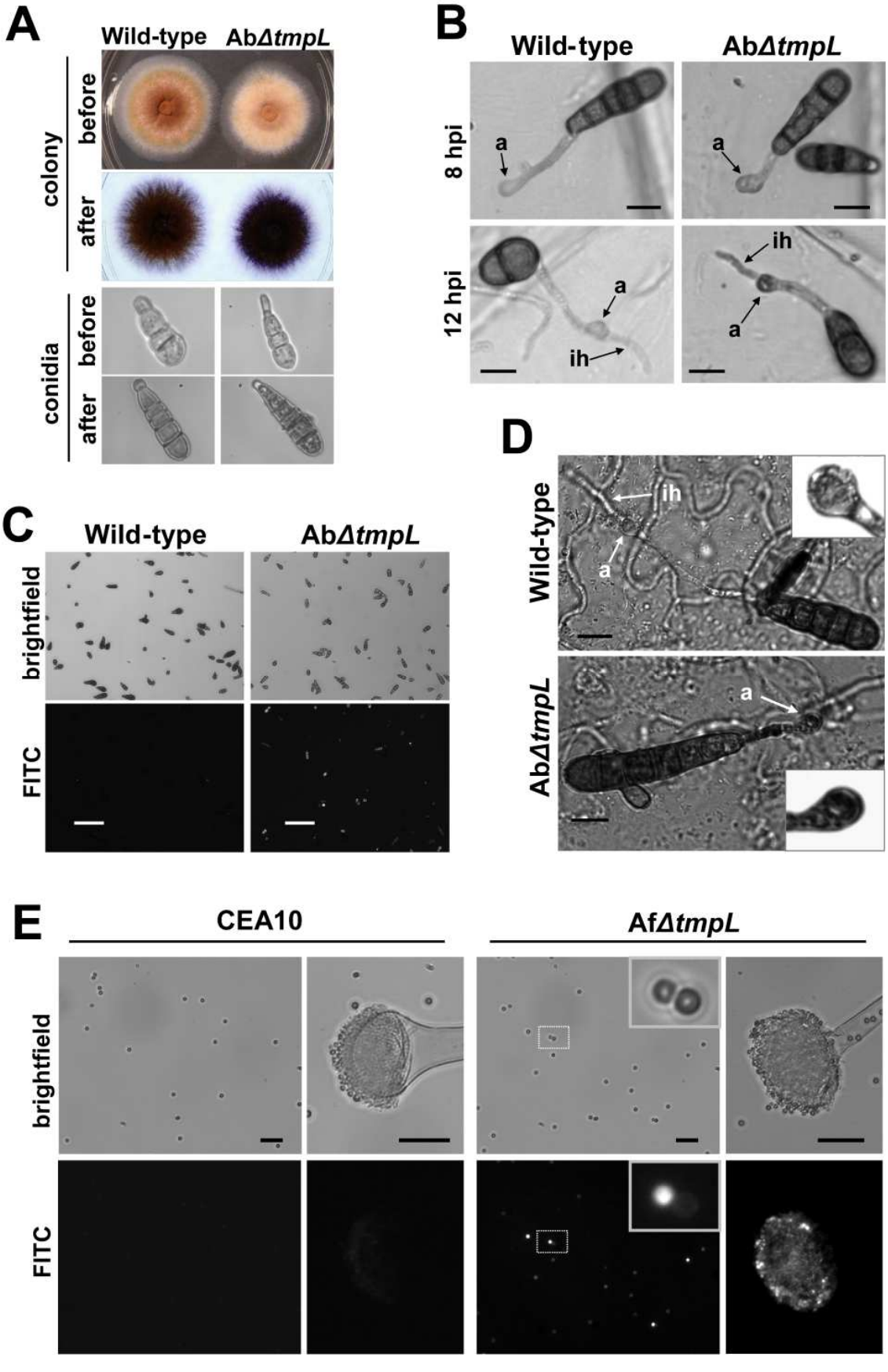
A
Wild-type
AbΔtmpL
colony
before
after
conidia
before
after
B
Wild-type
AbΔtmpL
8 hpi
12 hpi
a
ih
C
Wild-type
AbΔtmpL
brightfield
FITC
D
Wild-type
AbΔtmpL
ih
a
E
CEA10
AfΔtmpL
brightfield
FITC

**Figure 12. Excess ROS production during conidiation and infection in *ΔtmpL* mutants.** **(A)** Accumulation of excess superoxide in the colonies and conidia of the *A. brassicicola ΔtmpL* mutants. 7-day-old colonies (upper panels) and conidia (lower panels) of *A. brassicicola* wild-type and *ΔtmpL* mutant grown on a nutrient-rich medium were strained with nitroblue tetrazolium (NBT) to detect superoxide. Each panel shows the picture before or after NBT staining. **(B)** Accumulation of excess superoxide in the mature appressoria and emerging infection hyphae of the *A. brassicicola ΔtmpL* mutants. Conidia of *A. brassicicola* wild-type and *ΔtmpL* mutant were inoculated on onion epidermis, incubated at room temperature for 8 and 12 hr, and stained with NBT. Bars = 10 μm. Abbreviations: a, appressorium; ih, infection hypha. **(C)** Accumulation of excess ROS in the conidia of the *A. brassicicola ΔtmpL* mutants. Conidia released from 7-day-old colonies were stained with $H_2$DCFDA and viewed by epifluorescence microscopy. Bars = 50 μm. **(D)** Accumulation of excess $H_2O_2$ on mature appressoria of the *A. brassicicola ΔtmpL* mutants. Conidia of the *A. brassicicola* wild-type and *ΔtmpL* mutant were inoculated on green cabbage cotyledons and incubated at room temperature for 12 hr before being stained with 3,3′-diaminobenzidine tetrahydrochloride (DAB). Insets are the magnified view of each appressorium. Bars = 10 μm. Abbreviations: a, appressorium; ih, infection hyphae. **(E)** Accumulation of excess ROS in the conidia of the *A. fumigatus ΔtmpL* mutants. Conidia and conidiophores of the *A. fumigatus* wild-type (CEA10) and *ΔtmpL* mutant were released from 3-day-old colonies and subsequently stained with $H_2$DCFDA for 30 min and 1 hr, respectively, and viewed by confocal microscopy. Bars = 20 μm.

**Deletion of *A. brassicicola tmpL* causes increased expression of antioxidant genes and nuclear localization of the Yap1 transcription factor during conidiation**

Given the increased ROS accumulation in the absence of TmpL, we next sought to determine whether the ROS scavenging system was impaired in the *ΔtmpL* strains of *A. brassicicola*. We compared the expression of general antioxidant and redox control gene orthologs: *ctt1* (catalase T), *sod1* (Cu,Zn superoxide dismutase), *gsh1* (gamma glutamylcysteine synthetase), *gsh2* (glutathione synthetase), *trx2*

(thioredoxin), *gpx1* (glutathione peroxidase 1), and two redox-regulating genes *yap1* and *skn7* in *A. brassicicola* wild-type and *ΔtmpL* strains (Fig. 13A). In the wild-type strain, the relative transcript levels of all genes increased up to nine-fold during conidiation (36 hr air-exposed mycelia) compared with the transcript levels in vegetative mycelia. During conidiation all stress-associated genes examined showed up to a two-fold increase in mRNA abundance in the Ab*ΔtmpL* strain compared with the wild-type, while there was a very slight difference observed between the two strains during vegetative growth. These observations indicate a higher ROS level in the Ab*ΔtmpL* conidia, based on the fact that increased ROS levels result in higher expression of the enzymes that decompose them (Chen et al., 2003; Moye-Rowley, 2003). When combined with excess ROS accumulation observed in Ab*ΔtmpL* conidia (Fig. 12), these results also indicate a fundamental inability of the mutant to reduce cellular ROS level possibly because it's already beyond the cellular capability to neutralize them, even by the increased activity of the antioxidants. These results also strongly suggest that the Yap1 and Skn7 regulators are not downstream of TmpL activity.

It has been demonstrated in multiple yeast and fungal systems that during oxidative stress, the transcription factor Yap1 facilitates targeted gene expression by migrating into the nucleus from its location in the cytosol (Kuge et al., 1997). This cellular movement of Yap1 might provide additional information about the state of oxidative stress in the Ab*ΔtmpL* strain. Wild-type and Ab*ΔtmpL* strains were transformed with a GFP-Yap1 construct under the control of the *A. brassicicola yap1*

promoter. Cellular localization of the GFP-Yap1 strains was examined by confocal microscopy (Fig. 13B). During normal conidiation on solid CM, fluorescence of GFP-Yap1 was distributed evenly throughout the cytoplasm of wild-type conidia (Fig. 13B, 0 mM $H_2O_2$). In contrast, the Ab*ΔtmpL*:pYap1-GFP-Yap1 strains showed a focal, condensed GFP signal typical of nuclear localization, suggesting the mutant is in a state of constitutive oxidative stress during conidiation. By constrast, there was cytoplasmic distribution of the GFP signals observed in mycelia of the Ab*ΔtmpL*:pYap1-GFP-Yap1 strains (data not shown). This observation not only indicates excess ROS accumulation only in conidial cells, but also excludes any possible involvement of environmental factors generating ROS in fungal cells, such as UV radiation, temperature shift, mechanical damage, etc (Gessler et al., 2007). In a parallel experiment, treatment of WT:pYap1-GFP-Yap1 and Ab*ΔtmpL*:pYap1-GFP-Yap1 strains with 1 mM $H_2O_2$ for 1 hr resulted in substantial nuclear localization of GFP-Yap1 in both strains (Fig. 13B, 1 mM $H_2O_2$). This indicates that the GFP-Yap1 proteins in both strains are functional. Staining with DAPI confirmed our observations that GFP-Yap1 was indeed localized to the nucleus in these experiments (data not shown).

**TmpL is required for *A. brassicicola* and *A. fumigatus* virulence**

Given the above phenotypes of the *ΔtmpL* strains, we hypothesized that TmpL may play a key role in fungal virulence. To investigate the role of TmpL in *A. brassicicola* virulence, susceptible green cabbage (*Brassica oleracea*) were inoculated with two different concentrations of young, 7 day old conidia ($2\times10^5$ and $5\times10^4$

conidia $ml^{-1}$) (Fig. 14A). Plants inoculated with either wild-type or ectopic mutant (A1E1) developed extensive, typical black spots on leaves at both concentrations of conidia tested. However, the black necrotic spots resulting from inoculation with Ab*ΔtmpL* strains (A1-3 and A1-4) at both conidial concentrations was significantly smaller than those produced by the wild-type or ectopic mutant inoculations ($p<0.01$). The reconstituted strain AbtmpL rec (A1C2) was found to be just as virulent as the wild-type at both concentrations of conidia. The average reduction in disease severity caused by the mutants compared with the wild-type was more than 62% and 80% when using the higher and lower conidial concentrations, respectively. Similar results were obtained in virulence assays with *Arabidopsis*.

We next asked the question whether *tmpL* is also involved in fungal virulence in the human fungal pathogen *Aspergillus fumigatus*. Deletion of *tmpL* in *A. fumigatus* led to a statistically significant reduction ($p<0.01$) in virulence in a chemotherapeutic murine model of invasive pulmonary aspergillosis (Fig. 14B). Mice infected with the Af*ΔtmpL* strain did not display normal symptoms associated with invasive aspergillosis (IA) in contrast to wild-type and reconstituted strain infected mice which displayed well described symptoms of IA including ruffled fur, hunched posture, weight loss, and increased respiration. Consequently, like the *ΔtmpL* mutant in *A. brassicicola* that has reduced virulence on plants, TmpL is also required for fungal virulence in mammalian hosts.

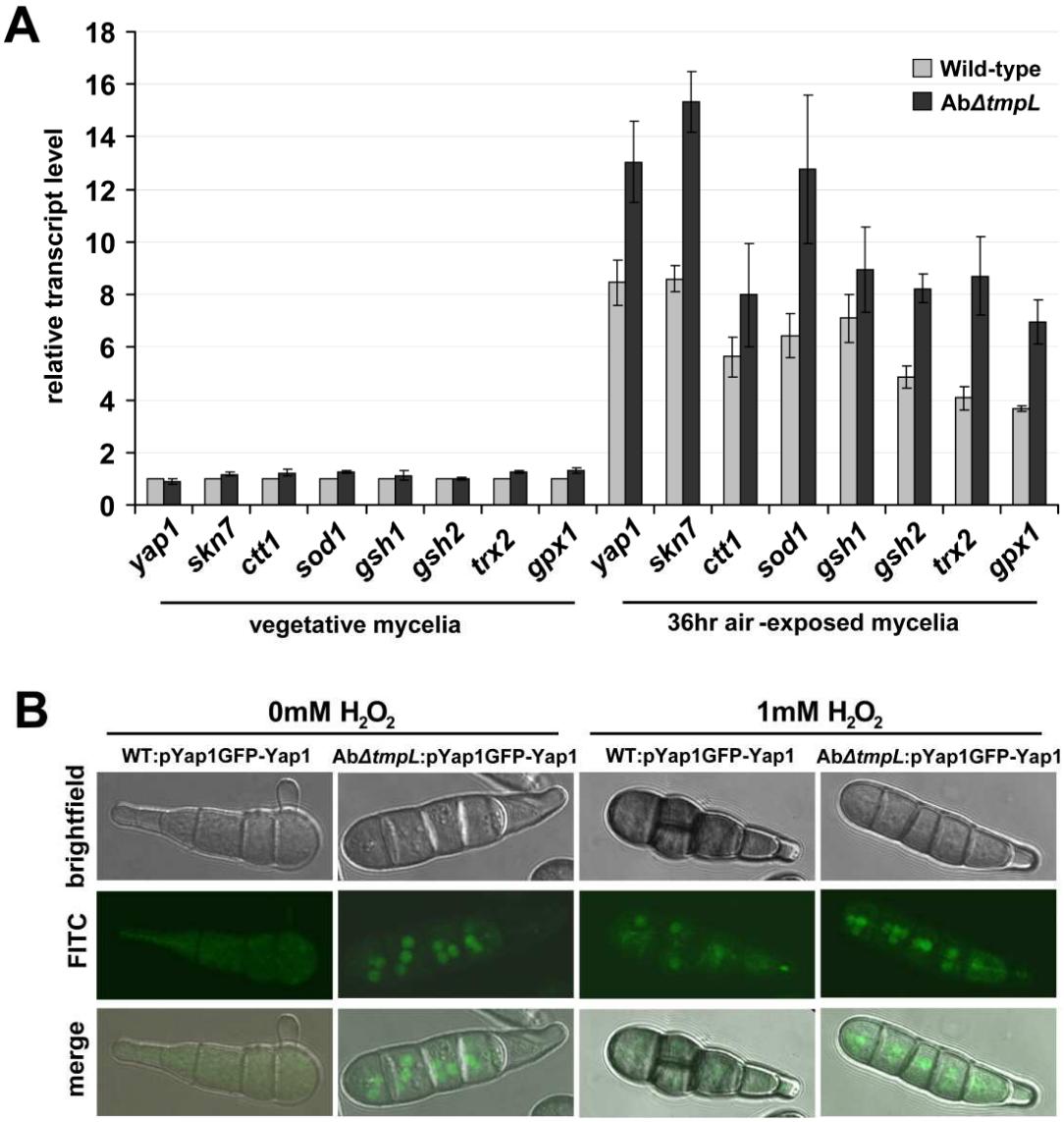


**Figure 13. Expression of antioxidant-related genes and nuclear localization of GFP-Yap1 in *A. brassicicola ΔtmpL* mutants. (A)** Transcript levels of antioxidants-related genes in vegetative mycelia and 36 hr air-exposed mycelia of *A. brassicicola* wild-type and *ΔtmpL* mutant. Relative transcript abundance was determined by comparing each gene transcript level with the transcript level of the same gene in vegetative mycelia of wild-type (set to transcript level 1). Data are mean ± SD of three independent experiments. **(B)** Constitutive nuclear localization of GFP-Yap1 in *A. brassicicola ΔtmpL* mutant conidia. Distribution of GFP-Yap1 in the wild-type (WT:pYap1GFP-Yap1) and the Ab*ΔtmpL* mutant (Ab*ΔtmpL*:pYap1GFP-Yap1) strains during normal conidiation on CM (0 mM $H_2O_2$) and following treatment of wild-type and Ab*ΔtmpL* mutant with $H_2O_2$ for 1 hr (1 mM $H_2O_2$).

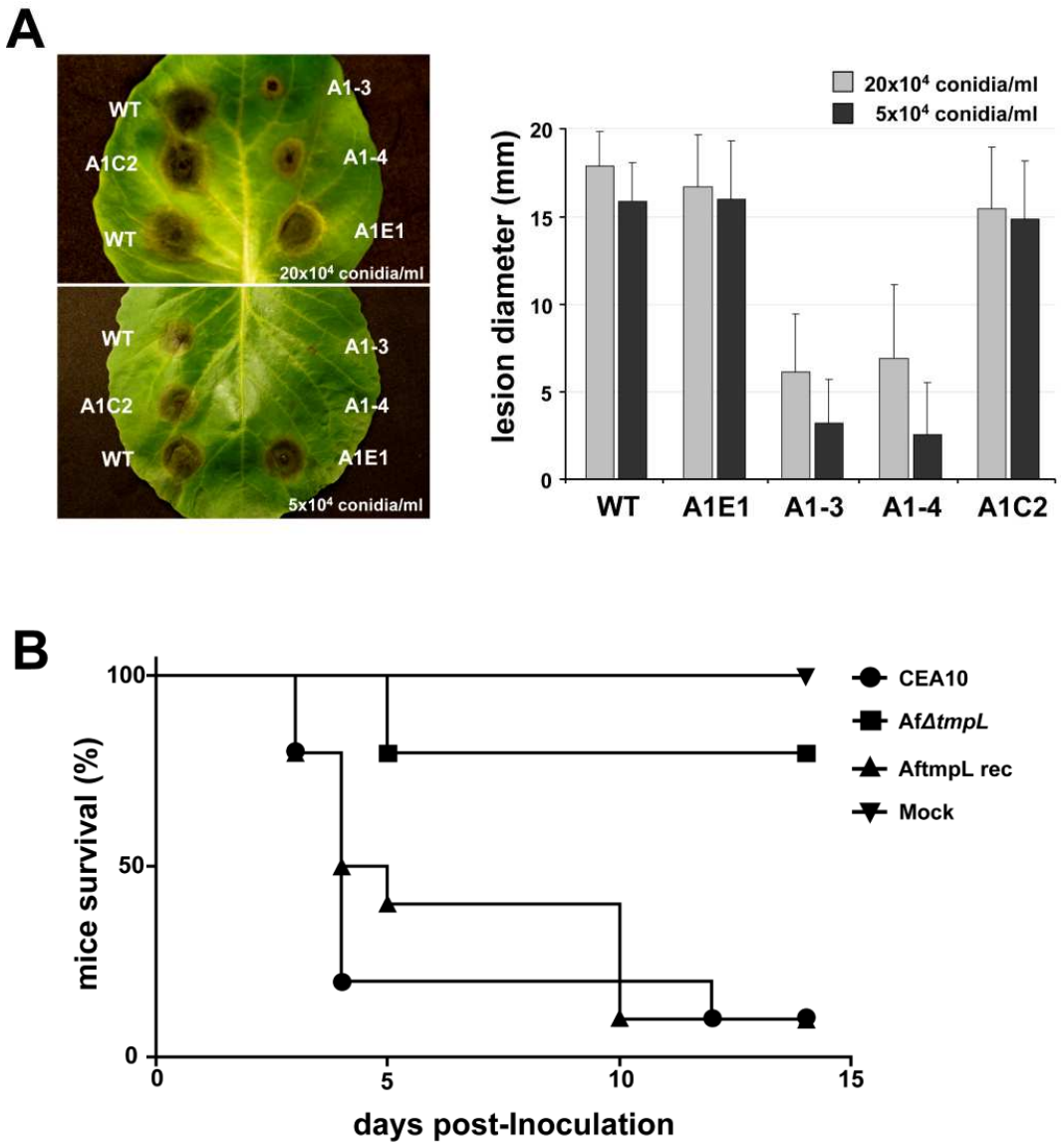


**Figure 14. Reduced virulence of *ΔtmpL* mutants.** **(A)** Virulence assay on green cabbage leaves using two conidial concentrations, $20 \times 10^4$ and $5 \times 10^4$ conidia $ml^{-1}$ of *A. brassicicola* wild-type (WT), ectopic (A1E1), two *ΔtmpL* mutants (A1-3 and A1-4), and a reconstituted mutant (A1C2) strains. Five days after inoculation (graph), disease severity was calculated based on the lesion diameter. Columns and error bars represent average and SD, respectively, of five independent experiments. **(B)** Virulence assay on mice inoculated intranasally with $10^6$ conidia/ 25 µl of *A. fumigatus* wild-type (CEA10), *ΔtmpL* mutant (Af*ΔtmpL*), and reconstituted mutant (AftmpL rec) strains. P value for comparison between Af*ΔtmpL* mutant and wild-type CEA10, $P = 0.0006$. Af*ΔtmpL* is significantly less virulent than the wild-type CEA10 and the reconstituted strain AftmpL rec.

### *A. brassicicola ΔtmpL* strains fail to penetrate plant tissue and induce active callose deposition *in planta*

To understand the reasons for the reduced virulence of *A. brassicicola ΔtmpL* strains on green cabbage, we performed microscopic analyses of the infection processes. Examination of green cabbage cotyledons using light microscopy at 12 hpi revealed that the mutants formed appressoria on the plant surface similar to those formed by wild-type (Fig. 15A). Intracellular infection hyphae formed directly under the appressoria of the Ab*ΔtmpL* strain, however, rarely developed inside of plant epidermal cells, while development of infection hyphae from wild-type appressoria was consistently observed. An onion epidermis assay also showed similar results as the cotyledon assay (Fig. 16A). Only 7% of Ab*ΔtmpL* appressoria produced visible intracellular infection hyphae at 12 hpi (Figure 16B), but initial penetration hyphae from most individual appressoria were frequently visible (Fig. 16A, inset). At 24 hpi, ~ 11% of the Ab*ΔtmpL* appressoria developed intracellular infection hyphae. The remaining Ab*ΔtmpL* appressoria did not develop infection hyphae, but in some cases, produced one or several germ tubes that formed additional appressoria (Fig. 16A, 24 hpi). In contrast, more than half of the wild-type appressoria successfully produced intracellular infection hyphae at 12 hpi (Fig. 16B), which usually penetrated cross-walls and spread within 24 hr (Fig. 16A, 24 hpi).

To characterize the host-pathogen interface, inoculated green cabbage leaves were examined by light and electron microscopy. In vertical leaf sections inoculated with the compatible wild-type, fungal appressoria successfully penetrated, formed intracellular infection hyphae, and killed most plant tissue below the infection sites

within 24 hr (Fig. 15B and 16C). In contrast, leaf sections inoculated with the less virulent Ab*ΔtmpL* strain appeared undamaged, though it was noted that necrosis similar to a hypersensitive response or papillae formation (callose deposition) developed below the infection site (Fig. 15B). Transmission electron microscopy revealed penetration hyphae and appressoria of the Ab*ΔtmpL* strain showing cell death-like phenotypes (cytoplasmic fragmentation, enlarged vacuoles, and distorted organelles) and the penetration hyphae were completely arrested by papillae formation in plant epidermal cells (Fig. 16C). Callose deposition was also detected by cytological staining using aniline blue (Fig. 16D). The wild-type induced small, scattered deposits in close proximity to the sites of penetration and tissue necrosis was extensive. In contrast, callose deposits observed following Ab*ΔtmpL* inoculation were much more pronounced and often localized at the site of penetration.

In order to investigate whether the Ab*ΔtmpL* strains can colonize the host plant when the first physical barrier, the plant cell wall, is removed, wounded leaf assays were performed (Fig. 15C). Symptoms produced by inoculation of the wild-type on wounded tissue were more severe than on intact (non-wounded) tissue. The Ab*ΔtmpL* strain formed larger lesions on wounded leaves than on intact leaves, but were still smaller than wild-type lesions on wounded leaves.

Together, these results indicate that *A. brassicicola ΔtmpL* strains have defects in pathogenicity associated primarily with very early stages of plant infection, resulting in the failure of appressoria penetrating into epidermal cells and an induction of callose deposition.

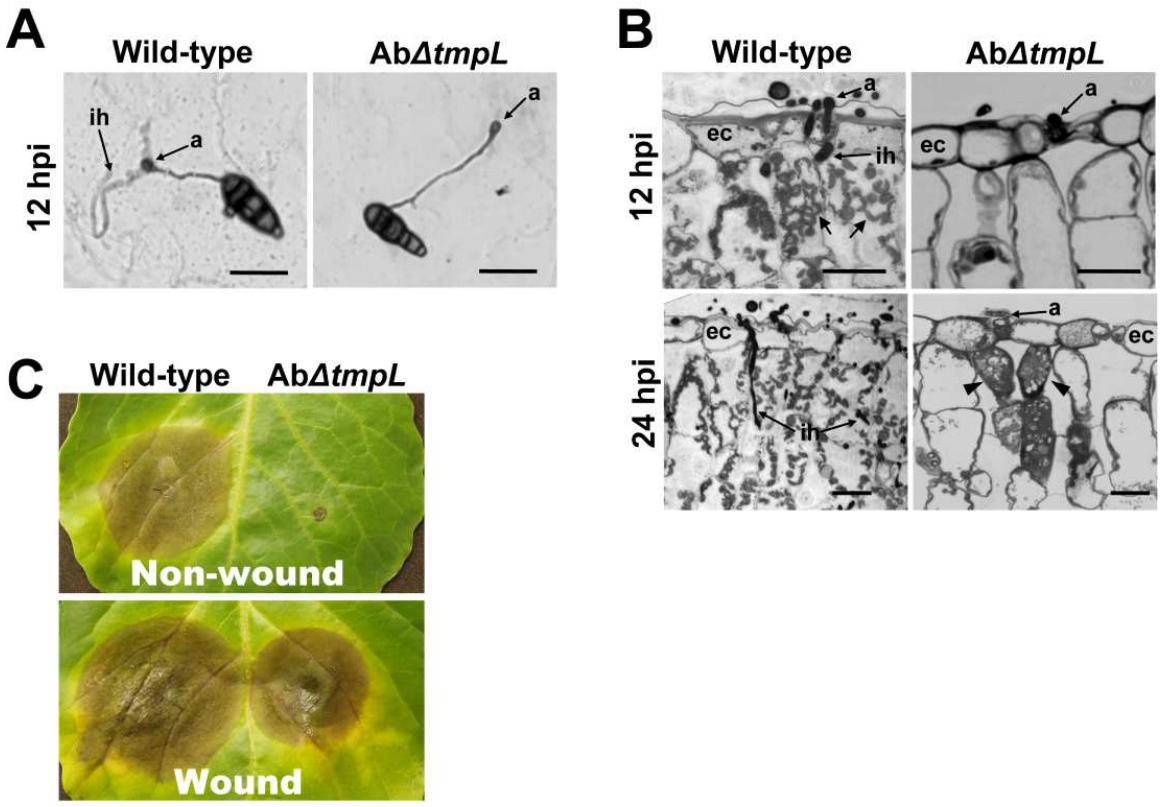


**Figure 15. Formation of appressoria and infection hyphae and a virulence assay of wounded and non-wounded green cabbage leaves inoculated with *A. brassicicola* wild-type and *ΔtmpL* mutant.** **(A)** Green cabbage cotyledons were used to examine the appressoria and infection hyphae formation of wild-type and Ab*ΔtmpL* mutant infection. Intracellular infection hyphae of the Ab*ΔtmpL* mutant were rarely developed inside of the plant epidermal cells, while infection hyphae of the wild-type appressoria were consistently observed. Bars = 20 μm**.** Abbreviations: a, appressorium; ih, infection hypha. **(B)** Green cabbage leaves inoculated with wild-type and Ab*ΔtmpL* mutant were collected at 12 and 24 hpi, embedded epoxy resin, sectioned, and stained with 0.1% toluidine blue O. Plant tissues around the wild-type fungal cells were extensively macerated and degraded and plastids were abnormally inflated (arrows). By contrast, leaf sections inoculated with the Ab*ΔtmpL* mutant maintained almost intact plant tissue (12 hpi) and plant cells below the infection site showed cell necrosis or callose-deposition-like phenomenon at 24 hpi (arrowheads). Bars = 20 μm. Abbreviations: a, appressorium; ec, epidermal cell; ih, infection hypha. **(C)** Wounded leaf infection assay of wild-type and Ab*ΔtmpL* mutant. The upper panel indicates intact (non-wounded) leaf inoculated with the wild-type and Ab*ΔtmpL* mutant, and the lower panel depicts wounded leaf infection by needle scratching.

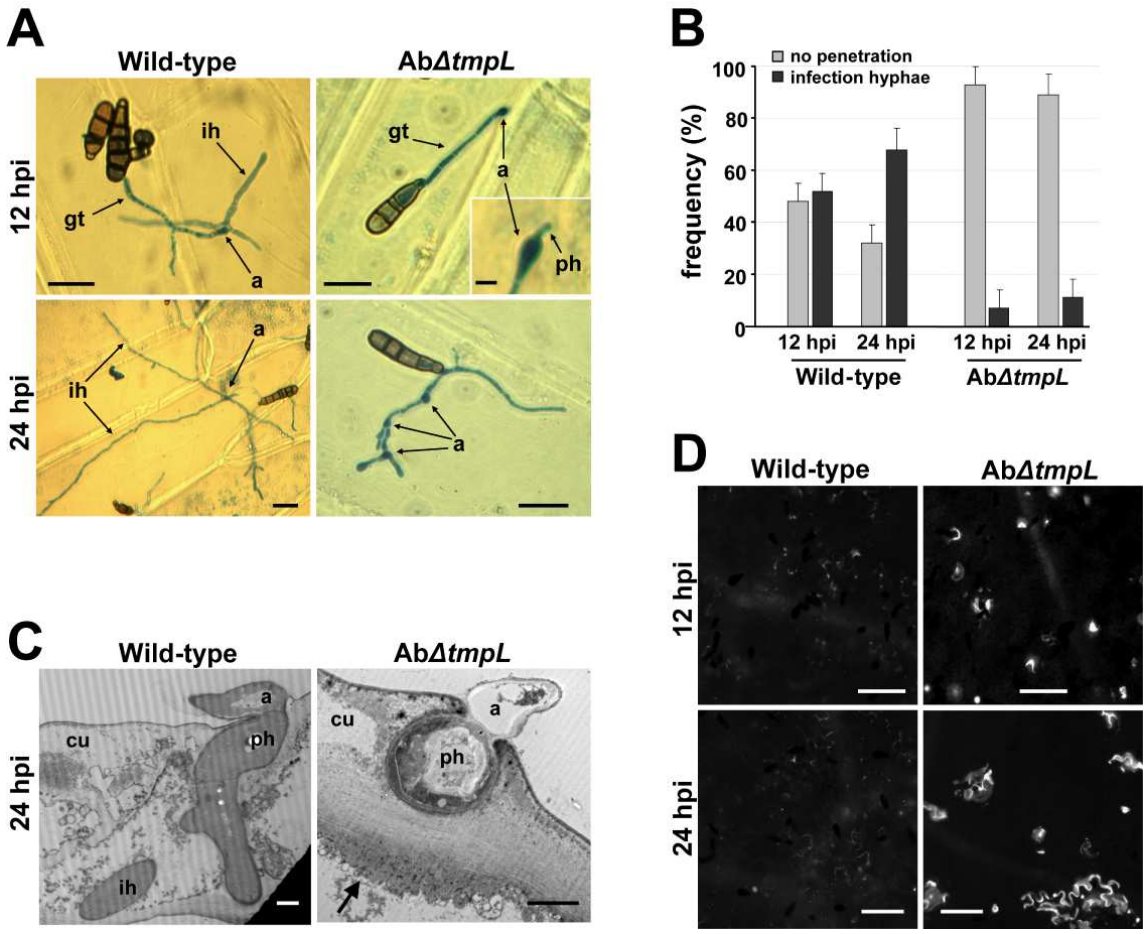


**Figure 16. Appressoria and infection hyphae formation, ultrastructure, and callose detection assays of *A. brassicicola ΔtmpL* mutant infection.** **(A)** Light micrographs of onion epidermis inoculated with *A. brassiciola* wild-type and *ΔtmpL* mutants at 12 and 24 hpi. Bars = 20 μm, except for the inset where it denotes 5 μm. Abbreviations: a, appressorium; gt, germ tube; ih, infection hypha; ph, penetration hypha. **(B)** Frequency of infection hyphae formation beneath appressoria of the *A. brassicicola* wild-type and *ΔtmpL* mutants on onion epidermis. Columns and error bars represent average and SD, respectively, of four independent experiments. **(C)** Transmission electron micrographs showing transverse sections of green cabbage leaves inoculated with *A. brassicicola* wild-type and *ΔtmpL* mutants. Arrow indicates papillae formation (callose deposition) around a fungal penetration hypha. Bars = 2 μm. Abbreviations: a, appressorium; cu, cuticle layer; ih, secondary infection hypha; ph, penetration hypha. **(D)** Callose deposition on green cabbage cotyledons inoculated with *A. brassicicola* wild-type and *ΔtmpL* mutants. White spots indicate callose deposition of the inoculation sites stained by aniline blue and viewed by epifluorescence microscopy. The tiny black spots dispersed on plant surface are fungal conidia. Bars = 50 μm.

**Overexpression of *yap1* in *A. brassicicola ΔtmpL* background leads to partial complementation of abnormal conidiation, oxidative stress tolerance, and reduced virulence**

Given the excess oxidative burst phenotypes of the *ΔtmpL* strains, we hypothesized that overexpression of *yap1* may rescue the *ΔtmpL* mutant phenotypes. To determine whether overexpression of the Yap1 transcriptional regulator can enhance the cellular scavenging ability of fungal cells and consequently restore the abnormal phenotype and reduced virulence in *ΔtmpL* strains, we generated a *ToxA* promoter-driven *yap1* overexpression cassette using fusion PCR methods. Subsequently, we introduced the overexpression cassette into both *A. brassicicola* wild-type and *ΔtmpL* backgrounds and examined its effect on each strain. As shown in Figure 17A, the mRNA abundance of *yap1* significantly increased at least 25-fold compared with each recipient strain: wild-type and Ab*ΔtmpL*, indicating that *yap1* overexpression cassettes were successfully integrated in the genome and expressed under the control of the *ToxA* promoter. To evaluate whether Yap1 overproduction affected the induction of the antioxidant defense system, we monitored the transcriptional activation of *ctt1* and *sod1* orthologs as representative downstream genes regulated by Yap1. During vegetative growth, there was no induction of the *ctt1* and *sod1* transcripts. During conidiation in 36 hr air-exposed mycelia, however, the *yap1* overexpression mutant in the Ab*ΔtmpL* background (Ab*ΔtmpL*:pToxA-Yap1) showed significantly increased expression (almost two-fold) of antioxidant genes. Yet, *yap1* overexpression in the wild-type (WT:pToxA-Yap1) resulted only in a slight increase of these antioxidant genes, possibly because of the mechanism of Yap1

activation; Yap1 is post-translationally activated only in the presence of cellular ROS (Kuge et al., 1997; Yan et al., 1998).

Overexpression of *yap1* restored oxidative stress tolerance of the Ab*ΔtmpL* strain, resulting in comparable sensitivity to $H_2O_2$ as the wild-type (Fig. 17B). Furthermore, the Ab*ΔtmpL*:pToxA-Yap1 strain produced wild-type-like conidia (Fig. 17C), indicating that *yap1* overexpression complemented, at least to a substantial degree, the *ΔtmpL* phenotypes. There was no distinguishable phenotypic difference between the WT:pToxA-Yap1 strain and the wild-type recipient strain. In addition to the conidial phenotype, green cabbage infection assays showed that the Ab*ΔtmpL*:pToxA-Yap1 strain partially restored its virulence compared with the Ab*ΔtmpL* recipient strain, but was still not comparable to the wild-type (Ab*ΔtmpL*, 4.1 ± 2.83 nm, n = 26; Ab*ΔtmpL*:pToxA-Yap1, 12.9 ± 4.52 mm, n = 26; $p<0.01$) (Fig. 17D). Interestingly *yap1* overexpression in the wild-type caused slightly decreased lesion size compared with its wild-type recipient strain (wild-type, 17.2 ± 2.5 mm, n = 22; WT:pToxA-Yap1, 15.7 ± 3.8 mm, n = 22; $p<0.05$), indicating that excess antioxidant activity resulting from *yap1* overexpression did indeed negatively affect the pathogenesis of the *A. brassicicola* wild-type. Overall, *yap1* overexpression in the Ab*ΔtmpL* strain strongly suggested that the phenotypic defects and reduced virulence were attributable to failure in the regulation of intracellular ROS levels, particularly in conidia and infection-related structures during the conidiation process and during plant infection, respectively. However, the residual virulence defect in the presence of *yap1* overexpression may suggest additional roles of *tmpL* in fungal virulence.

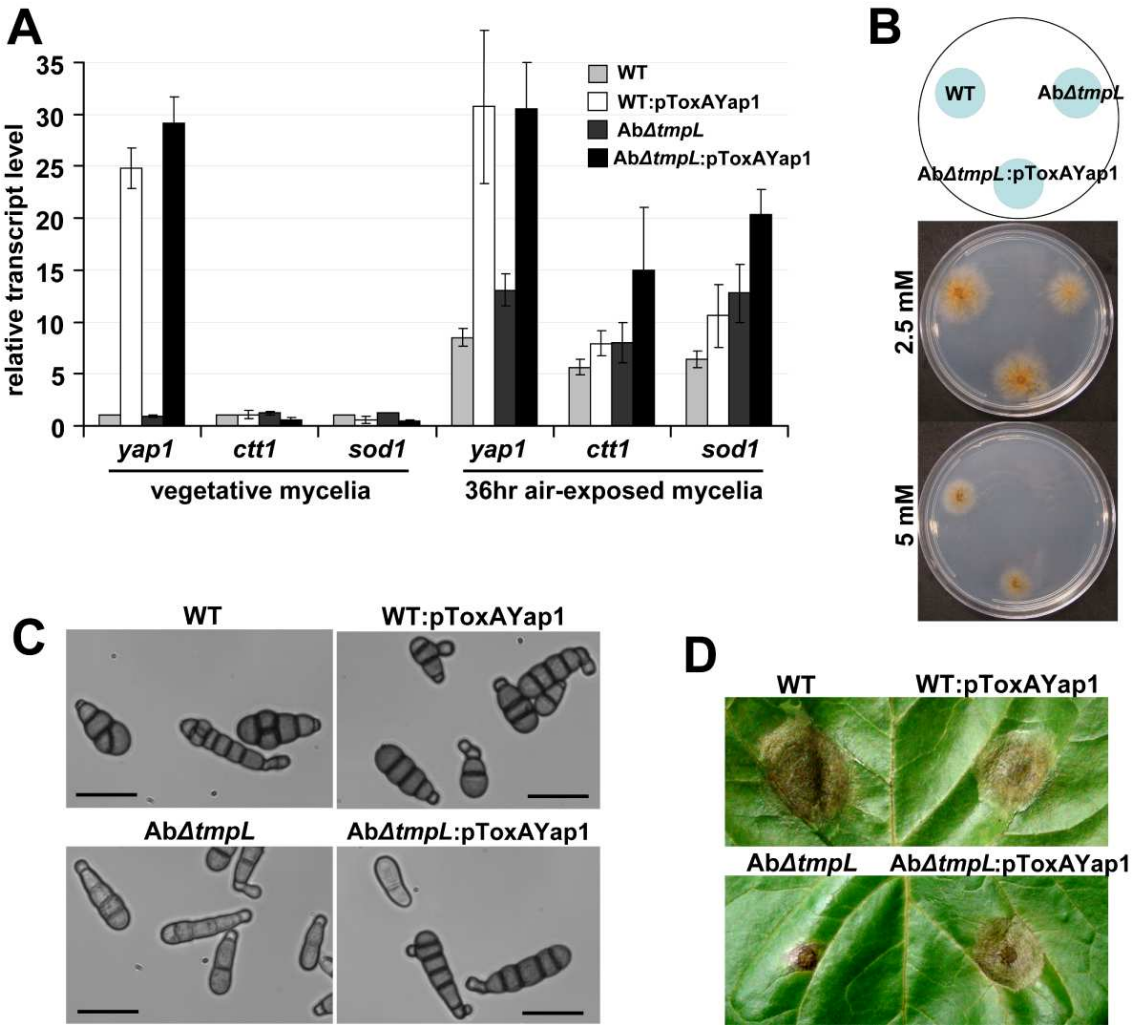


**Figure 17. Restoration of the abnormal phenotypes and reduced virulence of the *A. brassicicola ΔtmpL* mutants by a redox regulator *yap1* overexpression. (A)** Transcript levels of *yap1*, *sod1*, and *ctt1* in vegetative mycelia and 36 hr air-exposed mycelia of *A. brassicicola* wild-type (WT), *yap1* overexpression mutant on wild-type background (WT:pToxAYap1), *ΔtmpL* mutant (Ab*ΔtmpL*), and *yap1* overexpression mutant on *ΔtmpL* mutant background (Ab*ΔtmpL*:pToxAYap1). Relative transcript abundance was determined by comparing each gene transcript level with the transcript level of the same gene in vegetative mycelia of wild-type (set to transcript level 1). Data are mean ± SD of two independent experiments. **(B)** Hypersensitivity to oxidative stress generated by $H_2O_2$ was recovered by *yap1* overexpression in Ab*ΔtmpL* mutants. **(C)** Light micrographs showing restoration of the abnormal conidiogenesis of Ab*ΔtmpL* mutants in Ab*ΔtmpL*:pToxAYap1 overexpression strain. Bars = 20 μm. **(D)** Partial restoration of the reduced virulence of Ab*ΔtmpL* mutants in Ab*ΔtmpL*:pToxAYap1 overexpression strain.

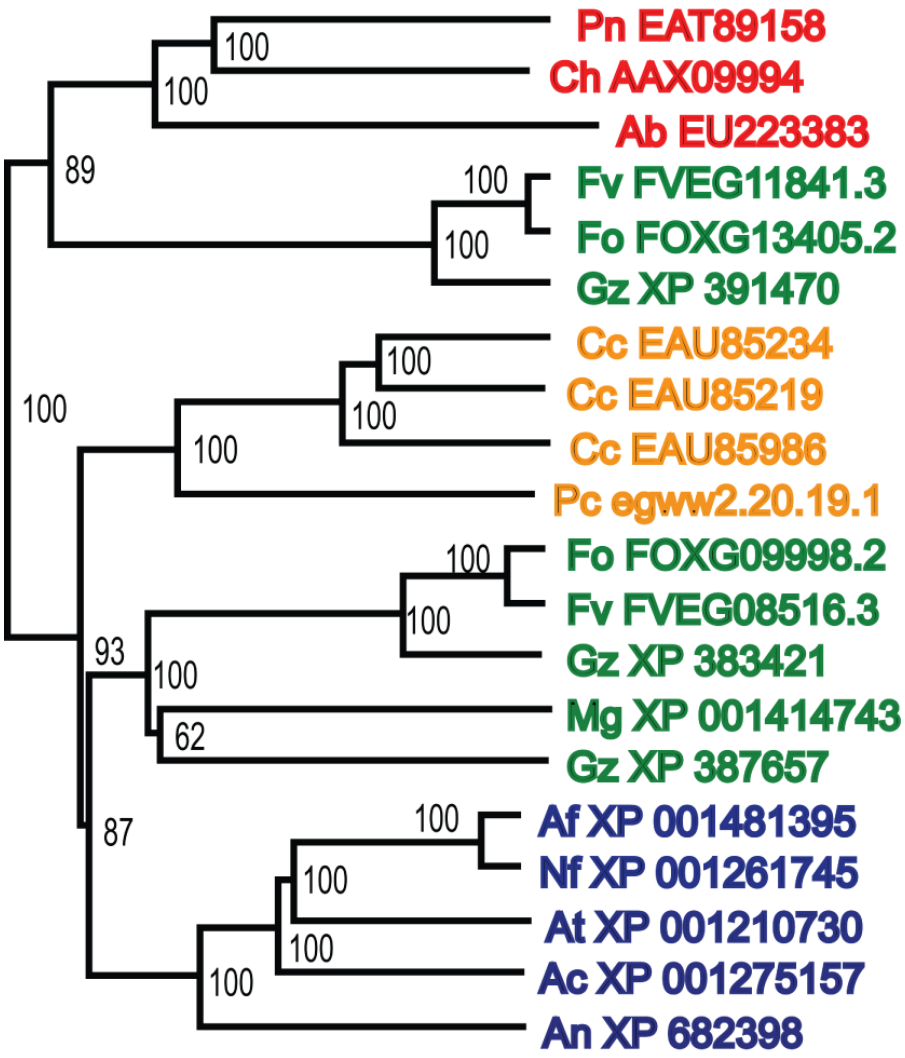


**Figure 18. Phylogenetic analysis of the TmpL orthologs.** TmpL orthologs were aligned with ClustalW, the alignment imported into PFAAT, and a neighbor joining tree generated based on its predicted amino acid sequences. Numbers at the node represent the result of 100 bootstrap replications. GenBank or organism-specific accession numbers follow species abbreviations. Red indicates Dothideomycetes, green for Sordariomycetes, yellow for Homobasidiomycota, and blue for Eurotiomycetes. Abbreviations: Pn *Phaeosphaeria nodorum*, Ch *Cochliobolus heterostrophus*, Ab *Alternaria brassicicola*, Fv *Fusarium verticillioides*, Fo *Fusarium oxysporum*, Gz *Gibberella zeae*, Cc *Coprinopsis cinerea*, Pc *Phanerochaete chrysosporium*, Mg *Magnaporthe grisea*, Af *Aspergillus fumigatus*, Nf *Neosartorya fischeri*, At *Aspergillus terreus*, Ac *Aspergillus clavatus*, An *Aspergillus nidulans*.

## Discussion

Mechanisms for adapting to stress either from intracellular or extracellular sources are among the most relevant and timely topics in fungal biology. During normal developmental processes, a fungal organism encounters various stresses from toxic by-products of its metabolism or oxidative stress generated mainly through aerobic respiration (Belozerskaia and Gessler, 2007; Del Sorbo et al., 2000). The cellular environment within a host, whether plant or animal, also represents a major source of stress to an invading fungal pathogen (Finn et al., 2006; Hammond-Kosack and Jones, 1996; Osbourn, 2001). In order to evade or circumvent stress, the fungus must possess special adaptation mechanisms. In this study we provide the first evidence that a novel, pathogenicity-related gene from a plant and animal fungal pathogen, *tmpL,* is critical for proper conidiogenesis and infection of healthy host tissues. Furthermore, *tmpL* appears to be associated with a filamentous fungi-specific stress defense system that particularly responds to oxidative stress.

TmpL is a novel hybrid protein consisting of an AMP-binding domain, six putative transmembrane domains, and a FAD/NAD(P)-binding domain. Based on our phylogenetic analysis, TmpL and its putative orthologs are present only in filamentous fungi (Fig. 18) and not highly related to proteins with known functions. Although portions of the predicted TmpL amino acid sequence showed high similarity to putative NPS protein sequences in the GenBank NR database, its sequence lacked thiolation and condensation domains necessary to create a minimal module in typical NPS proteins. The AMP-binding domain is very similar to an adenylation domain.

The latter is most often associated with modular NPS enzymes, where it activates amino acids prior to their incorporation into nonribosomal peptides (NRP) (Stachelhaus and Marahiel, 1995). Interestingly, all fungi that contained a TmpL homolog also contain numerous *NPS* genes. Though the exact function of TmpL remains to be determined, it may modify or activate specific amino acids associated with certain nonribosomal peptides acting as a signal molecule for oxidative stress responses in filamentous fungi. It is also proposed that based on the similarity of the C-terminal sequences of TmpL to a previously identified, although smaller, plasma membrane flavoprotein in *A. nidulans*, TmpA, TmpL might be involved in production of a regulatory signal, which eventually leads to fungal differentiation. As predicted in TmpA (Soid-Raggi et al., 2006), we suspected that the C-terminal region of TmpL had enzymatic activity. Bioinformatics analysis also showed TmpL and its orthologs contain proposed sites for FAD and NAD(P)-binding, based on protein modeling and the existence of two important consensus sequences, suggesting that the protein is specifically reduced by NAD(P)H with a reduction potential. Indeed in our study, a partial recombinant protein of TmpL, which includes FAD/NAD(P)-binding domain, supports this hypothesis by showing that the partial protein is capable of binding flavin. In addition, NCBI conserved domain BLAST searches identified a ferric reductase (FRE) domain with low similarity (*E*-value 0.004) in the FAD/NAD(P)-binding domain of the TmpL protein, suggesting that TmpL might be distantly related to the FRE group of proteins. Indeed several FRE proteins are known to be involved in the response to oxidative stress in various organisms (Lee et al., 2007; Yannone and Burgess, 1998), as part of a system that activates a number of different enzymes

involved in redox control. When considered together, it is likely that TmpL uses electrons from NAD(P)H, transferred via FAD, to activate or modify unknown substrates or possibly downstream proteins in a redox-related signal transduction pathway.

Our localization assays indicated that TmpL is associated with the Woronin body (WB) in filamentous fungi. WBs are known to plug septal pores in response to fungal cell injury, preventing excess cytoplasmic leaking (Galagan et al., 2003; Woronin, 1864). Early TEM studies indicated a peroxisomal origin for WBs (Camp, 1977). More recently, genetics and cell biology research confirmed that the WB is first assembled in large peroxisomes (Liu et al., 2008; Tey et al., 2005). Our confocal microscopy analysis showing a sequential association between TmpL and peroxisomes suggests that TmpL is first targeted into peroxisomes by an unknown peroxisomal targeting signal and then goes through WB biogenesis, eventually becoming part of a mature WB. However, WB in *A. brassicicola* conidia appeared to be divided into two groups based on their location and the localization of TmpL. It is generally accepted that depending on the organism, cell type, and metabolic requirements, distinct sets of proteins could be housed within certain multipurpose organelles or microbodies (Managadze et al., 2007; Titorenko and Rachubinski, 2004). Confocal analyses with TmpL-GFP and DsRed-AbHex1 double-labeled strain and TEM analysis of *A. brassicicola* conidia showing existence of one or two WB located in the cytoplasm near the cell cortex support this hypothesis. In addition, cytoplasmic redistribution of the TmpL-GFP fluorescence in a *Δpex14* strain indirectly, albeit strongly, supports the

idea that TmpL is associated with a specific WB where AbHex1 is localized. Several reports on WB from other fungi have established the presence of WB in non-septal regions, such as the tips of the germlings and secondary infectious hyphae, or at the cell periphery (Markham and Collinge, 1987; Momany et al., 2002; Soundararajan et al., 2004). These WB showed no association with the hyphal septum, suggesting other possible functions than plugging septal pores in response to cell injury. For example, loss of WB in *Magnaporthe grisea ⊿hex1* strains led to increased cell death in response to nitrogen starvation. This suggests that WB may function in response to environmental stress (Soundararajan et al., 2004). PRO40, associated with WB in *Sordaria macrospora*, was pivotal in triggering the developmental switch from protoperithecia to perithecia (Engh et al., 2007). Together, these findings indicate other possible functions of the WB associated with development or the multicellular growth characteristic of filamentous fungi. On the other hand, it is also true that very little is known about the WB function in other fungal structures such as conidia and specialized infection structures. Although we cannot rule out the possibility that DsRed-AbHex1 was targeted incorrectly to the peroxisome-like organelles where TmpL-GFP was localized because of its ectopic expression, it is more likely that these observations reflect the existence of a specific WB which is associated with TmpL. To confirm the association between TmpL and WB in the future, more detailed biochemical analyses are needed. These include either immunodetection assays using TmpL- and Hex1-specific antibodies following differential and density gradient centrifugation, or immunofluorescence microscopy.

It has been well documented that regulation of ROS level is important during fungal development (Aguirre et al., 2005; Gessler et al., 2007). In this study, we also highlighted the significance of intracellular ROS concentration in relation to fungal development. Given the observations that *tmpL* was highly expressed during conidiation and the loss-of-function mutation resulted in abnormal conidiogenesis and excess ROS accumulation in conidia, we can speculate that TmpL is involved in important mechanisms for balancing ROS level during conidiation. Deletion of a catalase gene (*CATB*) in *M. grisea* caused similar phenotypic changes as was observed in the *ΔtmpL* strains, such as less pigmentation, fragile conidia, and reduced virulence (Skamnioti et al., 2007), indicating a possible common effect of excess intracellular ROS in filamentous fungi. In many fungi, inhibition of ROS generation or excess intracellular ROS levels affected various fungal developmental processes (Egan et al., 2007; Gessler et al., 2007; Hansberg et al., 1993; Sun et al., 2006). Even a fungus-plant mutualistic symbiosis requires a sophisticated regulation of the ROS production (Takemoto et al., 2006; Tanaka et al., 2006). Consistent with the involvement of ROS in cell-wall biosynthesis (Takemoto et al., 2007), it seems probable that the excess ROS levels in *ΔtmpL* strains caused lighter pigmention in the *A. brassicicola* conidia. Several studies also reported that accumulation of ROS within the cytoplasm played a central role in apoptosis-like cell death (Greenlund et al., 1995; Madeo et al., 1999), as shown in our observations of apoptosis-like cell death phenomena in aged conidia of both *A. brassicicola* and *A. fumigatus ΔtmpL* strains.

Increased expression of antioxidant genes in *A. brassicicola ΔtmpL* strains is another indicator of increased ROS levels in the cell. Indeed, several reports in different microorganisms have shown a correlation between the up-regulation of specific antioxidant enzymes and increased cellular ROS levels (Aguirre et al., 2005; Chang and Petrash, 2008; Kawasaki and Aguirre, 2001), suggesting that increased ROS levels result in higher expression of the enzymes that decompose them. On the other hand, it could be questioned why the increased antioxidant expression in the *ΔtmpL* strains did not result in reducing cellular ROS levels in the mutant cells. The possible reason for that would be excess ROS levels in the *ΔtmpL* strains were far beyond the cellular capability (or threshold) to neutralize them. Our results from experiments of *yap1* overexpression in *ΔtmpL* mutant background provide a major evidence for this hypothesis. Upon oxidative stress, Yap1 is involved in activating genes involved in a cellular antioxidant system, such as *GSH1* (γ-glutamylcysteine synthetase), *TRX2* (thioredoxin), *GLR1* (glutathione reductase), and *TRR1* (thioredoxin reductase) (Lee et al., 1999). Therefore we can speculate that Yap1 overproduction led to the increase of the cellular antioxidant defense capability in the *ΔtmpL* strain that produces excess intracellular ROS in conidia. Indeed, *yap1* overexpression suppressed most of the phenotypic defects shown in the *ΔtmpL* strain, indicating excess intracellular ROS was most likely the primary reason for the phenotypic changes observed in the *ΔtmpL* mutants. Interestingly *yap1* overexpression in the wild-type strain did not affect the expression levels of downstream antioxidant genes *ctt1* and *sod1*, consistent with the post-translational activation model of the Yap1 protein by intracellular ROS. When considered together, these results demonstrate that TmpL

may be associated with a filamentous fungi-specific oxidative stress defense system. However, we cannot rule out another possibility that TmpL is involved in cellular ROS production. As a consequence of the loss of TmpL-operated ROS production, an additional means of ROS generation may be up-regulated during conidiation, resulting in excess production of ROS. Indeed *M. grisea Δnox1Δnox2* mutant displayed increased ROS generation during hyphal growth compared with wild-type strain (Egan et al., 2007), indicating that there is an alternative ROS source that is activated upon loss of the Nox enzymes. Similarly, in *Podospora anserina* inactivation of *panox1* led to an enhanced ROS production in mycelia (Malagnac et al., 2004). However there was no difference observed in the expression levels of *A. brassicicola nox* homologs, *AbnoxA* and *AbnoxB* between wild-type and *ΔtmpL* stains during conidiation process (data not shown), suggesting the NADPH oxidase-mediated ROS production is not the cause of oxidative stress in the *ΔtmpL* stains.

A major question from our work is the role of TmpL in fungal virulence. We observed that loss of TmpL function resulted in avirulence in both plant and animal fungal pathogens. With regard to plant pathogenesis, *A. brassicicola ΔtmpL* conidia successfully germinated and formed normal appearing appressoria on plant surfaces at similar rates as wild-type. Thus, a defect in germination or appressoria development cannot explain the mutant phenotype during plant pathogenesis. However, only 7% of the total appressoria were capable of penetrating the host and growth was rapidly arrested in the epidermal cells. Additionally, the mutant appressoria and penetration hyphae observed by TEM showed a cell-death-like phenotype that we speculate may

be due to excess oxidative stress, as indicated by NBT and DAB staining. To understand whether the infection failure in *ΔtmpL* strains was related to the excess buildup of ROS therein, we tried to reduce the levels of ROS during *in planta* appressoria development and penetration using a NADPH oxidase inhibitor diphenylene iodonium or antioxidant ascorbic acid. However, none of the treatments were successful in restoring the infection failure of the *ΔtmpL* strains. Even the infection of wild-type strains treated with these agents was seriously suppressed and resulted in tiny lesions on host leaves (data not shown). The latter result seems to be explained by the same reasoning with the observation that *yap1* overexpression in the wild-type strain caused reduced lesion size compared with its wild-type recipient strain. All of these results suggest that an excess reduction in intracellular but not extracellular oxidative stress also leads to a significant suppression of fungal infection. In other words, a sophisticated balancing of ROS levels during pathogenesis is critical in fungal pathogenesis of plants. As an alternative method of reducing excess ROS in appressoria and/or penetration hyphae of the *ΔtmpL* mutants, we chose to manipulate the existing antioxidant system present in filamentous fungi by overexpressing *yap1*. NBT staining showed less superoxide accumulation in the appressoria of the Ab*ΔtmpL*:pToxA-Yap1 overexpression strain compared with the AbΔ*tmpL* recipient strain (data not shown). Although the overexpression strain exhibited significantly restored virulence, it still was not comparable to the wild-type. Thus, our *yap1* overexpression analyses clearly demonstrated that the infection failure in *ΔtmpL* strains was related to the intracellular accumulation of excess ROS in fungal infection structures.

Regulation of ROS level during pathogenesis has been a critical factor that governs success or failure of the infection process. For example, *M. grisea* showed considerable amount of oxidative burst in appressoria during its pathogenesis, and inhibition of the ROS production by some inhibitors resulted in abnormal appressoria and further failure of plant infection (Egan et al., 2007). Deletion of the Yap1 oxidative stress response protein in *Ustilago maydis* caused avirulence on corn, resulting from an excess oxidative stress on infection structures (Molina and Kahmann, 2007). In addition, numerous fungal pathogens of animals have been reported to possess a defined genetic program to respond to oxidative killing by the host (Akhter et al., 2003; Cuellar-Cruz et al., 2008; Moye-Rowley, 2002; Moye-Rowley, 2003). However, *yap1* deletion mutants in the human fungal pathogen *A. fumigatus* are still virulent in chemotherapeutic models of invasive aspergillosis (Lessing et al., 2007). This observation, coupled with the lack of full virulence restoration in the *A. brassicicola ΔtmpL* mutant strains overexpressing *yap1* may suggest that the virulence defect of *tmpL* deficient strains is due to additional unknown causes. Indeed, in our studies the virulence of the *A. fumigatus ΔtmpL* mutant was also attenuated in $gp91^{phox-/-}$ mice, which are deficient in generating a respiratory burst and highly susceptible to *A. fumigatus* infection (data not shown). Collectively, these studies and our observations suggest that production and accumulation of excess intracellular ROS, and not increased sensitivity to extracellular ROS, in both *ΔtmpL* mutants of plant and animal pathogenic fungi is the primary cause for reduced virulence. Thus increased sensitivity to and detoxification of host derived, extracellular ROS, is most likely not the reason for the avirulence observed in *ΔtmpL* mutants in both pathosystems. Recent

discoveries of functional ROS-generating enzymes within filamentous fungi have elucidated some possible roles of the fungus-derived ROS in pathogenic species (Egan et al., 2007; Lara-Ortiz et al., 2003). Fungal contributions to ROS production have been obtained from fungi showing such activity without any contact of host cells. For example, spores of *M. grisea* germinating in water generated $H_2O_2$, $O_2^-$, and $OH^+$ extracellularly (Aver'yanov et al., 2007) and ROS production was associated with the development of infection structures on glass coverslips (Egan et al., 2007). Previous studies have also speculated the possible involvement of fungus-derived ROS production in the rapid growth and spread of the pathogens inside their hosts (Govrin and Levine, 2000; Schouten et al., 2002). Together with the excess ROS accumulation in the *ΔtmpL* conidia it is more plausible to speculate that the failure of regulating intracellularly produced ROS caused the penetration failure of the *ΔtmpL* strains, and thus the reduced virulence. While *A. fumigatus* is not known to produce penetration structures like appresoria to invade mammalian hosts, it may be possible that failure to handle fungal ROS accumulation during the initial stages of host infection result in the avirulence of the *ΔtmpL* mutants.

In conclusion, we have identified a novel transmembrane protein, TmpL, involved in plant and animal fungal virulence. Our results suggest that TmpL is involved in a complex redox homeostasis mechanism in *A. brassicicola* and *A. fumigatus* during fungal development and pathogenesis. Although the biochemical function of TmpL needs to be further investigated, it is plausible that the AMP-binding domain may activate signaling molecules and, together with the enzymatic

activity generated by the FAD/NAD(P)-binding domain, regulate intracellular redox homeostasis. Since WBs have a peroxisomal origin (Tey et al., 2005), we can speculate that the TmpL protein, associated with WB, might also have a peroxisomal origin. Considering that peroxisomes play a key role in both the production and scavenging of ROS in the cell, $H_2O_2$ in particular (Elgersma et al., 1997), the peroxisome-originated TmpL may act as a detoxifier of ROS in the same way as many enzymatic peroxisomal membrane proteins and previously identified peroxisomal antioxidant regulators (Iida et al., 2006; Mullen and Trelease, 1996). Another recent finding to support this connection between fungal WB and oxidative stress is that disruption of *abhex1* in *A. brasscicola* resulted in mutant strains lacking WBs and were more sensitive to oxidative stress ($H_2O_2$) than wild-type (Kim et al., unpublished data). This result was meaningful because the deletion of *hex1* in other fungi also causes the complete loss of WB in the resulting mutants (Jedd and Chua, 2000; Soundararajan et al., 2004). Of further interest is that the *Δabhex1* mutants are not as hypersensitive as *ΔtmpL* strains, suggesting a possible, complicated relationship between the antioxidant involvement of the TmpL protein and its association with WB. Future studies will focus on identification of the specific substrate(s) directly or indirectly interacting with TmpL, and definitively determining the role of this interesting protein in plant and animal fungal virulence.

# Materials and Methods

### *Fungal strains, media, fungal culture*

*Alternaria brassicicola* strain ATCC 96866 was used in this study (American Type Culture Collection, Manassas, VA). The growth and maintenance of *A. brassicicola* and media composition were performed as described by Kim (2007) except for a minimal medium (MM) (1% glucose, 0.5% $(NH_4)_2SO_4$, 0.2% $KH_2PO_4$, 0.06% $MgSO_4$, 0.06% $CaCl_2$, 0.0005% $FeSO_4.7H_2O$, 0.00016% $MnSO_4.H_2O$, 0.00014% $ZnSO_4.7H_2O$, 0.00037% $CoCl_2.6H_2O$). *Aspergillus fumigatus* strain CEA10 was used as the wild-type, stored as frozen stock in 20% glycerol at -80°C, and grown at 37°C, on glucose minimal medium (GMM) with appropriate supplements as previously described (Shimizu and Keller, 2001) . *A. fumigatus* strain CEA17, a uracil auxotroph derived from CEA10, was used as the recipient strain for generation of the *ΔtmpL* mutant. In our study, solid complete medium (CM) refer to potato-dextrose agar and liquid CM to glucose-yeast extract broth (1% glucose, 0.5% yeast extract).

***Plant Virulence Assays***

The virulence test on green cabbage (*Brassica oleracea*) was performed as described by Kim (2007). Briefly, *A. brassicicola* was inoculated with a 10 µl drop of conidial suspension ($5\times10^4$ or $20\times10^4$ conidia $ml^{-1}$) on each leaf of 5-week-old plants. Inoculated plants were kept in a plastic box at ambient temperatures and incubated at 100% humidity for 24 hr in the dark, followed by 16 hr fluorescent lights per day for 4-6 days. Lesion diameters were measured for all virulence tests. Statistical analyses were performed to test the differences in lesion diameters among the tested strains by a pairwise t-test using JMP software (SAS Institute Inc.). P-values $\leq 0.01$ were considered statistically significant. To test the ability of Ab*ΔtmpL* strain to colonize on

wounded plants, the same conidial suspensions were applied to needle scratches on host plant leaves.

### *Generation of tmpL replacement constructs, fungal transformation, and complementation in A. brassicicola*

A *tmpL* replacement construct was made by a double-joint PCR method from three PCR fragments, with slight modifications (Yu et al., 2004). Using *A. brassicicola* genomic DNA as a template, a 993 bp *tmpL* 5′ flanking region was amplified with primers TMPLR1 and TMPLR2, and a 992 bp *tmpL* 3′ flanking region was generated with primers TMPLR5 and TMPLR6. Using pCB1636 (Sweigard et al., 1997) as a template, a ~1.4 kb hygromycin B phosphotransferase (*hph*) gene cassette was amplified with primers TMPLR3 and TMPLR4 . The reverse primer TMPLR2 that amplifies the 5′ flanking region and the forward primer ATMR5 that amplifies the 3′ flanking region, contained 20 bp tail sequences that overlapped the 5′ and 3′ ends of the *hph* cassette. Likewise, the forward and reverse primer TMPLR3 and TMPLR4 that amplified the *hph* cassette also contained a 20 bp tail sequences that overlapped the 5′ and 3′ flanking regions. The three PCR fragmentswere purified with the QIAquick PCR purification kit (Qiagen, Valencia, CA), were then diluted 10-fold , and subjected to fusion PCR with primers TMPLR1 and TMPLR6. The final 3.4 kb *tmpL* replacement construct was purified again with the QIAquick PCR purification kit and reduced to 1 µg/µl under vacuum before transformation. Fungal transformation was based on protocol described previously (Cho et al., 2006). Transformants with expected genetic integrations were identified by PCR and Southern blot analysis.

In order to reintroduce wild-type *tmpL* into the *ΔtmpL* mutant, we amplified the wild-type *tmpL* allele from *A. brassicicola* genomic DNA using primer set TMPLcomF and TMPLcomR. The resulting PCR product covers 5.2 kb between the 953 bp upstream in relation to the start codon and the 1132 bp downstream in relation to the stop codon. A 1449 bp long nourseothricin resistance gene (*NAT*) cassette was amplified with primer set PNRcomF and PNRcomR from pNR1 plasmid (Malonek et al., 2004). The final two PCR products were used simultaneously to transform *ΔtmpL* mutant A1-3, and the transformants were selected using a nourseothricin antibiotic. PCR and Southern blot analyses were used to identify transformants with expected genetic integrations.

***Generation of tmpL replacement constructs, fungal transformation, and complementation in A. fumigatus***

Generation of a *tmpL* null mutant in *A. fumigatus* strain CEA17 was accomplished by replacing an ~1.9 kb internal fragment of the *tmpL* coding region (~3.36 kb; GenBank accession no. EDP49089) with *A. parasiticus pyrG*. The disruption construct was generated by cloning a sequence homologous to the *tmpL* locus into plasmid pJW24 (donated by Nancy Keller, University of Wisconsin—Madison). The 5' and 3' *tmpL* homologous sequences, each ~1 kb in length, were cloned to flank *A. parasiticus pyrG* in pJW24. The resulting plasmid, pTMPLKO, was used as a template to amplify the ~5.2 kb disruption construct (primer RAC39 and RAC41) for use in fungal transformation. To complement the *ΔtmpL* strain, a plasmid with the *tmpL* gene connected to the *hph* gene was constructed. Therefore, the *tmpL* gene was amplified using genomic DNA of CEA10 as template and the primers RAC357 and RAC110.

The ~5.3 kb PCR product and the plasmid pBC-Hygro were digested with *Not*I and *Spe*I. The PCR product was then ligated into the vector. The resulting plasmid, pTMPLREC, was used as a template to amplify the ~9.5 kb reconstitution construct (primer RAC325 and RAC326) for use in fungal transformation.

Generation of fungal protoplasts and polyethylene glycol-mediated transformation of *A. fumigatus* were performed as previously described (Bok and Keller, 2004). Briefly, 10 µg of the *tmpL*KO PCR-generated disruption construct was incubated on ice for 50 min with 1 x $10^7$ fungal protoplasts in a total volume of 100 µl. Gene disruption transformants were initially screened by PCR to identify potential homologous recombination events at the *tmpL* locus. PCR was performed with primers designed to amplify only the disrupted *tmpL* locus - RAC109 and RAC22 (PCR product: 2077 bp); RAC21 and RAC110 (PCR product: 1595 bp). For the reconstituted strain, 10 µg of the *tmpL*REC PCR-generated reconstitution construct was used in the protoplast transformation. Colonies were selected for growth on hygromycin containing media. Reconstitution events were then screened by PCR by amplifying a part of the *tmpL* that was replaced by *pyrG* in the mutant [RAC351 and RAC352 (PCR product: 778 bp)]. Homologous recombination of the disruption cassette and random integration of the reconstituition construct was confirmed by Southern analysis with the digoxigenin labeling system (Roche Molecular Biochemicals, Mannheim, Germany) as previously described (Cramer and Lawrence, 2003). To eliminate the chance of heterokaryons, each transformant was streaked with sterile toothpicks a minimum of two times to obtain colonies from single conidia.

***Preparation of A. brassicicola nucleic acids***

DNA isolation and Southern blot analysis were performed as described by Kim (2007). The *tmpL* 3′ fragment was used as an *tmpL* specific probe and a 500 bp *hph* fragment from the pCB1636 plasmid was used as a *hph* specific probe, and a ~1 kb *NAT* fragment from pNR1 plasmid as a *NAT* specific probe. All sequencings were done using the ABI Prism 310 automated sequencer (Applied Biosystems, Forster City, CA). Total RNA was extracted from fungal samples using the RNeasy Plant Kit according to the manufacturer's protocol (Qiagen, Valencia, CA). For the expression analysis with QRT-PCR, leaves of green cabbage were inoculated with 10 μl drops of wild-type conidial suspension ($1\times10^7$ conidia $ml^{-1}$), and infected samples were collected at 12, 24, 48, 60, 72, 96, and 120 hr after inoculation. Total RNA was also extracted from mycelia grown in liquid CM for 72 hr. In order to maintain vegetative growth with no stress, the liquid CM was changed every 24 hr. About 20 mycelial balls collected from the above 72 hr-liquid culture were spread onto sterilized filter paper, incubated for conidiation, and collected at 24 and 48 hr for total RNA extraction.

***Expression and purification of TmpL FAD/NAD(P)-binding region and FAD-binding assay***

First-strand cDNA was generated from the total RNA of 48 hr air-exposed mycelial balls with random primers using SuperScript™ First-Strand Synthesis System (Invitrogen™ Life Technologies, Carlsbad, CA, USA). A 635 bp *tmpL* partial coding sequence containing the FAD/NAD(P)-binding region was amplified from the cDNA using primers A1fn_ExpKpnFor and A1fn_ExpHndRev, and cloned between the *Kpn*I

and *Hind*III sites in plasmid pKLD66 (Rocco et al., 2008) to obtain plasmid pA1FN. *E. coli* BL21(DE3) was transformed with pA1FN. *E. coli* BL21(DE3)(pA1FN) was grown to an optical density of 0.6-0.8, followed by induction with 0.2 mM IPTG. After 3 hr of induction, cells were harvested by centrifugation at 7000 x g for 10 min at 4°C. The resulting 2 g cell pellet was resuspended in 2.5 ml nickel-nitrilotriacetic acid (Ni-NTA) 50 mM sodium phosphate buffer, pH 7.5. The cell suspension was passed three times through a French pressure cell at a pressure of $1.28 \times 10^8$ Pa. The resulting cell lysate was centrifuged at 8000 x g for 25 min at 4°C to remove cell debris. The resulting supernatant was mixed with l ml Ni-NTA His Bind Resin (Novagen) and incubated for 1 hr at 4°C with constant agitation. The incubated solution was loaded onto a column bed and the column was washed with 10 ml Ni-NTA washing buffer (50 mM sodium phosphate (pH 7.5) and 20 mM imidazole). The column was sequentially eluted with 50-500 mM imidazole containing 50 mM sodium phosphate buffer (pH 7.5). Fractions at about 250 mM imidazole were pooled and concentrated on an YM-30 membrane (Amicon). The 1 mg protein concentrate was incubated with 0.2 mM FAD at 4°C for 5 hr. Free flavin was removed by filtration and three 1 mL washes with 50 mM sodium phosphate buffer (pH7.5), on the membrane of a YM-3 concentrator (Amicon). The product was recovered in 50 mM sodium phosphate buffer (pH7.5) and assayed for protein content. A UV-visible spectrum of the protein was analysed with 200-800 nm wavelength range.

***Generation of fusion protein constructs***

A *tmpL* C-terminal *gfp* fusion construct was generated by fusion PCR. Using *A. brassicicola* genomic DNA as a template, an 1 kb *tmpL* 3′ region was amplified with primers TMPLGFP1 and TMPLGFP2-GA. Another set of primers, TMPLGFP3-GA and TMPLGFP4, were used to amplify a 2.4 kb *gfp* and *hph* cassette from template plasmid pCB16G6-Nac (Cho et al., 2006). Two resulting fragments, the 1 kb *tmpL* 3′ fragment and the 2.4 kb *gfp* and *hph* cassette, were mixed and subjected to second fusion PCR with primers TMPLGFP1 and TMPLGFP4. The resulting 3.4 kb PCR products were transformed in the *A. brassicicola* wild-type to make TmpL-GFP fusion transformants. Transformants with expected genetic integration events were identified by PCR and Southern blot analyses.

The same fusion PCR strategy was applied to generate a series of fusion proteins in which different portions of *tmpL*, an AMP-binding and transmembrane domain, were appended to the N terminus of the *gfp*. For the tmpL AMP-binding-*gfp* fusion construct, two primers, A1AdeGFP1 and A1AdeGFP2-GA, were used to amplify an 881 bp *tmpL* AMP-binding domain region. Another set of primers, A1AdeGFP3-GA and A1AdeGFP4, were used to amplify a 2.4 kb *gfp* and *hph* cassette from template plasmid pCB16G6-Nac. The two resulting PCR fragments were subjected to second fusion PCR with primers A1AdeGFP1 and A1AdeGFP4. The resulting 3.4 kb PCR products were transformed in the wild-type. In the same way, four primers were designed to generate the *tmpL* transmembrane-*gfp* fusion construct as follows: A1TmGFP1 and A1TmGFP2-GA for a 756 bp *tmpL* transmembrane region; A1TmGFP3-GA and A1TmGFP4 for a *gfp* and *hph* cassette.

To generate the *DsRed-abhex1* fusion construct by fusion PCR, three PCR fragments were amplified as follows: a 573 bp *Pyrenophora tritici- repentis ToxA* promoter fragment using primers ToxAFor and ToxA-DsRedRev from template plasmid pCB16G6-Nac; a 728 bp *DsRed* ORF fragment using primers DsRed-ToxAFor and DsRed-AbHEX1Rev from template plasmid pCAG-DsRed (Matsuda and Cepko, 2004); a 969 bp *abhex1* fragment using primers AbHEX1-DsRedFor and AbHEX1Rev from *A. brassicicola* genomic DNA. These final three PCR fragments were subjected to second fusion PCR with primers ToxAFor and AbHEX1Rev. The final construct was transformed into the TmpL-GFP fusion strain to generate TmpL-GFP:DsRed-AbHex1 dual fluorescence-labeled strains.

To construct the *DsRed*-PTS1 construct that serves as marker of peroxisomal matrix, the *DsRed* fragment was amplified from pCAG-DsRed plasmid using primers DsRedPTS1For and DsRedPTS1Rev, which append the PTS1 tripeptide SRL to the C terminus of *DsRed*. Using pNR1 as template, a 1.4 kb nourseothricin resistance gene (*NAT*) cassette was amplified with primers DsRedPTS1NATFor and DsRedPTS1NATRev. These final two PCR fragments were subjected to second fusion PCR with primers DsRedPTS1For and DsRedPTS1NATRev. The final construct was transformed into the TmpL-GFP strain to generate TmpL-GFP:DsRed-PTS1 dual fluorescence-labeled strains.

To disrupt *pex14* in TmpL-GFP and DsRed-AbHex1 strains, a linear minimal element (LME) construct was generated as previously described (Cho et al., 2006). Primers pex14KOFor and pex14KORev were used to amplify a 415 bp *pex14* partial

fragment from the *A. brassicicola* genomic DNA and another set of two primers, pex14HygFor and pex14HygRev, were used to amplify an 1.4 kb *NAT* cassettes from the plasmid pNR1. The two fragments were subjected to second fusion PCR with primers pex14KOFor and pex14HygRev. The final construct was transformed into the TmpL-GFP and DsRed-AbHex1 strains to generate TmpL-GFP:*Δpex14* and DsRed-AbHex1:*Δpex14* mutant strains, respectively.

To generate *gfp-yap1* construct under the control of the *yap1* promoter, four PCR fragments were amplified by fusion PCR. A 500 bp fragment of the *yap1* promoter region was produced from *A. brassicicola* genomic DNA using primers PromoYap1For and PromoYap1Rev, a 570 bp fragment of the *gfp* ORF region from pCB16G6-Nac plasmid using primers GFPYap1For and GFPYap1Rev, an 1 kb *yap1* ORF from the genomic DNA using primers Yap1For and Yap1Rev, and an 1.4 kb *NAT* cassette from plasmid pNR1 using primers Yap1NATFor and Yap1NATRev. These four fragments were subjected to second fusion PCR with primers PromoYap1For and Yap1NATRev. The final construct was transformed into the wild-type and *A. brassicicola ΔtmpL* mutant.

To generate *ToxA-yap1* overexpression construct, a 400 bp fragment of the *ToxA* promoter region from pCB16G6-Nac plasmid using primers ToxAFor and ToxAYap1Rev, and a 3.4 kb *yap1* and *NAT* cassette from the above *gfp-yap1* construct using primers Yap1overFor and Yap1NATRev were subjected to second fusion PCR with primers ToxAFor and Yap1NATRev. The final construct was transformed into wild-type and the *A. brassicicola ΔtmpL* mutant.

All construct were subject to sequence verification with the ABI Prism 310 automated sequencer (Applied Biosystems, Forster City, CA). All transformants with expected genetic integration events were identified by PCR and Southern blot analysis.

***Quantitative real-time PCR***

To analyze the mRNA abundance of *tmpL* by quantitative real-time (QRT) PCR, 1 µg of total RNA was used for first-strand cDNA with random primers using SuperScript™ First-Strand Synthesis System (Invitrogen™ Life Technologies, Carlsbad, CA, USA) according to the manufacturer's instruction and diluted 1:3 with nuclease-free water. Reactions were performed in a 25 µl volume containing 100 nM of each primer, 2 µl of cDNA (25 ng of input RNA) and 12.5 µl of 2X iQ™ SYBR® Green Supermix (Bio-Rad, Hercules, CA, USA). QRT-PCR was run on the iCycler iQ Real-Time PCR Detection System (Bio-Rad, Hercules, CA, USA). After a 3 min denaturation at 95°C, samples were run for 40 cycles of 15 s at 95°C, 30 s at 60°C and 30 s at 72°C. After each run, amplification specificity was checked with a dissociation curve acquired by heating the samples from 60 to 95°C. To compare relative abundance of *tmpL* transcripts, average threshold cycle (Ct) was normalized to that of Glyceraldehyde-3-phosphate dehydrogenase (*GAPDH*) for each condition as $2^{-\Delta Ct}$, where $-\Delta Ct = (C_{t,tmpL} - C_{t,GAPDH})$. Fold changes during conidial development and during infectious growth compared with growing fungus in liquid CM were calculated as $2^{-\Delta\Delta Ct}$, where $-\Delta\Delta Ct = (C_{t,tmpL} - C_{t,GAPDH})_{\text{test condition}} - (C_{t,tmpL} - C_{t,GAPDH})_{\text{liquid}}$ (Livak and Schmittgen, 2001). The same real-time PCR strategy was used to analyze the expression of *yap1* and other antioxidant-related genes in *A. brassicicola* wild-type,

WT:pToxAYap1 mutant, Ab*ΔtmpL*, and Ab*ΔtmpL*:pToxAYap1 strains, except for the method of calculating relative fold change. It was determined by comparing each expression level with the one of vegetatively growing wild-type in liquid CM, where - $\Delta\Delta Ct = (C_{t,\text{gene of interest}} - C_{t,GAPDH})_{\text{rest conditions}} - (C_{t,\text{gene of interest}} - C_{t,GAPDH})_{\text{WT,vegetative mycelia}}$. Each QRT-PCR was conducted twice with two replicates and all the data is presented. The primer pairs for the transcript amplification of each gene were as follows: For the *tmpL* gene, TMPL-expFor and TMPL-expRev; *yap1*, Yap1-expFor and Yap1-expRev; *skn7*, SKN7-expFor and SKN7-expRev; *ctt1*, CTT1-expFor and CTT1-expRev; *sod1*, SOD1-expFor and SOD1-expRev; *gsh1*, GSH1-expFor and GSH1-expRev; *gsh2*, GSH2-expFor and GSH2-expRev; *trx2*, TRX2-expFor and TRX2-expRev; *gpx1*, GPX1-expFor and GPX1-expRev. For amplification of the internal control *GAPDH* gene, AbGAPDH-For and AbGAPDH-Rev were used.

***Oxidative stress assays***

For the oxidative stress tests, *A. brassicicola* and *A. fumigatus* were grown on solid MM with or without the stress agents $KO_2$ and $H_2O_2$. Sensitivity to each stressor was determined by comparing the colony radius of 5-day-old *A. brassicicola* cultures on media containing each stressor. The tests were repeated at least three times for each condition. For the germling susceptibility assay in *A. fumigatus*, a protocol from the laboratory of Judith Rhodes University of Cincinnati was followed. Briefly, conidia from CEA10, Af*ΔtmpL* and AftmpL rec were harvested after growth on GMM plates for 3 days and incubation at 37˚C. The conidia were diluted and counted in a hemocytometer. The strains were adjusted to 200 colonies per plate when 100 µl was

plated. The strains were challenged in triplicate on GMM plates with 1.25mM $H_2O_2$, plus the control. The plates were incubated at 30˚C until microscopic germlings appeared on the plates (about 16 hrs). Then the plates were overlaid with 10 ml of 1.25mM $H_2O_2$ or 10 ml distilled water as a control and incubated at 37˚C for 10 minutes. After aspirating off the $H_2O_2$ and washing the plate twice with 10 ml of sterile distilled water the plates were returned to the 30˚C incubator and incubated until colonies were large enough to count.

***Murine virulence assays***

In this study, an outbred CD1 (Charles River Laboratory, Raleigh, NC) strain was used. All animals were kept in specific pathogen-free housing, and all manipulations were approved by the institutional internal review board (IACUC). Male mice (26 to 28 g in size, 6-8 weeks old), were housed five per cage and had access to food and water ad libitum. Mice were immunosuppressed with intraperitoneal (i.p.) injections of cyclophosphamide at 150 mg/kg 3 days prior to infection and with Kenalog injected subcutaneously (s.c.) at 40 mg/kg 2 days prior to infection. On day 3 post-infection (p.i.), repeat injections were given with cyclophosphamide (150 mg/kg i.p.) and on day 6 p.i. with Kenalog (40 mg/kg s.c.). Ten mice per A. fumigatus strains (CEA10, tmpL-deficient mutant, or the reconstituted strain AftmpL rec) were infected intranasally. The mice were inoculated intranasally following brief isoflurane inhalation, returned to their cages, and monitored at least twice daily.

Infection inoculum was prepared by growing the *A. fumigatus* isolates on GMM agar plates at 37 °C for 3 days. Conidia were harvested by washing the plate

surface with sterile phosphate-buffered saline-0.01% Tween 80. The resulting conidial suspension was adjusted to the desired concentration of 1 x $10^6$ conidia/25 μl by hemacytometer count. Mice were observed for survival for 14 days after *A. fumigatus* challenge. Any animals showing distress were immediately sacrificed and recorded as deaths within 24 hr. Mock mice were included in all experiments and inoculated with sterile 0.01% Tween 80. Survival was plotted on a Kaplan-Meier curve and a log-rank test used to determine significance of pair-wise survival (two-tailed $P < 0.01$). The animal experiments were repeated on two separate occasions with similar results.

***Microscopy***

For confocal microscopy, an inverted confocal laser scanning microscope (LSM-510, Carl Zeiss, Göttingen, Germany) and an argon ion laser for excitation at 488 nm wavelength and GFP filters for emission at 515–530 nm were used. Transformants carrying each fluorescent protein fusion construct were grown on solid and liquid CM. Newly formed conidia and conidiophores from solid CM plates and vegetative mycelia from liquid CM were collected for viewing. For *in planta* expression analysis, the lower epidermis of green cabbage cotyledons was peeled off at 4 and 12 hpi and observed. For the DsRed fusion strains, a He-Ne laser (543 nm excitation, 560-615 nm emission) was used. The imaging parameters used produced no detectable background signal from any source other than from each fluorescent protein. Confocal images were captured with LSM-510 software (version 3.5; Carl Zeiss) and recorded simultaneously by phase contrast microscopy and fluorescence confocal microscopy.

Brightfield and DIC images were captured with a photomultiplier for transmitted light using the same laser illumination for fluorescence.

For the electron microscopy, conidia from each strain were released in sterile water and processed as described previously for transmission electron microscopy (Kim et al., 2007). Examination was conducted with a JEM-1010 transmission electron microscope (JEOL, Tokyo, Japan) operating at 60 kV. For cross-sections of the green cabbage leaves inoculated with *A. brassicicola* wild-type and *ΔtmpL* strains, leaf samples were collected, embedded in Epon resin, cut thick sections with an ultramicrotome (MT-X, RMC, USA), and stained with 1% toluidine blue O. The thick sections were observed using a light microscope (Eclipse E600; Nikon, Tokyo, Japan).

***Cytological assays***

For cytological analysis, the lower epidermis of green cabbage cotyledons was peeled off 12 hpi, stained with lactophenol-cotton blue (Parmeter et al., 1969), and observed by light microscopy. For the onion epidermis assay, the epidermis was peeled off, carefully washed with distilled water,then inoculated with the conidia on the adaxial surface. After 12, 24, 48, and 72 hr incubation in a closed Petri dish at 100% RH, the epidermis was stained with lactophenol-cotton blue and observed by light microscopy.

For the detection of callose papillae, green cabbage cotyledons inoculated with *A. brassicicola* were fixed and decolorized in boiling 95% ethanol, then stained in aniline blue (0.005% (w/v) in 0.07 M $K_2HPO_4$). Callose was observed by mounting stained tissue in 70% glycerin and water viewing on an Axioplan Universal

microscope (Carl Zeiss Microscope Division, Oberkochen, Germany) with a fluorescein filter set with excitation at 365 nm and emission at 420 nm.

ROS was detected by staining with following solutions. For superoxide detection, nitroblue tetrazolium (Sigma-Aldrich) was used at 5 $mg \cdot ml^{-1}$ and the staining performed for 1 hr at room temperature prior to observation. *A. brassicicola* conidia collected from a nutrient-rich medium (5 g yeast extract, 5 g casamino acid, 340 g sucrose, 15 g agar in 1 L deionized water) and fungus-inoculated leaves at each time point were subjected to the staining. For detection of ROS other than superoxide, *A. brassicicola* and *A. fumigatus* conidia were collected from PDA and GMM media, respectively, and stained with 5 $\mu g \cdot ml^{-1}$ 5-(and 6)-carboxy-2´,7´-dichlorodihydrofluorescein diacetate (carboxy-$H_2$DCFDA; Molecular Probes, Eugene, OR). The intracellular distribution of ROS in appressoria was visualized after staining with 2 mg/ml DAB 2 hr, followed by a short rinse PBS.

***Accession Number***

Sequence data for *tmpL* can be found in the GenBank data libraries under accession number EU223383 for *A. brassicicola* and EDP49089 for *A. fumigatus*.

# Literature Cited


Agrios, G.N. (1997) Plant Pathology. San Diego, CA: Academic Press, pp.300-333.

Aguirre, J., Rios-Momberg, M., Hewitt, D., and Hansberg, W. (2005) Reactive oxygen species and development in microbial eukaryotes. Trends Microbiol, 13(3), 111-118.

Akhter, S., McDade, H.C., Gorlach, J.M., Heinrich, G., Cox, G.M., and Perfect, J.R. (2003) Role of alternative oxidase gene in pathogenesis of Cryptococcus neoformans. Infect Immun, 71(10), 5794-5802.

Apel, K., and Hirt, H. (2004) Reactive oxygen species: metabolism, oxidative stress, and signal transduction. Annu Rev Plant Biol, 55, 373-399.

Aver'yanov, A.A., Pasechnik, T.D., Lapikova, V.P., Gaivoronskaya, L.M., Kuznetsov, V., and Baker, C.J. (2007) Possible contribution of blast spores to the oxidative burst in the infection droplet on rice leaf. Acta Phytopathologica et Entomologica Hungarica, 42, 305-319.

Belozerskaia, T.A., and Gessler, N.N. (2007) [Reactive oxygen species and the strategy of the antioxidant defense in fungi: a review]. Prikl Biokhim Mikrobiol, 43(5), 565-575.

Bendtsen, J.D., Nielsen, H., von Heijne, G., and Brunak, S. (2004) Improved prediction of signal peptides: SignalP 3.0. J. Mol. Biol., 340(4), 783-795.

Bindschedler, L.V., Dewdney, J., Blee, K.A., Stone, J.M., Asai, T., Plotnikov, J., Denoux, C., Hayes, T., Gerrish, C., Davies, D.R., Ausubel, F.M., and Paul Bolwell, G. (2006) Peroxidase-dependent apoplastic oxidative burst in Arabidopsis required for pathogen resistance. Plant J, 47(6), 851-863.

Bok, J.W., and Keller, N.P. (2004) LaeA, a regulator of secondary metabolism in Aspergillus spp. Eukaryot Cell, 3(2), 527-535.

Borkovich, K.A., Alex, L.A., Yarden, O., Freitag, M., Turner, G.E., Read, N.D., Seiler, S., Bell-Pedersen, D., Paietta, J., Plesofsky, N., Plamann, M., Goodrich-Tanrikulu, M., Schulte, U., Mannhaupt, G., Nargang, F.E., Radford, A., Selitrennikoff, C., Galagan, J.E., Dunlap, J.C., Loros, J.J., Catcheside, D., Inoue, H., Aramayo, R., Polymenis, M., Selker, E.U., Sachs, M.S., Marzluf, G.A., Paulsen, I., Davis, R., Ebbole, D.J., Zelter, A., Kalkman, E.R., O'Rourke, R., Bowring, F., Yeadon, J., Ishii, C., Suzuki, K., Sakai, W., and Pratt, R. (2004) Lessons from the genome sequence of Neurospora crassa: tracing the path from genomic blueprint to multicellular organism. Microbiol Mol Biol Rev, 68(1), 1-108.

Brummer, E., Choi, J.H., and Stevens, D.A. (2005) Interaction between conidia, lung macrophages, immunosuppressants, proinflammatory cytokines and transcriptional regulation. Med Mycol, 43 Suppl 1, S177-179.

Buck, V., Quinn, J., Soto Pino, T., Martin, H., Saldanha, J., Makino, K., Morgan, B.A., and Millar, J.B. (2001) Peroxide sensors for the fission yeast stress-activated mitogen-activated protein kinase pathway. Mol Biol Cell, 12(2), 407-419.

Camp, R.R. (1977) Association of microbodies, Woronin bodies, and septa in intercellular hyphae of Cymadothea trifolii. Can. J. Bot.-Revue Canadienne De Botanique, 55, 1856-1859.
Champagne, M., Pierre, D., Sergei, O., Martin, B., Pavel, H., and Johanne, T. (1999) Protection against necrosis but not apoptosis by heat stress proteins in vascular smooth muscle cells: evidence for distinct modes of cell death. Hypertension, 33, 906-913.
Chang, Q., and Petrash, J.M. (2008) Disruption of aldo-keto reductase genes leads to elevated markers of oxidative stress and inositol auxotrophy in Saccharomyces cerevisiae. Biochim Biophys Acta, 1783(2), 237-245.
Chen, D., Toone, W.M., Mata, J., Lyne, R., Burns, G., Kivinen, K., Brazma, A., Jones, N., and Bahler, J. (2003) Global transcriptional responses of fission yeast to environmental stress. Mol Biol Cell, 14(1), 214-229.
Cho, Y., Davis, J.W., Kim, K.H., Wang, J., Sun, Q.H., Cramer, R.A., Jr., and Lawrence, C.B. (2006) A high throughput targeted gene disruption method for Alternaria brassicicola functional genomics using linear minimal element (LME) constructs. Mol Plant Microbe Interact, 19(1), 7-15.
Cramer, R.A., and Lawrence, C.B. (2003) Cloning of a gene encoding an Alt a 1 isoallergen differentially expressed by the necrotrophic fungus Alternaria brassicicola during Arabidopsis infection. Appl Environ Microbiol, 69(4), 2361-2364.
Cuellar-Cruz, M., Briones-Martin-del-Campo, M., Canas-Villamar, I., Montalvo-Arredondo, J., Riego-Ruiz, L., Castano, I., and De Las Penas, A. (2008) High resistance to oxidative stress in the fungal pathogen Candida glabrata is mediated by a single catalase, Cta1p, and is controlled by the transcription factors Yap1p, Skn7p, Msn2p, and Msn4p. Eukaryot Cell, 7(5), 814-825.
De Smet, K., Eberhardt, I., Reekmans, R., and Contreras, R. (2004) Bax-induced cell death in Candida albicans. Yeast, 21(16), 1325-1334.
Del Sorbo, G., Schoonbeek, H., and De Waard, M.A. (2000) Fungal transporters involved in efflux of natural toxic compounds and fungicides. Fungal Genet Biol, 30(1), 1-15.
Diamond, R.D., and Clark, R.A. (1982) Damage to Aspergillus fumigatus and Rhizopus oryzae hyphae by oxidative and nonoxidative microbicidal products of human neutrophils in vitro. Infect Immun, 38(2), 487-495.
Diamond, R.D., Krzesicki, R., Epstein, B., and Jao, W. (1978) Damage to hyphal forms of fungi by human leukocytes in vitro. A possible host defense mechanism in aspergillosis and mucormycosis. Am J Pathol, 91(2), 313-328.
Dym, O., and Eisenberg, D. (2001) Sequence-structure analysis of FAD-containing proteins. Protein Sci, 10(9), 1712-1728.
Egan, M.J., Wang, Z.Y., Jones, M.A., Smirnoff, N., and Talbot, N.J. (2007) Generation of reactive oxygen species by fungal NADPH oxidases is required for rice blast disease. Proc Natl Acad Sci U S A, 104(28), 11772-11777.
Elgersma, Y., Kwast, L., van den Berg, M., Snyder, W.B., Distel, B., Subramani, S., and Tabak, H.F. (1997) Overexpression of Pex15p, a phosphorylated peroxisomal integral membrane protein required for peroxisome assembly in

S.cerevisiae, causes proliferation of the endoplasmic reticulum membrane. EMBO J, 16(24), 7326-7341.
Engh, I., Wurtz, C., Witzel-Schlomp, K., Zhang, H.Y., Hoff, B., Nowrousian, M., Rottensteiner, H., and Kuck, U. (2007) The WW domain protein PRO40 is required for fungal fertility and associates with Woronin bodies. Eukaryot Cell, 6(5), 831-843.
Finkel, T. (2003) Oxidant signals and oxidative stress. Curr Opin Cell Biol, 15(2), 247-254.
Finn, R.D., Mistry, J., Schuster-Bockler, B., Griffiths-Jones, S., Hollich, V., Lassmann, T., Moxon, S., Marshall, M., Khanna, A., Durbin, R., Eddy, S.R., Sonnhammer, E.L., and Bateman, A. (2006) Pfam: clans, web tools and services. Nucleic Acids Res, 34(Database issue), D247-251.
Galagan, J.E., Calvo, S.E., Borkovich, K.A., Selker, E.U., Read, N.D., Jaffe, D., FitzHugh, W., Ma, L.J., Smirnov, S., Purcell, S., Rehman, B., Elkins, T., Engels, R., Wang, S., Nielsen, C.B., Butler, J., Endrizzi, M., Qui, D., Ianakiev, P., Bell-Pedersen, D., Nelson, M.A., Werner-Washburne, M., Selitrennikoff, C.P., Kinsey, J.A., Braun, E.L., Zelter, A., Schulte, U., Kothe, G.O., Jedd, G., Mewes, W., Staben, C., Marcotte, E., Greenberg, D., Roy, A., Foley, K., Naylor, J., Stange-Thomann, N., Barrett, R., Gnerre, S., Kamal, M., Kamvysselis, M., Mauceli, E., Bielke, C., Rudd, S., Frishman, D., Krystofova, S., Rasmussen, C., Metzenberg, R.L., Perkins, D.D., Kroken, S., Cogoni, C., Macino, G., Catcheside, D., Li, W., Pratt, R.J., Osmani, S.A., DeSouza, C.P., Glass, L., Orbach, M.J., Berglund, J.A., Voelker, R., Yarden, O., Plamann, M., Seiler, S., Dunlap, J., Radford, A., Aramayo, R., Natvig, D.O., Alex, L.A., Mannhaupt, G., Ebbole, D.J., Freitag, M., Paulsen, I., Sachs, M.S., Lander, E.S., Nusbaum, C., and Birren, B. (2003) The genome sequence of the filamentous fungus Neurospora crassa. Nature, 422(6934), 859-868.
Gessler, N.N., Aver'yanov, A.A., and Belozerskaya, T.A. (2007) Reactive oxygen species in regulation of fungal development. Biochemistry (Mosc), 72(10), 1091-1109.
Govrin, E.M., and Levine, A. (2000) The hypersensitive response facilitates plant infection by the necrotrophic pathogen Botrytis cinerea. Curr Biol, 10(13), 751-757.
Greenlund, L.J., Deckwerth, T.L., and Johnson, E.M., Jr. (1995) Superoxide dismutase delays neuronal apoptosis: a role for reactive oxygen species in programmed neuronal death. Neuron, 14(2), 303-315.
Hagiwara, D., Asano, Y., Yamashino, T., and Mizuno, T. (2008) Characterization of bZip-type transcription factor AtfA with reference to stress responses of conidia of Aspergillus nidulans. Biosci Biotechnol Biochem, 72(10), 2756-2760.
Halliwell, B., and Gutteridge, J.M. (1986) Oxygen free radicals and iron in relation to biology and medicine: some problems and concepts. Arch Biochem Biophys, 246(2), 501-514.
Halliwell, B., and Gutteridge, J.M. ( 2002) Free radicals in biology and medicine. Oxford, UK: Oxford University Press.

Hammond-Kosack, K.E., and Jones, J.D. (1996) Resistance gene-dependent plant defense responses. Plant Cell, 8(10), 1773-1791.
Hansberg, W., de Groot, H., and Sies, H. (1993) Reactive oxygen species associated with cell differentiation in Neurospora crassa. Free Radic Biol Med, 14(3), 287-293.
Hasan, R., Leroy, C., Isnard, A.D., Labarre, J., Boy-Marcotte, E., and Toledano, M.B. (2002) The control of the yeast H2O2 response by the Msn2/4 transcription factors. Mol Microbiol, 45(1), 233-241.
Horton, P., Park, K.J., Obayashi, T., Fujita, N., Harada, H., Adams-Collier, C.J., and Nakai, K. (2007) WoLF PSORT: protein localization predictor. Nucleic Acids Res, 35(Web Server issue), W585-587.
Iida, R., Yasuda, T., Tsubota, E., Takatsuka, H., Matsuki, T., and Kishi, K. (2006) Human Mpv17-like protein is localized in peroxisomes and regulates expression of antioxidant enzymes. Biochem Biophys Res Commun, 344(3), 948-954.
Jedd, G., and Chua, N.H. (2000) A new self-assembled peroxisomal vesicle required for efficient resealing of the plasma membrane. Nat Cell Biol, 2(4), 226-231.
Kargel, E., Menzel, R., Honeck, H., Vogel, F., Bohmer, A., and Schunck, W.H. (1996) Candida maltosa NADPH-cytochrome P450 reductase: cloning of a full-length cDNA, heterologous expression in *Saccharomyces cerevisiae* and function of the N-terminal region for membrane anchoring and proliferation of the endoplasmic reticulum. Yeast, 12(4), 333-348.
Kawasaki, L., and Aguirre, J. (2001) Multiple catalase genes are differentially regulated in Aspergillus nidulans. J Bacteriol, 183(4), 1434-1440.
Kim, K.H., Cho, Y., La Rota, M., Cramer, R.A., Jr., and Lawrence, C.B. (2007) Functional analysis of the *Alternaria brassicicola* non-ribosomal peptide synthetase gene *AbNPS2* reveals a role in conidial cell wall construction. Mol. Plant Pathol., 8(1), 23-39.
Kuge, S., Jones, N., and Nomoto, A. (1997) Regulation of yAP-1 nuclear localization in response to oxidative stress. EMBO J, 16(7), 1710-1720.
Lambeth, J.D. (2004) NOX enzymes and the biology of reactive oxygen. Nat Rev Immunol, 4(3), 181-189.
Lara-Ortiz, T., Riveros-Rosas, H., and Aguirre, J. (2003) Reactive oxygen species generated by microbial NADPH oxidase NoxA regulate sexual development in Aspergillus nidulans. Mol Microbiol, 50(4), 1241-1255.
Lee, B.N., Kroken, S., Chou, D.Y., Robbertse, B., Yoder, O.C., and Turgeon, B.G. (2005) Functional analysis of all nonribosomal peptide synthetases in *Cochliobolus heterostrophus* reveals a factor, NPS6, involved in virulence and resistance to oxidative stress. Eukaryot. Cell, 4(3), 545-555.
Lee, J., Godon, C., Lagniel, G., Spector, D., Garin, J., Labarre, J., and Toledano, M.B. (1999) Yap1 and Skn7 control two specialized oxidative stress response regulons in yeast. J Biol Chem, 274(23), 16040-16046.
Lee, Y., Yeom, J., Kang, Y.S., Kim, J., Sung, J.S., Jeon, C.O., and Park, W. (2007) Molecular characterization of fprB (ferredoxin-NADP+ reductase) in Pseudomonas putida KT2440. J Microbiol Biotechnol, 17(9), 1504-1512.

Lessing, F., Kniemeyer, O., Wozniok, I., Loeffler, J., Kurzai, O., Haertl, A., and Brakhage, A.A. (2007) The Aspergillus fumigatus transcriptional regulator AfYap1 represents the major regulator for defense against reactive oxygen intermediates but is dispensable for pathogenicity in an intranasal mouse infection model. Eukaryot Cell, 6(12), 2290-2302.

Liu, F., Ng, S.K., Lu, Y., Low, W., Lai, J., and Jedd, G. (2008) Making two organelles from one: Woronin body biogenesis by peroxisomal protein sorting. J Cell Biol, 180(2), 325-339.

Livak, K.J., and Schmittgen, T.D. (2001) Analysis of relative gene expression data using real-time quantitative PCR and the 2(-Delta Delta C(T)) Method. Methods, 25(4), 402-408.

Madeo, F., Frohlich, E., Ligr, M., Grey, M., Sigrist, S.J., Wolf, D.H., and Frohlich, K.U. (1999) Oxygen stress: a regulator of apoptosis in yeast. J Cell Biol, 145(4), 757-767.

Malagnac, F., Lalucque, H., Lepere, G., and Silar, P. (2004) Two NADPH oxidase isoforms are required for sexual reproduction and ascospore germination in the filamentous fungus Podospora anserina. Fungal Genet Biol, 41(11), 982-997.

Malonek, S., Rojas, M.C., Hedden, P., Gaskin, P., Hopkins, P., and Tudzynski, B. (2004) The NADPH-cytochrome P450 reductase gene from *Gibberella fujikuroi* is essential for gibberellin biosynthesis. J. Biol. Chem., 279(24), 25075-25084.

Managadze, D., Wurtz, C., Sichting, M., Niehaus, G., Veenhuis, M., and Rottensteiner, H. (2007) The peroxin PEX14 of Neurospora crassa is essential for the biogenesis of both glyoxysomes and Woronin bodies. Traffic, 8(6), 687-701.

Markham, P., and Collinge, A.J. (1987) Woronin bodies of filamentous fungi. FEMS Microbiol Rev, 46, 1-11.

Matsuda, T., and Cepko, C.L. (2004) Electroporation and RNA interference in the rodent retina in vivo and in vitro. Proc Natl Acad Sci U S A, 101(1), 16-22.

Mehdy, M.C. (1994) Active Oxygen Species in Plant Defense against Pathogens. Plant Physiol, 105(2), 467-472.

Missall, T.A., Lodge, J.K., and McEwen, J.E. (2004) Mechanisms of resistance to oxidative and nitrosative stress: implications for fungal survival in mammalian hosts. Eukaryot Cell, 3(4), 835-846.

Molina, L., and Kahmann, R. (2007) An Ustilago maydis gene involved in H2O2 detoxification is required for virulence. Plant Cell, 19(7), 2293-2309.

Momany, M., Richardson, E.A., Van Sickle, C., and Jedd, G. (2002) Mapping Woronin body position in *Aspergillus nidulans*. Mycologia, 94(2), 260-266.

Moye-Rowley, W.S. (2002) Transcription factors regulating the response to oxidative stress in yeast. Antioxid Redox Signal, 4(1), 123-140.

Moye-Rowley, W.S. (2003) Regulation of the transcriptional response to oxidative stress in fungi: similarities and differences. Eukaryot Cell, 2(3), 381-389.

Mullen, R.T., and Trelease, R.N. (1996) Biogenesis and membrane properties of peroxisomes: Does the boundary membrane serve and protect? Trends Plant Sci, 1, 389-394.

Myhre, O., Andersen, J.M., Aarnes, H., and Fonnum, F. (2003) Evaluation of the probes 2',7'-dichlorofluorescin diacetate, luminol, and lucigenin as indicators of reactive species formation. Biochem Pharmacol, 65(10), 1575-1582.

Nakai, K., and Horton, P. (1999) PSORT: a program for detecting sorting signals in proteins and predicting their subcellular localization. Trends Biochem. Sci., 24(1), 34-36.

Nathues, E., Joshi, S., Tenberge, K.B., von den Driesch, M., Oeser, B., Baumer, N., Mihlan, M., and Tudzynski, P. (2004) CPTF1, a CREB-like transcription factor, is involved in the oxidative stress response in the phytopathogen Claviceps purpurea and modulates ROS level in its host Secale cereale. Mol Plant Microbe Interact, 17(4), 383-393.

Osbourn, A.E. (2001) Tox-boxes, fungal secondary metabolites, and plant disease. Proc Natl Acad Sci U S A, 98(25), 14187-14188.

Parmeter, J.R., Sherwood, R.T., and Platt, W.D. (1969) Anastomosis grouping among isolates of *Thanatephorus cucumeris*. Phytopathology, 59, 1270-1278.

Pasquier, C., Promponas, V.J., Palaios, G.A., Hamodrakas, J.S., and Hamodrakas, S.J. (1999) A novel method for predicting transmembrane segments in proteins based on a statistical analysis of the SwissProt database: the PRED-TMR algorithm. Protein Eng, 12(5), 381-385.

Passardi, F., Cosio, C., Penel, C., and Dunand, C. (2005) Peroxidases have more functions than a Swiss army knife. Plant Cell Rep, 24, 255-265.

Philippe, B., Ibrahim-Granet, O., Prevost, M.C., Gougerot-Pocidalo, M.A., Sanchez Perez, M., Van der Meeren, A., and Latge, J.P. (2003) Killing of Aspergillus fumigatus by alveolar macrophages is mediated by reactive oxidant intermediates. Infect Immun, 71(6), 3034-3042.

Rocco, C.J., Dennison, K.L., Klenchin, V.A., Rayment, I., and Escalante-Semerena, J.C. (2008) Construction and use of new cloning vectors for the rapid isolation of recombinant proteins from *Escherichia coli*. Plasmid, 59, 231-237.

Rossmann, M.G., Moras, D., and Olsen, K.W. (1974) Chemical and biological evolution of nucleotide-binding protein. Nature, 250(463), 194-199.

Royall, J.A., and Ischiropoulos, H. (1993) Evaluation of 2',7'-dichlorofluorescin and dihydrorhodamine 123 as fluorescent probes for intracellular H2O2 in cultured endothelial cells. Arch Biochem Biophys, 302(2), 348-355.

Santos, J.L., and Shiozaki, K. (2001) Fungal histidine kinases. Sci STKE, 2001(98), RE1.

Schouten, A., Tenberge, K.B., Vermeer, J., Stewart, J., Wagemakers, L., Williamson, B., and van Kan, J.A.L. (2002) Functional analysis of an extracellular catalase of Botrytis cinerea. Molecular Plant Pathology, 3(4), 227-238.

Schwarzer, D., Finking, R., and Marahiel, M.A. (2003) Nonribosomal peptides: from genes to products. Nat Prod Rep, 20(3), 275-287.

Shatkay, H., Hoglund, A., Brady, S., Blum, T., Donnes, P., and Kohlbacher, O. (2007) SherLoc: high-accuracy prediction of protein subcellular localization by integrating text and protein sequence data. Bioinformatics, 23(11), 1410-1417.

Shatwell, K.P., Dancis, A., Cross, A.R., Klausner, R.D., and Segal, A.W. (1996) The FRE1 ferric reductase of *Saccharomyces cerevisiae* is a cytochrome b similar to that of NADPH oxidase. J. Biol. Chem., 271, 14240-14244.

Shibuya, K., Paris, S., Ando, T., Nakayama, H., Hatori, T., and Latge, J.P. (2006) Catalases of Aspergillus fumigatus and inflammation in aspergillosis. Nippon Ishinkin Gakkai Zasshi, 47(4), 249-255.

Shimizu, K., and Keller, N.P. (2001) Genetic involvement of a cAMP-dependent protein kinase in a G protein signaling pathway regulating morphological and chemical transitions in Aspergillus nidulans. Genetics, 157(2), 591-600.

Singh, A., Kaur, N., and Kosman, D.J. (2007) The metalloreductase Fre6p in Fe-efflux from the yeast vacuole. J. Biol. Chem., 282(39), 28619-28626.

Skamnioti, P., Henderson, C., Zhang, Z., Robinson, Z., and Gurr, S.J. (2007) A novel role for catalase B in the maintenance of fungal cell-wall integrity during host invasion in the rice blast fungus Magnaporthe grisea. Mol Plant Microbe Interact, 20(5), 568-580.

Soid-Raggi, G., Sanchez, O., and Aguirre, J. (2006) TmpA, a member of a novel family of putative membrane flavoproteins, regulates asexual development in *Aspergillus nidulans*. Mol. Microbiol., 59(3), 854-869.

Sonnhammer, E.L., von Heijne, G., and Krogh, A. (1998) A hidden Markov model for predicting transmembrane helices in protein sequences. Proc Int Conf Intell Syst Mol Biol, 6, 175-182.

Soundararajan, S., Jedd, G., Li, X., Ramos-Pamplona, M., Chua, N.H., and Naqvi, N.I. (2004) Woronin body function in Magnaporthe grisea is essential for efficient pathogenesis and for survival during nitrogen starvation stress. Plant Cell, 16(6), 1564-1574.

Sridhar Prasad, G., Kresge, N., Muhlberg, A.B., Shaw, A., Jung, Y.S., Burgess, B.K., and Stout, C.D. (1998) The crystal structure of NADPH:ferredoxin reductase from Azotobacter vinelandii. Protein Sci, 7(12), 2541-2549.

Stachelhaus, T., and Marahiel, M.A. (1995) Modular structure of genes encoding multifunctional peptide synthetases required for non-ribosomal peptide synthesis. FEMS Microbiol Lett, 125(1), 3-14.

Stohs, S. (1995) The role of free radicals in toxicity and disease. J Basic Clin Physiol Pharmacol, 6(3-4), 205-228.

Sun, C.B., Suresh, A., Deng, Y.Z., and Naqvi, N.I. (2006) A multidrug resistance transporter in Magnaporthe is required for host penetration and for survival during oxidative stress. Plant Cell, 18(12), 3686-3705.

Sweigard, J., Chumly, F., Carroll, A., Farrall, L., and Valent, B. (1997) A series of vectors for fungal transformation. Fungal Gen. Newsl., 44, 52-53.

Takemoto, D., Tanaka, A., and Scott, B. (2006) A p67Phox-like regulator is recruited to control hyphal branching in a fungal-grass mutualistic symbiosis. Plant Cell, 18(10), 2807-2821.

Takemoto, D., Tanaka, A., and Scott, B. (2007) NADPH oxidases in fungi: diverse roles of reactive oxygen species in fungal cellular differentiation. Fungal Genet Biol, 44(11), 1065-1076.

Tanaka, A., Christensen, M.J., Takemoto, D., Park, P., and Scott, B. (2006) Reactive oxygen species play a role in regulating a fungus-perennial ryegrass mutualistic interaction. Plant Cell, 18(4), 1052-1066.
Temple, M.D., Perrone, G.G., and Dawes, I.W. (2005) Complex cellular responses to reactive oxygen species. Trends Cell Biol, 15(6), 319-326.
Tey, W.K., North, A.J., Reyes, J.L., Lu, Y.F., and Jedd, G. (2005) Polarized gene expression determines woronin body formation at the leading edge of the fungal colony. Mol Biol Cell, 16(6), 2651-2659.
Thorpe, G.W., Fong, C.S., Alic, N., Higgins, V.J., and Dawes, I.W. (2004) Cells have distinct mechanisms to maintain protection against different reactive oxygen species: oxidative-stress-response genes. Proc Natl Acad Sci U S A, 101(17), 6564-6569.
Titorenko, V.I., and Rachubinski, R.A. (2004) The peroxisome: orchestrating important developmental decisions from inside the cell. J Cell Biol, 164(5), 641-645.
Torres, M.A., Jones, J.D., and Dangl, J.L. (2006) Reactive oxygen species signaling in response to pathogens. Plant Physiol, 141(2), 373-378.
Wojtaszek, P. (1997) Oxidative burst: an early plant response to pathogen infection. Biochem J, 322 ( Pt 3), 681-692.
Woronin, M. (1864) Zur Entwicklungsgeschichte der *Ascobolus pulcherrimus* Cr. und einiger Pezizen. Abh. Senkenb. Naturforsch., 5, 333-344.
Yamamoto, A., Ueda, J., Yamamoto, N., Hashikawa, N., and Sakurai, H. (2007) Role of heat shock transcription factor in Saccharomyces cerevisiae oxidative stress response. Eukaryot Cell, 6(8), 1373-1379.
Yan, C., Lee, L.H., and Davis, L.I. (1998) Crm1p mediates regulated nuclear export of a yeast AP-1-like transcription factor. EMBO J, 17(24), 7416-7429.
Yannone, S.M., and Burgess, B.K. (1998) The seven-iron FdI from Azotobacter vinelandii regulates the expression of NADPH: ferredoxin reductase via an oxidative stress response. Journal of biological inorganic chemistry, 3, 253-258.
Yu, J.H., Hamari, Z., Han, K.H., Seo, J.A., Reyes-Dominguez, Y., and Scazzocchio, C. (2004) Double-joint PCR: a PCR-based molecular tool for gene manipulations in filamentous fungi. Fungal Genet. Biol., 41(11), 973-981.

# Chapter VI

## Summary and Conclusion

*Alternaria brassicicola* (Schwein.) Wiltshire is a phytopathogenic fungus that causes one of the most economically important diseases of *Brassica* species, Alternaria black spot (also called dark leaf spot). As a necrotrophic pathogen, *A. brassicicola* secretes numerous secondary metabolites, which include host-selective and nonhost-selective phytotoxins, to kill cells from a large spectrum of Brassica plants. Understanding of the *A. brassicicola* secondary metabolites, its biosynthetic mechanisms, and their roles in necrotrophic interactions with its hosts is still rather incomplete. For example, brassicicolin A was the first metabolite reported as an "antibiotic complex" (Ciegler and Lindenfelser, 1969) and recently demonstrated as the major host-selective phytotoxin (Pedras et al., 2009), whereas the encoding gene and the mechanism of action *in planta* has not been determined. As well, *A. brassicicola* was reported to produce a host-selective toxin protein called AB toxin (Otani et al., 1998), from spores germinating on host leaves. AB toxin was induced by a host-derived oligosaccharide of 1.3 kDa, but the encoding gene and its function remain unknown (Oka et al., 2005). In addition, several fusicoccane-like diterpenes were isolated from phytotoxic extracts of cultures of *A. brassicicola*, but their phytotoxicity was not determined due to the small quantities obtained (MacKinnon et al., 1999).

With all this necessity, my study had two goals: first, to identify all *NPS* and *PKS* genes in the genome of *A. brassicicola* and determine the phenotype resulting from mutation of each *NPS* and *PKS* gene, with emphasis on discovery of any that might be involved in fungal virulence; Second, to further characterize several genes of interest to determine their functions in *A. brassicicola* biology and pathogenesis. In a genome-wide search for NPS- and PKS-encoding genes in *A. brassicicola*, we determined that the genome encodes seven *NPS*, one *NPS*-like, and 10 *PKS* genes, and that, when deleted singly, *AbNPS2*, *AbNPS4*, *AbNPS7*, *tmpL* (*NPS*-like), *AbPKS1*, and *AbPKS8* disruption mutants showed significant reductions in virulence (20 % to 80 %), indicating that the products of those genes are necessary for the full virulence of *A. brassicicola* on green cabbage and Arabidopsis when tested. In addition, several mutants showed interesting phenotypes such as abberant "bumpy" conidial cell walls resulting in hydrophilic conidial surface (*AbNPS2*), conidia with lighter pigmentation and thin cell walls (*tmpL*), melanin-deficient albino mutants (*AbPKS7*), and hypersensitivity to oxidative stress (*AbNPS6-7* and *tmpL*).

Through in-depth functional analysis we determined that AbNPS2 plays an important role in conidial cell wall construction and in virulence. However, the end product of AbNPS2 remains undetermined. Based upon gene expression and microscopic analyses we speculate that the putative secondary metabolite produced by AbNPS2 is a compound connecting or attaching the outermost cell wall layer to the outer part of the middle layer, resulting in producing conidia with an improved ability to survive in adverse environmental conditions. This study further illustrated the

versatile and essential role of secondary metabolites in fungal biology and was the first report that a fungal NPS metabolite is associated with conidial cell wall construction. Although melanin functions to protect fungal conidia from UV damage, most secondary metabolites are known to play no obvious roles in conidiation or conidial protection but are secreted into the environment at a time in the life cycle of the fungus. Identification of the putative secondary metabolite produced by AbNPS2 and its role in conidial development will not only provide new insights in fungal cell wall architecture and cell wall construction, but also allow us to get an important handle on the precise molecular events that give rise to these drastic effects on spore viability.

Polyketides and nonribosomal peptides represent two natural product classes with tremendous therapeutic value (Cane and Walsh, 1999). Erythromycin (a polyketide antibiotic), vancomycin (a nonribosomal peptide antibiotic), and epothilone (a mixed polyketide-nonribosomal peptide antitumor agent) represent just a few of these important natural compounds. In our study, we identified and characterized a gene cluster containing *AbPKS9* (renamed as *DEP5*) responsible for depudecin biosynthesis. Depudecin is an inhibitor of histone deacetylases (HDACs) (Matsumoto et al., 1992). Although depudecin is well known as anti-parasitic and anti-angiogenic, we wondered why a plant pathogen possesses an HDAC inhibitor; what is the role of HDAC in plant disease resistance? *AbPKS9* deletion mutants caused only ~10% reduced lesion size on susceptible green cabbage compared with wild-type strain, indicating depudecin is a minor virulence factor. Although it is not as strong an HDAC inhibitor as HC toxin produced by *Cochliobolus carbonum*, this system can be utilized

to exploit the genetic resources of both partners to address the role of HDACs in disease resistance. It is also possible that depudecin's main role is yet to be determined and/or could act synergistically with other secondary metabolites in regards to virulence or as an antimicrobial substance.

The critical roles of ROS in fungal development or virulence have been well established over the past half a century since the first experimental detection of hydrogen peroxide in fungal cells in Bach's works (1950). ROS in the cell act as signaling molecules regulating physiological responses and developmental processes, and are also involved in sophisticated virulence processes for many pathogenic fungi. Therefore uncovering the role of cellular ROS appears to be very important in understanding fungal development and virulence. Currently we have a limited understanding of how ROS are generated or decomposed inside fungal cells and what are the cellular ROS regulatory mechanisms. In chapter 5, we demonstrated that a NPS-like protein named TmpL is involved in fungal development and virulence in both plant and animal pathogenic fungi. Based upon the structure of the *tmpL* with only a single putative AMP-binding domain similar to an adenylation domain, followed by six transmembrane domains, we concluded that it is not a true *NPS* gene. In the absence of TmpL, dysregulation of oxidative stress homeostasis in both fungi caused developmental and virulence defects. Our finding provides new insights into mechanisms underlying the complex webs of interactions between ROS and cell differentiation and the involvement of ROS for both plant and animal fungal

pathogenesis, which presents an opportunity to develop efficient control methods for both plant and animal fungal disease.

During our studies, *AbNPS6* and *AbNPS7* were concomitantly identified as NPS enzymes responsible for siderophore biosynthesis by Turgeon and colleagues (Oide et al., 2007; Turgeon et al., 2008). Through the functional analyses of those siderophore-producing NPS enzymes, they suggested that iron metabolism is involved in oxidative stress tolerance and virulence by supplying an essential nutrient iron. However the exact relationship between siderophore-mediated iron metabolism and oxidative stress tolerance remains to be defined.

Several metabolites have been isolated from the organic extracts of the *A. brassicicola* culture broths (Pedras et al., 2009). These include phomapyrone (A, G, and F), brassicicene (C, G, H, and I), infectopyrone, and brassicicolin A. In this study phomapyrone and infectopyrone were found to be non-phytotoxic, while diterpene brassicicene and the host-selective toxin brassicicolin A were found in phytotoxic fraction (Pedras et al., 2009). Among them, only one biosynthetic cluster for diterpene brassicicene C has been identified so far (Minami et al., 2009). We have also functionally analyzed the brassicene terpene synthase and found it to be a virulence factor (Kim et al., unpublished). Thus our study involving the identification, analysis, and production of knock out mutant strains corresponding to *NPS* and *PKS* genes identified in the *A. brassicicola* genome may be considered a substantial resource to identify gene clusters responsible for the *A. brassicicola* metabolites thus far identified. For example, it is highly plausible that the NPS and PKS enzymes, which were shown

to be related to the virulence of *A. brassicicola* in our study, are involved in the production of phytotoxic metabolites. Indeed some fungal secondary metabolites derived from NPSs were found to be host-selective phytotoxins involved in the virulence of pathogens, such as HC toxin (Walton, 2006) and destruxin B (Pedras et al., 2003). In addition, the four polyketides phomapyrones (A, F and G) and infectopyrone are definitely connected to the PKS pool identified in our study. Therefore, a goal for the future is to further characterize each *NPS* and *PKS* gene with the aim of identifying the metabolite product synthesized by the enzyme that each gene encodes in *A. brassicicola*. It may also be valuable to test individual small molecules from *A. brassicicola* for other activites and applications (antimicrobial, anticancer, antiviral, cholesterol lowering activity, herbicidal, etc.).

Our study, and those of others, demonstrates that small molecule secondary metabolites play diverse, but also fundamental, roles in the producing organisms themselves, in addition to better known roles as effectors of interactions between organisms. Some are crucial for basic biological processes, such as asexual development and nutrient gathering (e.g. iron metabolism), demonstrating the significance of these molecules to survival and proliferation of the fungus. The task at hand is, as mentioned, identification of the natural biological function of the remaining NPS and PKS metabolites through additional comparative screens of mutants versus wild-type, accompanied by whole-genome approaches, now made possible by the release of the genome sequences of many fungi. Considerable work also remains to be done in understanding the biosynthetic mechanism and regulation of the NPSs and

PKSs. The availability of the genetic information could eventually allow "combinatorial biosynthesis" of the novel compounds, like depudecin, through genetic manipulation (i.e. heterologous expression in improved production hosts) (Bode and Muller, 2005). Furthermore, comparisons among studies of *NPS* and *PKS* genes from other fungi will further our understanding of the evolution and ecological significance of these diverse groups of compounds.

Some nonribosomal peptides and polyketides produced by *A. brassicicola* seem to function as virulence factors, as suggested in our study. Some of them may be phytotoxins (HST or non-HST) that disable host cellular functions or kill host cells. Based on *AbNPS2* study, some metabolites may play a role of a shield or a structural component, specifically protecting infection-related structures such as appressoria and infection hyphae. Considerable secondary metabolic potential of *A. brassicicola* also makes it plausible that many effector-type functions are fulfilled by secreted metabolites during plant infection. Elucidating their precise roles in pathogenicity is of the first priority for durable control of *A. brassicicola* disease. However, fungal pathogenicity is affected not just by one or two factors, but multiple factors such as simultaneous production of several toxic materials and defense against enzymes and toxins from hosts. Understanding this complexity may ultimately lead to efficient control of fungal disease of important crops. Over the past 50 years, the control of plant fungal diseases has relied mainly on chemical pesticides. However, it is clear that sustainable agricultural practices demand control strategies other than massive application of potentially environmentally harmful fungicides. It is anticipated that

future approaches to control diseases will rely on more selective and environmentally friendly control methods. Considering the diversity of pathogenicity strategies that fungal pathogens use as well as their ability to quickly adapt, it is difficult to predict which developments will lead to durable and broad-spectrum disease resistance. No matter what sophisticated methodologies may be discovered, it is clear that effective plant protection will require a much better understanding of the diverse roles of fungal pathogenicity factors.

# Literature Cited


Bach, A.N. (1950) Collected Works in Chemistry and Biochemistry [in Russian]. Moscow, Russia: Academy of Sciences of the USSR Publisher.

Bode H, Mu ¨ ller R, 2005. The impact of bacterial genomics onnatural product research. Angewandte Chemie International Edition 44: 6828–6846.

Cane, D.E., and Walsh, C.T. (1999) The parallel and convergent universes of polyketide synthases and nonribosomal peptide synthetases. Chem Biol, 6(12), R319-325.

Ciegler, A., and Lindenfelser, L.A. (1969) An antibiotic complex from Alternaria brassicicola. Experientia, 25(7), 719-720.

MacKinnon, S.L., Keifer, P., and Ayer, W.A. (1999) Components from the phytotoxic extract of *Alternaria brassicicola*, a black spot pathogen of canola. Phytochemistry, 51, 215-221.

Matsumoto, M., Matsutani, S., Sugita, K., Yoshida, H., Hayashi, F., Terui, Y., Nakai, H., Uotani, N., Kawamura, Y., Matsumoto, K., and et al. (1992) Depudecin: a novel compound inducing the flat phenotype of NIH3T3 cells doubly transformed by ras- and src-oncogene, produced by Alternaria brassicicola. J Antibiot (Tokyo), 45(6), 879-885.

Minami, A., Tajima, N., Higuchi, Y., Toyomasu, T., Sassa, T., Kato, N., and Dairi, T. (2009) Identification and functional analysis of brassicicene C biosynthetic gene cluster in Alternaria brassicicola. Bioorg Med Chem Lett, 19(3), 870-874.

Oide, S., Krasnoff, S.B., Gibson, D.M., and Turgeon, B.G. (2007) Intracellular siderophores are essential for ascomycete sexual development in heterothallic Cochliobolus heterostrophus and homothallic Gibberella zeae. Eukaryot Cell, 6(8), 1339-1353.

Oka, K., Akamatsu, H., Kodama, M., Nakajima, H., Kawada, T., and Otani, H. (2005) Host-specific AB-toxin production by germinating spores of Alternaria brassicicola is induced by a host-derived oligosaccharide. Physiol. Mol. Plant Pathol., 66, 12-19.

Otani, H., Kohnobe, A., Kodama, M., and Kohmoto, K. (1998) Production of a host-specific toxin by germinating spores of *Alternaria brassicicola*. Physiol. Mol. Plant Pathol., 52, 285-295.

Pedras, M.S., Chumala, P.B., Jin, W., Islam, M.S., and Hauck, D.W. (2009) The phytopathogenic fungus Alternaria brassicicola: phytotoxin production and phytoalexin elicitation. Phytochemistry, 70(3), 394-402.

Pedras, M.S., Montaut, S., Zaharia, I.L., Gai, Y., and Ward, D.E. (2003) Transformation of the host-selective toxin destruxin B by wild crucifers: probing a detoxification pathway. Phytochemistry, 64(5), 957-963.

Turgeon, B.G., Oide, S., and Bushley, K. (2008) Creating and screening Cochliobolus heterostrophus non-ribosomal peptide synthetase mutants. Mycol Res, 112(Pt 2), 200-206.
Walton, J.D. (2006) HC-toxin. Phytochemistry, 67(14), 1406-1413.